Sentinel-1A/B flood inundation mapping of Hurricane Harvey in Texas and DInSAR time series analysis to map subsidence of the Ganges-Brahmaputra-Meghna Delta

By

**Clay D. Woods**

B.S., University of Utah, 2018

A thesis submitted to the

Faculty of the Graduate School of the

University of Colorado in partial fulfillment

of the requirement for the degree of

Master of Geology

Department of Geological Sciences

2022

Committee Members:

Irina Overeem

Kristy Tiampo

Michael Willis

**Abstract**

The increasing number of flood events, combined with coastal urbanization, has contributed to significant economic losses and damage to buildings and infrastructure. Here I present two several methods for characterizing flood inundation using Sentinel-1A/B synthetic aperture radar (SAR). In the first part, an amplitude thresholding technique is developed to characterize flood inundation and compared to machine learning (ML) methods. Both are very effective at identifying both large- and small-scale flood inundation at very high-resolution. In the second part, differential interferometric synthetic aperture radar (DInSAR) is used to map subsidence of the Ganges-Brahmaputra-Meghna (GBM) delta. The GBM delta is the largest delta in the world with an area of ~150,000 km^2 and approximately 200 million inhabitants (Becker et al., 2020) subject to both subsidence and coastal flooding (Higgins et al., 2014; Rogers et al. 2018). Thus, the need to quantify spatial patterns of deformation rates of the GBM is critical for future planning to mitigate the impacts of changes in sedimentation rates and sea level rise in the Bangladesh coastal region. In this study, DInSAR images at ~100 meter pixelization are used to generate interferograms and associated time series to determine current deformation rates over the GBM. Approximately 650 ascending and 550 descending Sentinel-1A Single Look Complex (SLC) images were acquired spanning from March 2017 to June 2021 resulting in approximately 2300 interferograms. The availability of both ascending and descending images in the regions allows for construction of 11 vertical time series using MSBAS which are then mosaicked into a singular deformation map. Overall, the region is subsiding with a rate of 3.36 mm/yr, with 95% of the vertical linear deformation rates ranging between -28.11 and 22.09 mm/yr. Time series display a strong sinusoidal signal with a local maximum during the middle of the year (June) and a local minimum at the start of the year (January) and an amplitude ranging from 8-12 cm.

Minimal correlation between the vertical linear deformation rates and either topography or vegetation (as quantified by NDVI) was found, while a strong correlation with geologic units was observed. Comparison of GPS-derived rates and MSBAS-derived rates shows reasonable comparison between some stations. Removal of the monsoon sinusoidal signal shows a more stable time series with potential underlying deformation dynamics.

## Dedication

Nugget

**Contents**


1. **Introduction/Background.....1**
2. **Flooding inundation analysis of Hurricane Harvey using Sentinel-1A data....7**
   - **2.1. Flooding inundation methods .....7**
   - **2.2. Flood inundation mapping.....9**
3. **DInSAR time series analysis to map the subsidence/uplift of the Ganges-Brahmaputra-Meghna Delta.....17**
   - **3.1. Data for DInSAR.....18**
   - **3.2. DInSAR Time Series Methods Overview .....20**
   - **3.3. DInSAR processing.....21**
   - **3.4. Multidimensional Small Baseline Subset Inversion.....35**
   - **3.5. Time Series Mosaicking.....39**
   - **3.6. Normalized Differenced Vegetation Index .....43**
4. **DInSAR Time Series Results .....45**
   - **4.1. Linear deformation rate map .....45**
   - **4.2. Individual Time Series.....47**
5. **DInSAR Discussion.....53**
   - **5.1. Topography Comparison .....53**
   - **5.2. Normalized Differenced Vegetation Index Comparison .....58**
   - **5.3. Geological Overlay Comparison.....64**
   - **5.4. Points of interest and GPS comparison .....69**
   - **5.5. Error sources.....84**
   - **5.6. Future Work.....84**

**6. DInSAR Time Series Conclusion.....85**

**References.....88**

**Appendix.....98**

**List of Figures**

**Figure 1.1:** Ganges-Brahmaputra-Meghna delta base map .....3

**Figure 1.2:** Previous DInSAR-based subsidence map (from Higgins et al., 2014). .....6

**Figure 2.2.1:** Initial inundation threshold results .....10

**Figure 2.2.2:** Inundation comparison results .....12

**Figure 2.2.3:** NOAA optical data overview .....14

**Figure 2.2.4:** NOAA enlarged region 1 .....15

**Figure 2.2.5:** NOAA enlarged region 2 .....16

**Figure 2.2.6:** NOAA enlarged region 3 .....17

**Figure 3.1.1:** DInSAR frame base map of this study .....19

**Figure 3.3.1:** Sentinel-1A/B acquisition modes .....22

**Figure 3.3.2:** Basic repeat pass SAR example .....23

**Figure 3.3.3:** DInSAR workflow .....24

**Figure 3.3.4:** Sentinel-1A/B TOPSAR swaths and bursts .....26

**Figure 3.3.5:** Speckle noise phenomenon .....28

**Figure 3.3.6:** Geometric distortions 1 .....29

**Figure 3.3.7:** Geometric distortions 2 .....30

**Figure 3.3.8:** Mosaicked averaged coherence .....31

**Figure 3.3.9:** GACOS example....32

**Figure 3.3.10:** Interferogram masking example....33

**Figure 3.4.1:** L-curves....36

**Figure 3.4.2:** MSBAS Tikhonov regularization parameters examples images....38

**Figure 3.4.3:** MSBAS Tikhonov regularization parameters examples histograms....39

**Figure 3.4.4:** Time series region of overlapping pixels....40

**Figure 3.6.1:** SAR backscatter characteristics....44

**Figure 4.1.1:** Linear deformation rate map....45

**Figure 4.1.2:** Linear deformation rate histogram....46

**Figure 4.2.1:** Time Series 1....48

**Figure 4.2.2:** Time Series 2....49

**Figure 4.2.3:** Time Series 3....50

**Figure 4.2.4:** Time Series 4....51

**Figure 4.2.5:** Time Series 5....52

**Figure 5.1.1:** Topography versus deformation correlation....54

**Figure 5.1.2:** Topography and deformation cross sections....56

**Figure 5.2.1 (a):** NDVI compared to vertical linear deformation rate map....59

**Figure 5.2.1 (b):** NDVI compared to averaged coherence....61

**Figure 5.3.1:** Linear deformation rate map with geological overlay .....65

**Figure 5.3.2:** Region one enlarged vertical linear deformation rate map .....66

**Figure 5.3.3:** Region two enlarged vertical linear deformation rate map .....66

**Figure 5.3.4:** Geological unit descriptions.....67

**Figure 5.4.1 (a):** GPS w/ MSBAS-derived time series comparison .....70

**Figure 5.4.1 (b):** GPS w/ sinusoid removed MSBAS-derived time series comparison....70

**Figure 5.4.2 (a):** Time series with sinusoid removed .....74

**Figure 5.4.2 (b):** Time series with sinusoid removed regression recalculated .....75

**Figure 5.4.3 (a):** Time series with sinusoid removed .....76

**Figure 5.4.3 (b):** Time series with sinusoid removed regression recalculated .....77

**Figure 5.4.4 (a):** Time series with sinusoid removed .....78

**Figure 5.4.4 (b):** Time series with sinusoid removed regression recalculated .....79

**Figure 5.4.5 (a):** Time series with sinusoid removed .....80

**Figure 5.4.5 (b):** Time series with sinusoid removed regression recalculated .....81

**Figure 5.4.6 (a):** Time series with sinusoid removed .....82

**Figure 5.4.6 (b):** Time series with sinusoid removed regression recalculated .....83

**List of Tables**

**Table 3.3.1:** Data pairing for MSBAS .....34

**Table 5.3.1:** Continuous GPS comparison to MSBAS-derived vertical linear rates .....71

**Table 5.3.2:** Campaign GPS comparison to MSBAS-derived vertical linear rates .... 71-72

## 1. Introduction/Background

Coastal regions around the world are at increased risk of flooding due to coastal subsidence and sea level rise which is likely to be exacerbated by continued climate change. Particularly sensitive regions include deltaic regions, with an estimated 340 million people worldwide living in these regions (Edmonds et al., 2020). Thus, we have a need to be able to quantify flood inundation and subsidence to assess associated risk to best prepare for future flooding and mitigate potential damages. This study both quantifies flood inundation using an automatic histogram threshold-based technique and estimates the subsidence/uplift of the Ganges-Brahmaputra-Meghna (GBM) delta using differential interferometric synthetic aperture radar (DInSAR). The ability to quantify subsidence can provide useful information regarding flood hazard as regions which are subsiding quicker may be at more risk than others.

Flooding is one of the most prevalent natural disasters in the world, causing many fatalities and high economic losses. While the aggregate average annual flood loss estimate for 136 cities was estimated at US$6billion per year in 2013, it is estimated that, without adaptation, those average losses are projected to increase to more than US$1trillion per year by 2050 (Hallegatte 2013). The combination of climate change, growing populations and regional subsidence is likely to make the problem worse, especially for large coastal cities. As a result, it is critical that we better assess the risk of flooding and quantify the dynamics of water bodies worldwide through improved remote sensing data acquisition and analysis and their incorporation into flood risk mapping, impact assessments, forecasting, alerting and emergency response systems. The European Space Agency's (ESA's) C-band Sentinel-1A/B synthetic aperture radar (SAR)

satellite data has sufficient spatial and temporal resolutions to allow for the detailed study of those dynamic water bodies of interest to both decision makers and the public.

Commonly applied methods in the detection of inundation include simple and automatic histogram thresholding-based methods (Refice et al., 2018; Cao et al., 2019) and multitemporal change detection-based methods (Ajadi et al., 2016; D'Addabbo et al., 2018; Meyer et al., 2019). In this study an automatic histogram thresholding method, based on the methods Cao et al., 2019, is used to map flooding inundation.

The combination of sea level rise caused by climate change and the natural and anthropogenic subsidence in deltas has the potential to cause significant, damaging impacts to those living within deltaic regions (Brown et al., 2015; Kay et al., 2015; Rogers et al., 2018; Becker et al., 2020; Syvitski et al., 2009). Deltaic regions are particularly sensitive to the changing climate and anthropogenic impacts which can alter sedimentation rates of deltas, given that they are commonly near or at sea level over large regions (Brown et al., 2015; Rogers et al., 2018). Subsidence in deltas occurs at a variety of spatial and temporal scales and can be caused by a multitude of different factors ranging from naturally occurring processes such as tectonics, erosion, sediment compaction to anthropogenic drivers, including farming practices, deforestation, hydrocarbon extraction and the construction of levees or embankments to manage coastal and river processes and prevent flooding (Syvitski et al., 2009; Brown et al., 2015; Rogers et al., 2018). Thus, the need to quantify the potential impacts of sea level rise and associated subsidence in vulnerable deltas for a more complete understanding of delta sustainability and future planning.

The Ganges-Brahmaputra-Meghna (GBM) delta, shown in Figure 1.1, is the largest delta in the world, with an area of ~150,000 $km^2$ and approximately 200 million inhabitants (Becker et

al., 2020). It is situated in a tectonically active region, forming a triple junction of the Indian Plate, the Eurasian Plate and the Burmese Plate.

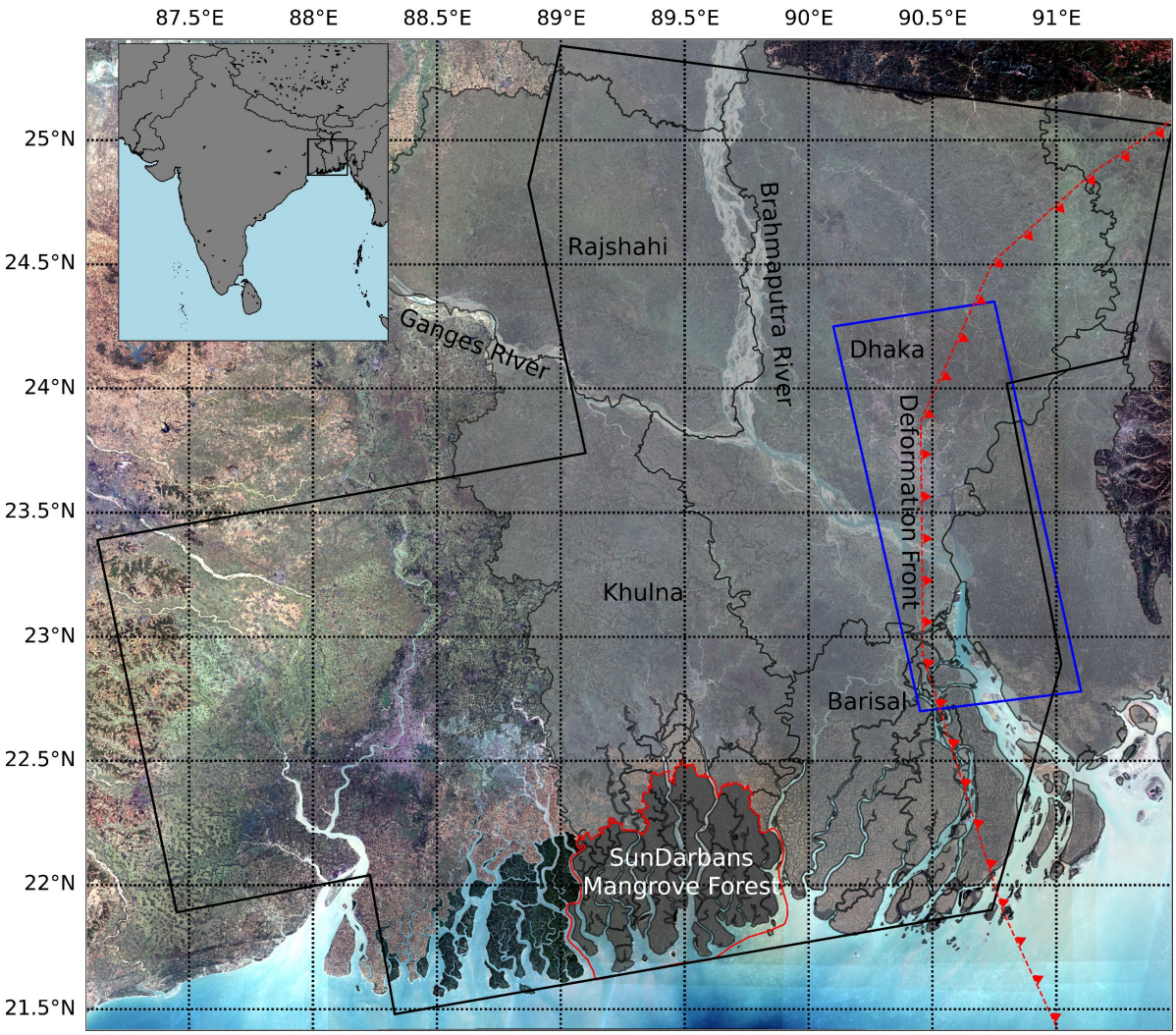


**Figure 1.1:** Base map of the GBM. Black outline is the approximate location of the results in this study, red line is the deformation front of the Burma thrust-fold belt in the region. Background image is an RGB composite of the mean of ESA Sentinel-2 optical data from March 2017 to June 2021, processed using Google Earth Engine (GEE) at 30 m resolution. Blue rectangle is approximate location of DInSAR results from Higgins et al., 2014.

The GBM is particularly vulnerable to increased sea level rise, as at least 10% of the delta is less than 1 m above mean sea level. Half of the entire area of Bangladesh lies within 10 m of sea level, and it has one of the highest population densities in the world, at ~1000 people per square

kilometer (Becker et al., 2020; Steckler et al., 2022). Thus, for the more than140 million people who inhabit the GBM, even small changes in the magnitude or rate of sea level rise or subsidence in the region can have significant consequences for its inhabitants. This deltaic region also experiences extreme river flooding during the monsoon season, with 20-25% of the land being submerged in a normal monsoon season and 60-70% in an extreme flood (Steckler et al., 2022). Increased sea level rise, potential subsidence and anthropogenic alterations of the delta and its natural processes has the potential to impact ongoing flood risk.

The GBM is maintained by natural river sedimentation processes, including flooding within the active river floodplain and tidal reworking of fluvial sediments into the lower deltaic floodplain (Rogers et al,. 2013; Rogers et al., 2018). To date, these processes have been able to maintain the natural mangrove forests in the GBM and offset recent sea level rise and have resulting in a net gain of land in the main locus of deposition in the Meghna estuary (Rogers et al., 2018; Steckler et al., 2022). In other parts of the lower delta plain, due to the high risk of flooding in the region, infrastructure has been constructed to mitigate the risk and damages of potential flooding. These include dikes, polders, and similar infrastructure in at risk areas which can alter the natural depositional processes of the delta that would normally naturally sustain the elevation (Auerbach et al., 2015; Rogers et al., 2018). The overall aggradation rates of the delta sampled by Rogers et al., 2018, an average $2.3 \pm 9\ cm\ y^{-1}$, is more than double the estimated average rate of local sea level rise (Rogers et al., 2018). However, there is a compelling need to incorporate subsidence into this overall view of the delta, as sea level rise alone is not the only risk factor in the GBM. Understanding the combination of sea level rise and subsidence, which can occur at rates significantly higher than sea level rise, would allow for a better modeling and

assessment of the potential increased risk of flooding, considering the overall aggradation rate of the GBM.

To date, several methods have been applied to quantify the overall subsidence in the GBM. These methods include GPS stations, which can provide point-based measurements of the rate of subsidence over time periods of several years. GPS stations in our area of interest (MPUR and DHAK) have estimated subsidence rates of 0.6 mm/yr (2007-2013) and 12.25 mm/yr (2003-2008), respectively (Steckler et al., 2010, 2013). In addition, a large seasonal signal of up to 5-6 cm in amplitude is expected in this region due to elastic deformation under shallow groundwater loading during the monsoon season (Steckler et al. 2013) which has been previously measured by GPS data. Models also have been applied to determine subsidence rates. Krien et al., 2019, estimated subsidence caused by sediment compaction at 2-3 mm/year. GPS methods are limited by their point-based spatial resolution, which constrains their ability to accurately estimate an overall map of subsidence of the GBM. To overcome these spatial resolution limitations, Higgins et al., 2014, used ALOS1 L-band SAR data from 2007-2011 to map subsidence in the eastern portion of the GBM using DInSAR methods. Using 18 ALOS PALSAR scenes at ~100 meter pixelization, they found subsidence rates ranging from 0 to more than 18 mm/yr shown in Figure 1.2.

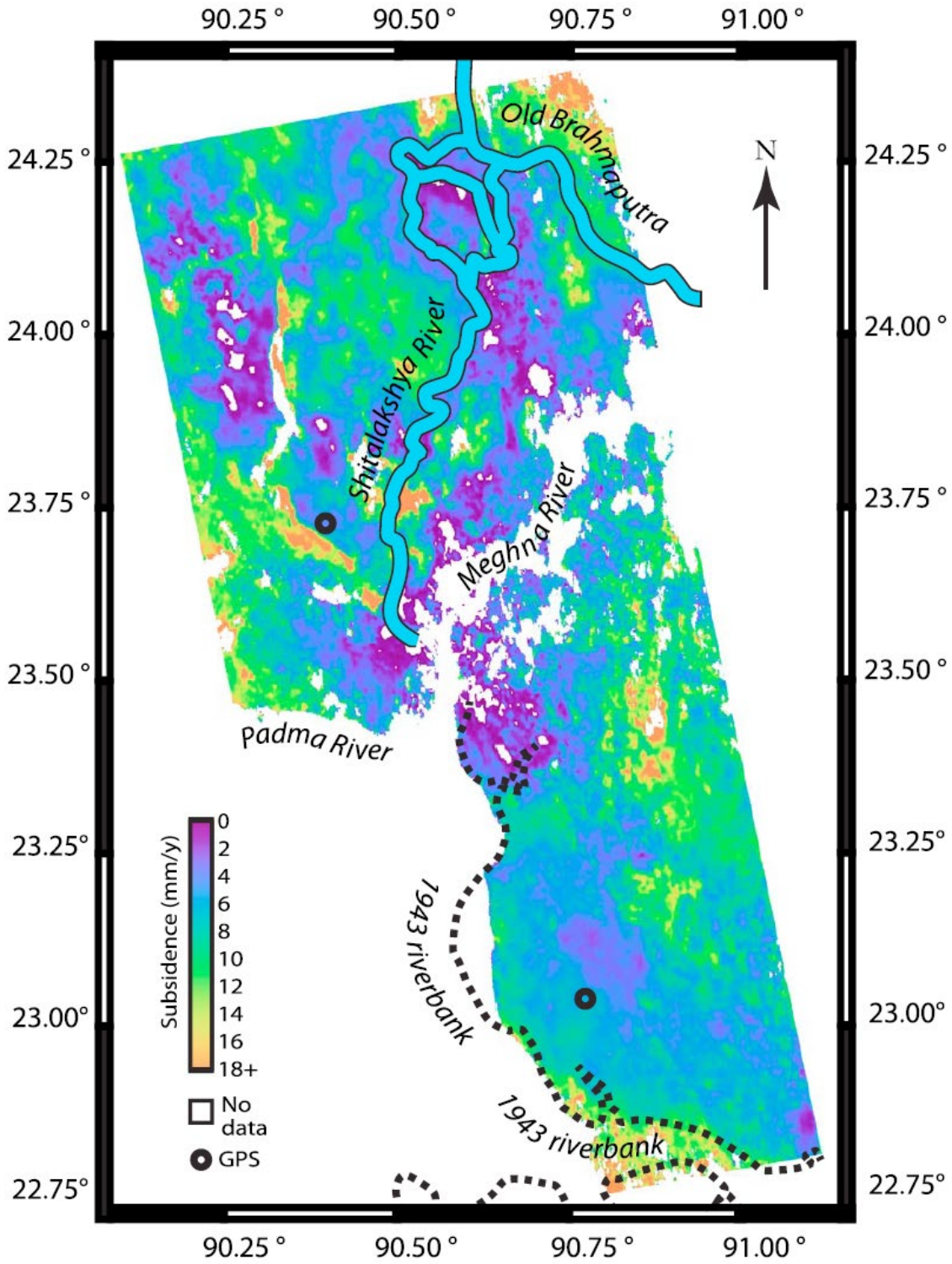


**Figure 1.2:** DInSAR based annual subsidence rates of the GBM between 2007-2011, from Higgins et al. 2014.

The launch of the Sentinel-1A/B C-band SAR satellites ESA in 2014 and 2016, with 6-to-12-day temporal resolution, provides the opportunity to expand the study of the GBM using DInSAR at high temporal and spatial resolution using freely available data. DInSAR allows for the quantification of ground motion using repeat pass SAR measurements. The study area covers the vast majority of the GBM, including coastal regions at ~100 m pixelization, as shown in Figure 1.1. This area essentially includes every land cover type in the GBM, including both urban and agricultural, regions of embankment and polders, and the natural Sundarbans, a large area of mangrove forest at the confluence of the GBM and Hoogly rivers in the Bay of Bengal. SAR acquisitions with high temporal resolution is important in a region affected by both short- and long-term processes, such as monsoon rains, agriculture, flooding and sediment transport that can reduce coherence and make retrieval of repeat pass deformation difficult at the relatively short wavelengths of Sentinel-1A/B. The dense temporal resolution of Sentinel-1A/B allows for the formulation of dense vertical deformation time series from the period of March 2017 to June 2021. The continuous GPS station located in Dhaka (DHAK) allows us to calibrate the deformation rates and reconcile multiple DInSAR time series deformation maps into a single deformation map covering most of the GBM. Subsidence in the region is analyzed in the context of regional geology, soil types, sediment compaction, sediment aggradation and potential anthropogenic impacts such as groundwater or hydrocarbon extraction. This study provides an overall deformation map of the majority of the GBM including both subsidence and uplift of the region at high spatial resolution.

## 2. Flooding inundation analysis of Hurricane Harvey using Sentinel-1A data

### 2.1 Flooding inundation methods

SAR offers the unique advantage of all-weather data collection at Earth's surface, which is advantageous for flood mapping due to the likelihood of heavy cloud cover during heavy rainfall events. In this study, imagery from the ESA Sentinel-1A/B C-band SAR satellite, which has a 6-12 day repeat period with a large spatial extent (~100s of km) was employed, providing high temporal and spatial resolution imagery over large regions ideal for flood mapping. This data is publicly available from NASA's Alaska Satellite Facility Distributed Active Archive Center (ASF DAAC) in both single look complex (SLC) and high-resolution ground range detected (GRD) data (Copernicus, 2015).

A threshold method was employed to map inundated regions based on the low backscatter coefficient of the ground range detected (GRD) SAR data which has an approximate resolution of 15 m. Using the method of Cao et al., (2019), SAR data with the appropriate power transform will follow a bimodal Gaussian distribution. We exploit this characteristic to automatically determine a threshold for the image to classify water and non-water regions. The image is split into tiles due to different sections of the SAR scene behaving differently because of a wide swath (Cao et al., 2019). Each tile is analyzed separately to determine its unique threshold. Each tile is further split into an array of $s$ x $s$ pixels to determine which sets of pixels within this tile behaves as a bimodal Gaussian distribution using the maximum normalized between-class variance (BCV) (Cao et al., 2019; Demirkaya et al., 2004). Based on simulations, it was determined that a maximum value of BCV greater than 0.65 can be assumed to be bimodal. Within each tile, we determine which set of $s$ x $s$ pixels are bimodal and determine the threshold for that tile. The value of $s$ is varied to maximize the number of bimodal sets of pixels within each tile to determine an optimal threshold for that tile. An automatic threshold is selected using either the mode of the distribution or the local minimum separating the peaks in the

bimodal distribution. The mean of the thresholds for each set of *s* x *s* pixels is used as the threshold for the entire tile. This process is repeated for each tile in the image to generate a binary output displaying the classified water regions. Because this method also classifies water which is more permanent rather than a result of flooding events, a set of images is used to remove the common classifications among all images, assuming sufficient temporal coverage. This method can be applied to both VV (vertical-vertical) and VH (vertical-horizontal) polarizations to improve accuracy as well as to coherence images to further refine the method. Coherence images are formed from two SLC images and essentially estimate the change in pixel characteristics from the first image to the second. Thus, when there is flooding the GRD images should exhibit a significant change in backscatter coefficient between pre-flood and flooding, which should be captured with coherence image estimation. Then the coherence image estimation can be used as validation for comparison with the threshold results from GRD images. This assumes data is available for coherence image estimations before, during and after a flood event. This method of tiling also has the potential to be used in machine learning algorithms to detect changes among tiles for flood detection (Tiampo et al., 2021a; Tiampo et al., 2021b).

### 2.2 Flood inundation mapping

The initial results for flood inundation mapping of Hurricane Harvey using the automatic histogram threshold method of SAR GRD data are presented in Tiampo et al. 2021b, shown in Figure 2.2.1.

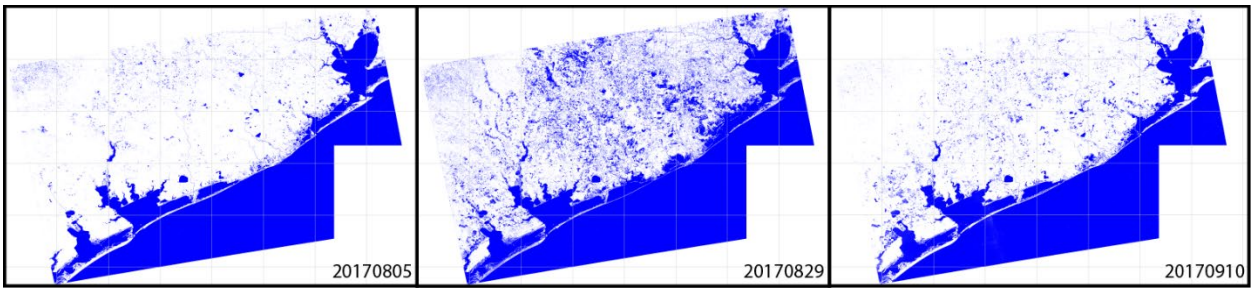


**Figure 2.2.1:** Initial results for the SAR threshold analysis of SAR GRD data (Tiampo et al.. 2021b) for identification of flood extent caused by Hurricane Harvey. Blue denotes pixels identified as water at 15 m resolution. The left image is from before the rainfall began, the middle is during the storm and the right image was after the waters had receded significantly.

Figure 2.2.1 displays before flooding, during flooding and after flooding classification of water at ~15 m resolution. Visual comparison of the images clearly shows a large increase in the number of flooded pixels from pre-flood to flooding and overall recession or decrease in the number of flooded pixels in the post-flood binary classified images. Given that we know the dates Hurricane Harvey occurred, we do expect an increase in the number of flooded pixels during the flooding period, but these initial results did not have any ground truth methods applied. Thus, these initial results were not verified and could potentially contain many false positives.

In collaboration with Lingcao Huang and Conor Simmons and advised by Kristy Tiampo (Department of Geological Sciences & the Collaborative Institute of Research in Environmental Sciences (CIRES), University of Colorado Boulder), the flood inundation mapping research continued, developing various methods which include machine learning (ML) methods using DeepLabV3+ (Chen et al., 2015) and various potential ground truth comparisons. Their initial ML method is described briefly in Tiampo et al., (2021b) and in detail in Tiampo et al., (2021a). These methods will be described briefly here as well as the results they derived, which will be

compared to the initial results of the SAR threshold analysis shown in Figure 2.2.1, the primary method I initially implemented on for flood inundation mapping.

Several different methods and data sources were used in Tiampo et al., (2021a) to map flooding inundation. These include, water pixels classified using MODIS (Moderate Resolution Imaging Spectroradiometer) data supplied by the Dartmouth Flood Observatory (DFO) (Brakenridge 2021), normalized differenced water index (NWDI) analysis of Sentinel-2 optical data, DeepLabv3+ analysis of SAR GRD data, thresholding analysis of SAR GRD data and an RGB classification based method. The NWDI analysis was based on a manually chosen threshold of 0 to separate water pixels from other pixels. The machine learning method was based on a tiling-based approach as discussed in Section 2.1. Essentially, the SAR GRD data was divided into varying sized tiles, water pixels were then manually identified in these tiles as polygons and used as training data for the machine learning algorithm. The polygons which were identified to contain water pixels were then altered in various ways to improve the robustness of the machine learning model. The RGB classification was based on plotting the SAR GRD data and its various polarizations in each color band, i.e., SAR GRD VV as red, SAR GRD VH as blue, and their ratio VH/VV as blue and then applying the DeepLabv3+ methodology to this RGB image. The basic idea in this approach is that VH/VV will be the most sensitive to pixels inundated in water and thus blue in this image will show up as water pixels. The combination of these different methods and results is shown in Figure 2.2.2.

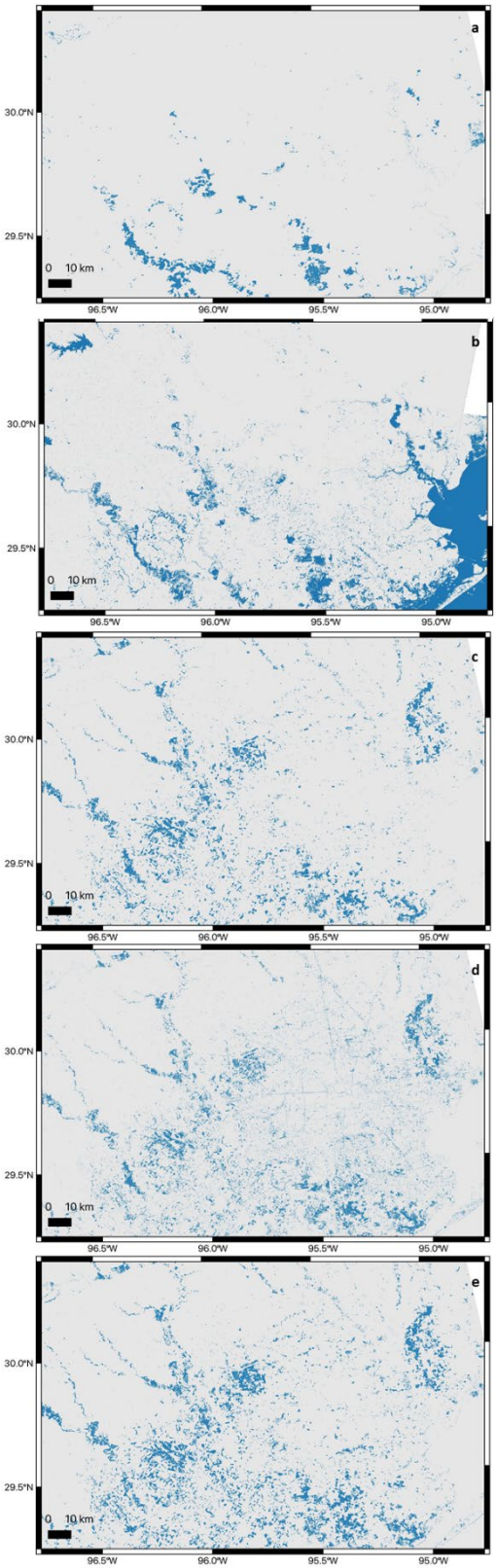


**Figure 2.2.2:** a) Water pixels identified by MODIS data, courtesy of the DFO (Brakenridge 2021) 250

m pixel spacing; water pixels identified from NDWI analysis of Sentinel-2 data, 10 m pixel spacing; c) water pixels identified by the DeepLabv3+ analysis of SAR GRD data, August 29, 2017, 10 m pixel spacing; d) water pixels identified from thresholding analysis of the same SAR GRD data, 10 m pixel spacing; and e) water pixels identified by the classification analysis of the SAR GRD data, 10 m pixel spacing. The Global Water Mask is removed from all results except the NDWI, Figure 10b (Tiampo et al., 2021a).

Of all the methods described above, none have been compared with ground truth to date, but can be used in direct comparison. We should at least expect some reasonable agreement between the different classified images. The best available potential ground truth data for these results is provided by National Oceanic and Atmospheric Administration (NOAA) optical imagery during the dates of Hurricane Harvey (https://storms.ngs.noaa.gov/storms/harvey/download/metadata.html). The images were acquired from an altitude between 2500 to 5000 feet using a Trimble Digital Sensor System (DSS) between August 27 and September 3, 2017. The NOAA optical data has a ground sample distance (GSD) of 35 to 50 cm. Several regions contain both the NOAA optical data and the inundated classified results as shown in Figure 2.2.3.

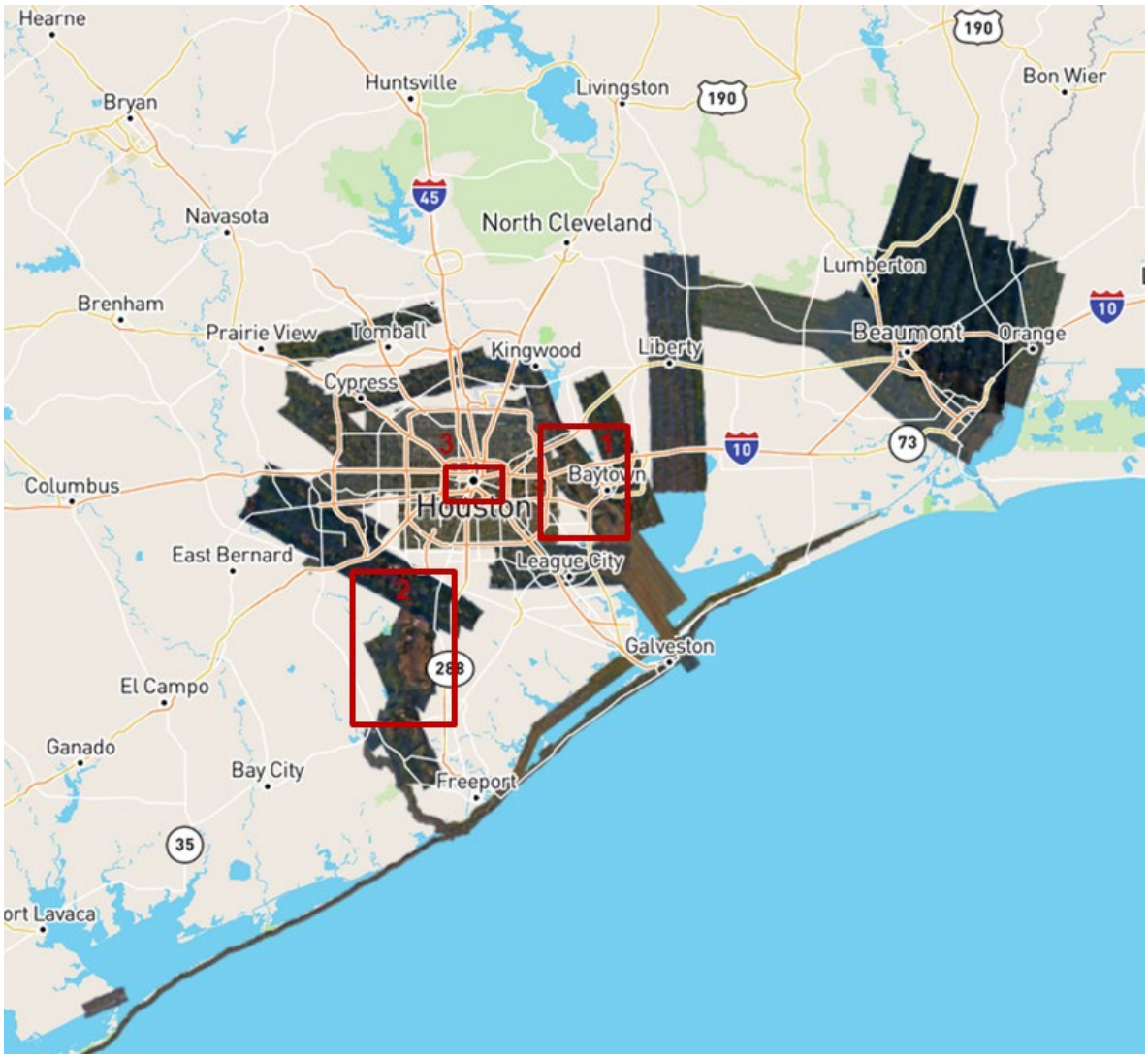


**Figure 2.2.3:** NOAA Remote Sensing Division airborne digital optical imagery of the Houston area acquired between August 27 and September 3, 2017, in response to Hurricane Harvey. Approximate GSD for each pixel ranges between 35 and 50 cm (https://storms.ngs.noaa.gov/storms/harvey/download/metadata.html). Red squares outline three areas selected for comparison with results of flood detection and DeepLabv3+ analysis (Tiampo et al., 2021a).

The first of these regions is shown in Figure 2.2.4.

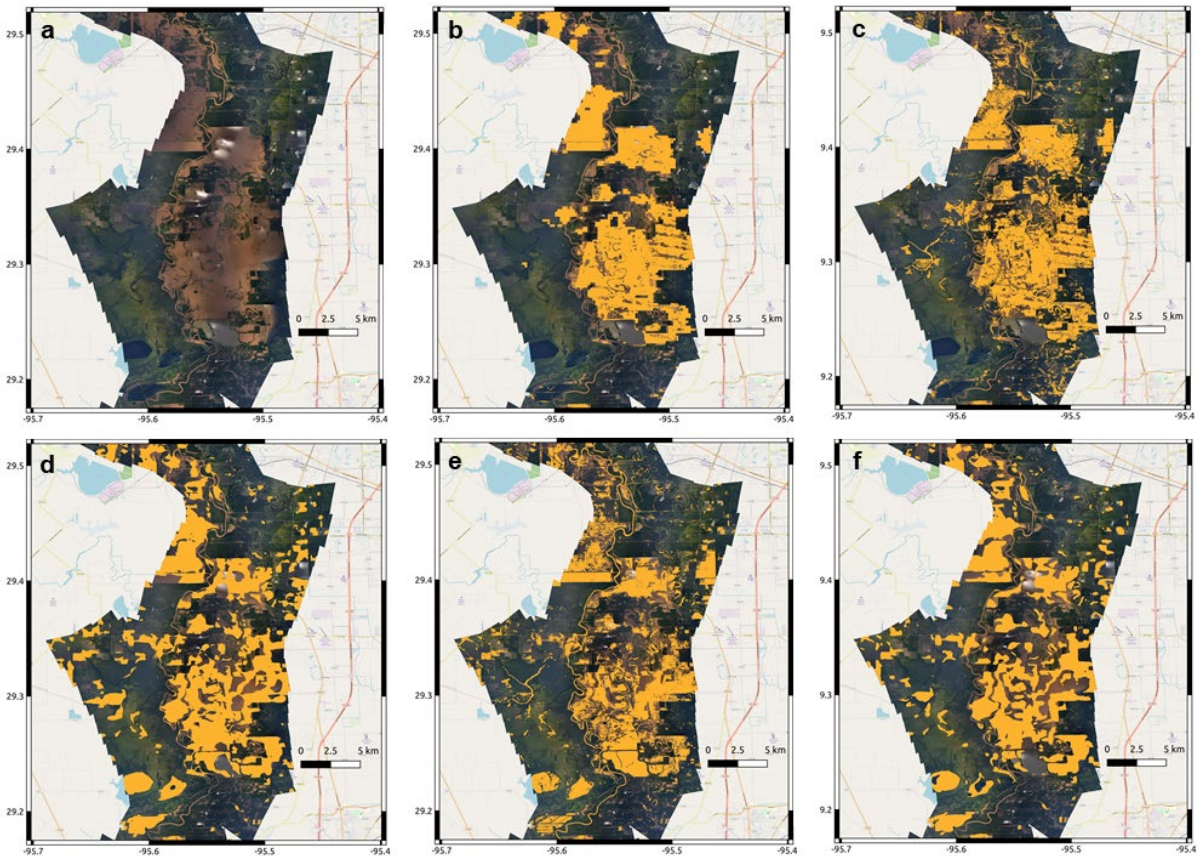


**Figure 2.2.4:** a) NOAA Remote Sensing Division airborne digital optical imagery of the Houston area acquired between August 27 and September 3, 2017, subregion 1, as shown in Figure 2.2.3; b) water pixels identified by DFO MODIS data, 250 m pixel spacing, courtesy of the DFO (Brakenridge 2021); c) water pixels identified from NDWI analysis of Sentinel-2 data, 10 m pixel spacing; d) water pixels identified by the DeepLabv3+ analysis of SAR GRD data, August 29, 2017, 10 pixel spacing; e) water pixels identified from thresholding analysis of the same SAR GRD data, 10 m pixel spacing; and f) water pixels identified by the classification analysis of the SAR GRD data, 10 m pixel spacing. The GWM is not removed from the analyses of b through f (Tiampo et al., 2021a).

Thus, we can directly visually compare subregions of results as shown in Figure 2.2.1 to the NOAA optical data in Figure 2.2.4. All the methods applied in this case seem to produce similar results, although with minor differences. The second comparison is shown in Figure 2.2.5.

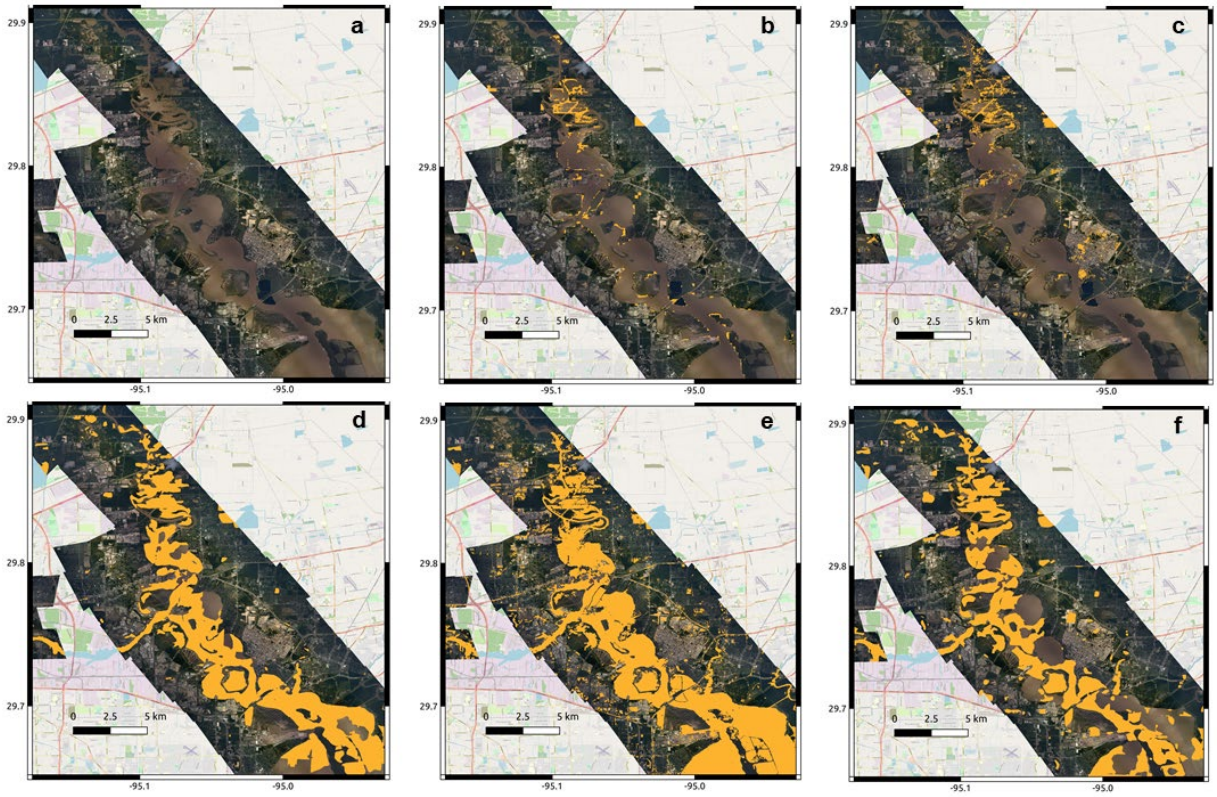


**Figure 2.2.5:** a) NOAA Remote Sensing Division airborne digital optical imagery of the Houston area acquired between August 27 and September 3, 2017, subregion 2, as shown in Figure 2.2.3; b) water pixels identified by MODIS data, 250 m pixel spacing, courtesy of the DFO (Brakenridge 2021); c) water pixels identified from NDWI analysis of Sentinel-2 data, 10 m pixel spacing; d) water pixels identified by the DeepLabv3+ analysis of SAR GRD data, August 29, 2017, 10 m pixel spacing; e) water pixels identified from thresholding analysis of the same SAR GRD data, 10 m pixel spacing; and f) water pixels identified by the classification analysis of the SAR GRD data, 10 m pixel spacing (Tiampo et al., 2021a).

Figure 2.2.5 shows more significant differences for the classification results at this location than in Figure 2.2.4. Clearly, (a), (b) and (c) identify almost no pixels as being inundated, whereas we can clearly see there is water in this location from the NOAA imagery. We do see most of this water covered region classified as inundated as shown in (d), (e) and (f). They approximately classify the same region but there are clearly minor differences in the actual classifications. Thus, in this case the DeepLabv3+, thresholding, and RGB classification method were successful in identifying the flooded and permanent waters of this sinusoidal channel. Whereas the MODIS

data classification and NWDI largely failed. The third region tested for comparison is shown in Figure 2.2.6.

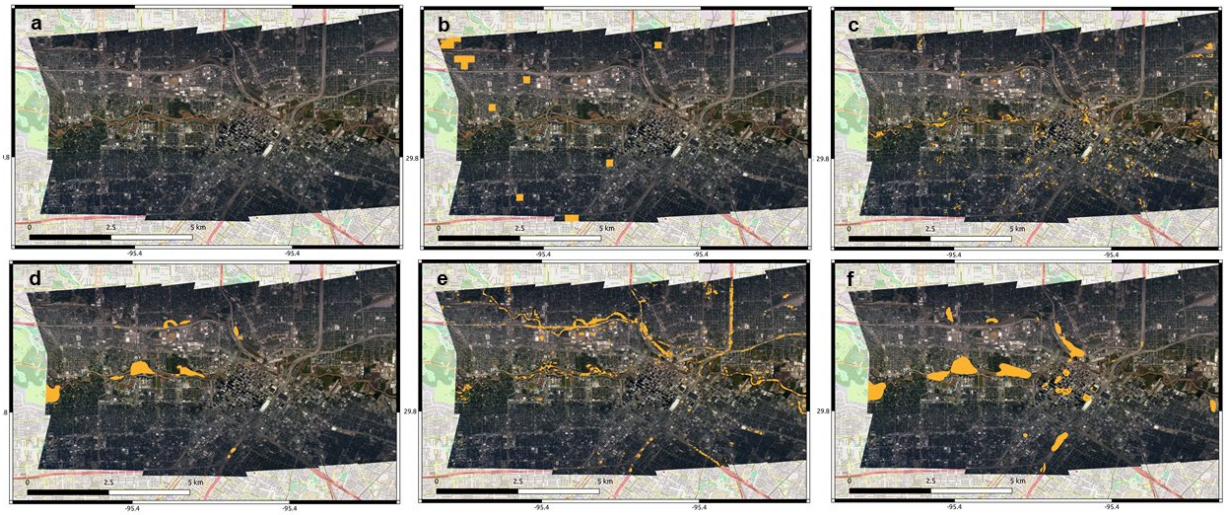


**Figure 2.2.6:** a) NOAA Remote Sensing Division airborne digital optical imagery of the Houston area acquired between August 27 and September 3, 2017, subregion 3, as shown in Figure 2.2.3; b) water pixels identified by MODIS data, 250 m pixel spacing, courtesy of the DFO (Brakenridge 2021); c) water pixels identified from NDWI analysis of Sentinel-2 data, 10 m pixel spacing; d) water pixels identified by the DeepLabv3+ analysis of SAR GRD data, August 29, 2017, 10 m pixel spacing; e) water pixels identified from thresholding analysis of the same SAR GRD data, 10 m pixel spacing; and f) water pixels identified by the classification analysis of the SAR GRD data, 10 m pixel spacing (Tiampo et al., 2021a).

The classification results in Figure 2.2.6 are primarily permanent water bodies and ponds which can clearly be seen in (d) and (f) but are largely missing in (b), (c) and (e). In this case the thresholding method shown in (e) almost entirely fails to classify any permanent water bodies as seen in (d) and (f) and largely has classified roadways as flooded. Thus (e) exhibits many false positives that the DeepLabv3+ analysis does not. Comparison between the different methods and the initial automatic histogram-based thresholding method shown in Figure 2.2.1 demonstrate the merit in the application of SAR GRD data in the identification of flood inundation. Further refinement is needed for all these methods, but initial results are promising.

## 3. DInSAR time series analysis to map the subsidence/uplift of the Ganges-Brahmaputra-Meghna Delta

### 3.1 Data for DInSAR

The ESA Sentinel-1A/B synthetic aperture radar (SAR) single look complex (SLC) imagery was selected for this region because of the short repeat pass time (6-to-12 days), high initial resolution of ~3 m x 22 m in range and azimuth respectively with high final spatial resolution of ~100 m and data extending from March 2017 to June 2021. The wavelength of Sentinel-1A/B SAR is $\lambda = 5.6\ cm$, which generally results in a greater loss of coherence in vegetated areas compared to an L-band ($\lambda = 23.6\ cm$) SAR satellite, such as ALOS1, the Japanese satellite carrying a SAR sensor. However, given short repeat time of 6 to 12 days, we expect reliable results. Sentinel-1A/B SAR SLC images from five ascending and five descending frames for the GBM were obtained from the ASF (https://search.asf.alaska.edu/) , the frames are shown in Figure 3.1.1.

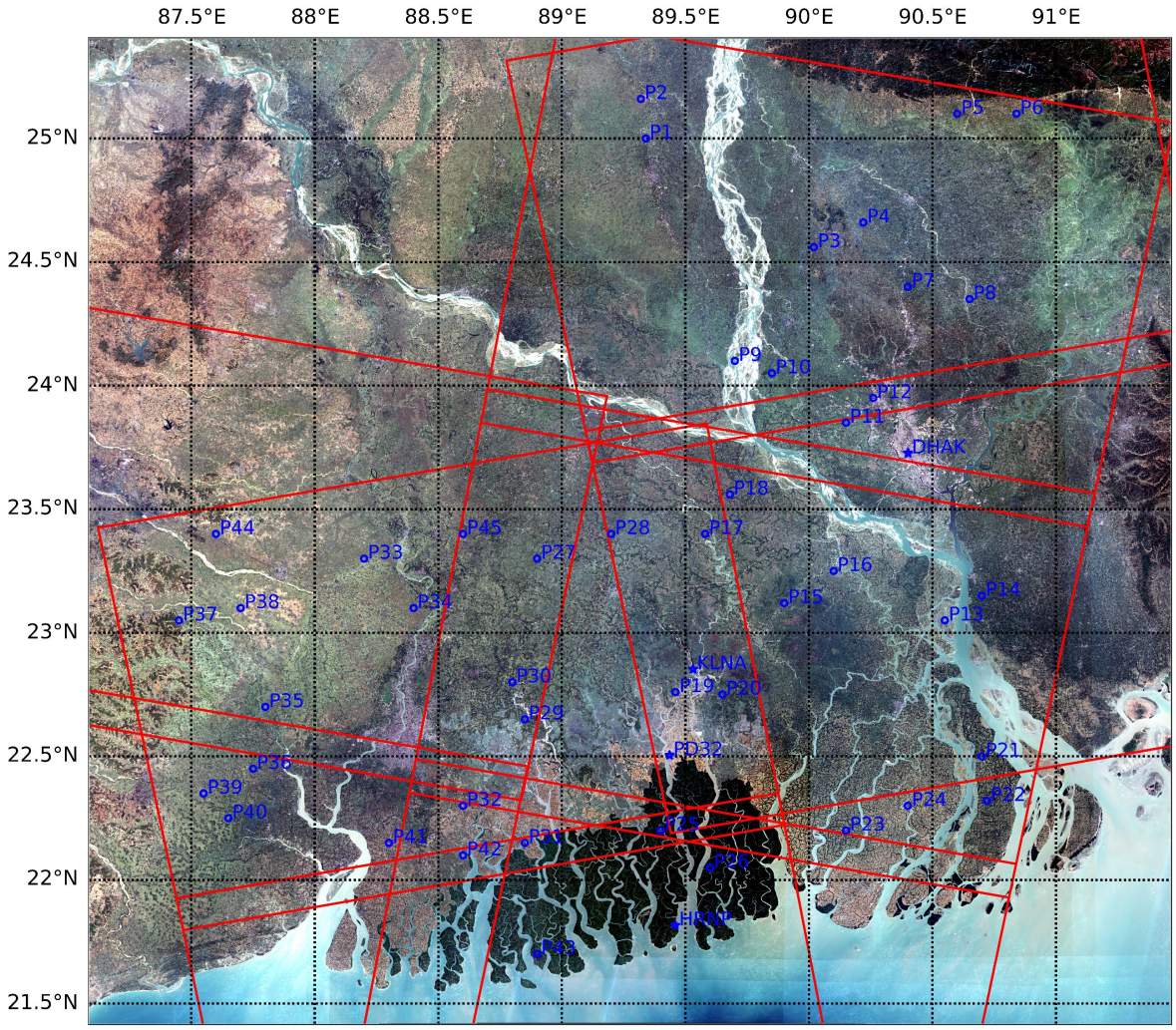


**Figure 3.1.1:** Base map showing generated time series points as P, in blue and, GPS sites used in this study. Red frames are the approximate boundaries of SAR frames used in this study.

These frames include one ascending orbit with three frames, Path 114, Frame 65, 71 and 76, and another with two frames, Path 12, Frame 64 and 69. Descending orbits include Path 150, Frames 510, 515 and 520, and Path 48 Frames 514 and 519. The dataset from these 10 frames includes approximately 650 ascending and 550 descending SLC's spanning March 2017 to June 2021 (see Supplemental Materials Data Granules in the Appendix for all data that was used in this study). The raw SLC data used to form the interferograms was processed using Sentinel-1 toolbox

(st1bx), which is freely available from the ESA Sentinel Application Platform (SNAP) v8.0.0, http://step.esa.int.

GPS station data used in this study was provided by Dr. Michael Steckler (Lamont Research Professor, Marine Geology and Geophysics, Lamont-Doherty Earth Observatory (LDEO), The Earth Institute). These data and methods of GPS data collection are described in detail in Steckler et al., 2010, 2013 and 2022. Available GPS data is used in referencing the Time Series described in methods below and are used to compare GPS derived deformation rates to DInSAR-multidimensional small baseline subset (MSBAS) derived deformation rates (Samsonov et al., 2012). We expect reasonable agreement between DInSAR-MSBAS derived deformation rates and GPS derived deformation rates. Differences between MSBAS derived and GPS derived rates can be caused by a variety of different factors, such as different error sources, processing, resolution (spatial map-based data versus point-based GPS data. These different data types are potentially indicators of different deformation processes as well. For example, a continuous GPS station mounted on a stable building will not measure sediment aggradation, whereas DInSAR may have the potential to measure this as deformation, given reasonable coherence is maintained. These potential differences between MSBAS derived and GPS derived deformation rates will be described in greater detail in the discussions section of this study.

### 3.2 DInSAR Time Series Methods Overview

To extract deformation rates from our Sentinel-1A/B SAR data we need to apply various processing techniques common to DInSAR. Our data consists of SLC images which contain phase information used in deriving an interferogram. We combine two SLC images from either an ascending or descending orbit which overlap and are generally collected close in time, typically 12 or 24 days, to form an ascending or descending interferogram. DInSAR is the

extraction of the phase difference in the line-of-site direction (LOS) which is the change in distance between the ground and the satellite at the time of the initial SAR orbit pass and the secondary SAR orbit pass, for a location. These results are only reliable given multiple processing steps including precisely aligning the two SAR images, creation of the interferogram, or phase differenced image, and then correcting for any SAR image collection artifacts, including topographic and atmospheric effects. Topographic issues are corrected using the Shuttle Radar Topography Mission (SRTM) 30 m Digital Elevation Model (DEM) of the region and atmospheric errors are corrected using the Generic Atmospheric Correction for InSAR (GACOS) (Yu et al., 2018). In this study we use 12 or 24 days to form an interferogram because any longer periods result in a high loss of coherence between repeat pass images. Because lower coherence pixels typically produce less reliable results, we remove pixels below a chosen coherence threshold and apply a Goldstein phase filter (Goldstein et al., 1998) to improve the reliability of the results. Processing details are provided below.

After the creation of reliable interferograms, we implement the MSBAS software to create time series and deformation maps for each pixel (Samsonov et al., 2012). Deformation maps are relative to whenever the first SAR image was collected. We benchmark particular deformation maps to GPS data available in the region to provide an absolute reference frame. That GPS benchmarking allows us to combine all the time series results generated by MSBAS into a singular deformation map for the entire GBM.

### 3.3 DInSAR processing

In this study we will be using Sentinel-1A SLC data. The various potential acquisition modes of Sentinel-1A/B are shown in Figure 3.3.1. We are interested in Interferometric Wide Swath Mode (IW) to apply DInSAR methods. Sentinel-1A/B uses a method of data collection

called Terrain Observation with Progressive Scans SAR (TOPSAR) meant to replace the conventional ScanSAR mode of data collection. This results in the data being collected in three swaths spanning approximately 250 km as shown in Figure 3.3.1 with each Swath consists of nine overlapping bursts.

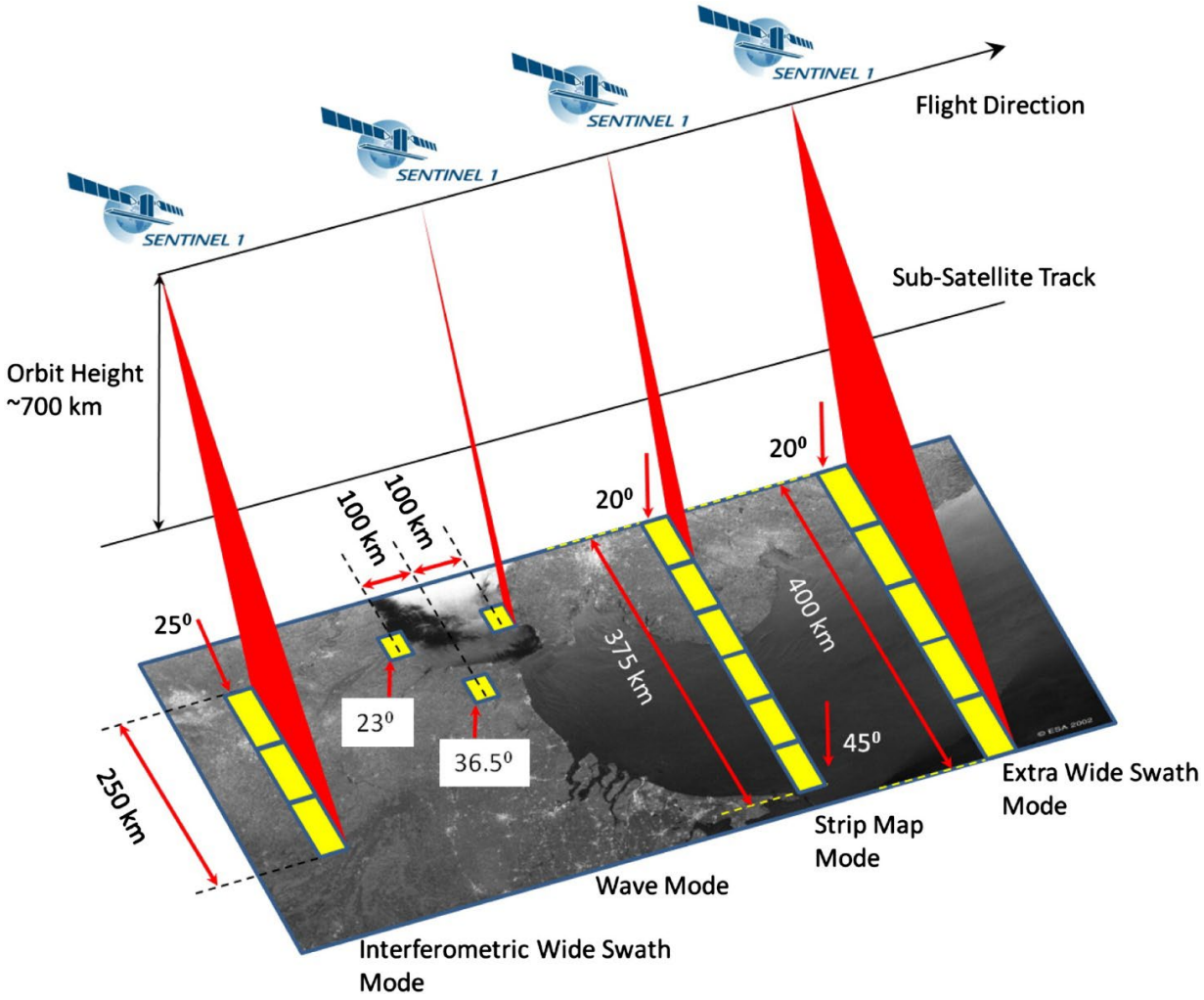


**Figure 3.3.1:** Sentinel-1A/B acquisition mode. Figure from (https://sentinels.copernicus.eu/web/sentinel/missions/sentinel-1/instrument-payload)

The basic principle for interferogram formation is based on repeat pass interferometry and the ability to measure a difference in the phase from the initial (reference) and secondary passes of the SAR satellite. The basic set up is shown in Figure 3.3.2, $\emptyset_M$ is the phase measured at the reference time $t_1$ and $\emptyset_S$ is the phase measured at the secondary time $t_2$.

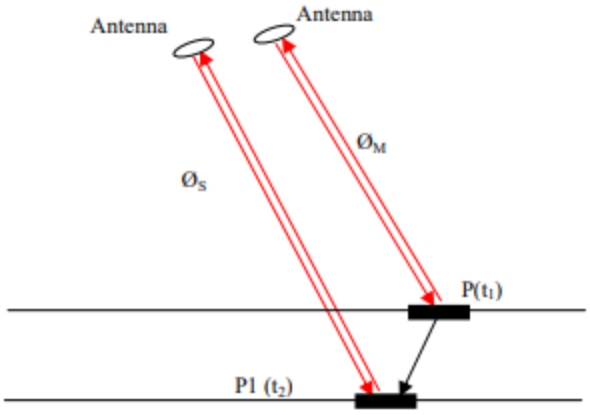


**Figure 3.3.2:** Basic set up of repeat pass SAR and the application to DInSAR (Sheng et al., 2012).

This results in a phase difference which is given in equation 3.1 (Gabriel et al., 1989).

$$\Delta\phi = \frac{4\pi}{\lambda}\big(\rho(t_2) - \rho(t_1)\big) = \frac{4\pi}{\lambda}\Delta\rho_d \tag{3.1}$$

With DInSAR we are essentially interested in $\Delta\rho_d = \rho(t_2) - \rho(t_1)$ as this is the displacement which occurred between $t_1$ and $t_2$ which is related to the phase difference $\Delta\phi$ which is measured by the repeat pass SAR as shown in Figure 3.3.2. This is complicated by several factors, as $\Delta\phi$ contains phase information not only related to the potential deformation between $t_1$ and $t_2$. Thus, we need to be able to correct for these additional contributions to the phase difference $\Delta\phi$ to be able to extract meaningful results related to actual deformation. We can more generally write the phase difference which contains all phase contribution terms as given in equation 3.2.

$$\Delta\phi = \phi_{deformation} + \phi_{curve} + \phi_{topography} + \phi_{atmosphere} + \phi_{orbit} + \phi_{noise} \tag{3.2}$$

It is possible to remove the additional phase terms besides the $\phi_{noise}$ as this is generally random. To improve the signal to noise ratio (SNR) both multilooking and the Goldstein phase filter is applied which will help remove phase contribution $\phi_{noise}$. Successful removal of the additional

phase terms will leave us with $\phi_{deformation}$ which is primarily what we are interested in with DInSAR as this allows us to estimate the deformation at a given pixel.

The basic workflow used in this study is shown in Figure 3.3.4. DInSAR processing steps were completed using the sentinel application platform (SNAP) software.

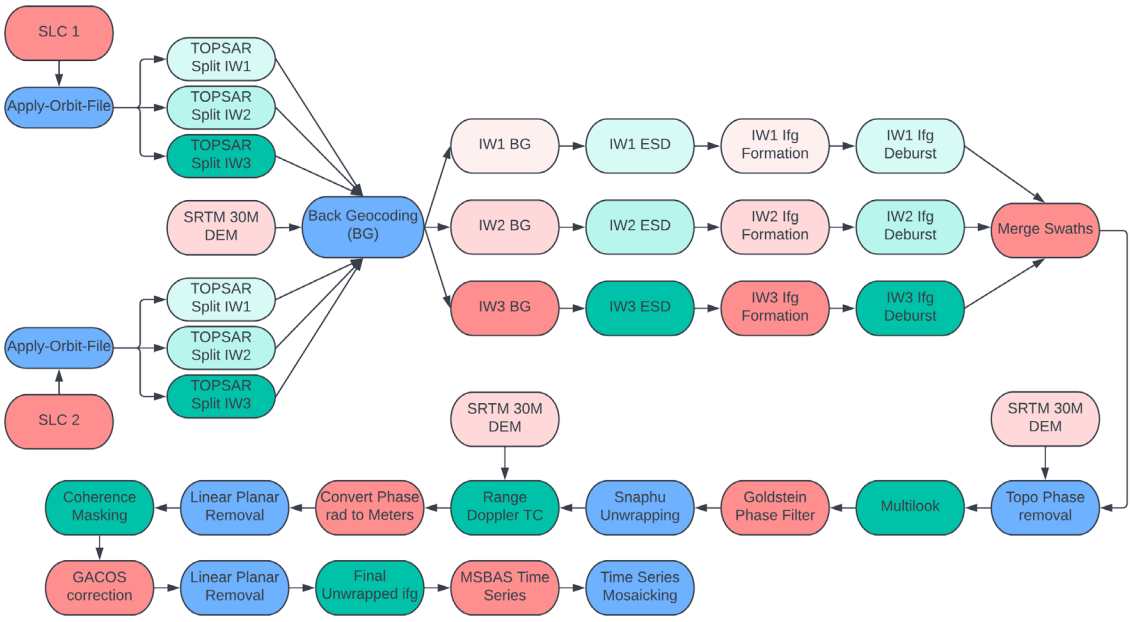


**Figure 2.3.3:** Workflow for creation of interferograms for time series mosaicking. Using the Sentinel1 toolbox developed by ESA.

Sentinel-1A/B typically has precise orbit files available within three weeks of data acquisition. Thus, we can generally accurately correct for and remove phase contributions due to the orbital parameters of Sentinel-1A at each acquisition time and correct for $\phi_{orbit}$ in equation 3.2. This is the first step in the processing as shown in Figure 3.3.3 which is completed using SNAP. We then need to precisely align pixel by pixel SLC 1 and SLC 2 as shown in Figure 3.3.3. This is accomplished by applying the back geocoding (BG) algorithm in SNAP to each swath of SLC 1

and SLC 2. This precise alignment is further refined on a fractional pixel basis using the enhanced spectral diversity (ESD) method implemented in SNAP.

Sentinel-1A/B SLC data consists of complex numbers at each pixel, consisting of both phase and amplitude terms which can be written as equation 3.3 (Sandwell et al., 2011).

$$C(x) = A(x)e^{i\phi(x)} \tag{3.3}$$

As seen in equation 3.1 we want to determine a phase difference between the reference SLC 1 and secondary SLC 2. This can be determined by taking the complex conjugate of the reference SLC 1 and simply multiplying them together as shown in equation 3.4 (Sandwell et al., 2011).

$$C_2 C_1^* = A_1 A_2 e^{i(\phi_2 - \phi_1)} = R(x) + il(x) \tag{3.4}$$

Where $C_1^*$ is the complex conjugate of the reference SLC. The phase difference is then simply extracted as in equation 3.5 (Sandwell et al., 2011).

$$\Delta\phi = (\phi_2 - \phi_1) = \tan^{-1}\left(\frac{I}{R}\right) \tag{3.5}$$

Equation 3.5 includes all terms of equation 3.2 besides the $\phi_{orbit}$ phase term as this was removed in the first step of our processing shown in Figure 3.3.3. This process results in the generation of an interferogram as shown in Figure 3.3.3 and is accomplished using SNAP. The interferogram generation step also accounts for the $\phi_{curve}$ phase term in equation 3.2. To remove the earths curvature from equation 3.2 a 6$^{th}$ degree polynomial is fit with 601 points with SNAP.

Because the data is collected in swaths which consists of nine bursts (Figure 3.3.1) we will have distinct overlapping areas within each interferogram shown in Figure 3.3.4.

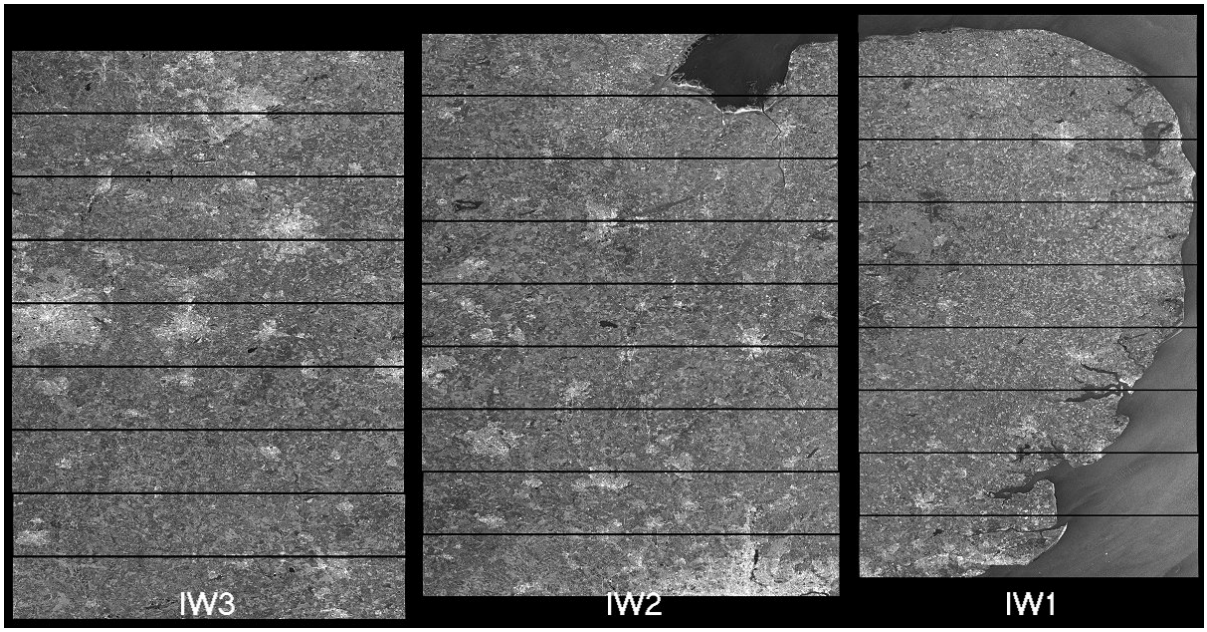


**Figure 3.3.4:** Sentinel-1A/B TOPSAR collection mode results in three swaths and nine overlapping bursts (https://sentinels.copernicus.eu/web/sentinel/user-guides/sentinel-1-sar/acquisition-modes/interferometric-wide-swath).

Thus, to create a seamless interferogram, which contains nine bursts of overlapping data per swath, we need to apply debursting to the interferogram using the overlapping data from the bursts to identify the correct parameters to use which is implemented in SNAP. This results in a seamless interferogram with all bursts combined. We can then merge the three individual interferogram swaths to create a singular interferogram.

Sentinel-1A data is collected every 12 days at the same location on Earth. Thus, we have a repeat interval of 12 days between each Sentinel-1A SLC. As shown in equation 3.1 our phase difference is based on the using repeat pass Sentinel-1A SLC data at two distinct time points $t_1$ and $t_2$ to generate interferograms shown in equation 3.5. Thus, if we have another Sentinel-1A SLC at $t_3$, the repeat time of this SLC 3 would be 24 days from the first SLC 1. In this study we used a maximum 24 day repeat time to generate interferograms. Thus, for every SLC which is at $t_1$ there will potentially be two distinct SLCs at $t_2$ or? $t_3$ (SLC 2 and SLC 3) which we can use

to form interferograms as in equation 3.5, which would result in the formation of two interferograms using SLC 1 as the reference. The creation of an interferogram using SLC 1 as the reference and SLC 2 and SLC 3 as secondaries provides additional information related to potential deformation between $t_1$ and $t_3$. This is because when we use SLC 2 and the reference, we will form an interferogram between SLC 2 and SLC 3 as well. Thus, we will have the deformation at each time step between $t_1$ and $t_2$ and $t_2$ and $t_3$ as well as between $t_1$ and $t_3$ which essentially constrains the possible deformation that occurred within the 24 days repeat time. As discussed in the data section, we have approximately 1200 distinct Sentinel-1A SLC data, and thus using a maximum 24 day repeat time to results in approximately 2300 interferograms formed.

After merging the interferograms we still have several phase terms shown in equation 3.2 to remove. The topography phase term $\phi_{topography}$ is removed using the Shuttle Radar Topography Mission (SRTM) 1sec HGT dem at approximately 30-meter resolution (Farr et al., 2007). SAR SLC data typically displays a phenomenon known as speckle noise as shown in Figure 3.3.5. To correct for this and reduce the potential speckle noise, the interferograms are multilooked using 28 range and 7 azimuth looks, which results in an approximate interferogram pixel resolution of 100 meters.

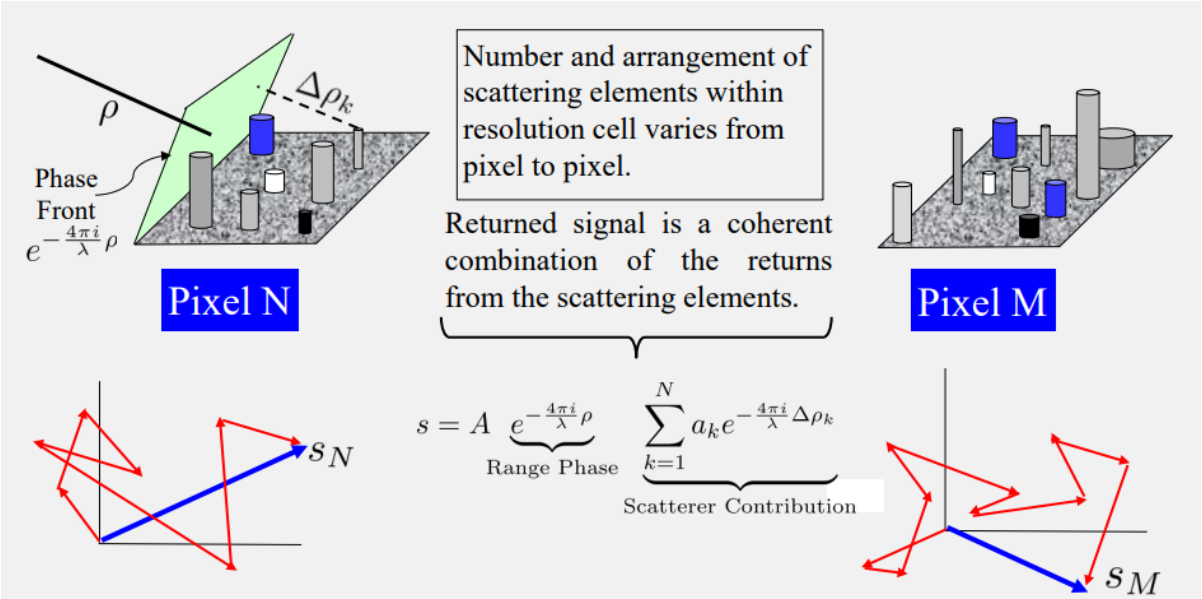


**Figure 3.3.5:** Displays various pixels with a variety of objects the SAR signal can bounce off and return coherently to the sensor (Rosen 2014). This type of coherent scattering results in speckle noise in SAR data.

A Goldstein phase filter (Goldstein et al., 1998) is then applied using the specific parameters of adaptive filter exponent of $\alpha = 1$, fast frequency transform (FFT) window size of 256 pixels, and a coherence threshold of 0.2 to only consider pixels with this coherence or greater in the Goldstein phase filter. Interferograms typically contain high speckle noise and decorrelation due to low coherence making the individual interferometric fringes difficult to distinguish. Thus, the Goldstein phase filter is a necessary step for interferometric processing of the GBM due to the overall lower coherence of this region. Applying this filter results in improving the ability to distinguish fringes and reduce overall noise and thus error. It is important to note that the Goldstein phase filter can introduce artifacts into the interferograms, i.e., it can potentially overcorrect the interferograms. The resulting filtered interferograms are input into the snaphu unwrapping program (Chen et al., 2002) (https://web.stanford.edu/group/radar/softwareandlinks/sw/snaphu/), resulting in the line-of-sight (LOS) phase unwrapped interferograms. To correct for topographical variations and the tilt of the

satellite sensor which can cause geometric distortions in the unwrapped interferograms the Range Doppler Terrain Correction (RTC) is applied to the final unwrapped interferogram using the SRTM 1 sec HGT DEM with SNAP (Small et al., 2008; Schreier et al., 1993). These potential topographic variations with potential geometric distortions are shown in Figure 3.3.6.

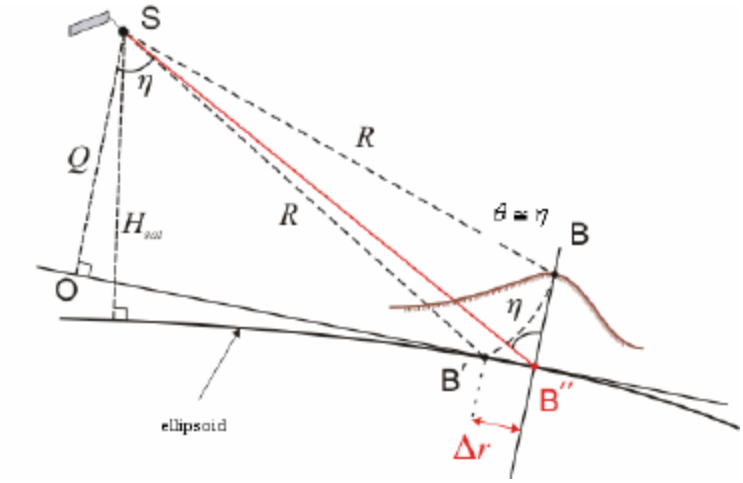


**Figure 3.3.6:** Potential geometric distortions corrected using the Range Doppler Terrain Correction and orthorectification algorithm (Cossu et al., 2007). Point B is imaged by the SAR sensor at B' although its true location is B''. Thus, we need to correct the location by $\Delta r$.

Additional potential geometric distortions which need to be corrected using the RTC are shown in Figure 3.3.7.

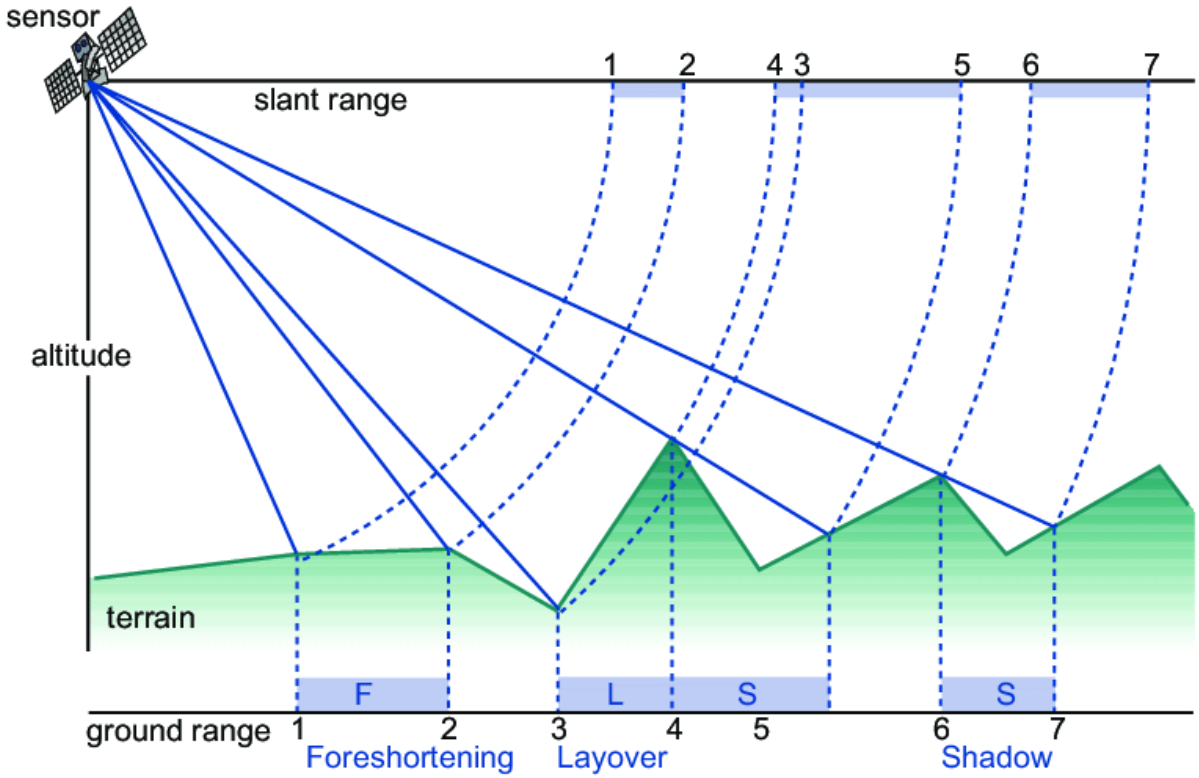


**Figure 3.3.7:** Displays additional potential geometric distortions due to the terrain, which needed to be corrected using the RTC (Tempfli et al., 2009).

Orthorectification also is applied to precisely geocode the final unwrapped interferogram (Small et al., 2008; Schreier et al., 1993). Finally, a simple linear planar model was fit (Appendix: Python Code Snippets 1) to the unwrapped interferogram to remove any linear ramps caused by either remaining orbital, topographic or earth curvature artifacts.

C-band SAR tends to have a low average coherence outside of cities in the Bangladesh region, due to widespread agricultural use, marshy and swampy terrain, and monsoonal landscape changes such as standing water on the landscape. An average coherence mask was created that includes both the overlapping ascending and descending datasets. Any pixel with an average coherence less than 0.15 was removed from the uncorrected unwrapped interferograms (see Figure 3.3.3), detailed below. Figure 3.3.8 displays the averaged coherence of the region.

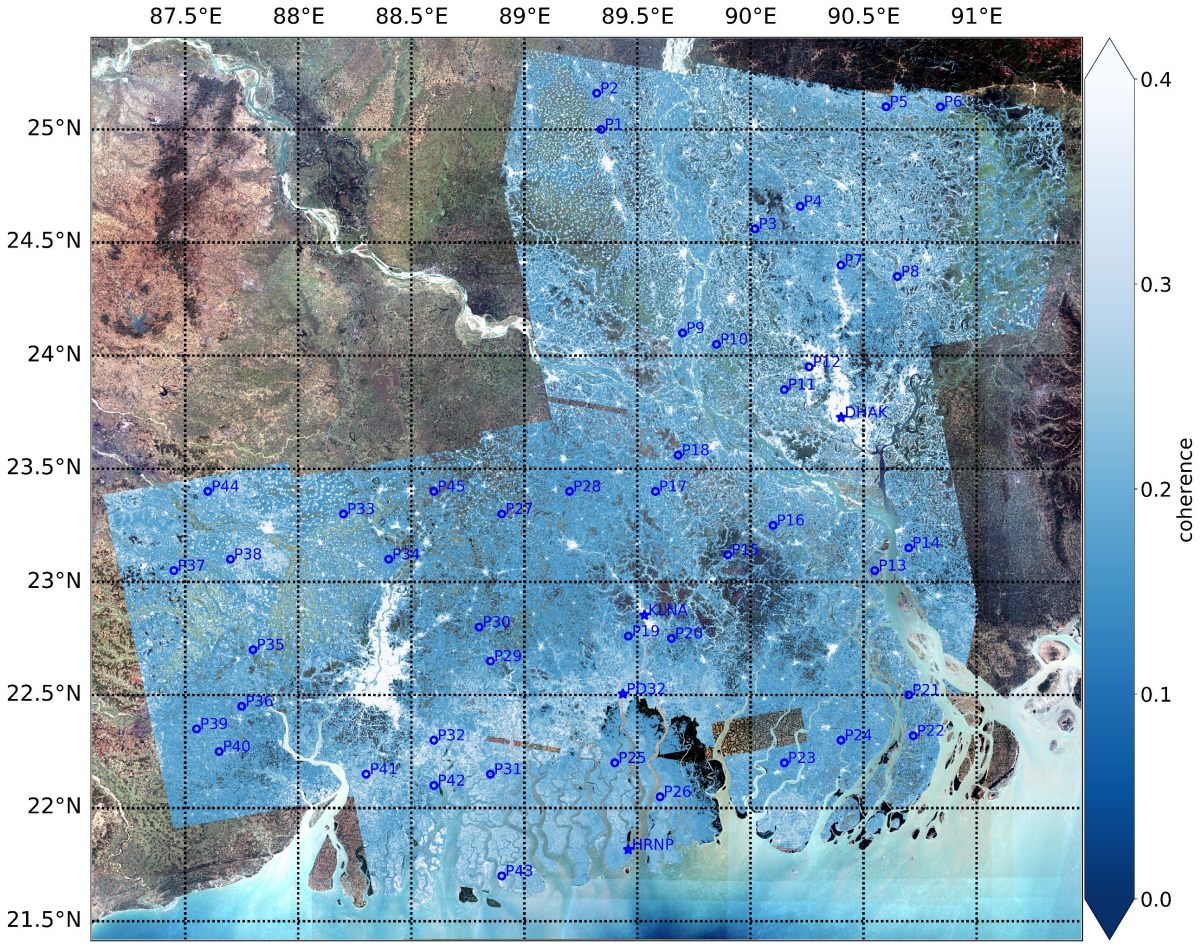


**Figure 3.3.8:** Mosaicked average coherence combing both ascending and descending data.

The next step shown in Figure 3.3.3 is to remove the atmospheric phase term shown in equation 3.2. Bangladesh has significant atmospheric signal from increased water vapor due to the monsoon season (June to October) which can cause systematic errors in estimating surface deformation. Thus, to extract meaningful results from DInSAR analysis in this region we need to apply an atmospheric correction to each unwrapped interferogram. To do so we need accurate atmospheric data which preferably has a high spatial resolution, ~100 meters, and availability every 12 days. This is made possible through the availability of the Generic Atmospheric Correction Online Service for InSAR (GACOS) (Yu et al., 2018). GACOS is freely available from http://www.gacos.net/, provides high temporal (6 hours) and spatial resolution (~90m)

correction model which can be applied to mitigate tropospheric error and topographic correlation in our analysis (Yu et al., 2018). GACOS correction includes the following datasets, within their Iterative Tropospheric Decomposition (ITD) model, High Resolution ECMWF weather model at 0.1-degree and 6-hour resolutions, SRTM DEM (90m, 60°S-60°N) and ASTER GDEM (90m, 60°N-83°N, 60°S-83°S) (Yu et al., 2018). We applied GACOS corrections to the unwrapped interferograms from the 10 sets of ascending and descending frames to correct for the $\phi_{atmosphere}$ phase term in equation 3.2. GACOS can introduce linear planar artifacts and thus a simple model was fit to the GACOS corrected unwrapped interferograms to remove any linear ramps introduced by the correction (Figure 3.3.3). An example of an unwrapped interferogram which was corrected with GACOS is shown in Figure 3.3.9.

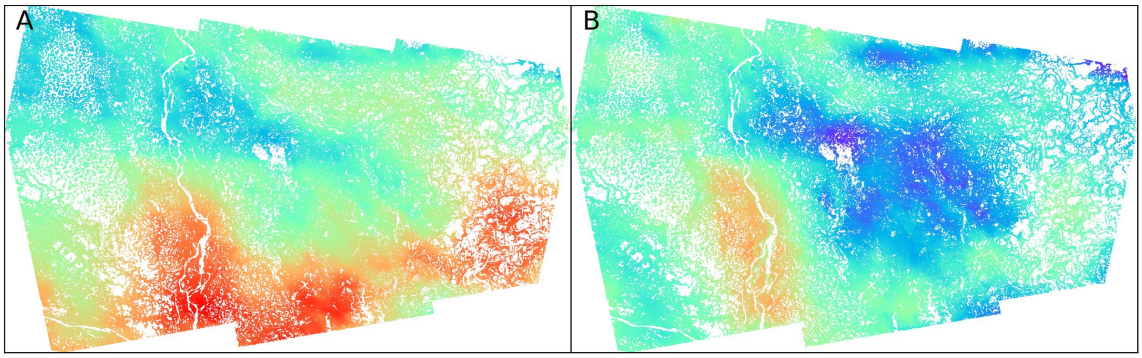


**Figure 3.3.9:** (A) Original uncorrected unwrapped interferogram in units of mm, with standard deviation of $\sigma_{uncorrected} = 32.77\ mm$, (B) GACOS corrected unwrapped interferogram, with standard deviation of $\sigma_{corrected} = 26.50\ mm$. Reds are higher deformation values and blues are lower deformation values, data is plotted on the same scale.

The goal of the GACOS correction is to reduce the standard deviation, as shown in Figure 3.3.9. This is because the atmospheric signal can cause SAR signal delays resulting in potentially larger derived vertical linear deformation rates than physically exist. This will in turn increase the standard deviation as we will have a larger spread of vertical linear deformation rates. Thus, if GACOS was successful or needed we should expect an improved or reduced standard deviation.

Ruyu et al., (2021) found for 1250 Sentinel-1 interferograms that GACOS reduced the interferometric phase standard deviation in 84.6% of the interferograms by an average of 36.4%.

At this point, we have corrected for the $\phi_{orbit}$, $\phi_{topography}$, $\phi_{atmosphere}$ and $\phi_{curve}$ and should be left with $\phi_{\text{deformation}}$ . The phase also has been converted from radians to meters, as shown in Figure 3.3.3. The final step includes removing any linear ramp introduced from the GACOS correction. This results in the final GACOS unwrapped corrected interferogram.

Figure 3.3.10 provides an example of coherence masking, a typical wrapped and unwrapped interferogram, as well the coherence mask applied for this specific image.

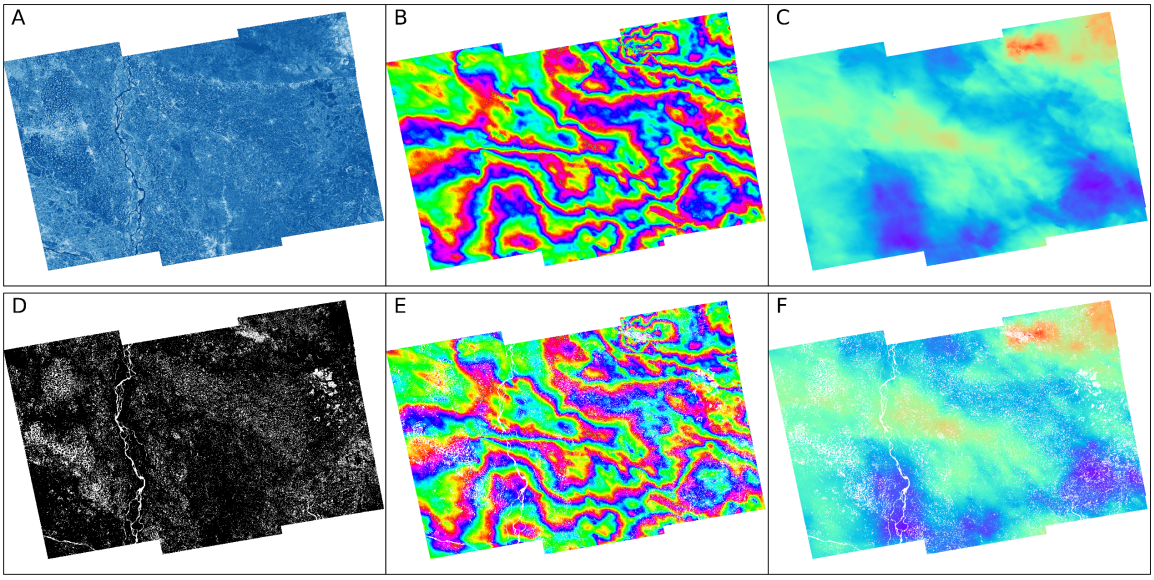


**Figure 3.3.10:** (A) A typical coherence image, with dark blues as the lowest coherence compared to white. (B) An unwrapped interferogram with no coherence mask applied, (C) The unwrapped interferogram with no mask applied. (D) The coherence mask computed from (A) where coherence less than 0.15 is excluded. White is excluded pixels and black are included pixels. (E) and (F) Wrapped and unwrapped interferograms, respectively, with (D) applied to (B) and (C).

The unwrapped interferograms potentially contain significant unwrapping errors which can cause erroneous time series and deformation map results. Three methods were tested to subset each unwrapped interferogram dataset from the ascending and descending frames to be used in

producing time series results and vertical linear deformation rates from the MSBAS analysis (Table 3.3.1).

| Time Series Name | Ascending Frame | Descending Frame | Exclusion Method |
|---|---|---|---|
| | | | |
| Time Series 1 (TS1) | Path 114 Frame 65 | Path 150 Frame 515 | Method 1 |
| Time Series 2 (TS2) | Path 114 Frame 65 | Path 150 Frame 520 | Method 2 |
| Time Series 3 (TS3) | Path 114 Frame 71 | Path 150 Frame 510 | Method 2 |
| Time Series 4 (TS4) | Path 114 Frame 71 | Path 150 Frame 515 | Method 3 |
| Time Series 5 (TS5) | Path 114 Frame 76 | Path 150 Frame 510 | Method 1 |
| Time Series 6 (TS6) | Path 12 Frame 64 | Path 150 Frame 520 | Method 3 |
| Time Series 7 (TS7) | Path 12 Frame 64 | Path 48 Frame 519 | Method 1 |
| Time Series 8 (TS8) | Path 12 Frame 69 | Path 150 Frame 515 | Method 3 |
| Time Series 9 (TS9) | Path 12 Frame 69 | Path 150 Frame 520 | Method 3 |
| Time Series 10 (TS10) | Path 12 Frame 69 | Path 48 Frame 514 | Method 2 |
| Time Series 11 (TS11) | Path 12 Frame 69 | Path 48 Frame 519 | Method 3 |

**Table 3.3.1:** Pairing of ascending and descending frames datasets used to create time series with MSBAS. Exclusion method is used to subset each time series data set both ascending and descending. This consists of method one, visual inspection, method, two standard deviation rule removal, and method three, no exclusion.

The first method includes manually viewing each unwrapped interferogram and determining visually if it meets data quality standards. The second method includes removing any unwrapped interferograms with a standard deviation outside the 95% interval estimate of the computed standard deviations for each unwrapped interferogram in the specific ascending or descending data set. The final method was to simply not exclude any unwrapped interferograms. Each of these three methods was tested for each of the eleven-time series (Table 3.3.1) and compared to determine the best method. Three distinct interferogram subsets were produced from this analysis and each input into MSBAS to derive three distinct vertical linear deformation rate maps. The histogram of each of the three vertical linear deformation rate maps was plotted with the corresponding standard deviation. We compared both these vertical linear deformation rate

maps visually with each other and the associated histograms to identify the optimal exclusion or non-exclusion method for that specific time series (Table 3.3.1). The MSBAS-derived vertical linear deformation rate map with the lowest standard deviation was chosen. The best subset method for each ascending and descending data set varied, as shown in Table 3.3.1.

### 3.4 Multidimensional Small Baseline Subset inversion

The MSBAS software was implemented to create time series and deformation rate maps (Samsonov et al., 2012). MSBAS has the capability to use overlapping data from ascending and descending tracks to derive two dimensional high spatial and temporal resolution deformation maps and time series. This results in denser time series and can extract vertical as well as horizontal (east-west) deformation. Our primary interest in this study is the vertical linear deformation rate, although horizontal east-west linear deformation rates are also derived from MSBAS. Analysis of the overlapping frames from both ascending and descending tracks resulted in eleven datasets (Table 3.3.1) of overlapped ascending and descending data. These eleven ascending and descending sets of unwrapped interferograms were used to create eleven distinct vertical linear deformation rate maps from MSBAS, overlapping only at common edges (Table 3.3.1). Because the ascending and descending frames only partially overlap, they were resampled and cropped to identical pixels.

The MSBAS inversion program was used to derive eleven distinct vertical linear deformation rate maps (Table 3.3.1). The parameter which stabilizes the inversion and thus the solution for the derived deformation maps include the Tikhonov regularization parameters $\lambda$ (Tikhonov et al., 1977). The L-curve method is used to determine the optimal regularization parameters $\lambda$ for each time series (Table 3.3.1). Eight values of $\lambda$ in the range 0.01-0.60 were tested for each time series. The resulting least squares or residual norm and solution norms were plotted to determine

the optimal trade off. Smaller solution norms will result in smaller deformation rates but larger residuals, and thus the need to determine an ideal trade-off value of $\lambda$. Here, for $\lambda = 0.108$ we have a large solution norm and a small residual norm, with $\lambda = 0.600$ we have a small solution norm and a large residual norm (Figure 3.4.1).

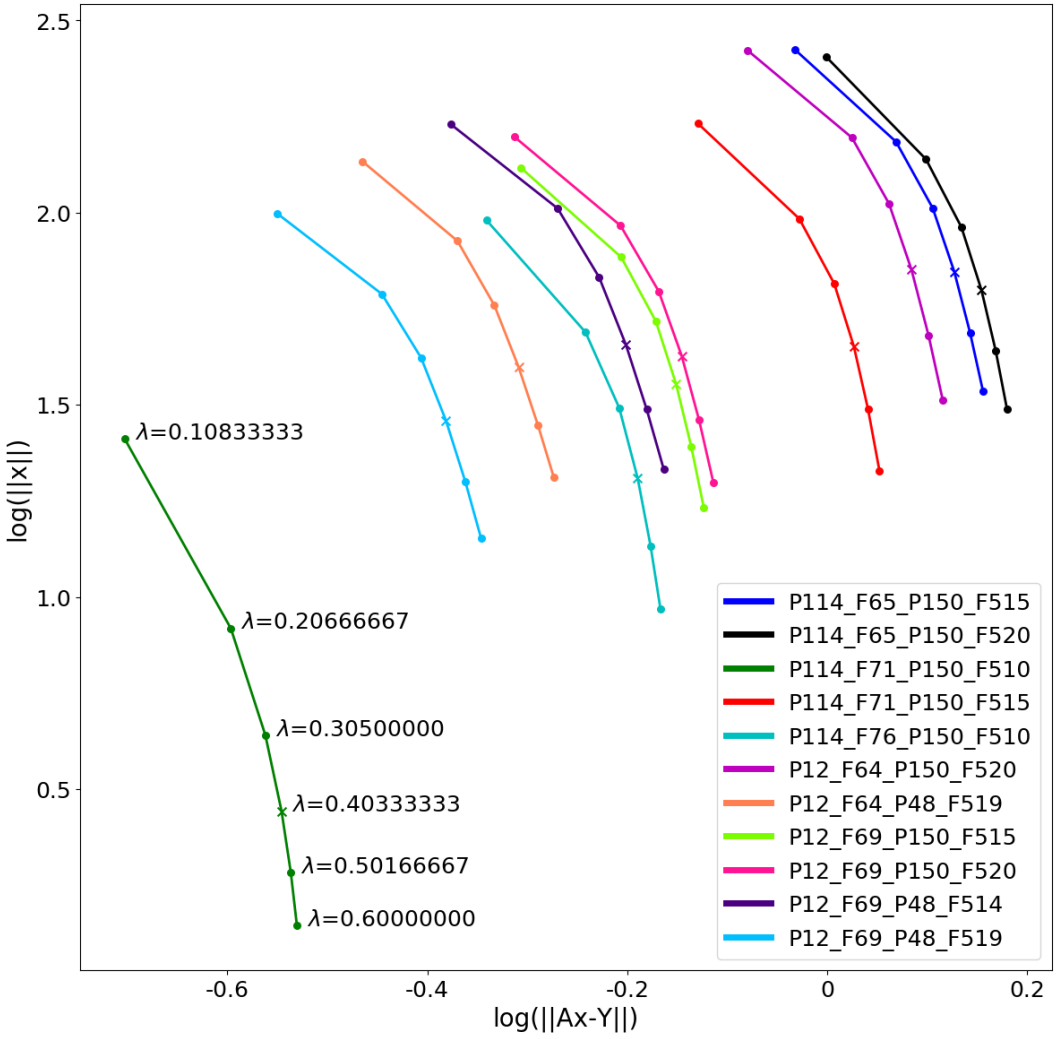


**Figure 3.4.1:** L-Curves for the MSBAS inversion of the 11-time series used in this study (Table 3.3.1). The x point on each L-curve is the value of lambda used in the Tikhonov regularization, λ = 0.403. $||x||$ is the solution norm and $||Ax - Y||$ is the residual norm.

Thus, we choose $\lambda = 0.403$ as the trade-off between both norms (Figure 3.4.1). This value of $\lambda$ has a solution and residual norm closest to the corner of the L-curve resulting in an optimal

trade-off between the solution norm and residual norm. The values of all eleven L-curves including lambda, residual norms and solution norms are shown in Figure 3.4.1.

The goal of Tikhonov regularization is to stabilize the inversion. Thus, we need to choose several values of the regularization parameter $\lambda$ and determine if the solution stabilizes. Then we can choose the optimal value of $\lambda$ as a trade off between solution norm and residual norm as shown in Figure 3.4.1. To identify if the solution has stabilized, we can plot various solutions and compare Figure 3.4.2. In Figure 3.4.2, four distinct solutions to the MSBAS inversion have been plotted. We see no visual differences and thus the solution is stable at this point, with only minor differences. This can be further analyzed as shown in Figure 3.4.3 with basic statistics. We see there are slight variations in the means as well as the histograms, but it is very small with a mean variation of about 4 mm/yr.

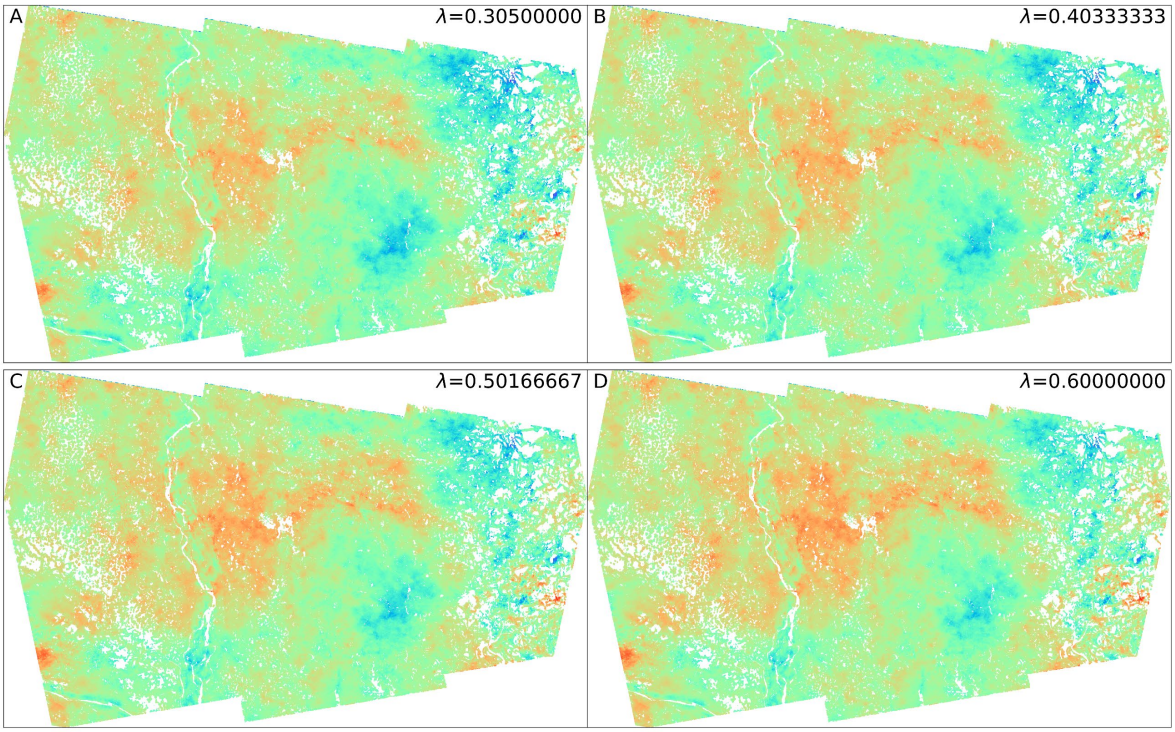


**Figure 3.4.2:** MSBAS-derived vertical linear deformation rates for a selection of Tikhonov regularization parameters $\lambda$.

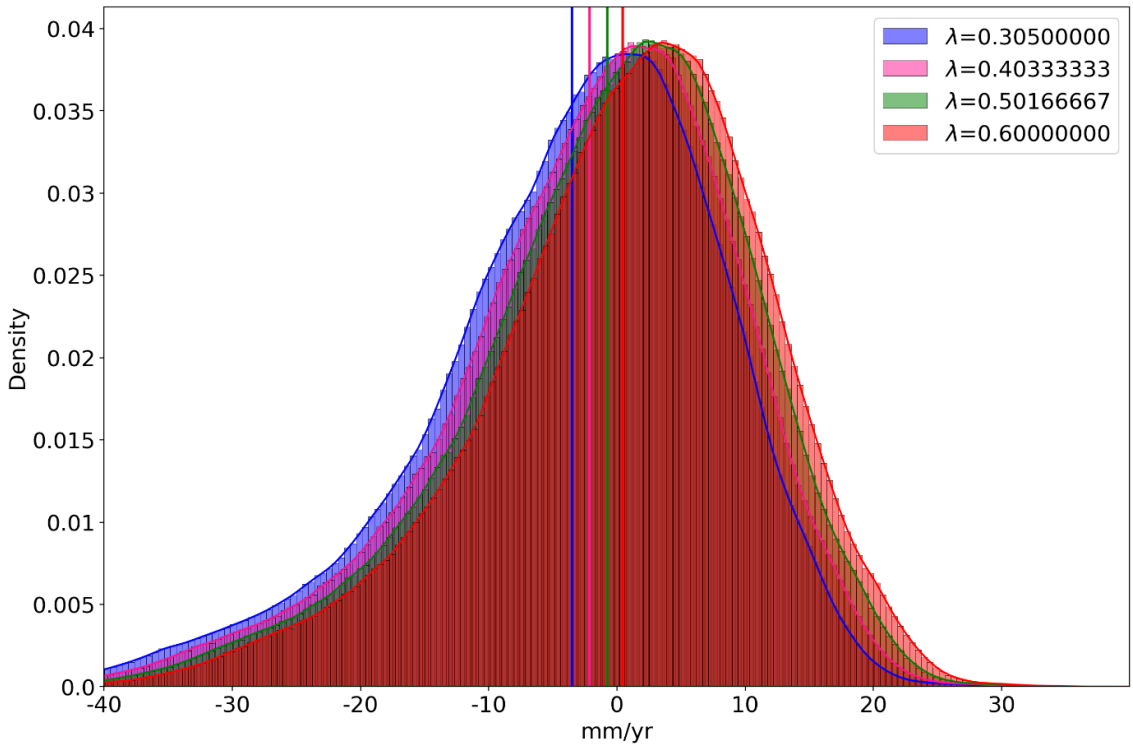


**Figure 3.4.3:** Histograms of the MSBAS derived linear rates shown in Figure 3.4.2. The vertical lines are the individual means of each inversion.

### 3.5 Time Series Mosaicking

Because unwrapped interferograms provide relative deformation over the acquisition time period, to compare the deformation calculated using DInSAR with MSBAS we need to determine either a stable point in our unwrapped interferograms or have available GPS data which can be used as an absolute point of reference. Here, we used available GPS data to derive an absolute reference frame, as currently there are no known stable points in Bangladesh that can be used as a fixed reference. The GPS station, DHAK, was employed as the primary reference point in MSBAS to calibrate the interferograms in time series 3 (TS3, Table 3.3.1), using a 9x9 pixel average resulting in an approximately one km square reference pixel centered at DHAK. Figure 3.4.4 displays the spatial location of the time series in Table 3.3.1.

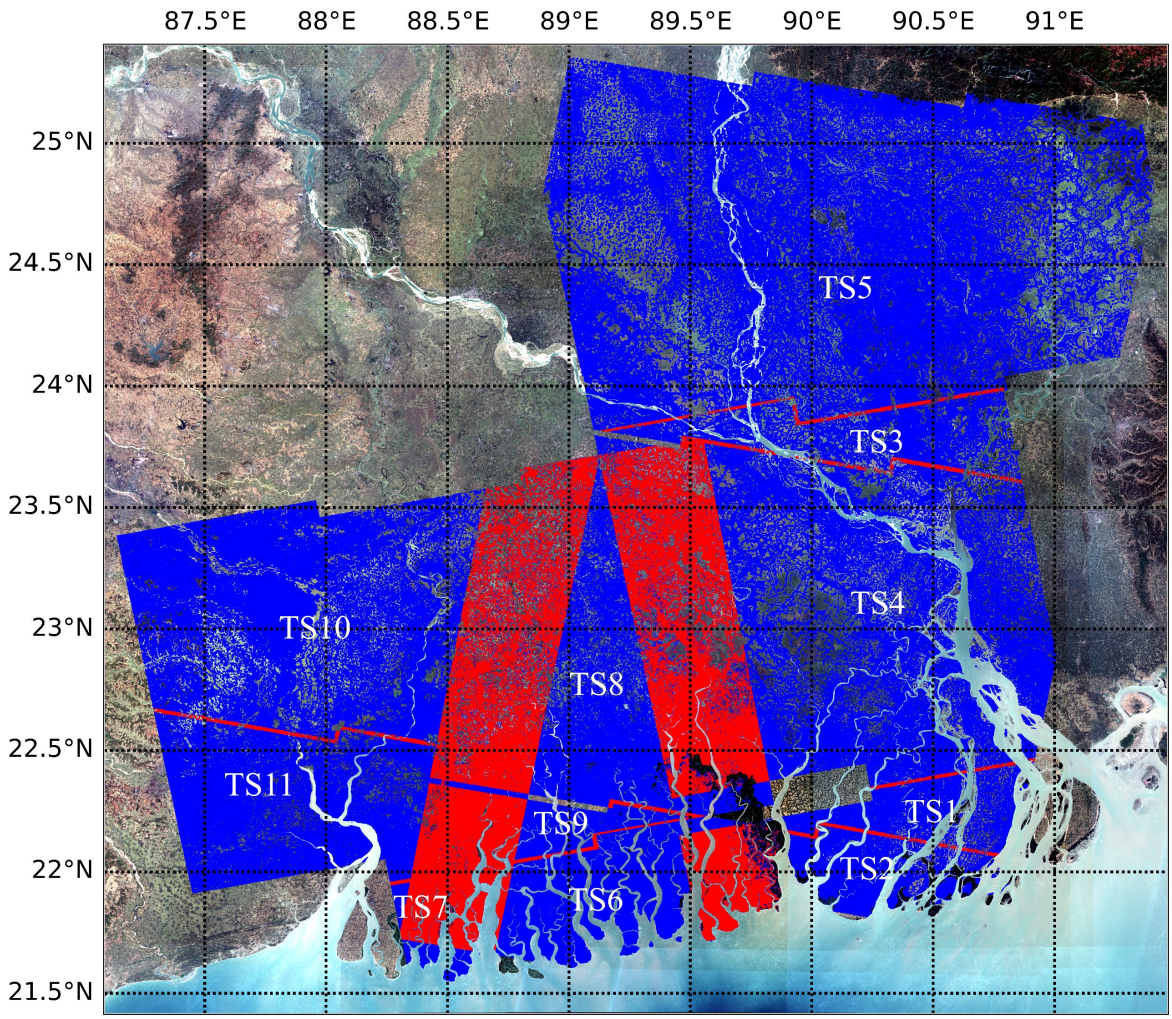


**Figure 3.4.4:** Blue pixels are location of time series, TS1-TS11 is shown. Red pixels represent the locations of overlapping pixels between the time series.

DHAK was used as the reference point in the MSBAS inversion for TS3, and thus each unwrapped interferogram in this inversion was referenced to DHAK. This is accomplished by subtracting the pixel value of the unwrapped interferogram at DHAK for each unwrapped interferogram in the inversion, effectively setting this point in TS3 to 0 before referencing it to the DHAK GPS-derived vertical linear rate. Because DHAK is a GPS station with approximately 20 years of continuous data, its estimated linear subsidence rate of 10.27 mm/yr was used as an absolute value to correct the resulting MSBAS-derived vertical linear deformation rate map. We use the vertical linear rate of motion at the DHAK GPS station to correct the MSBAS-derived

vertical linear deformation rate map and add the value of the DHAK GPS-derived vertical linear subsidence rate of 10.27 mm/yr to TS3 to estimate absolute rates.

The remaining ten MSBAS-derived vertical linear deformation rate maps were given no reference point when running MSBAS due to the lack of long-term GPS stations overlapping with suitable pixels or known stable points. Thus, the absolute MSBAS-derived vertical linear deformation rate TS3 is used to determine the appropriate reference value to correct for each of the time series TS2, TS4-TS11 (Table 3.3.1). This can be done because TS3 overlaps with several other time series, and those time series also overlap with the neighboring time series deformation maps, allowing us to determine the correct reference value for each time series and estimate absolute vertical linear deformation rates over the entire region.

To reference TS3 to the overlapping time series, we assume the vertical linear deformation rates at each overlapping pixel should be the same because they were both processed with the same methodology, parameters, and time frame and with similar error sources. We designate the pixels from TS3 $X_n$ and the pixels from the overlapping time series $Y_n$, i.e. $X_1$and $Y_1$ overlap between the two time series. We need to determine the correct value to add to the overlapping time series pixels to reconcile $Y_1$ with the reference pixel $X_1$ However, given that we have potentially thousands of overlapping pixels from TS3 and each overlapping time series, we cannot simply add that to the entire overlapping pixels to reference it to TS3. Because of the inherent noise between individual pixels in DInSAR time series, the overlapping pixels could differ significantly. Instead of equating individual pixels between the overlapping time series and TS3, we want to determine the best reference value to add to the overlapping time series which minimizes the overall difference between the overlapping region of TS3 and each overlapping time series. In other words, if there are two sets of pixels, one from TS3 and another from the

overlapping time series ,such that when we difference these two sets $X_1, \cdots, X_n$ from $Y_1, \cdots, Y_n$, we will minimize this difference by adding a specific reference value to the $Y_1, \cdots, Y_n$ values to produce the set $Y_1', \cdots, Y_n'$ which is $Y_1' = Y_1 + r$ where $r$ is the best reference value and $n$ is the number of pixels in the overlapping region. Thus, we want to minimize

$$S(r) = (X_1 - (Y_1 + r))^2 + \cdots + \left(X_n - (Y_n + r)\right)^2 = \sum_{i=1}^{n} (X_i - Y_i')^2 \qquad (3.5.1)$$

where $r$ is the best reference value or the value that minimizes Equation 3.5.1. It is important to note that the values of $r$ are constrained to be within the data set of the overlapped differenced pixels, i.e. when you subtract all the $Y_n$ from the $X_n$ this will produce the differenced data set and one of these values must be the best value of $r$. Thus, we simply subtract the pixel values of the overlapping pixels $Y_n$ from $X_n$ which creates a set of pixel differences. We then determine the maximum and minimum difference from this differenced set of pixels and create a vector of 5000 evenly spaced values between the minimum and maximum difference. Each of these 5000 values is a potential value of $r$ that minimizes Equation 3.5.1. We test every potential value of $r$ and determine the best value. Given that our overlapping region has overlapping coherence, we add a further constraint to Equation 3.5.1. We assume that pixels with lower coherence contribute less to the sum $S(r)$, while pixels with higher coherence contribute more to $S(r)$. Under this assumption, we are choosing the best value of $r$ to minimize $S(r)$, given that pixels with higher coherence are more reliable than pixels with lower coherence. We therefore modify Equation 3.5.1 to include overlapping coherence which we simply average from the two overlapping time series. This is given as

$$S_c(r) = c_1^2(X_1 - Y_1 + r)^2 + \cdots + c_n^2(X_n - Y_n + r)^2 = \sum_{i=1}^{n} c_i^2(X_i - Y_i')^2 \quad (3.5.2)$$

where $c_n$ is the average coherence value at the given pixel $n$. The value of $c_n$is given in equation 3.5.3.

$$c_n = \frac{\sum_{j=1}^{m} c_j(x_n, y_n)}{m} \quad (3.5.3)$$

where $c_j(x_n, y_n)$ is the coherence pixel value of coherence image number $j$ at location $(x_n, y_n)$, and $m$ is the total number of coherence images within the entire set of ascending and descending coherence images.

The best reference value $r$ is then determined using Equation 3.5.2 and we add this to the values for the pixels from the time series which overlaps with the absolute time series TS3, resulting in a new, absolute referenced time series. This new time series overlaps with its neighboring time series as well (Figure 3.3.4). We apply the same methodology as above to the new overlapping times series, using the time series we referenced to TS3 as the new absolute, reference time series. We then apply this out from overlapping time series to time series until all eleven of the time series or vertical linear deformation rate maps are absolute referenced back to TS3. Finally, we create an overall grid based on the total extent of the eleven-time series (Table 3.3.1) and place the complete, referenced vertical linear deformation rate map on this grid.

### 3.6 Normalized Differenced Vegetation Index

Regions in Bangladesh are potentially heavily vegetated or under intensive agriculture which can potentially cause lower coherence within DInSAR processing. The Sundarbans mangrove forests are an example of a heavily vegetated area which can potentially cause

DInSAR time series results to be unreliable. Specific wavelengths of SAR also will display difference backscatter characteristics with the same surface type shown in Figure 3.6.1.

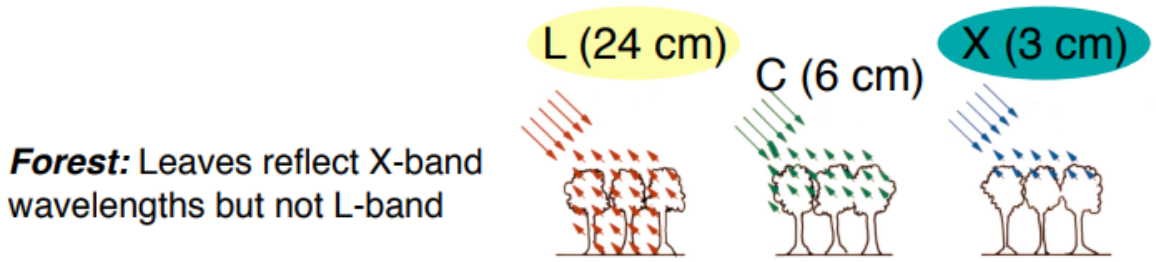


**Figure 3.6.1:** Displays different backscatter characteristics for difference SAR wavelengths, C-Band SAR is used in this study (Rosen 2014).

Figure 3.6.1 just shows a simple example of the backscatter characteristics of SAR signal and a forest. We are using Sentinel-1A/B C-band SAR in this study which will have some backscatter from a forest, whereas X-band SAR will have the most. Thus, we might expect to be able to retrieve SAR backscatter from the Sundarbans for example. To ensure that there is limited heavy decorrelation due to vegetation we compute the Normalized Differenced Vegetation Index and compare it to the MSBAS-derived vertical linear deformation rate mosaicked map (section 3.5) and the averaged coherence (Equation 3.5.3) of the region. Given there is not significant decorrelation due to vegetation, we should see limited correlation between the coherence and the NDVI images. We use Sentinel-2 optical data in this study to compute the NDVI given by Equation 3.6.1.

$$NDVI = \frac{NIR - RED}{NIR + RED} = \frac{B_8 - B_4}{B_8 + B_4} \tag{3.6.1}$$

Sentinel-2 data from March 2017 to June 2021 was used to compute the NDVI with Google Earth Engine (GEE). The NDVI was computed for each date and then the mean was taken of these NDVI calculations. Thus, we get a single averaged NDVI image over the approximate four-year period of this study for comparison.

# 4. DInSAR Time Series Results

## 4.1 Linear deformation rate map

The final mosaicked vertical linear deformation rate map as described in section 3.5 is shown in Figure 4.1.1.

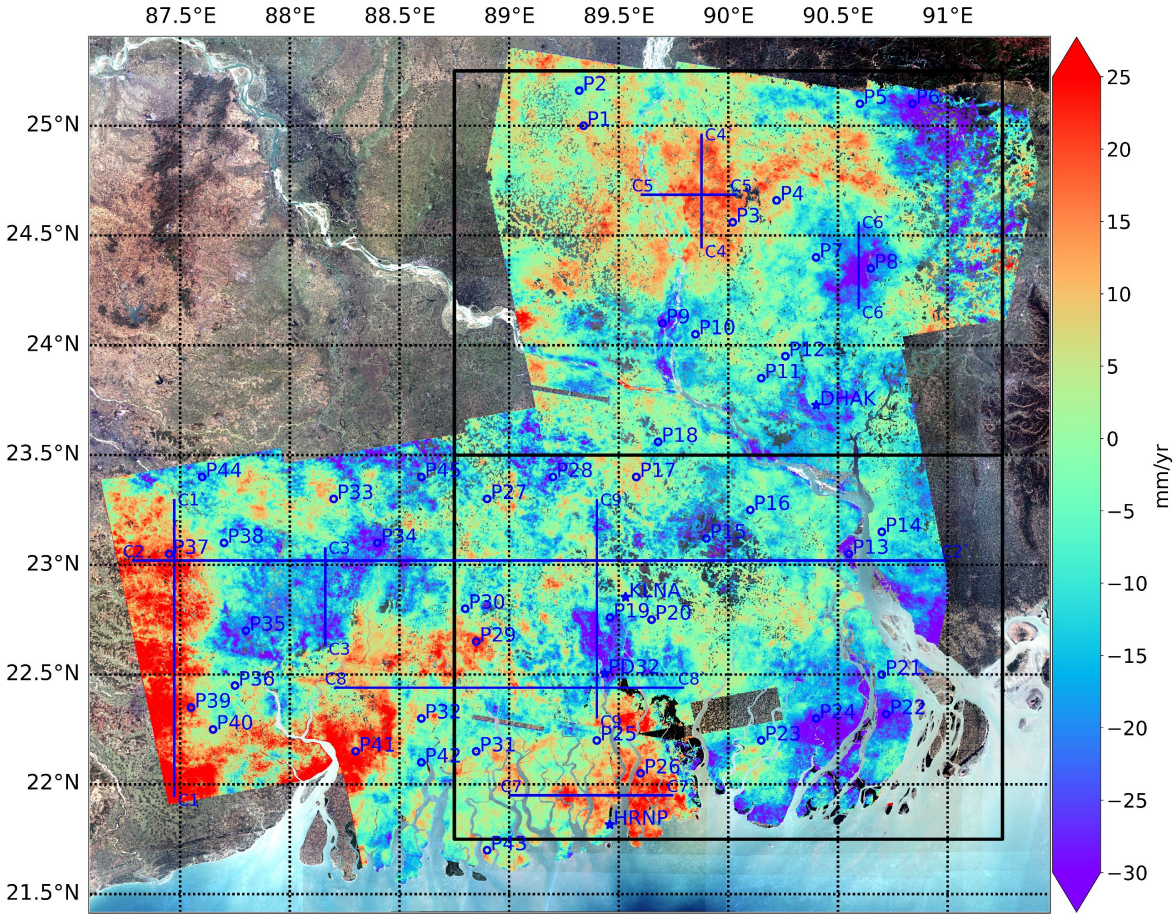


**Figure 4.1.1:** Linear rate deformation map with cross section lines for comparison with topography (see Figure 5.1.2). Selected time series locations are shown as blue circles. Black boxes are locations of enlarged vertical linear deformation rate map shown in Figure 5.3.2 and 5.3.3. Scale is in mm/yr and is clipped to 2*std from the mean.

Figure 4.1.1 shows a vertical linear deformation rate of the region ranging from 25 mm/yr to -30 mm/yr. This is not the absolute range of values as the scale has been clipped to 2*std from the mean to reduce saturation caused by outliers. Figure 4.1.1 also displays the location of 45 points

of interest, plotted with blue circles, for time series. Cross section lines are also plotted to compare topography from the SRTM 30 m DEM to the vertical linear deformation rate to identify any potential correlation between the two. The two black squares plotted are regions of interest which overlap with the geologic to be enlarged.

Figure 4.1.2 displays the histogram of the vertical linear deformation rate map shown in Figure 4.1.1.

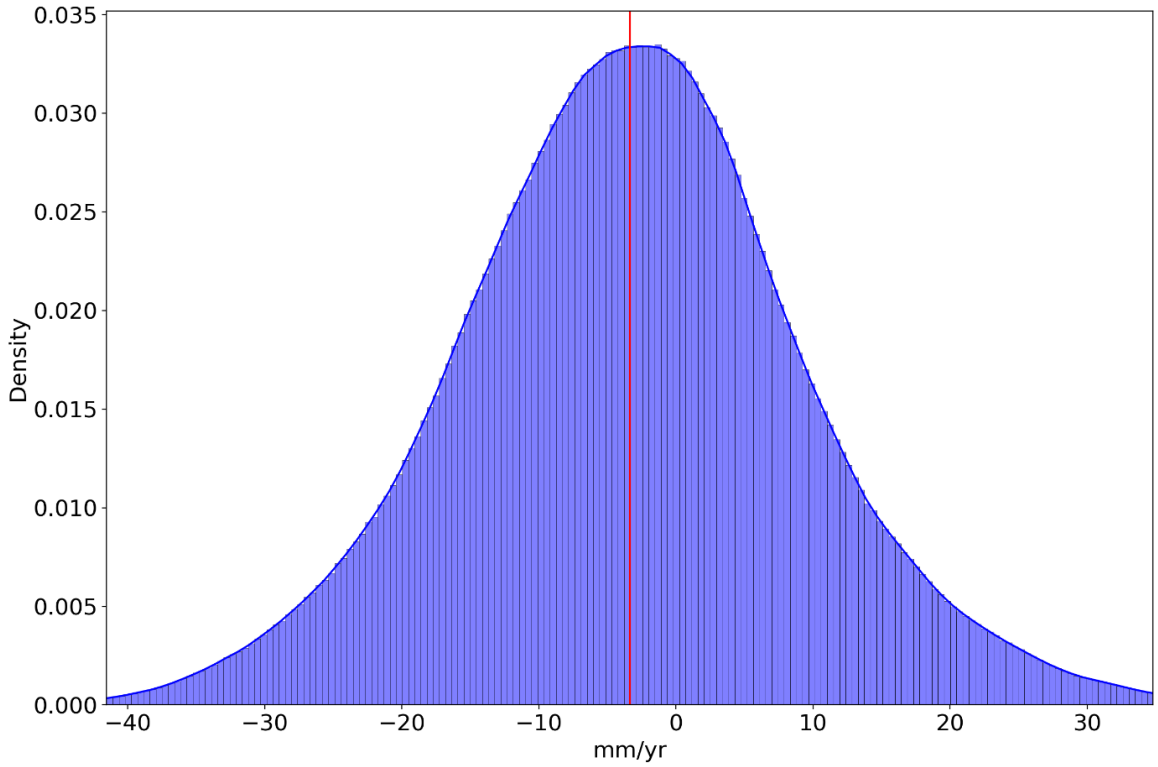


**Figure 4.1.2:** Histogram of vertical linear deformation rate map shown in Figure 4.1.1. The red line shows the mean of the distribution.

Visual inspection of the histogram clearly shows that the vertical linear deformation rates are approximately normally distributed. The mean vertical linear deformation rate is -3.36 mm/yr with a standard deviation of 12.72 mm/yr. The three-sigma rule is computed to be, (-16.09 to 9.36), (-28.81 to 22.09) and (-41.54 to 34.81) for the 68%, 95% and 99.7% intervals respectively.

Thus, we can expect approximately 95% of the MSBAS-derived vertical linear deformation rates to be between -28.81 mm/yr and 22.09 mm/yr.

### 4.2 Individual time series

Figure 4.1.1 displayed the vertical linear deformation rates as a map computed from linear regression of time series. MSBAS computes the deformation at each time step that data is available and then linear regression is applied to compute the overall vertical deformation map of the region, regardless of the time series being linear or not. Examples of these time series are shown Figures 4.2.1-4.2.5, with locations shown in Figure 4.1.1.

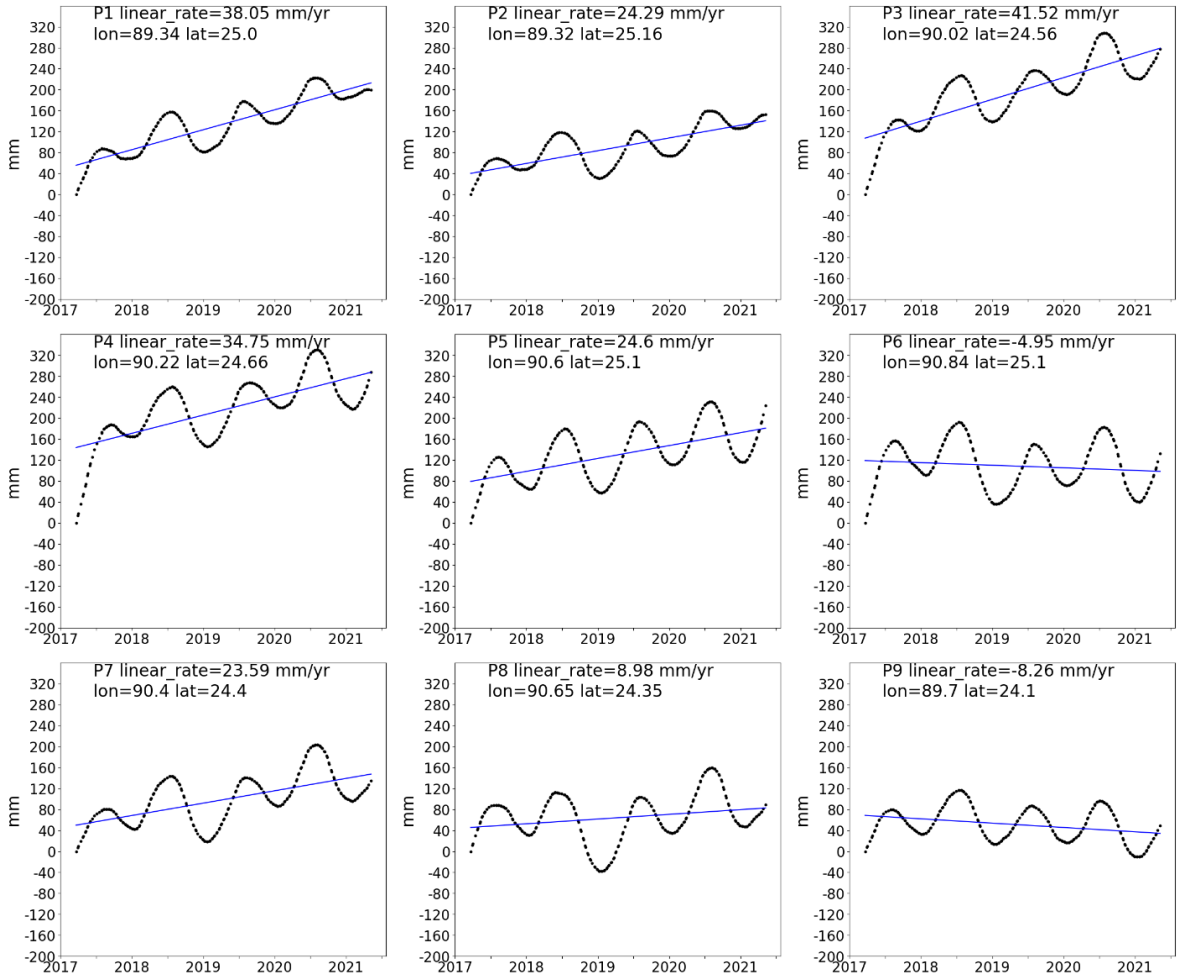


**Figure 4.2.1**: Time series with associated linear regression and estimated vertical linear deformation rate. Locations shown in Figure 4.1.1.

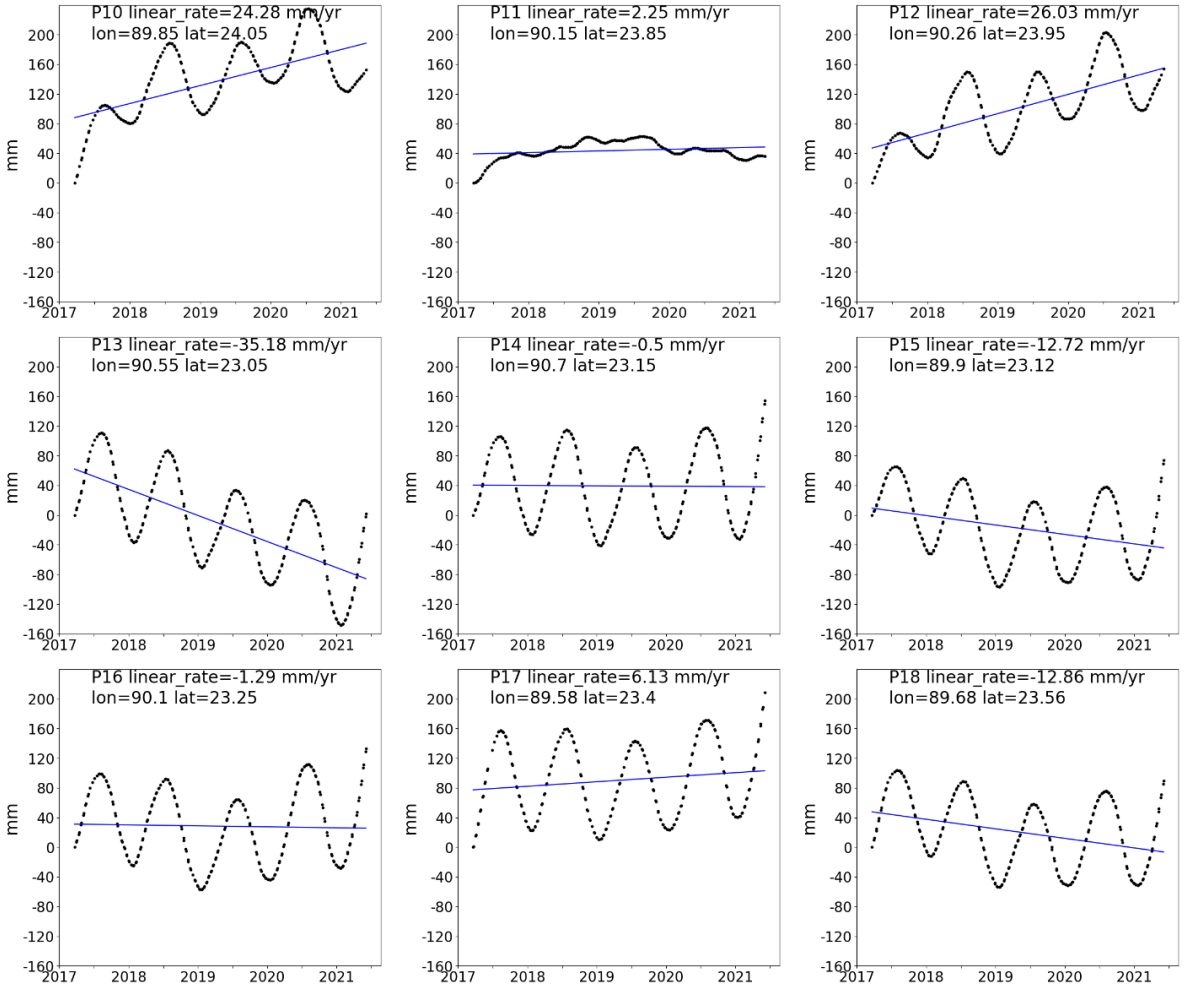


**Figure 4.2.2**: Time series with associated linear regression and estimated vertical linear deformation rate. Locations shown in Figure 4.1.1.

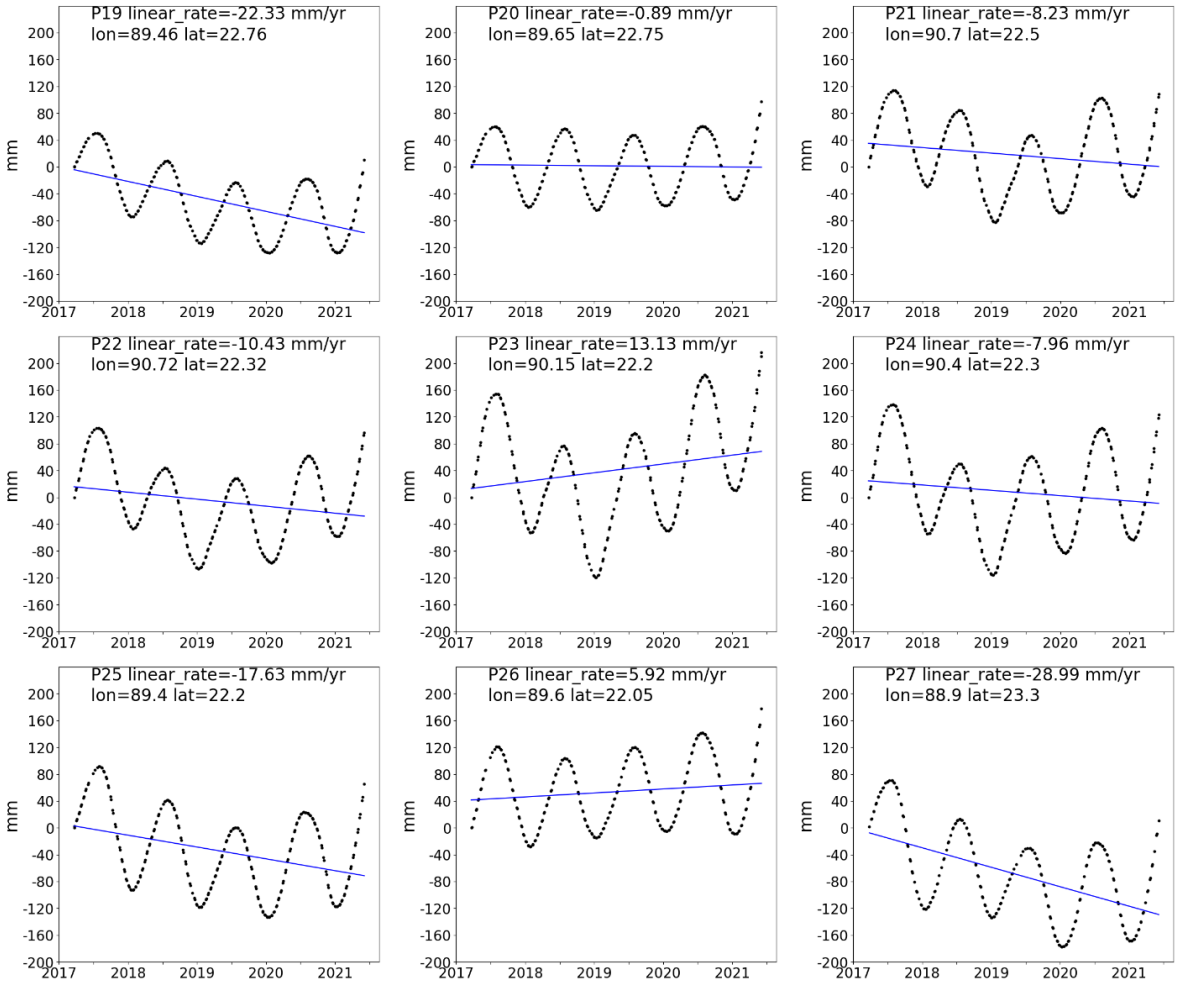


**Figure 4.2.3**: Time series with associated linear regression and estimated vertical linear deformation rate. Locations shown in Figure 4.1.1.

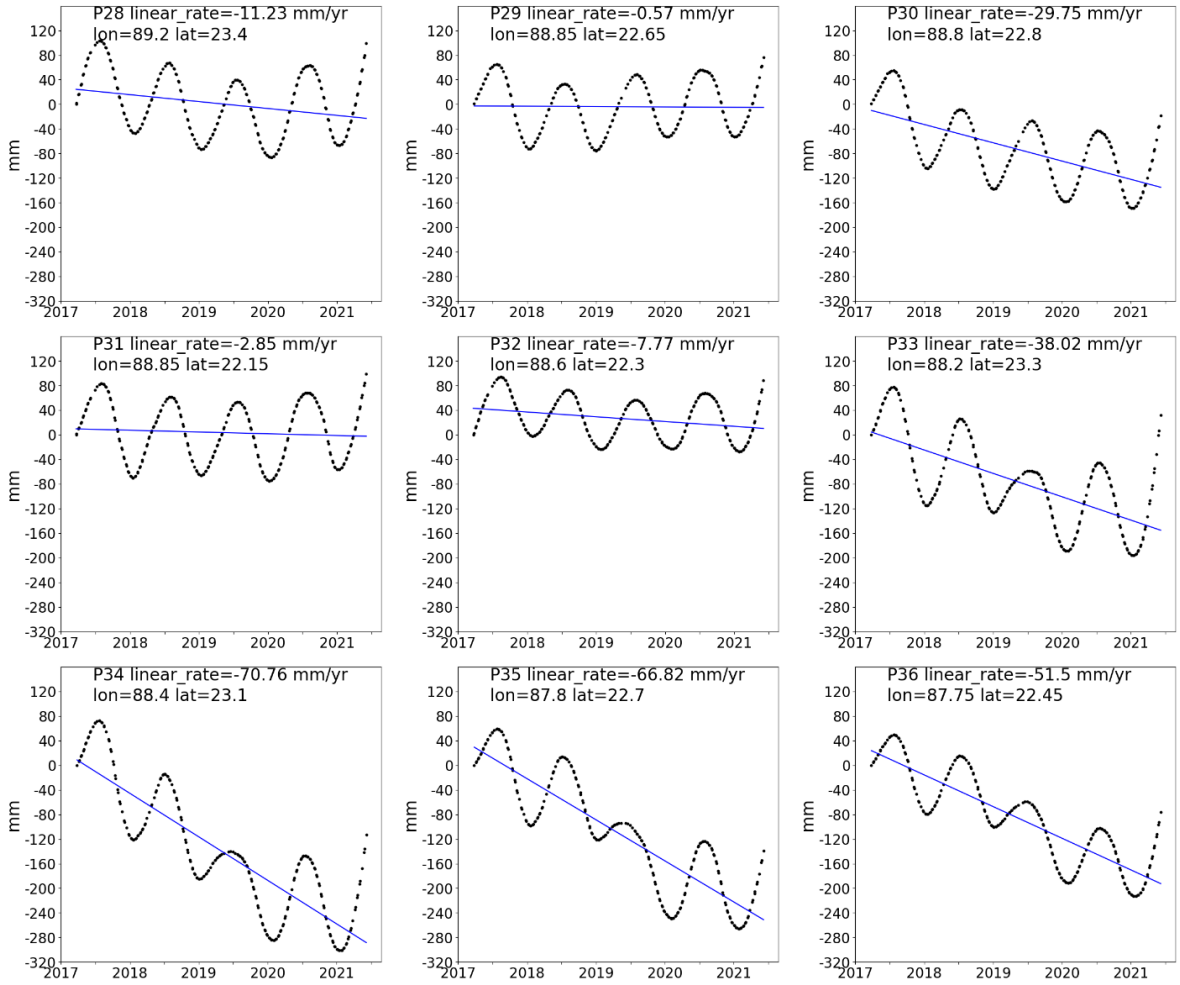


**Figure 4.2.4**: Time series with associated linear regression and estimated vertical linear deformation rate. Locations shown in Figure 4.1.1.

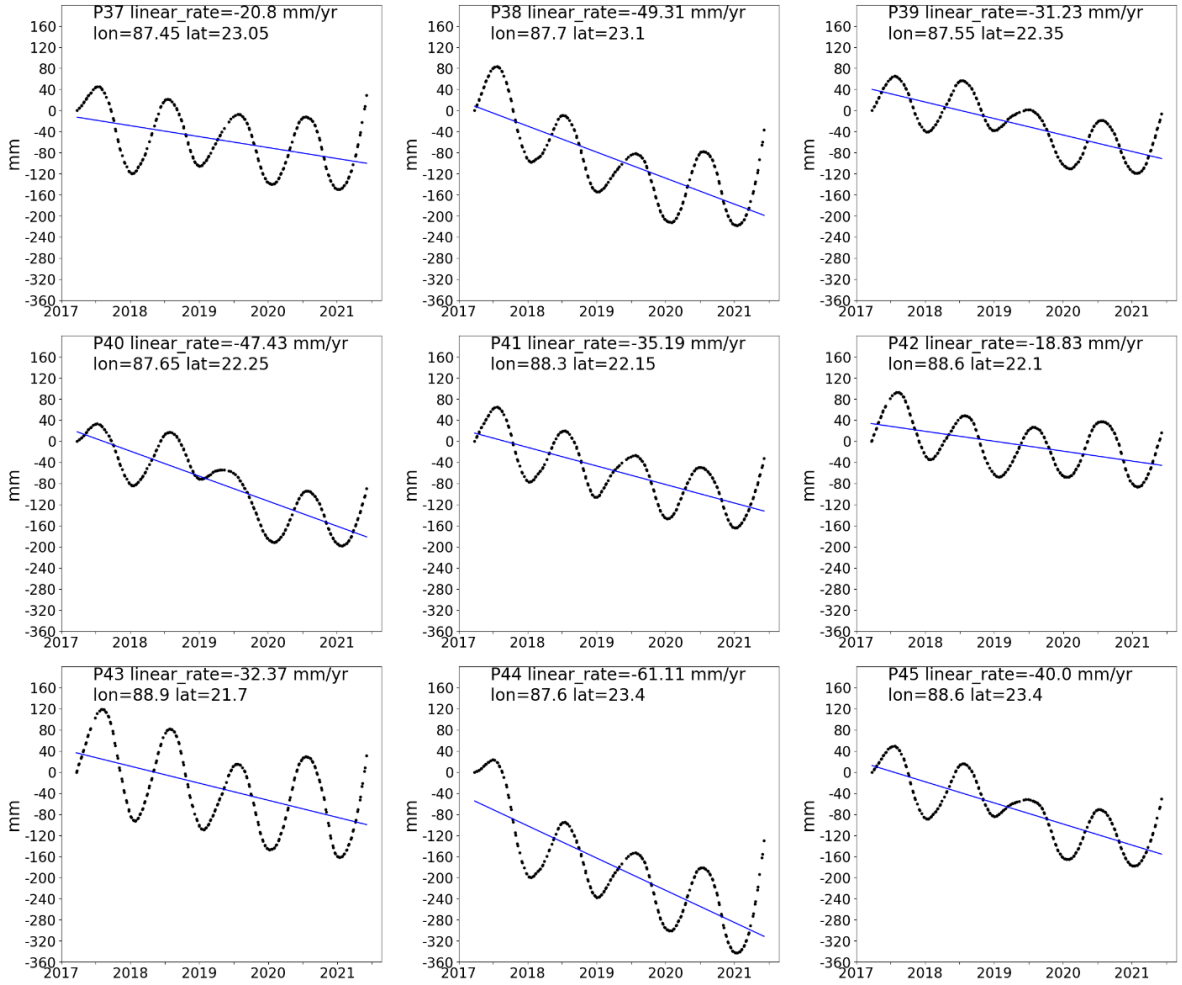


**Figure 4.2.5**: Time series with associated linear regression and estimated vertical linear deformation rate. Locations shown in Figure 4.1.1.

We expect strong seasonal signal due to the monsoon season which causes loading of the delta as well as poroelastic rebound when the ground has become fully saturated. This seasonal signal is clearly seen in most of the time series in Figures 4.2.1-4.2.5 besides P11 in Figure 4.2.2. The local maximum occurs at approximately mid-year and the local minimum at the approximate start of each year. The amplitude of the sinusoidal or seasonal signal ranges from approximately 8 to 12 cm.

## 5. DInSAR Discussion

In this section we will investigate whether the vertical linear deformation rates shown in Figure 4.1.1 could be an artifact of topography, heavy vegetation, or potential errors in processing. We will demonstrate that correlation with topography is limited in this region, except for the region near 87.5°E. We also will compare the NDVI to the vertical linear deformation rate map Figure 4.1.1 and the average coherence map Figure 3.3.8. Finally, we will compare the vertical linear deformation rates to the geology of the area and identify potential relationships between the two. We also will compare the GPS-derived vertical linear deformation rates and the MSBAS-derived vertical linear deformation rates will be compared. We also will remove the sinusoidal signal seen in the time series in Figures 4.2.1-4.2.5 to better investigate the non-seasonal dynamics occurring in the GBM. Additional potential error sources will be discussed that could have occurred in the processing and thus may have affected the vertical linear deformation rates shown in Figure 4.1.1.

### 5.1 Topography Comparison

The overall elevation of Bangladesh is low, as are the changes in elevation. The SRTM 30 m DEM was removed from the interferograms, but this does not guarantee it will be fully removed, as it was obtained at a unique moment in time (February 2000) and can contain physical topography errors. In addition, tropospheric signal associated with changes in height can result in errors that are correlated with topography. Thus, there may be potential topographic errors within the MSBAS-derived vertical linear deformation rate map shown in Figure 4.1.1. Assuming topographic error exists, we expect the topography to either positively or negatively correlate with the vertical linear deformation rate values. Thus, to ensure that topography

correlation is limited we plot both the overall deformation rates vs. SRTM 30 m DEM as well as cross sections of the two with spatial locations shown in Figure 4.1.1.

First, we plot the overall correlation between the entire vertical linear deformation rate map and the SRTM DEM, shown in Figure 5.1.1.

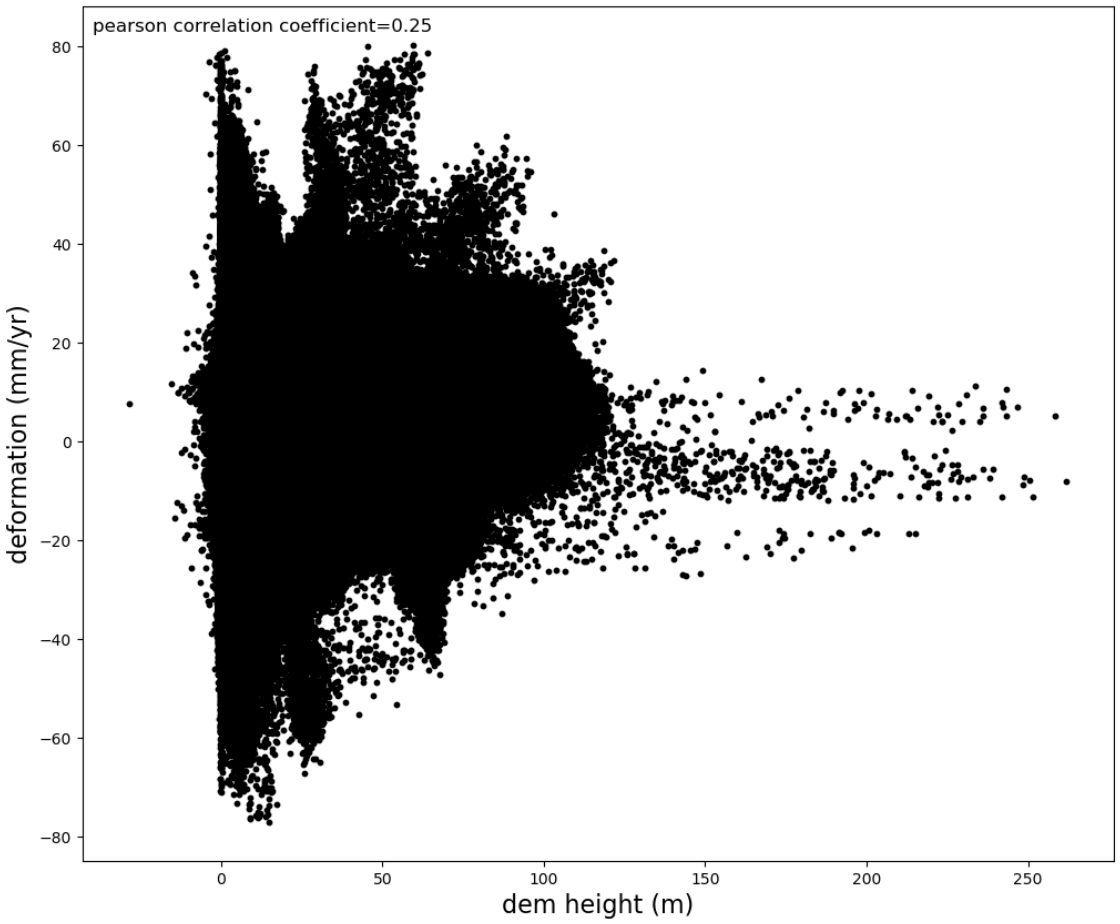


**Figure 5.1.1:** MSBAS-derived vertical linear deformation rate vs. SRTM DEM resampled to the MSBAS-derived vertical linear deformation rate map. The Pearson correlation coefficient is computed to identify any potential correlation between deformation and topography.

To identify the potential correlation between topography and the deformation rate, we can both visually compare the two for any potential correlation. We also calculate the Pearson correlation coefficient, which is a measure of the linear correlation between two data sets. Visually, there is

limited correlation between the two. The Pearson correlation coefficient has a value of 0.25 .Thus, with a value of 0.25 there is limited linear correlation between the topography and the linear deformation rate, but some still exists. The most likely location of this correlation is seen in Figure 4.1.1 as the large red region in the westernmost part of the image at a longitude of 87.5°E. Topography starts to increase significantly in this region, compared to the rest of the region, and this is potentially the cause for the uplift rates seen at 87.5°E. The most likely explanation is that there were errors in the SRTM topographic correction or the GACOS correction was not accurate in this region.

We can also identify any topographic correlation by plotting cross sections of both topography and vertical linear deformation rate. The locations of these nine cross section lines are shown in Figure 4.1.1. The basic idea is to plot the topography and the vertical linear deformation rate on the same plot with different scales, and to visually determine if the vertical linear deformation rate mirrors the topography, either negatively or positively. This is shown for the nine cross section lines in Figure 5.1.2.

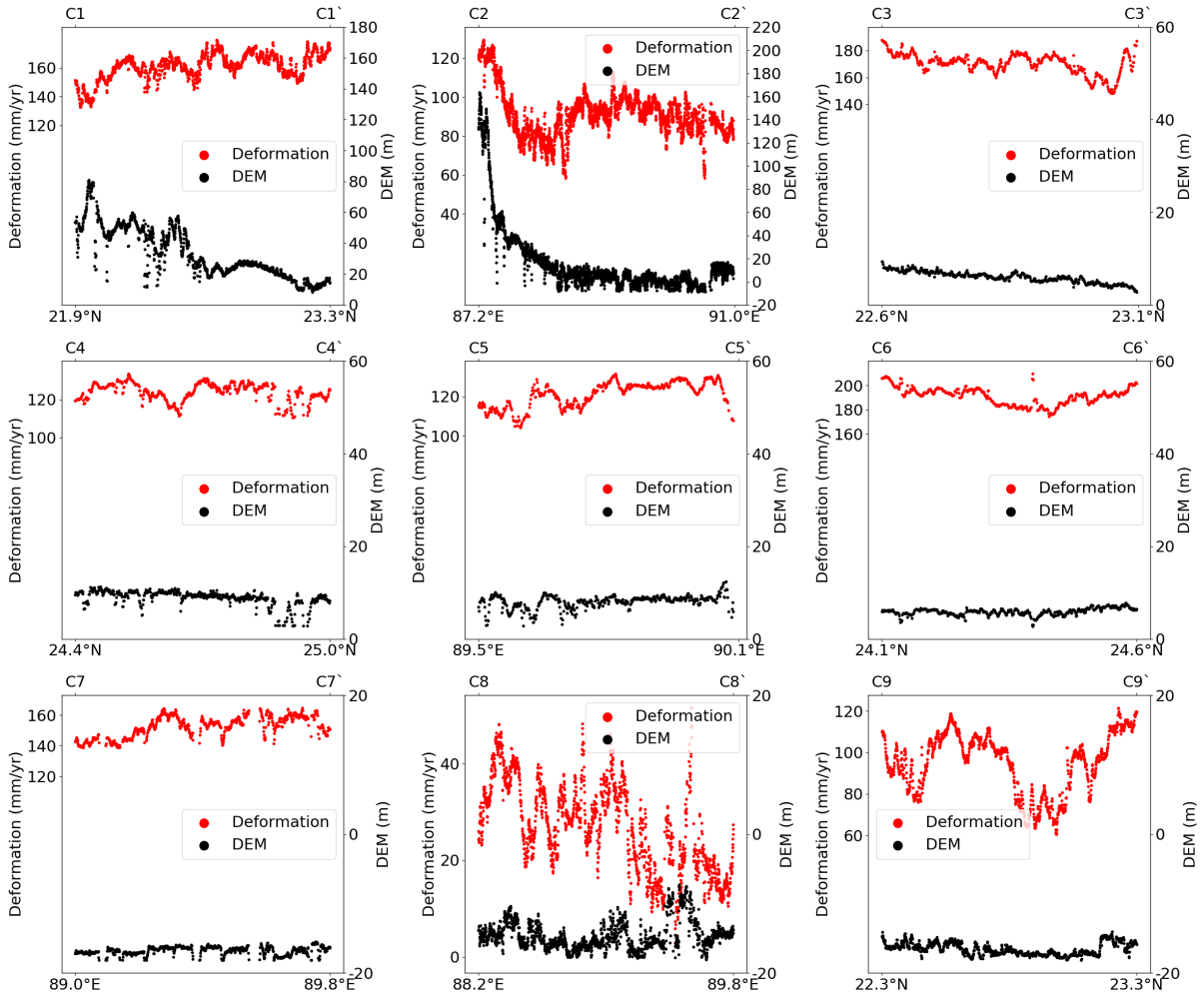


**Figure 5.1.2:** Cross sections as shown in Figure 4.1.1, of MSBAS-derived vertical linear deformation rate plotted in red and the SRTM DEM plotted in black. MSBAS-derived vertical linear deformation rates are shifted to facilitate comparison with deformation rates to topography.

These nine cross section locations were chosen due to the larger vertical linear deformation rate seen in these areas to determine if it was related to topographic effects. Essentially, we aim to identify deviations of the red dots from the black dots in Figure 5.1.2 or deviation from the vertical linear deformation rate and the SRTM DEM. In Figure 5.1.2, cross section C2-C2`, which overlaps with the region in the west at 87.5°E, there is a potential correlation starting at 87.2°E and continuing to approximately 87.6°E and becomes insignificant after that. There appears to be limited correlation between topography and the vertical linear deformation rate in

most of the remaining cross sections of Figure 5.1.2, although there is potentially some negative correlation in cross section C1-C1` and potentially some positive correlation in cross section C8-C8`. The cross section C8-C8` displays potential positive correlation and the vertical linear deformation rate appears to behave more erratically than the other cross sections. This could potentially be due to more variable terrain and soil type causing the vertical linear deformation rate to vary more rapidly. It is also important to note that the relative size of the scales differ from cross section to cross section. The range of C8-C8` is 40 mm/yr whereas the range of C9-C9` is 60 mm/yr, thus the oscillations in C8-C8` could be in part due to being plotted on a smaller scale.

It also is important to note that the longitude and latitude length of these cross sections varies significantly in some cases. For example, C2-C2` has a length of 3.8 degrees of longitude which covers most of the vertical linear deformation rate map, versus 0.5 degrees of latitude of C3-C3`, it also displays similar oscillations to C8-C8` but with a larger range and thus they appear smaller. This makes sense as it spans many different surface types and processes across a large longitude range. The cross sections with a smoother appearance and less oscillations are typically shorter in either longitude or latitude.

In summary, we identify potential correlation in the west at 87.5°E, shown in Figure 5.1.2 cross section C2-C2`. Potentially there is some other minor correlation between topography and the vertical linear deformation rate, as shown in Figure 5.1.1. Thus, we eliminate topography as a cause of vertical deformation for the vertical linear deformation rate map Figure 4.1.1, except for the large red uplift region in the western most part of the image, at 87.5°E, which is likely primarily residual topographic signal.

### 5.2 Normalized Differenced Vegetation Index Comparison

Significant vegetation of the study region may potentially cause errors with DInSAR processing, primarily due to the resulting lower coherence. Thus, to analyze the impacts of vegetation we compute the NDVI as discussed in section 3.6. We then visually compare this to the vertical linear deformation rate as well as the averaged coherence maps, shown in Figures 5.2.1 (a) and (b) respectively.

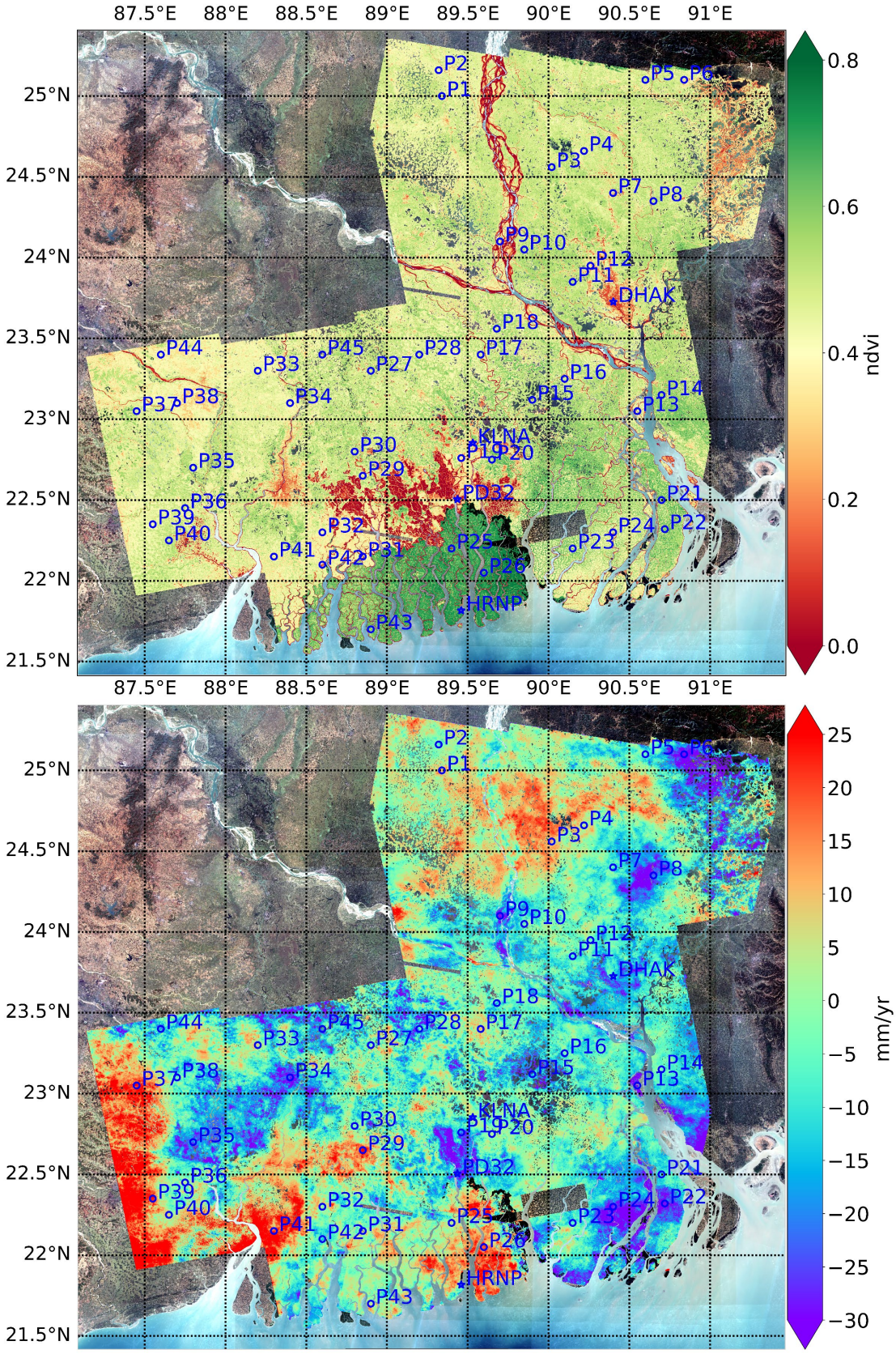
87.5°E
88°E
88.5°E
89°E
89.5°E
90°E
90.5°E
91°E
25°N
24.5°N
24°N
23.5°N
23°N
22.5°N
22°N
21.5°N
P1
P2
P3
P4
P5
P6
P7
P8
P9
P10
P11
P12
P13
P14
P15
P16
P17
P18
P19
P20
P21
P22
P23
P24
P25
P26
P27
P28
P29
P30
P31
P32
P33
P34
P35
P36
P37
P38
P39
P40
P41
P42
P43
P44
P45
DHAK
KLNA
HRNP
PD32
0.8
0.6
0.4
0.2
0.0
ndvi
25
20
15
10
5
0
−5
−10
−15
−20
−25
−30
mm/yr

**Figure 5.2.1 (a):** Average NDVI from March 2017 to June 2021 (top) derived using GEE with available Sentinel-2 data. MSBAS-derived vertical linear deformation rate map (bottom).

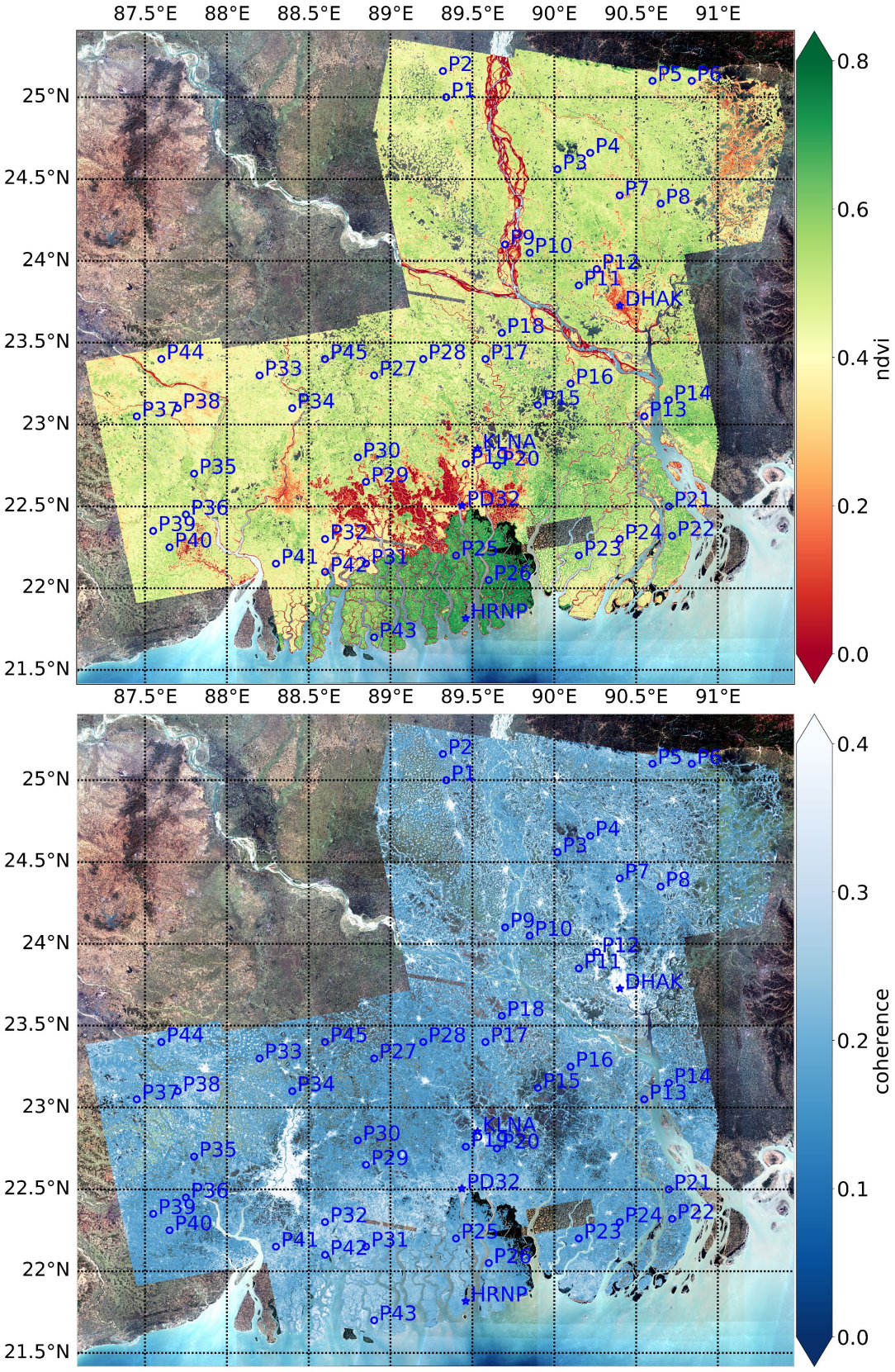
87.5°E
88°E
88.5°E
89°E
89.5°E
90°E
90.5°E
91°E
25°N
24.5°N
24°N
23.5°N
23°N
22.5°N
22°N
21.5°N
P1
P2
P3
P4
P5
P6
P7
P8
P9
P10
P11
P12
P13
P14
P15
P16
P17
P18
P19
P20
P21
P22
P23
P24
P25
P26
P27
P28
P29
P30
P31
P32
P33
P34
P35
P36
P37
P38
P39
P40
P41
P42
P43
P44
P45
DHAK
KLNA
PD32
HRNP
ndvi
0.8
0.6
0.4
0.2
0.0
coherence
0.4
0.3
0.2
0.1
0.0

**Figure 5.2.1 (b):** Average NDVI from March 2017 to June 2021 (top) derived using GEE with available Sentinel-2 data. Averaged coherence (bottom).

We first compare the vertical linear deformation rate map (Figure 5.2.1 (b)) with the NDVI map (Figure 5.2.1 (a)). There appears to be limited spatial correlation between the two, except for 90.25°E, 22.75°N, denoted Location 1, and in the Sundarbans, P26, denoted Location 2, Figure 5.2.2 (a). These two locations appear to show higher NDVI values. At Location ,1 the NDVI is lower than at Location 2, as is the vertical linear deformation rate, but they do appear to correlate spatially. At Location 2, within the Sundarbans, we see a much darker green in the NDVI map and a darker red in the vertical linear deformation rate map, again appearing to be spatially correlated. Visual inspection of the remainder of the map shows little spatial correlation between the two in Figure 5.2.1 (a).

In Figure 5.2.1 (b) we compare the NDVI to the averaged coherence image. In this comparison we should expect regions of low NDVI to show higher coherence relative to the regions of high NDVI. This clearly holds for the two major cities shown in Figure 5.2.1 (b), at 88.25°E, 22.75°N, and the location of DHAK. We would expect major cities to have a low NDVI and a high coherence, as is clearly observed here. There is also a region of low NDVI spanning approximately three degree-squares, starting at (88.75°E, 22.75°N). This region also displays a higher coherence relative to the other regions with a higher NDVI. The Sundarbans also have a lower coherence, and it is the most densely vegetated region, also seen in the NDVI image. Note that we do not expect perfect correlation between coherence and the NDVI, as vegetation is just one factor that can affect the coherence.

Given the visual comparisons of the NDVI and the vertical linear deformation rate map shown in Figure 5.2.1 (a), we expect limited impact on the DInSAR results from the vegetation in this region. The exceptions include Location 1 and Location 2, which demonstrate some

spatial correlation, including the Sundarbans. Visual comparison between NDVI and average coherence in Figure 5.2.1 (b) do confirm that regions of low NDVI are typically higher in coherence and regions of higher NDVI such as the Sundarbans typically display lower coherence over time. Thus, in these areas of higher vegetation we might expect less reliable results compared to the cities because the coherence is lower, here it would primarily affect Locations 1 and 2, and should be taken into consideration when interpreting the vertical linear deformation rates in these regions.

We are particularly interested in the possibility of measuring the vertical linear deformation rate caused by the growth of the Sundarbans. As shown in Figure 3.6.1, C-band SAR will partially reflect and partially absorb into forest canopies. Thus, we should expect some backscatter from the Sundarbans. As shown in Figure 4.1.1, we see positive rates for most of the Sundarbans, which potentially could be explained by vegetation growth of the Sundarbans. It could also simply be error due lower coherence in this region, as discussed above, it is also possible that we are measuring ~2cm/year of persistent sedimentation by annual tidal flooding (Rogers et al, 2014;2017; Bomer et al, 2020). Acquisition of repeat lidar data to map the Sundarbans canopy height with time would help to quantify potential changes. In addition, processing additional SAR bands, including L-band, which penetrates the canopy, and X-band, which largely bounces off leaf canopy, could allow us to differentiate between those behaviors. C-band SAR by itself simply does not provide enough information to explain the cause of this signal.

### 5.3 Geologic Overlay Comparison

In Sections 5.1 and 5.2 we discussed the potential effects of topography and NDVI in the interpretation of the vertical linear deformation rate map shown in Figure 4.1.1. We found minimal topographic effects besides at the western most part of the image located at 87.5°E as well as minimal NDVI correlation, primarily in the Sundarbans and the square located at (90.25°E, 22.75°N) or location 1. Here we attempt to attribute some of the vertical linear deformation rates we see in Figure 4.1.1 with to the general geology of the region (Alam et al., 2001). The comparison between the vertical linear deformation rate map and the geology of the region is shown in Figure 5.3.1, enlarged regions with extent shown in Figure 4.1.1 are shown in Figures 5.3.2 and 5.3.3 with geologic unit descriptions in Figure 5.3.4.

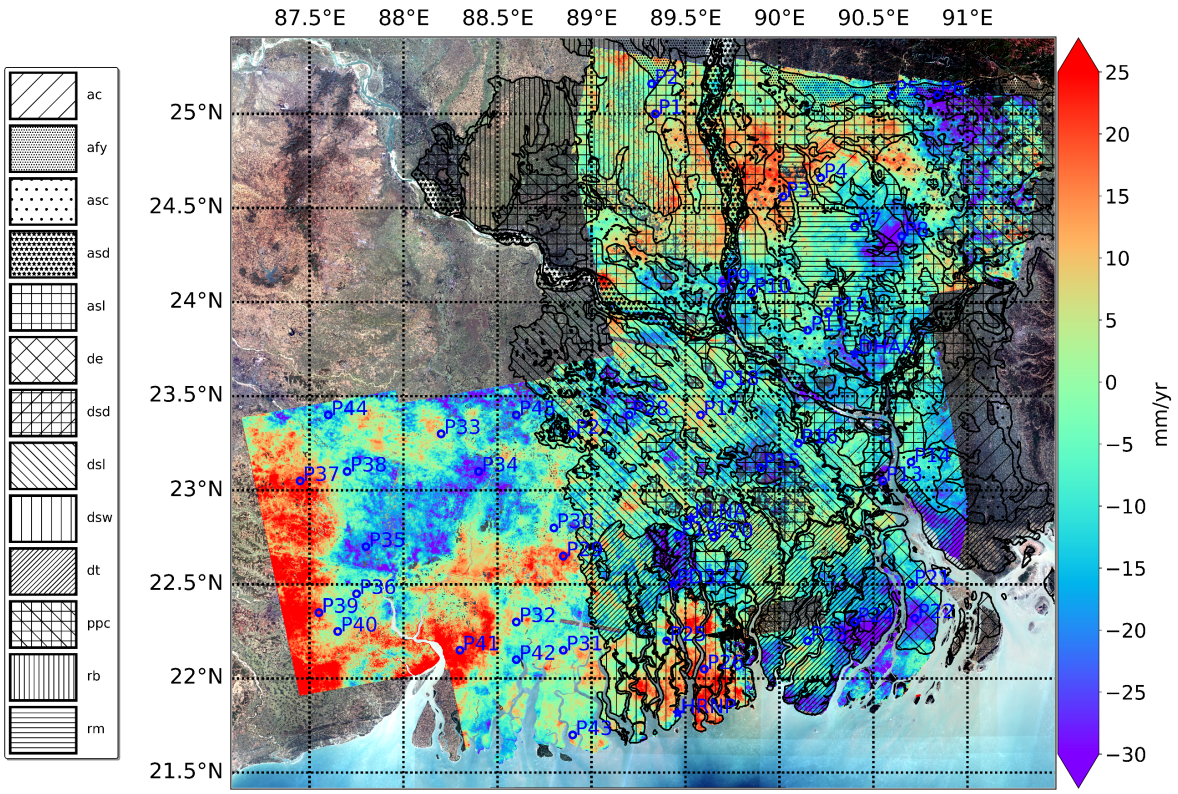


**Figure 5.3.1:** Geologic map (Alam et al., 2001) plotted on the MSBAS-derived vertical linear deformation rate map. **Ac** – Chandia Alluvium, **afy** – Young Gravelly Sand, **asc**- Alluvial Silt and Clay, **asd**- Alluvial Sand, **asl** – Alluvial Silt, **de** – Estuarine Deposits, **dsd** – Deltaic Sand, **dsl** – Deltaic Silt, **dsw** – Mangrove Swamp Deposits, **dt** – Tidal Deltaic Deposits, **ppc** – Marsh Clay and Peat, **rb** – Barind Clay Residuum, **rm** – Madhupur Clay Residuum.

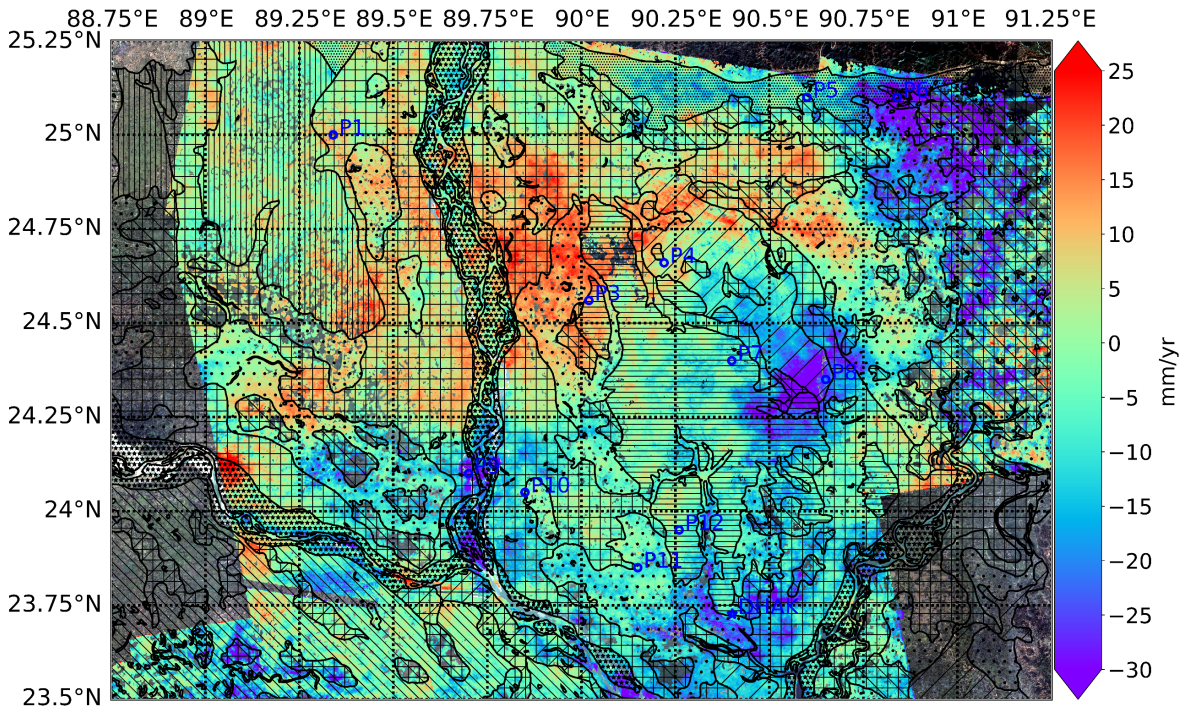


**Figure 5.3.2:** Enlarged vertical linear deformation rate map with geologic map (Alam et al., 2001). See Figure 5.3.4 for geologic unit description.

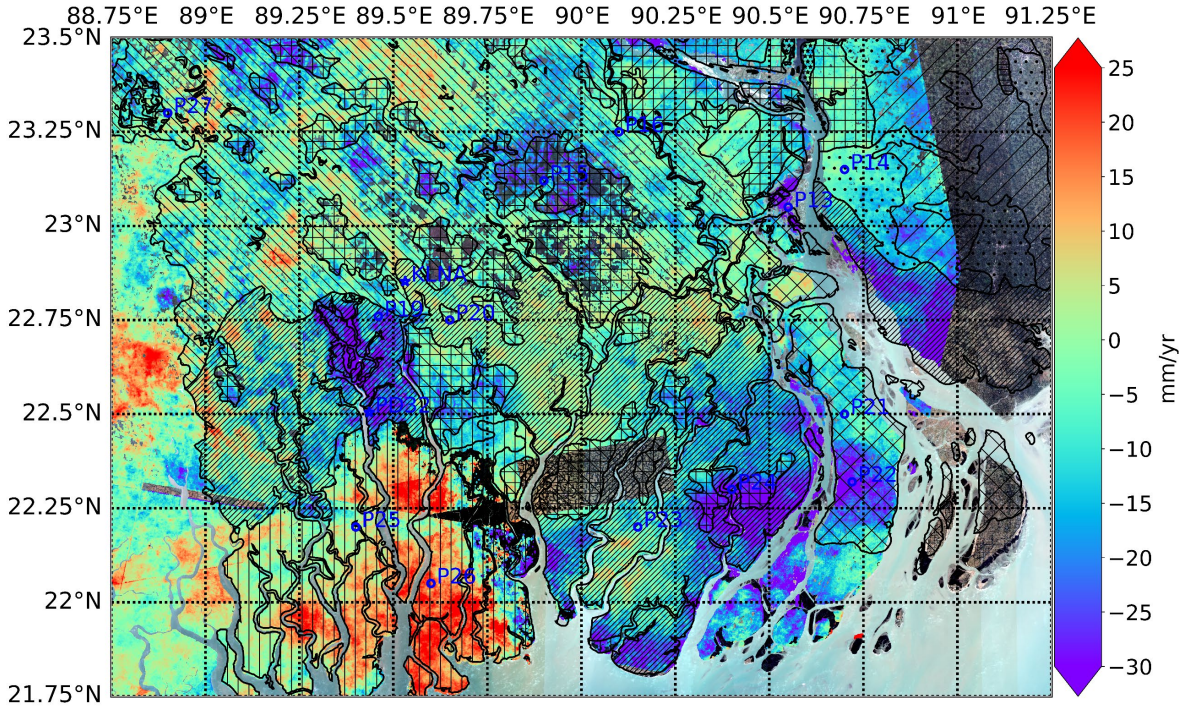


**Figure 5.3.3:** Enlarged vertical linear deformation rate map with geologic map (Alam et al., 2001). See Figure 5.3.4 for geologic unit description.

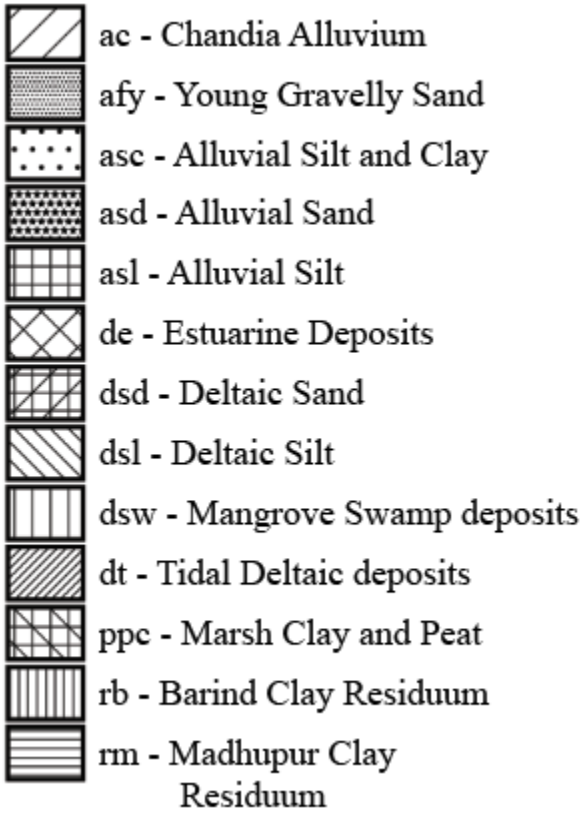


**Figure 5.3.4:** Geologic units and descriptions of geologic map (Alam et al., 2001) reference for Figures 5.3.1, 5.3.2 and 5.3.3.

Generally, we are looking for correlation between units and the vertical linear deformation rate, as we expect similar soil properties to possibly have similar rates. The vertical linear deformation rates north of 24N latitude tend to display uplift within the Barind Clay Residuum (rb), Alluvial Silts (asl), Madhupur Clay Residuum (rm) and the Alluvial Silts and Clays (asc). We see subsidence within the Marsh Clay and Peat (ppc) and the Young Gravelly Sand (afy). Thus, there appears to be uplift within the clays and subsidence within the peats and the young gravelly sand. In part, the uplift may be explained by clays expanding during the monsoonal season, associated with significant amplitude in the time series of Figures 4.2.1-4.2.5. In addition, some of the uplift signal could be related to aggradation, as this region is next to the Brahmaputra River, which is where we see the highest uplift (89.75°E, 24.75°N) in the region north of 24°N latitude. The Marsh and Clay Peat (ppc), which is in the northeastern most part of

the image, may be subsiding due to the general compaction of this material, whereas the Young Gravelly Sands (afy) may subside simply because they are young deposits. The Alluvial Silt and Clay (asc) begins to subside further south of 24°N located around P11 and DHAK.

South of 24°N we see more moderate rates of uplift and similar rates of subsidence. The Deltaic Silts (dsl) and the Mangrove Swamp Deposits (dsw) consist of primarily uplift with some subsidence. The Mangrove Swamp Deposits (dsw) include the Sundarbans Mangrove Forest, The uplift there potential could be explained by the canopy growth of the Sundarbans, but significantly more evidence is needed to support this claim. The Deltaic Silts in this region (dsl) show moderate uplift rates of up to 10 mm/yr due to potential aggradation from the Padma River and tributaries. There are also pockets of subsidence within the Deltaic Silts (dsl) of up to 10 mm/yr. We see a mix of subsidence and uplift as well in the Tidal Deltaic Deposits (dt). There appears to be more subsidence closer to the coast of the Tidal Deltaic Deposits (dt). Further inland this turns into a mix uplift and some subsidence, as seen in Figures 5.3.3. The Marsh and Clay Peat in this region, which is located at P15, shows primarily subsidence, as seen in the region to the northeast. The Estuarine Deposits (de) and the Deltaic Sands (dsd) both display subsidence. Both next to the Padma River where the deposits are potentially young, resulting in subsidence as they dewater and compact.

### 5.4 Points of interest and GPS comparison

As seen in Figures 4.2.1-4.2.5, there is significant monsoonal signal within almost every time series. This signal has a local maximum approximately mid-year and the local minimum approximately at the start of each year. When the monsoon initially starts, the pressure of the monsoon is competing with poreolastic expansion of the clays in the region. Thus, at the start of the year we are at a local minimum and as the monsoon progresses these sediments expand, causing relative uplift to the local minima. Eventually, approximately halfway through the year, the sediments become completely water loaded, reaching the local maxima and poreolastic expansion is minimized. The water loading begins to cause the entire delta to essentially subside relative to the local maxima and thus reaches the local minima again at the start of the year. These cycles are clearly seen in almost every time series of Figures 4.2.1-4.2.5.

Here we want to analyze the time series with no sinusoidal signal and thus we will fit a sinusoid to the time series and remove it. To accomplish this, we use the best fit sinusoid equation 5.4.1.

$$B(x;\ A, o, \omega, \phi) = A \cdot sin(\omega \cdot \phi \cdot x) + o \tag{5.4.1}$$

Where $x$ is time in years, $A$ is amplitude, $o$ is the offset of the sinusoid, $\omega$ is the frequency and $\phi$ is the phase. This equation is fit to the time series data using scipy.optimize import curve_fit function in python. The application of this equation and its fit can be seen in comparison with GPS in Figure 5.4.1 (a). We then perform a linear regression on the residual time series.

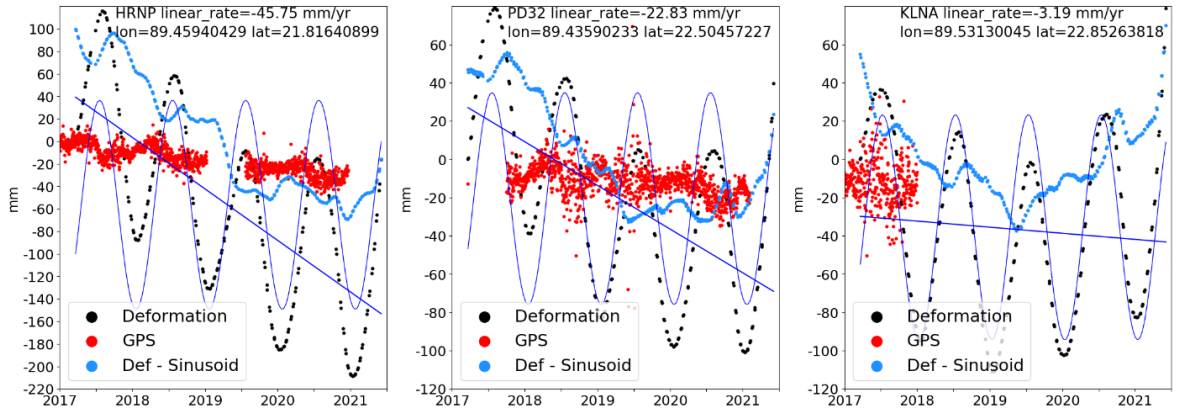


**Figure 5.4.1 (a):** Comparison of GPS-derived data and MSBAS-derived vertical linear deformation rates. Blue line is the regression of the MSBAS-derived deformation. The best fit sinusoid is fit to the deformation data and removed from the deformation data. The black dots represent MSBAS-derived deformation, red dots are GPS derived height change provided by Dr. Michael Steckler, the light blue dots are the MSBAS-derived deformation with the sinusoid removed and the blue line is the regression fit to the black dots.

Figure 5.4.1 (b) shows the comparison between GPS elevation change and MSBAS-derived vertical linear deformation rate with the sinusoid removed and the recomputed regression line.

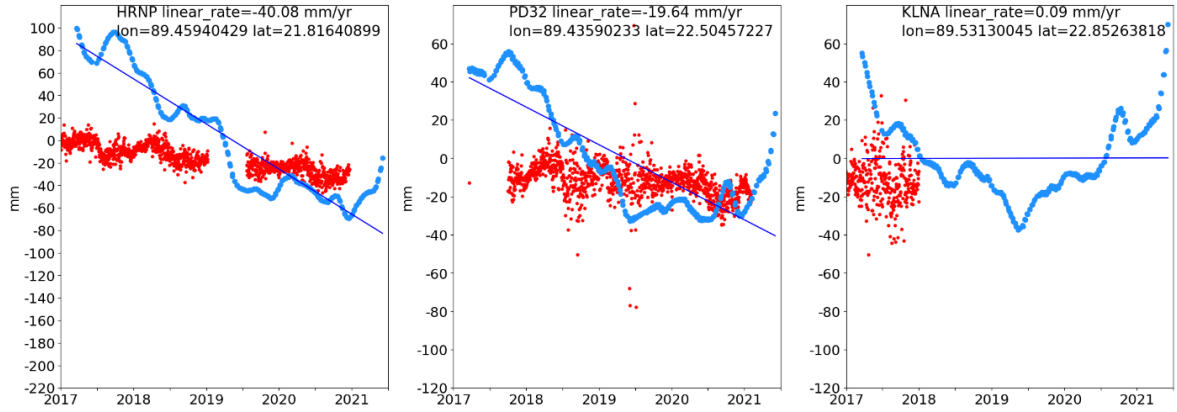


**Figure 5.4.1 (b):** Comparison of GPS-derived data and MSBAS-derived vertical linear deformation rates with best fit sinusoid removed. Blue line is the regression of the MSBAS-derived vertical linear deformation rate with best fit sinusoid removed. GPS derived height change provided by Dr. Michael Steckler in red, the light blue dots are the MSBAS-derived deformation with the sinusoid removed.

Figure 5.4.1 (a) shows the comparison between three continuous GPS stations vertical time series (red dots), HRNP, PD32 and KLNA and the MSBAS-derived vertical deformation (black dots). While the GPS and MSBAS rates are different, they are generally in the same direction.

We also compare every continuous GPS-derived vertical linear deformation rate and campaign

GPS-derived linear rate where there is DInSAR MSBAS-derived vertical linear deformation rates. These comparisons are shown in Tables 5.3.1 and 5.3.2.

| Deformation point | MSBAS vertical linear deformation rate (mm/yr) | GPS name | GPS vertical rates (mm/yr) | Longitude | Latitude | Start Date | End Date |
|---|---|---|---|---|---|---|---|
| deformation_point_0 | -8.86 | HRNP | -7.42 | 89.459404 | 21.816409 | 20121021 | 20201220 |
| deformation_point_1 | -19.01 | PD32 | -4.87 | 89.435902 | 22.504572 | 20121021 | 20210203 |
| deformation_point_2 | -1 | KLNA | -4.32 | 89.5313 | 22.852638 | 20130115 | 20171231 |
| deformation_point_3 | 5.73 | JAML | -5.41 | 91.2371 | 25.0005 | 20070215 | 20161204 |
| deformation_point_4 | -6.55 | KHUL | 5.38 | 89.4184 | 22.8029 | 20030515 | 20080804 |
| deformation_point_5 | 15.66 | MPUR | 0.43 | 90.014 | 24.6043 | 20070219 | 20110622 |
| deformation_point_6 | -12.26 | RPUR | 0.71 | 90.6708 | 23.0365 | 20070301 | 20161218 |
| deformation_point_7 | -5.12 | KHEP | -3.27 | 90.219694 | 21.986663 | 20121022 | 20210203 |
| deformation_point_8 | 0.3 | MBST | -10.59 | 89.890945 | 24.237413 | 20141018 | 20170116 |
| deformation_point_9 | -13.1 | WDBB | -45.34 | 90.411477 | 23.788679 | 20141022 | 20190920 |
| deformation_point_10 | -4.08 | WDBG | -11.01 | 90.388252 | 23.752921 | 20141022 | 20191027 |
| deformation_point_11 | -8.34 | DHK2 | -12.78 | 90.387897 | 23.804669 | 20130401 | 20171231 |
| deformation_point_12 | -3.39 | ICHA | 2.3 | 88.736028 | 22.899897 | 20131124 | 20170428 |
| deformation_point_13 | -21.85 | MPUC | -32.63 | 90.520803 | 23.781323 | 20140602 | 20170314 |
| deformation_point_14 | -9.59 | VLKA | -7.41 | 90.398868 | 24.409762 | 20121104 | 20171231 |
| deformation_point_15 | 10.01 | PAIK | 0.1 | 89.319425 | 22.584817 | 20140315 | 20200119 |

**Table 5.3.1:** Comparison between continuous GPS derived vertical linear deformation rates provided by Dr. Michael Steckler, and MSBAS derived vertical linear deformation rates.

| Deformation point | MSBAS vertical linear deformation rates (mm/yr) | GPS name | GPS vertical rates (mm/yr) | Longitude | Latitude |
|---|---|---|---|---|---|
| deformation_point_0 | -2.84 | GPS 101 | 0.21 | 88.96153 | 23.01559 |
| deformation_point_1 | -15.41 | GPS 103 | -21.42 | 89.98305 | 23.21988 |
| deformation_point_2 | 2.86 | GPS 104 | -23.94 | 89.81635 | 22.99384 |
| deformation_point_3 | 10.96 | GPS 105 | -22.35 | 89.16204 | 22.98069 |
| deformation_point_4 | 10.72 | GPS 106 | -21.29 | 89.05672 | 22.69431 |
| deformation_point_5 | -0.34 | GPS 107 | -13.08 | 89.18083 | 22.54799 |
| deformation_point_6 | 20.03 | GPS 109 | -13.83 | 89.03175 | 22.45898 |
| deformation_point_7 | -2.18 | GPS 111 | -13.52 | 89.09177 | 22.252 |
| deformation_point_8 | 2.99 | GPS 113 | -11.08 | 89.15082 | 22.05223 |
| deformation_point_9 | 1.35 | GPS 115 | -1.23 | 89.44509 | 22.98529 |

| | | | | | |
|---|---|---|---|---|---|
| deformation_point_10 | 5.75 | GPS 118 | -2.48 | 89.29447 | 22.84094 |
| deformation_point_11 | 2.65 | GPS 120 | -10.46 | 89.309 | 22.68775 |
| deformation_point_12 | -0.96 | GPS 122 | -9.1 | 89.3941 | 22.52778 |
| deformation_point_13 | -9.85 | GPS 124 | -15.45 | 89.28086 | 22.36339 |
| deformation_point_14 | 10.33 | GPS 126 | -23.61 | 89.49431 | 22.26438 |
| deformation_point_15 | 6.25 | GPS 128 | -23.12 | 89.27769 | 22.11651 |
| deformation_point_16 | 4.66 | GPS 132 | -22.07 | 89.71314 | 22.77314 |
| deformation_point_17 | -15.18 | GPS 134 | -23.29 | 89.51676 | 22.73242 |
| deformation_point_18 | 5.08 | GPS 138 | -15.57 | 89.64307 | 22.36879 |
| deformation_point_19 | 10.72 | GPS 140 | -27.96 | 89.71108 | 22.07861 |
| deformation_point_20 | -0.93 | GPS 142 | -16.92 | 89.94095 | 22.84938 |
| deformation_point_21 | -0.26 | GPS 144 | -12 | 89.84417 | 22.60676 |
| deformation_point_22 | 6.54 | GPS 146 | -13.15 | 89.83005 | 22.27658 |
| deformation_point_23 | -6.11 | GPS 148 | -23.72 | 89.96837 | 22.03402 |
| deformation_point_24 | 1.48 | GPS 150 | -22.38 | 89.07757 | 21.83469 |
| deformation_point_25 | -8.86 | GPS 154 | -31.38 | 89.45973 | 21.81691 |
| deformation_point_26 | 15.12 | GPS 158 | -19.17 | 89.5944 | 21.94589 |
| deformation_point_27 | -10.41 | GPS 164 | -25.82 | 90.25201 | 23.18743 |
| deformation_point_28 | 0.6 | GPS 170 | -13.28 | 90.42415 | 23.09837 |
| deformation_point_29 | 3.77 | GPS 182 | -14.59 | 90.05965 | 22.48932 |
| deformation_point_30 | 5.71 | GPS 186 | -14.31 | 90.23216 | 22.14161 |
| deformation_point_31 | -6.08 | GPS 188 | -16.53 | 90.48131 | 22.94554 |
| deformation_point_32 | -4.04 | GPS 190 | -13.24 | 90.24978 | 22.90534 |
| deformation_point_33 | 4.88 | GPS 192 | -27.62 | 90.31966 | 22.75451 |
| deformation_point_34 | -7.78 | GPS 194 | -20.42 | 90.29959 | 22.64415 |
| deformation_point_35 | -2.89 | GPS 196 | -14.28 | 90.3383 | 22.35867 |
| deformation_point_36 | -3.48 | GPS 199 | 0.61 | 89.198 | 23.12628 |
| deformation_point_37 | -4.74 | GPS 202 | -13.58 | 90.47616 | 22.67739 |
| deformation_point_38 | -20.03 | GPS 206 | -24.67 | 90.54721 | 22.48383 |
| deformation_point_39 | -21.76 | GPS 208 | -22.21 | 90.6057 | 22.3309 |
| deformation_point_40 | -26.66 | GPS 224 | -23.85 | 90.29541 | 21.98606 |
| deformation_point_41 | -5.76 | GPS 2867 | -50.92 | 89.54377 | 23.14247 |
| deformation_point_42 | 4.34 | GPS 2876 | 2.93 | 89.60598 | 23.01315 |
| deformation_point_43 | -8.38 | GPS 2957 | -15.38 | 89.94324 | 23.02261 |

**Table 5.3.2:** Comparison between campaign GPS-derived vertical linear deformations rates provided by Dr. Michael Steckler, and MSBAS derived vertical linear deformation rates.

We should expect reasonable agreement between the GPS-derived vertical linear deformation rates and MSBAS-derived vertical linear deformation rates, although methods are subject to their own errors sources. More importantly, they are sensitive to different processes at the surface.

GPS and MSBAS measurements are fundamentally different. GPS are a point-based elevation change method measuring the height change of a monument either buried in the ground or attached to a building. DInSAR measures the relative change between repeat pass satellite acquisitions, averaged over 100 m pixel areas. Table 5.3.1 shows some agreement between the rates at HRNP, KHEP, DHK2, MPUC and VLKA. There is also some agreement between the vertical linear deformation rates in Table 5.3.2.

In Figures 5.4.2-5.4.6 (a) we analyze the removal of the sinusoid as in Equation 5.4.1 and in Figures 5.4.2-5.4.6 (b) we recompute the regression line for the deformation signal with the sinusoid removed.

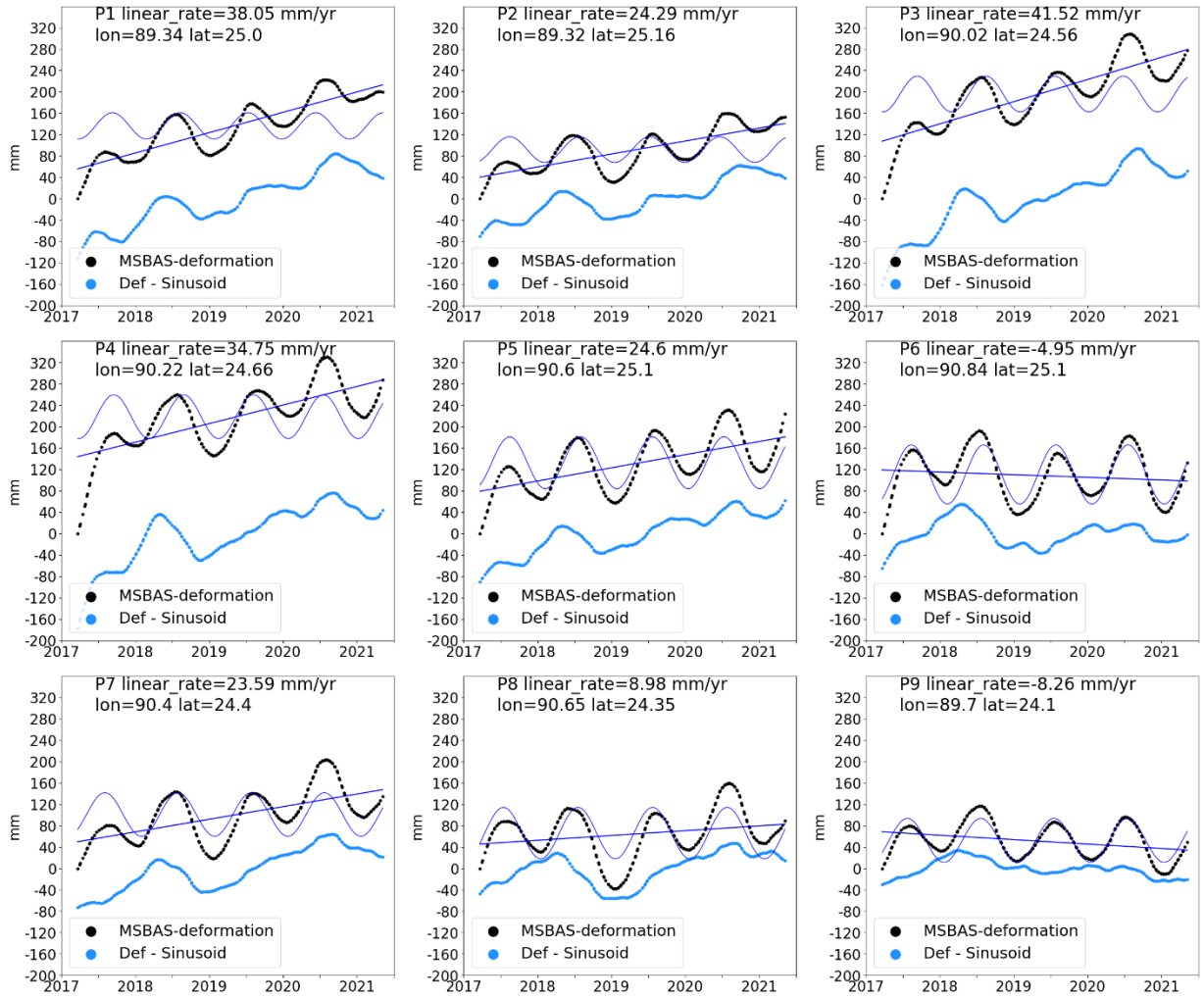


**Figure 5.4.2 (a):** Time series for locations shown in Figure 4.1.1 with best fit sinusoid. Regression line is shown for best fit linear trend of MSBAS-deformation points.

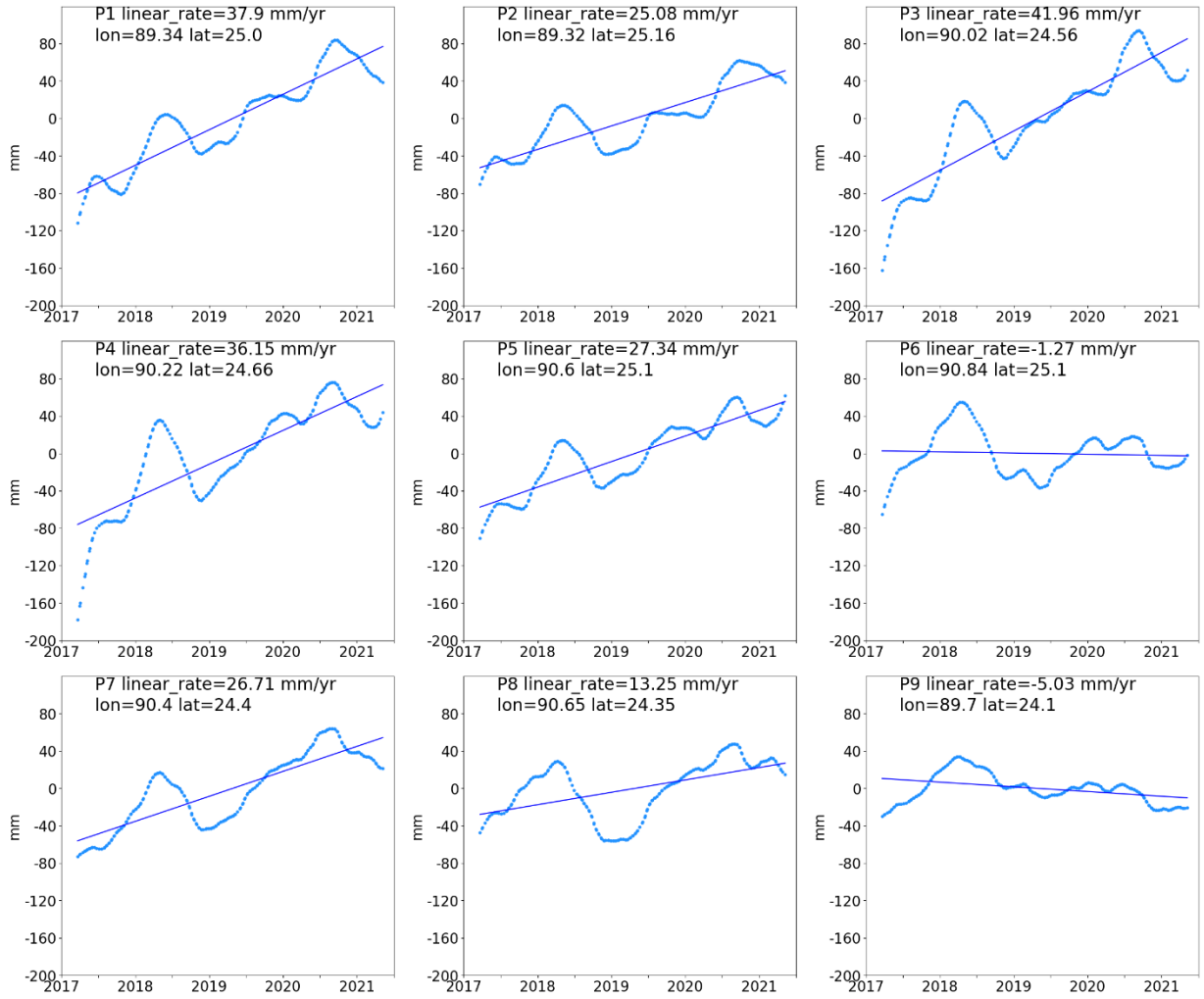


**Figure 5.4.2 (b):** Time series for locations as shown in Figure 4.1.1 with best fit sinusoid removed. Regression line is shown for the best linear trend.

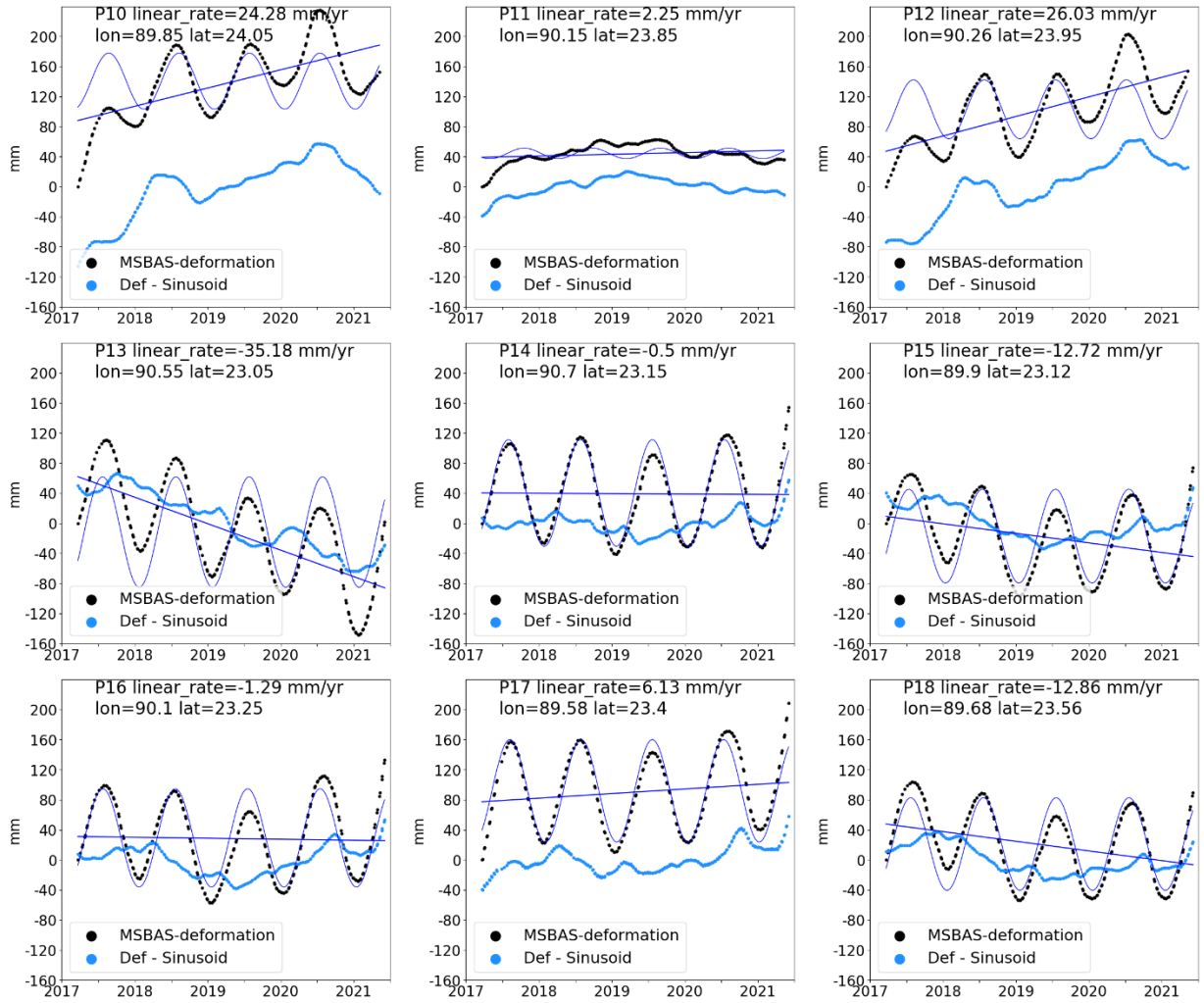


**Figure 5.4.3 (a):** Time series for locations as shown in Figure 4.1.1 with best fit sinusoid. Regression line is shown for best fit linear trend of MSBAS-deformation points.

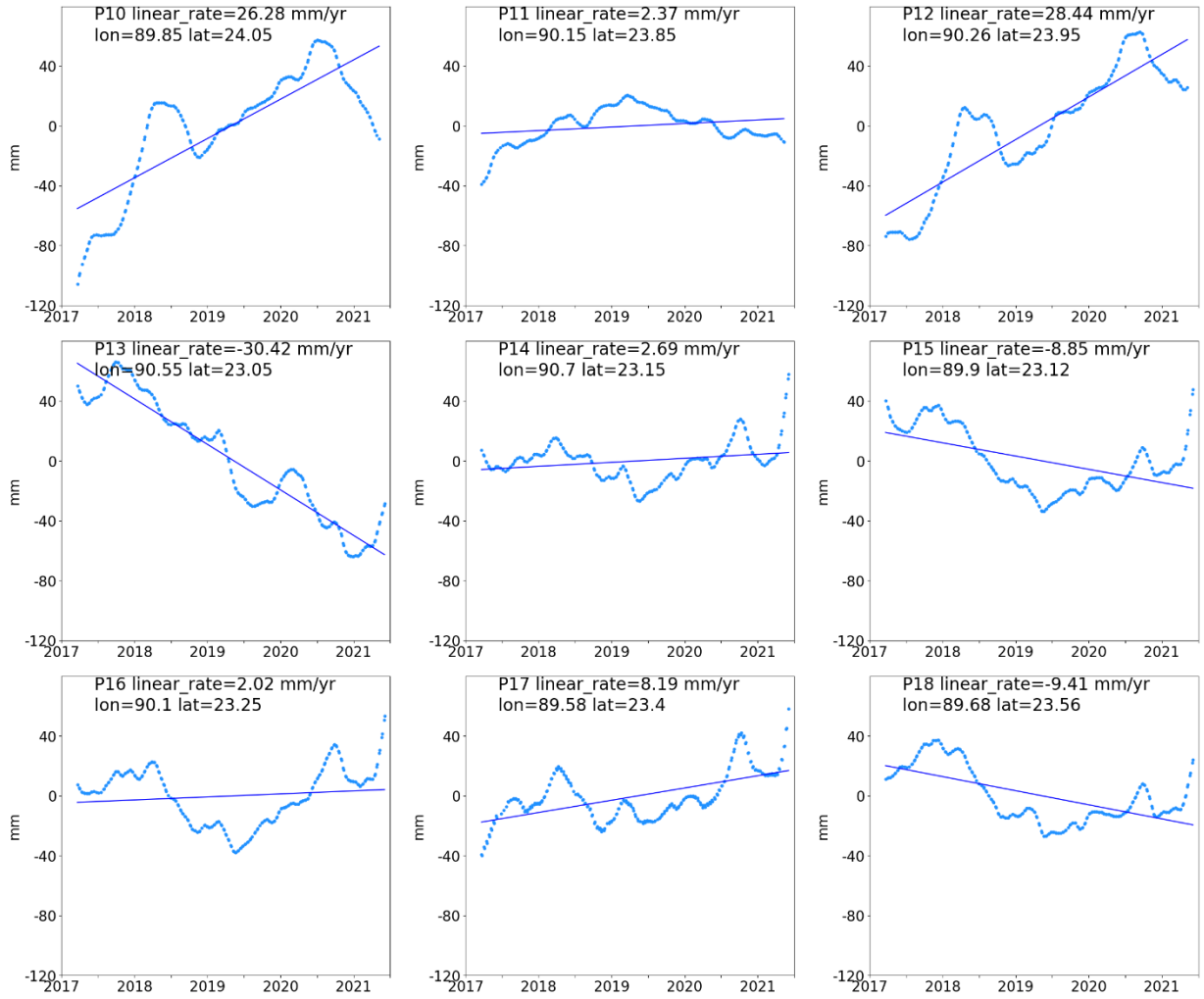


**Figure 5.4.3 (b):** Time series for locations as shown in Figure 4.1.1 with best fit sinusoid removed. Regression line is shown for the best linear trend.

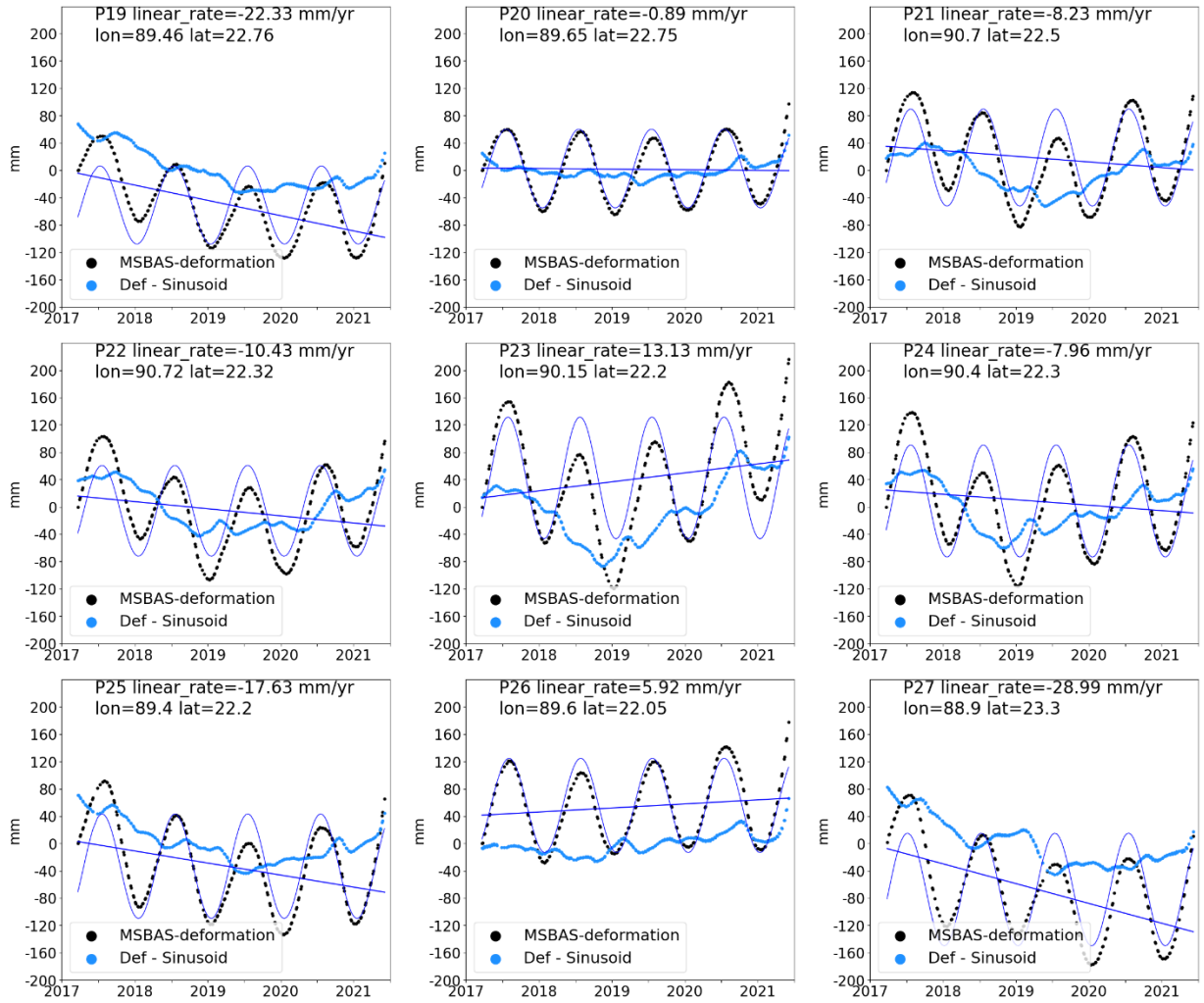


**Figure 5.4.4 (a):** Time series for locations as shown in Figure 4.1.1 with best fit sinusoid. Regression line is shown for best fit linear trend of MSBAS-deformation points.

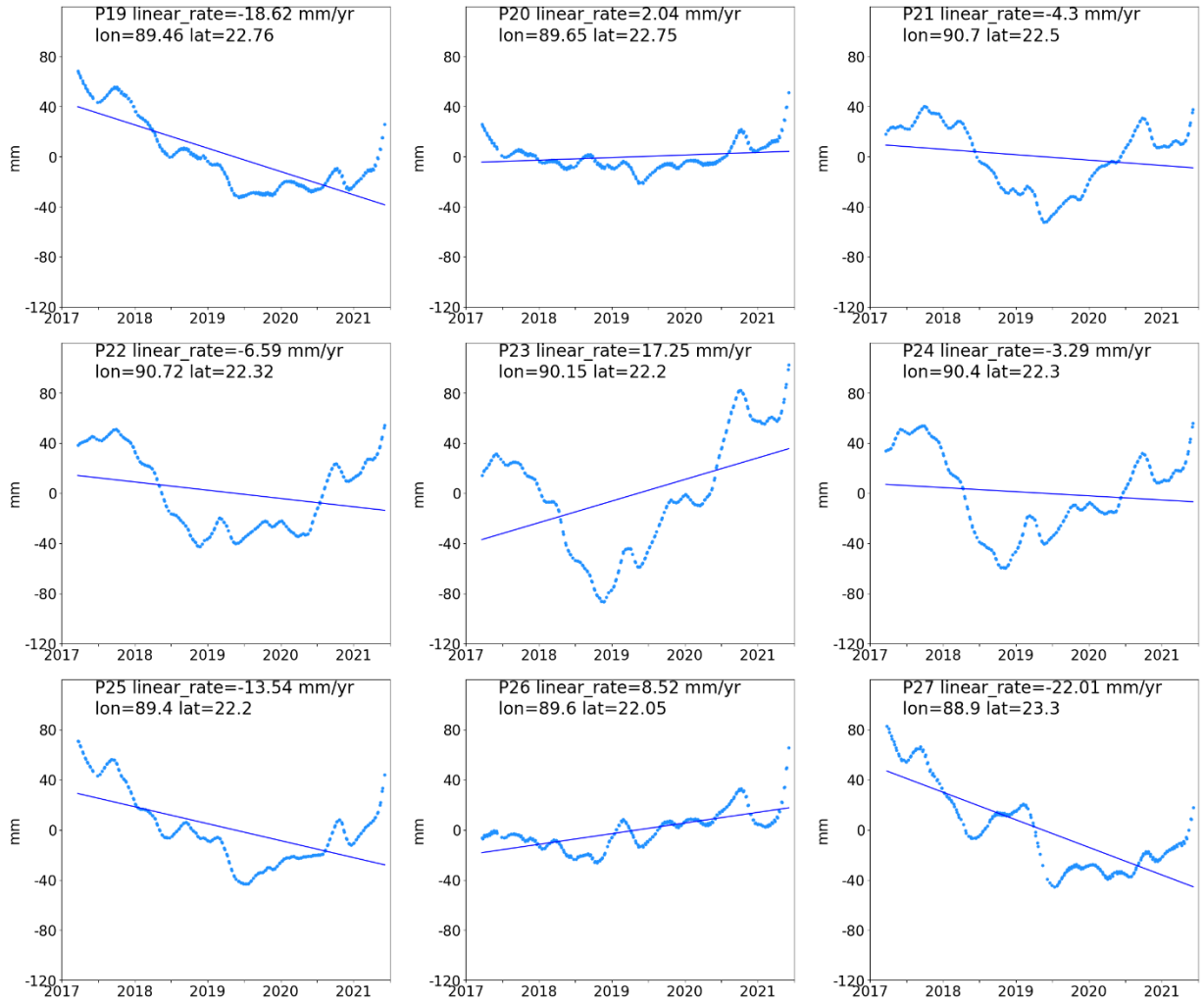


**Figure 5.4.4 (b):** Time series for locations as shown in Figure 4.1.1 with best fit sinusoid removed. Regression line is shown for the best linear trend.

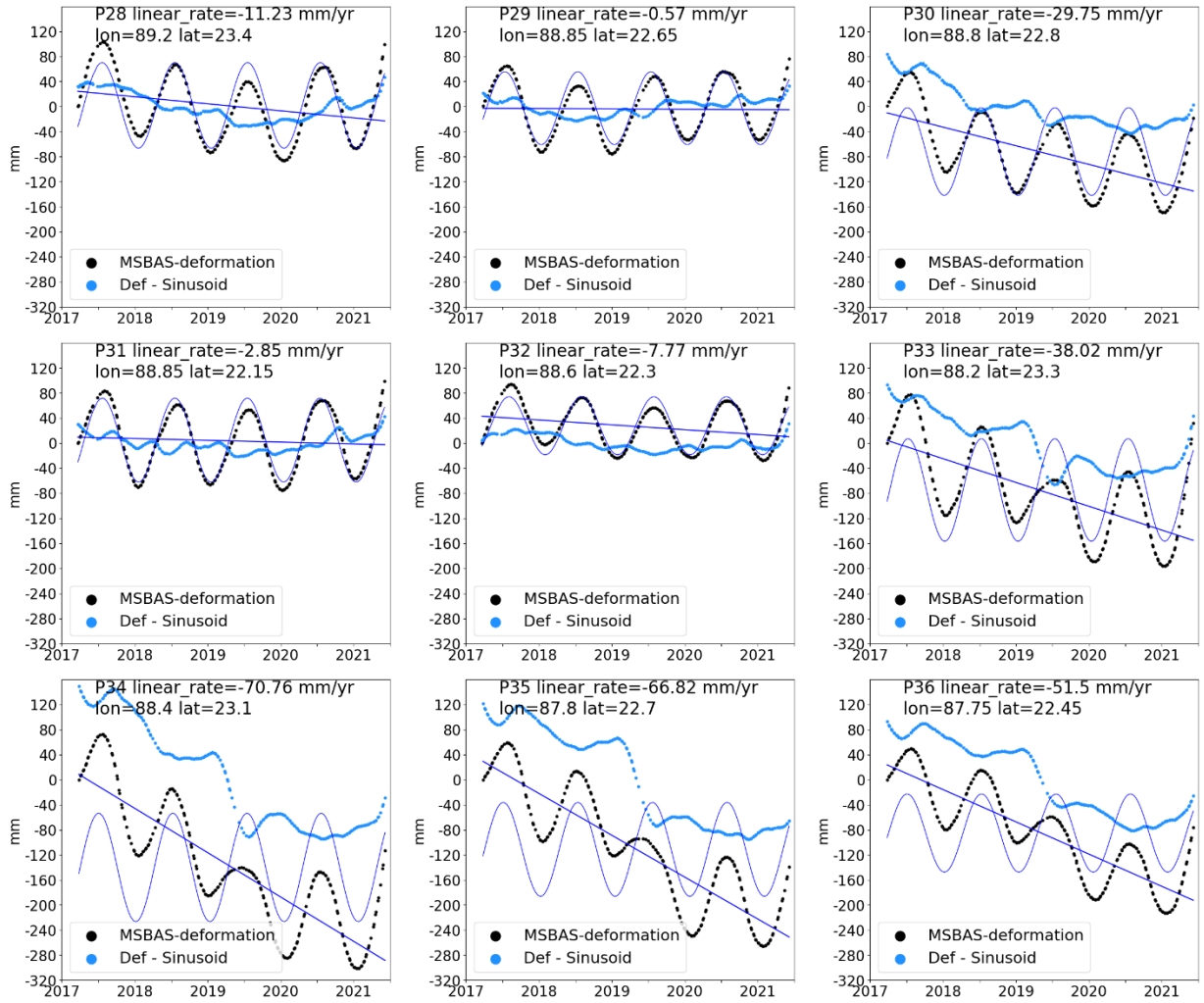


**Figure 5.4.5 (a):** Time series for locations as shown in Figure 4.1.1 with best fit sinusoid. Regression line is shown for best fit linear trend of MSBAS-deformation points.

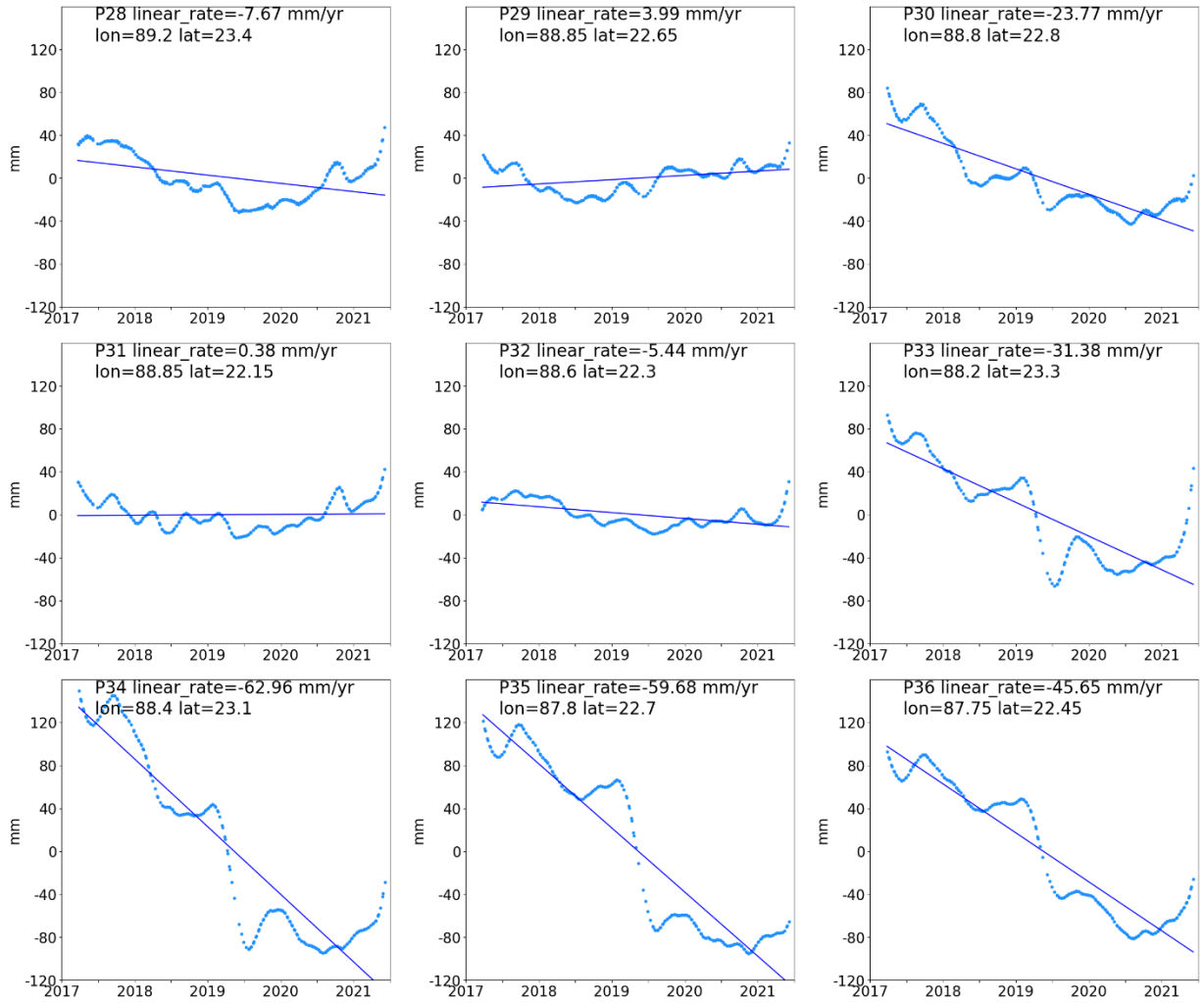


**Figure 5.4.5 (b):** Time series for locations as shown in Figure 4.1.1 with best fit sinusoid removed. Regression line is shown for the best linear trend.

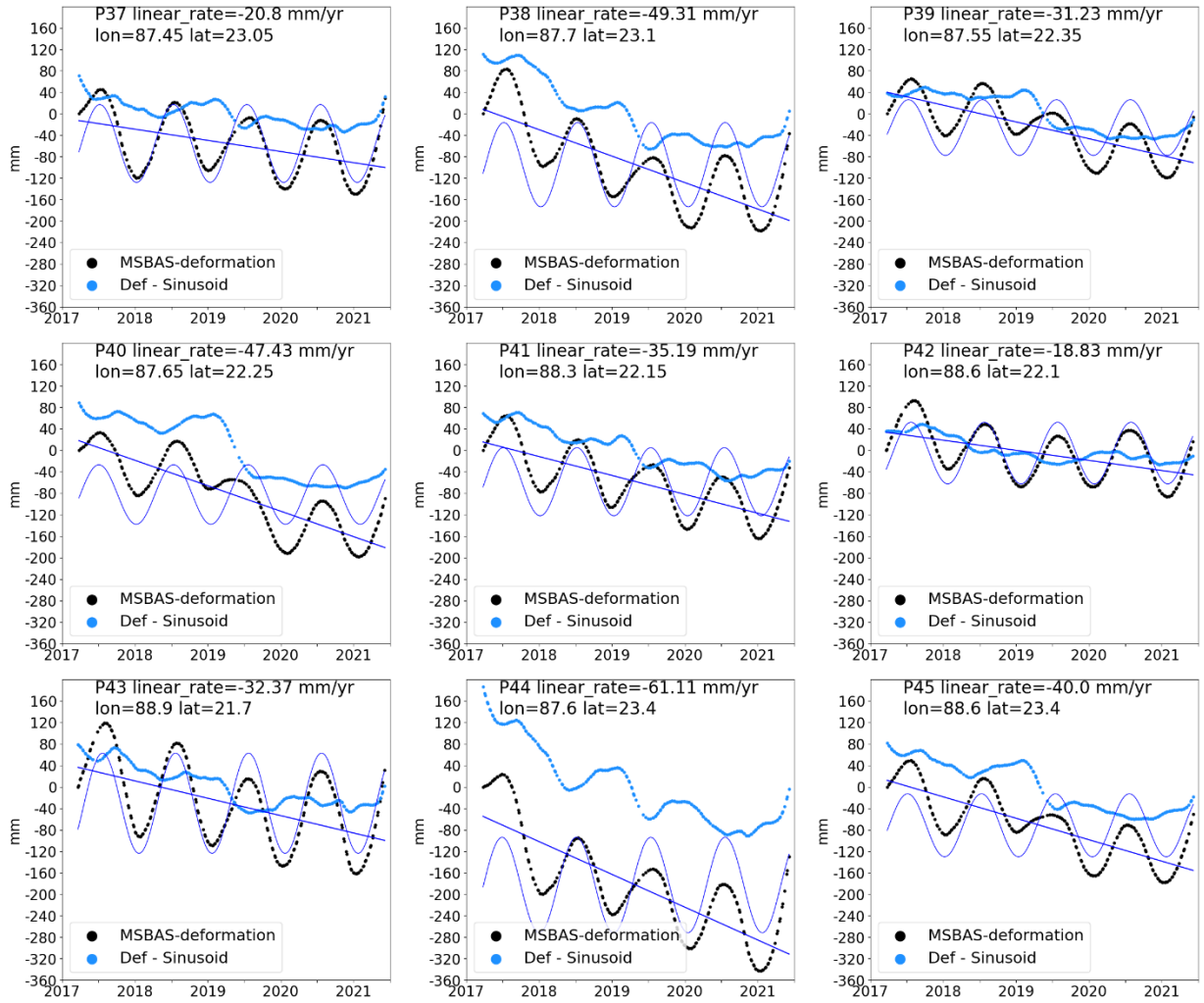


**Figure 5.4.6 (a):** Time series for locations as shown in Figure 4.1.1 with best fit sinusoid. Regression line is shown for best fit linear trend of MSBAS-deformation points.

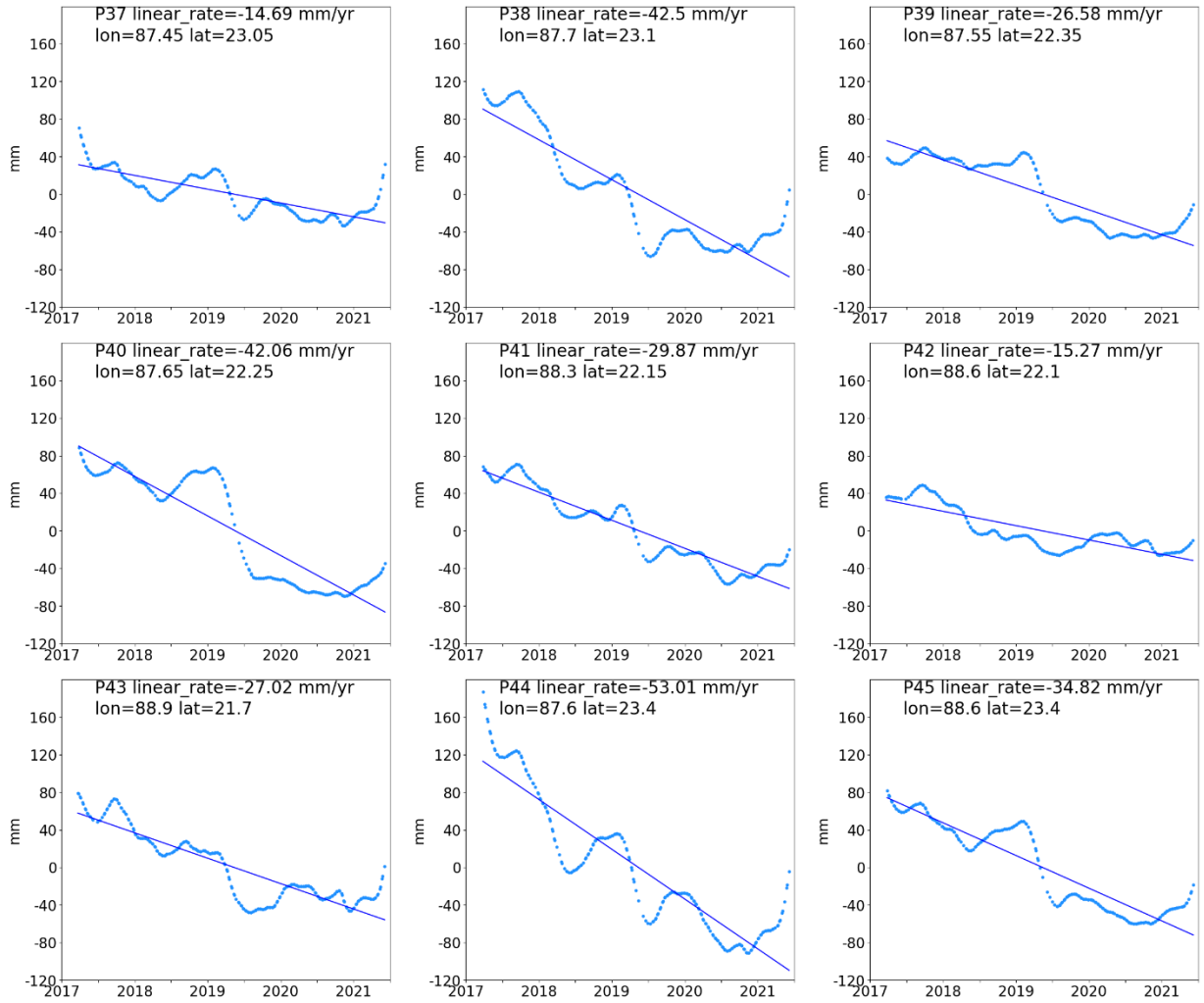


**Figure 5.4.6 (b):** Time series for locations as shown in Figure 4.1.1 with best fit sinusoid removed. Regression line is shown for the best linear trend.

The monsoonal sinusoidal signal in the original analysis essentially masks any other signal which might be present within the MSBAS time series, as the amplitude of the sinusoidal signal is so large. The goal of removing the sinusoidal signal is to better understand the processes occurring in this region. Thus, for the 45 points shown in Figure 4.1.1, we removed the sinusoidal signal from the time series and recomputed the regression lines for each. Given we are only removing the sinusoid, the vertical linear deformation rates should remain relatively unchanged from the vertical linear deformation rate calculated from the deformation with a sinusoidal signal. Comparing vertical linear deformation rates computed with the sinusoid and

the removal of the sinusoid does show that the vertical linear deformation rates do remain relatively unchanged, but they are different by up to 10 mm/yr in some cases. Figures 5.4.2-5.4.6 (b) show more stable deformation with most of the sinusoid removed, although it does still exist in a few cases, as the sinusoid is not uniform from year to year. In these residual time series, we observed both linear subsidence rates and nonlinear changes with time.

### 5.5 Error sources

There exist several potential error sources in the DInSAR and time series results. We discussed several sources of these potential errors earlier, including topography and NDVI related to coherence. There also exists potential atmospheric errors which were not fully accounted for with the GACOS, as it is a model built on existing data, available at varying resolutions and accuracy, and therefor is not perfect. This atmospheric signal is potentially significant in Bangladesh due to the monsoon season. Thus, any remaining atmospheric signal could potentially contaminate the final vertical linear deformation rate. Finally, to correct for the low coherence, which can cause decorrelation and speckle noise in the wrapped interferograms we apply the Goldstein phase filter. This filter itself can introduce artifacts, especially where the coherence is lowest. This could then potentially cause phase unwrapping errors and contaminate the final vertical linear deformation rates as well.

### 5.6 Future work

Future work will consist of increasing the length of the time series which should help significantly in computing more accurate vertical linear deformation rates. Incorporation of a high-resolution DEM into the processing also will significantly help by increasing the coherence in the region due to better back geocoding. Higher resolution deformation maps can be estimated, as the current resolution is100 m. In addition, future efforts should investigate whether

DInSAR can be used to measure canopy growth, as in the Sundarbans. Finally, the upcoming launch of NISAR in 2023 will provide L-band and S-band SAR data, which can be used in combination with C-band SAR to greatly improve results. L-band SAR can retain much higher coherence in a region such as Bangladesh (Higgins et al., 2014) and thus provide more reliable results with potentially less error. Combining these data sources would also provide much higher temporal resolution. L-band combined with C-band SAR also could potentially resolve what is happening in the Sundarbans, as they each have different backscatter characteristics for forest or canopy cover as shown in Figure 3.6.1.

### 6. DInSAR Time Series Conclusion

DInSAR time series analysis was used in this study to quantify the deformation (subsidence/uplift) of the GBM. We acquired approximately 650 ascending and 550 descending Sentinel-1A SLC's from 10 frames spanning from March 2017 to June 2021. We applied DInSAR processing to the SLC's using SNAP and where able to derive time series combing the ascending and descending data using the MSBAS inversion software. The resulting time series derived from MSBAS were mosaicked into a single image and referenced to the continuous GPS station DHAK. This resulted in a final vertical linear deformation rate map with rates ranging from 25 to -30 mm/yr. We found the overall mean to be -3.36 mm/yr and approximately 95% of the derived vertical linear deformation rates were in the range of -28.81 to 22.09 mm/yr. Thus, overall, the GBM has more subsidence than uplift. Further, time series results show a strong sinusoidal seasonal signal with a local maxima approximately mid-year and the local minima approximately at the start of each year. We interpret this to be caused by the poroelastic expansion of the clays in the GBM caused by the initial start of the monsoon. Eventually, the sediments become fully water loaded and there can be no more poroelastic expansion and thus

the pressure from the monsoon causes relative subsidence of the delta starting mid-year which continues until approximately the start of the next year as the monsoon eventually recedes.

To identify what was causing estimated vertical linear deformation rates we analyzed topography, NDVI and a geological overlay of the region. The GBM is relatively flat, except for the westernmost portion, which sees an increase in elevation by about 100 m relative to the rest of the delta. This causes the vertical linear deformation rate map at 87.5E to display a large region of uplift which we attribute to residual topography. The remainder of the deformation map is found not to be insignificantly correlated with the topography. We then compared the NDVI to the vertical linear deformation rate map as well the averaged coherence map. We found two potential locations of spatial correlation between the NDVI and the vertical linear deformation rate map. Comparison between the NDVI and the averaged coherence map suggests that for low NDVI we typically have higher coherence, such as within cities, and for regions of higher NDVI, such as the Sundarbans, we typically have lower coherence.

The geological map is overlain on the deformation map to identify potential regions of spatial correlation. The vertical linear deformation rates north of 24N latitude tend to display uplift within the Barind Clay Residuum (rb), Alluvial Silts (asl), Madhupur Clay Residuum (rm) and the Alluvial Silts and Clays (asc). We see subsidence within the Marsh Clay and Peat (ppc) and the Young Gravelly Sand (afy). The Alluvial Silt and Clay (asc) begins to subside further south of 24N located around P11 and DHAK. South of 24N we see more moderate rates of uplift and similar rates of subsidence. The Deltaic Silts (dsl) and the Mangrove Swamp Deposits (dsw) consist of primarily uplift with some subsidence. The Marsh and Clay Peat in this region, which is located at P15 shows primarily subsidence which is the same as we saw in the region to the northeast. The Estuarine Deposits (de) and the Deltaic Sands (dsd) both display subsidence.

We compare the MSBAS-derived vertical linear deformation rates to GPS derived rates and find somewhat reasonable agreement between the two rates. Specifically, we see reasonable agreement between continuous GPS-derived vertical linear rates at HRNP, KHEP, DHK2, MPUC and VLKA. There is variable agreement between the campaign-derived GPS-derived vertical linear rates and the MSBAS-derived vertical linear rates. The sinusoidal signal was removed from the selected 45 time series and the regression recomputed for each. This causes minimal change in the vertical linear deformation rates but allows us to better interpret what may be occurring in the region.

**References**

Ajadi, O.A.; Meyer, F.J.; Webley, P.W. Change Detection in Synthetic Aperture Radar Images Using a Multiscale-Driven Approach. Remote Sens. 2016, 8, 482.

Alam, M. K., A. K. M. Hasan, M. R. Khan, and J. W. Whitney (2001), Geological Map of Bangladesh, digitally compiled by F. M. Persits, C. J. Wandrey, R. C. Millici, and A. Manwar, U.S. Geological Survey Open-File Report 97-470-H, https://doi.org/10.3133/ofr97470H.

Alexey, N., Alois, K., Gradient boosting machines, a tutorial. Frontiers in Neurorobotics. 2013. DOI=10.3389/fnbot.2013.00021.

Alsdorf, D. E., E. Rodrı´guez, and D. P. Lettenmaier (2007), Measuring surface water from space, Rev. Geophys., 45, RG2002, doi:10.1029/2006RG000197.

Amitrano, D., Di Martino, G., Iodice, A., Riccio, D., Ruello, G.: A new framework for SAR multitemporal data RGB representation: rationale and products. IEEE Trans. Geosci. Remote Sens. 53(1), 117–133 (2015).

André Twele, Wenxi Cao, Simon Plank & Sandro Martinis (2016) Sentinel-1-based flood mapping: a fully automated processing chain, International Journal of Remote Sensing, 37:13, 2990-3004, DOI: 10.1080/01431161.2016.1192304

Auerbach, L., Goodbred Jr, S., Mondal, D. et al. Flood risk of natural and embanked landscapes on the Ganges–Brahmaputra tidal delta plain. Nature Clim Change 5, 153–157 (2015). https://doi.org/10.1038/nclimate2472

Barnard PL, Erikson LH, Foxgrover AC, Hart JAF, Limber P, O'Neill AC, van Ormondt M, Bates, P.D., Horritt, M.S., Aronica, G., Beven, K.: Bayesian updating of flood inundation likelihoods conditioned on flood extent data. Hydrol. Process. 18(17), 3347–3370 (2004). doi:10.1002/hyp.1499

Bates, P.D., Wilson, M.D., Horritt, M.S., Mason, D.C., Holden, N., Currie, A.: Reach scale floodplain inundation dynamics observed using airborne synthetic aperture radar imagery: data analysis and modelling. J. Hydrol. 328(1–2), 306–318 (2006). doi:10.1016/j.jhydrol.2005.12.028

Bayik, C., Abdikan, S., Ozbulak, G., Alasag, T., Aydemir, S., and Balik Sanli, F.: EXPLOITING MULTI-TEMPORAL SENTINEL-1 SAR DATA FOR FLOOD EXTEND MAPPING, Int. Arch. Photogramm. Remote Sens. Spatial Inf. Sci., XLII-3/W4, 109-113, https://doi.org/10.5194/isprs-archives-XLII-3-W4-109-2018, 2018.

Becker, Melanie & Papa, Fabrice & Karpytchev, Mikhail & Delebecque, Caroline & Krien, Yann & Khan, Md Jamal Uddin & Ballu, Valérie & Durand, Fabien & Le Cozannet, Goneri & Islam, A. & Calmant, Stéphane & Shum, C.K.. (2020). Water level changes, subsidence, and sea

level rise in the Ganges–Brahmaputra–Meghna delta. Proceedings of the National Academy of Sciences. 117. 201912921. 10.1073/pnas.1912921117.

Bovolo, F., Bruzzone, L.: A split-based approach to unsupervised change detection in largesize multitemporal images: application to tsunami-damage assessment. IEEE Trans. Geosci. Remote Sens. 45(6), 1658–1669 (2007). doi:10.1109/TGRS.2007.895835

Brakenridge, G.R., DFO Flood Observatory, University of Colorado, February 2021. Global Active Archive of Large Flood Events, 1985-Present, accessed 15 April 2021.

Breiman, L. Random Forests. Machine Learning 45, 5–32 (2001). https://doi.org/10.1023/A:1010933404324

Brown, Sally & Nicholls, R.J.. (2015). Subsidence and human influences in mega deltas: The case of the Ganges–Brahmaputra–Meghna. Science of The Total Environment. 527. 10.1016/j.scitotenv.2015.04.124.

Cao, H., Zhang, H., Wang, C., Zhang, B., 2019. Operational Flood Detection Using Sentinel-1 SAR Data over Large Areas. Water, 11(4), 786.

Cao, H.; Zhang, H.; Wang, C.; Zhang, B. Operational Flood Detection Using Sentinel-1 SAR Data over Large Areas. Water 2019, 11, 786.

Chen, C. W.and Zebker, H. A., "Phase unwrapping for large SAR interferograms: statistical segmentation and generalized network models," in IEEE Transactions on Geoscience and Remote Sensing, vol. 40, no. 8, pp. 1709-1719, Aug. 2002, doi: 10.1109/TGRS.2002.802453.

Chen, L.-C.; Papandreou, G.; Kokkinos, L.; Murphy, K.; Yuille, A.L. Semantic image segmentation with deep convolutional nets and fully connected CRFs. International Conference on Learning Representations (ICLR), 2015.

Cohen, J. (1960). A Coefficient of Agreement for Nominal Scales. Educational and Psychological Measurement, 20(1), 37–46. https://doi.org/10.1177/001316446002000104
Copernicus Sentinel Data, 2015. Retrieved from ASF DAAC on April, 2020, processed by ESA. https://search.asf.alaska.edu/

Cossu, Roberto & Brito, Fabrice & Colin, Olivier & Fusco, Luigi & Goncalves, P. & Lavalle, M. & Paces, M.. (2007). Global automatic orthorectification of asar products in ESRIN G-POD.

D. Small, "Flattening Gamma: Radiometric Terrain Correction for SAR Imagery," in IEEE Transactions on Geoscience and Remote Sensing, vol. 49, no. 8, pp. 3081-3093, Aug. 2011. doi: 10.1109/TGRS.2011.2120616.

D'Addabbo A., Refice A., Capolongo D., Pasquariello G., Manfreda S. (2018) Data Fusion Through Bayesian Methods for Flood Monitoring from Remotely Sensed Data. In: Refice A., D'Addabbo A., Capolongo D. (eds) Flood Monitoring through Remote Sensing. Springer Remote Sensing/Photogrammetry. Springer, Cham, Pierdicca N., Pulvirenti L., Chini M. (2018) Flood

Mapping in Vegetated and Urban Areas and Other Challenges: Models and Methods. In: Refice A., D'Addabbo A., Capolongo D. (eds) Flood Monitoring through Remote Sensing. Springer Remote Sensing/Photogrammetry. Springer, Cham

D'Addabbo, A., Refice, A., Pasquariello, G., Lovergine, F.P., Capolongo, D., Manfreda, S.: A Bayesian network for flood detection combining SAR imagery and ancillary data. IEEE Trans. Geosci. Remote Sens. 54(6), 3612–3625 (2016). doi:10.1109/TGRS.2016.2520487
Dellepiane S.G., Gemme L. (2018) Adaptive SAR Image Processing Techniques to Support Flood Monitoring from Earth Observation Data. In: Refice A., D'Addabbo A., Capolongo D. (eds) Flood Monitoring through Remote Sensing. Springer Remote Sensing/Photogrammetry. Springer, Cham

Dellepiane, S., De Laurentiis, R., & Giordano, F. (2004). Coastline extraction from SAR images and a method for the evaluation of the coastline precision. Pattern Recognition Letters, 25(13), 1461-1470. doi:10.1016/j.patrec.2004.05.022

Dellepiane, S.G., Angiati, E.: A new method for cross-normalization and multitemporal visualization of SAR images for the detection of flooded areas. IEEE Trans. Geosci. Remote Sens. 50(7), 2765–2779 (2012)

Demirkaya, O., H. Asyali, M., 2004. Determination of image bimodality thresholds for different intensity distributions. Signal Processing: Image Communication, 19(6), 507-516. doi:https://doi.org/10.1016/j.image.2004.04.002

doi: 10.1109/TNNLS.2015.2435783
Edmonds, D.A., Caldwell, R.L., Brondizio, E.S. et al. Coastal flooding will disproportionately impact people on river deltas. Nat Commun 11, 4741 (2020). https://doi.org/10.1038/s41467-020-18531-4

F. Ayoub, C.E. Jones, M.P. Lamb, B. Holt, J.B. Shaw, D. Mohrig, W. Wagner, Inferring surface currents within submerged, vegetated deltaic islands and wetlands from multi-pass airborne SAR, Remote Sensing of Environment, Volume 212, 2018, Pages 148-160, ISSN 0034-4257, https://doi.org/10.1016/j.rse.2018.04.035. (http://www.sciencedirect.com/science/article/pii/S0034425718301913)

Farr, T. G., et al. (2007), The Shuttle Radar Topography Mission, Rev. Geophys., 45, RG2004, doi:10.1029/2005RG000183.

G. R. Brakenridge , B. T. Tracy & J. C. Knox (1998) Orbital SAR remote sensing of a river flood wave, International Journal of Remote Sensing, 19:7, 1439-1445, DOI: 10.1080/014311698215559

Gabriel, A. K., Goldstein, R. M., and Zebker, H. A. (1989), Mapping small elevation changes over large areas: Differential radar interferometry, J. Geophys. Res., 94( B7), 9183– 9191, doi:10.1029/JB094iB07p09183.

Giordano, F., Goccia, M., Dellepiane, S.: Segmentation of coherence maps for flood damage assessment. In: IEEE International Conference on Image Processing 2005, ICIP 2005, Genova, Italy, vol. 2, pp. 233–236. IEEE (Institute of Electrical and Electronics Engineers Inc., Piscataway, New Jersey, US) (2005)

Giustarini, L., Hostache, R., Kavetski, D., Chini, M., Corato, G., Schlaffer, S., Matgen, P.: Probabilistic flood mapping using synthetic aperture radar data. IEEE Trans. Geosci. Remote Sens. 1–12 (2016). doi:10.1109/TGRS.2016.2592951
Goldstein, R.M. and Werner, C.L., "Radar Interferogram Phase Filtering for Geophysical Applications," Geophysical Research Letters, 25, 4035-4038, 1998

Hallegatte, S., et al. "Future Flood Losses in Major Coastal Cities." Nature Climate Change, vol. 3, no. 9, 2013, pp. 802-806.

Hallegatte, Stephane ,Green, Colin, Nicholls, Robert J., Corfee-Morlot, August 2013. Future flood losses in major coastal cities, Nature Publishing Group UR - https://doi.org/10.1038/nclimate1979 10.1038/nclimate1979

Hanqiu Xu (2006) Modification of normalised difference water index (NDWI) to enhance open water features in remotely sensed imagery, International Journal of Remote Sensing, 27:14, 3025-3033, DOI: 10.1080/01431160600589179

Hess, L. L., Melack, J. M., Novo, E. M. L. M., Barbosa, C. C. F., & Gastil, M. (2003). Dual-season mapping of wetland inundation and vegetation for the central amazon basin. Remote Sensing of Environment, 87(4), 404-428. doi:10.1016/j.rse.2003.04.001

Higgins, S. A., I. Overeem, M. S. Steckler, J. P. M. Syvitski, L. Seeber, and S. H. Akhter (2014), InSAR measurements of compaction and subsidence in the Ganges-Brahmaputra Delta, Bangladesh, J. Geophys. Res. Earth Surf., 119, 1768–1781, doi:10.1002/2014JF003117.

Horritt, M.S., Mason, D.C., Luckman, A.J.: Flood boundary delineation from synthetic aperture radar imagery using a statistical active contour model. Int. J. Remote Sens. 22(13), 2489–2507 (2001) https://www.nature.com/articles/nclimate1979#supplementary-information

Integrating SAR and derived products into operational volcano monitoring and decision support systems, ISPRS Journal of Photogrammetry and Remote Sensing, Volume 100, 2015, Pages 106-117, ISSN 0924-2716, https://doi.org/10.1016/j.isprsjprs.2014.05.009.

J.-B. Henry , P. Chastanet , K. Fellah & Y.-L. Desnos (2006) Envisat multi-polarized ASAR data for flood mapping, International Journal of Remote Sensing, 27:10, 1921-1929, DOI: 10.1080/01431160500486724.

Joyce, K. E., Belliss, S. E., Samsonov, S. V., McNeill, S. J., & Glassey, P. J. (2009). A review of the status of satellite remote sensing and image processing techniques for mapping natural hazards and disasters. Progress in Physical Geography: Earth and Environment, 33(2), 183–207. https://doi.org/10.1177/0309133309339563.

Kay, Susan & Caesar, John & Wolf, Judith & Bricheno, Lucy & Nicholls, Robert & Islam, A. & Haque, Anisul & Pardaens, Anne & Lowe, Jason. (2015). Modelling the increased frequency of extreme sea levels in the Ganges-Brahmaputra-Meghna delta due to sea level rise and other effects of climate change. Environ. Sci.: Processes Impacts. 17. 10.1039/C4EM00683F.

Krien, Y., Karpytchev, M., Ballu, V., Becker, M., Grall, C., Goodbred, S., et al. (2019). Present-day subsidence in the Ganges-Brahmaputra-Meghna Delta: Eastern amplification of the Holocene sediment loading contribution. Geophysical Research Letters, 46, 10,764–10,772. https://doi.org/10.1029/ 2019GL083601

Kussul, N., Shelestov, A., Skakun, S.: Flood monitoring from SAR data. In: Use of Satellite and In-Situ Data to Improve Sustainability, pp. 19–29. Springer, Netherlands (2011).
Long, S., Fatoyinbo, T., & Policelli, F. (2014). Flood extent mapping for namibia using change detection and thresholding with SAR. Environmental Research Letters, 9(3), 1-9. doi:10.1088/1748-9326/9/3/035002

M. Gong, J. Zhao, J. Liu, Q. Miao and L. Jiao, Change Detection in Synthetic Aperture Radar Images Based on Deep Neural Networks, IEEE Transactions on Neural Networks and Learning Systems, vol. 27, no. 1, pp. 125-138, Jan. 2016.

Manavalan, R.: SAR image analysis techniques for flood area mapping – literature survey. Earth Sci. Inf. (2016). doi:10.1007/s12145-016-0274-2

Manfreda S., Samela C., Troy T.J. (2018) The Use of DEM-Based Approaches to Derive a Priori Information on Flood-Prone Areas. In: Refice A., D'Addabbo A., Capolongo D. (eds) Flood Monitoring through Remote Sensing. Springer Remote Sensing/Photogrammetry. Springer, Cham

Manjusree, P., Prasanna Kumar, L., Bhatt, C.M., Rao, G.S., Bhanumurthy, V.: Optimization of threshold ranges for rapid flood inundation mapping by evaluating backscatter profiles of high incidence angle SAR images. Int. J. Disaster Risk Sci. 3(2), 113–122 (2012). doi:10.1007/s13753-012-0011-5

Markus Boldt, Antje Thiele, Karsten Schulz, Franz J. Meyer, and Stefan Hinz "Practical approach for synthetic aperture radar change analysis in urban environments," Journal of Applied Remote Sensing 13(3), 034528 (25 September 2019). https://doi.org/10.1117/1.JRS.13.034528.

Marti-Cardona, B., Lopez-Martinez, C., Dolz-Ripolles, J., Bladè-Castellet, E.: ASAR polarimetric, multi-incidence angle and multitemporal characterization of Doñana wetlands for

flood extent monitoring. Remote Sens. Environ. 114(11), 2802–2815 (2010). doi:10.1016/j.rse.2010.06.015

Martinis, S., Twele, A., Voigt, S.: Towards operational near real-time flood detection using a split-based automatic thresholding procedure on high resolution TerraSAR-X data. Nat. Hazards Earth Syst. Sci. 9(2), 303–314 (2009). doi:10.5194/nhess-9-303-2009

Martinis, S., Twele, A., Voigt, S.: Unsupervised extraction of flood-induced backscatter changes in SAR data using Markov image modeling on irregular graphs. IEEE Trans. Geosci. Remote Sens. 49(1), 251–263 (2011)
Matgen, P., Hostache, R., Schumann, G., Pfister, L., Hoffmann, L., Savenije, H.H.G.: Towards an automated SAR-based flood monitoring system: lessons learned from two case studies. Phys. Chem. Earth A/B/C. 36(7), 241–252 (2011).

Matgen, P., Schumann, G.J.P., Henry, J.B., Hoffmann, L., Pfister, L.: Integration of SARderived river inundation areas, high-precision topographic data and a river flow model toward near real-time flood management. Int. J. Appl. Earth Obs. Geoinf. 9(3), 247–263 (2007). doi:10.1016/j.jag.2006.03.003

Meyer, F. J., et al., "Applications of a SAR-Based Flood Monitoring Service During Disaster Response and Recovery," IGARSS 2019 - 2019 IEEE International Geoscience and Remote Sensing Symposium, Yokohama, Japan, 2019, pp. 4649-4652. doi: 10.1109/IGARSS.2019.8900495.

Meyer, F.J. , D.B. McAlpin, W. Gong, O. Ajadi, S. Arko, P.W. Webley, J. Dehn,
Meyer, Franz & Ajadi, Olaniyi & Schultz, Lori & Bell, Jordan & Arnoult, Ken & Gens, Rudiger & Nicoll, Jeremy. (2018). An Automatic Flood Monitoring Service from Sentinel-1 SAR: Products, Delivery Pipelines, and Performance Assessment. 6576-6579. 10.1109/IGARSS.2018.8517531.

Milly, P. C. D. Wetherald, R. T. Dunne, K. A. Delworth, T. L. Increasing risk of great floods in a changing climate Nature 2002/01/31/online 415 - 514 Macmillan Magazines Ltd. https://doi.org/10.1038/415514a 10.1038/415514

Musa, Z. N., Popescu, I., and Mynett, A.: A review of applications of satellite SAR, optical, altimetry and DEM data for surface water modelling, mapping and parameter estimation, Hydrol. Earth Syst. Sci., 19, 3755-3769, https://doi.org/10.5194/hess-19-3755-2015, 2015.

Nazir, F., Riaz, M.M., Ghafoor, A., Arif, F.: Brief communication: contrast-stretching-and histogram-smoothness-based synthetic aperture radar image enhancement for flood map generation. Nat. Hazards Earth Syst. Sci. 15(2), 273–276 (2015)

Niculescu, S., Lardeux, C., Hanganu, J.,Mercier, G., David, L.: Change detection in floodable areas of the Danube delta using radar images. Nat. Hazards 78(3), 1899–1916 (2015). doi:10.1007/s11069-015-1809-4

Ningthoujam, R.K.; Balzter, H.; Tansey, K.; Feldpausch, T.R.; Mitchard, E.T.A.; Wani, A.A.; Joshi, P.K. Relationships of S-Band Radar Backscatter and Forest Aboveground Biomass in Different Forest Types. Remote Sens. 2017, 9, 1116.

Ningthoujam, R.K.; Tansey, K.; Balzter, H.; Morrison, K.; Johnson, S.C.M.; Gerard, F.; George, C.; Burbidge, G.; Doody, S.; Veck, N.; Llewellyn, G.M.; Blythe, T. Mapping Forest Cover and Forest Cover Change with Airborne S-Band Radar. Remote Sens. 2016, 8, 577
O'Grady, D., Leblanc, M., Bass, A.: The use of radar satellite data from multiple incidence angles improves surface water mapping. Remote Sens. Environ. 140, 652–664 (2014). doi:10.1016/j.rse.2013.10.006

Physics and Chemistry of the Earth, 83-84, 84-95. doi:10.1016/j.pce.2015.05.002

Pierdicca, N., Pulvirenti, L., Chini,M., Boni, G., Squicciarino, G., Candela, L.: Flood mapping by SAR: possible approaches to mitigate errors due to ambiguous radar signatures. In: IEEE International Geoscience and Remote Sensing Symposium (IGARSS), Quebec City, Canada, pp. 3850–3853. IEEE (Institute of Electrical and Electronics Engineers Inc., Piscataway, New Jersey, US) (2014)

Rahman, M.S. & Di, L. Nat Hazards (2017) 85: 1223. https://doi.org/10.1007/s11069-016-2601-9.

Refice A. et al. (2018) Monitoring Flood Extent and Area Through Multisensor, Multi-temporal Remote Sensing: The Strymonas (Greece) River Flood. In: Refice A., D'Addabbo A., Capolongo D. (eds) Flood Monitoring through Remote Sensing. Springer Remote Sensing/Photogrammetry. Springer, Cham

Refice, A., D'Addabbo, A., & Capolongo, D. (2018;2017;). Flood monitoring through remote sensing (1st 2018 ed.). Cham: Springer. doi:10.1007/978-3-319-63959-8

Rogers, KG and Overeem, I 2017 Doomed to drown? Sediment dynamics in the human-controlled floodplains of the active Bengal Delta. Elem Sci Anth, 5: 66, DOI: https://doi.org/10.1525/elementa.250

Rogers, KG, Steven L. Goodbred, Dhiman R. Mondal, Monsoon sedimentation on the 'abandoned' tide-influenced Ganges–Brahmaputra delta plain, Estuarine, Coastal and Shelf Science, Volume 131, 2013, Pages 297-309, https://doi.org/10.1016/j.ecss.2013.07.014.

Rosen, A, Paul. Principles and Theory of Radar Interferometry. Aug. 2014.

Ruya Xiao, Chen Yu, Zhenhong Li, Xiufeng He. Statistical assessment metrics for InSAR atmospheric correction: Applications to generic atmospheric correction online service for InSAR (GACOS) in Eastern China. International Journal of Applied Earth Observation and Geoinformation. Volume 96, 2021, https://doi.org/10.1016/j.jag.2020.102289.

S. K. McFeeters (1996) The use of the Normalized Difference Water Index (NDWI) in the delineation of open water features, International Journal of Remote Sensing, 17:7, 1425-1432, DOI: 10.1080/01431169608948714

Samsonov, S., d'Oreye, N., Multidimensional time-series analysis of ground deformation from multiple InSAR data sets applied to Virunga Volcanic Province, Geophysical Journal International, Volume 191, Issue 3, December 2012, Pages 1095–1108, https://doi.org/10.1111/j.1365-246X.2012.05669.x

Sandwell, D., Mellors, R., Tong, X., Wei, M., & Wessel, P. (2011). GMTSAR: An InSAR Processing System Based on Generic Mapping Tools.

Schlaffer, S., Chini, M., Giustarini, L., Matgen, P.: Probabilistic mapping of flood-induced backscatter changes in SAR time series. Int. J. Appl. Earth Obs. Geoinf. 56, 77–87 (2017). doi:10.1016/j.jag.2016.12.003

Schreier G., SAR Geocoding: Data and Systems, Wichmann 1993.

Schumann, G., P. D. Bates, M. S. Horritt, P. Matgen, and F. Pappenberger (2009), Progress in integration of remote sensing– derived flood extent and stage data and hydraulic models, Rev. Geophys., 47, RG4001, doi:10.1029/2008RG000274.

Sharma, P., Wang, J., Zhang, M., Woods, C., Kar, B., Bausch, D., Chen, Z., Tiampo, K., Glasscoe, M., Schumann, G., Pierce, M., and Eguchi, R.: DisasterAWARE - A GLOBAL ALERTING PLATFORM FOR FLOOD EVENTS, ISPRS Ann. Photogramm. Remote Sens. Spatial Inf. Sci., VI-3/W1-2020, 107-113, https://doi.org/10.5194/isprs-annals-VI-3-W1-2020-107-2020, 2020.

Sheng, Yaobin & Wang, Yunjia & Ge, Linlin & Rizos, Chris. (2012). Differential radar interferometry and its application in monitoring underground coal mining-induced subsidence.

Singh, A., Meena, G. K., Kumar, S., and Gaurav, K.: ANALYSIS OF THE EFFECT OF INCIDENCE ANGLE AND MOISTURE CONTENT ON THE PENETRATION DEPTH OF L- AND S-BAND SAR SIGNALS INTO THE GROUND SURFACE, ISPRS Ann. Photogramm. Remote Sens. Spatial Inf. Sci., IV-5, 197-202, https://doi.org/10.5194/isprs-annals-IV-5-197-2018, 2018

Small D., Schubert A., Guide to ASAR Geocoding, RSL-ASAR-GC-AD, Issue 1.0, March 2008.

Steckler, M. S., et al. (2013), GPS velocity field in Bangladesh: Delta subsidence, seasonal water loading and shortening across the Burma Accretionary Prism, Poster presented at the 2013 Fall Meeting of the AGU, San Francisco, Calif., 9–12 Dec 2013, Abstract T13D-2566.

Steckler, M. S., Nooner, S. L., Akhter, S. H., Chowdhury, S. K., Bettadpur, S., Seeber, L., and Kogan, M. G. (2010), Modeling Earth deformation from monsoonal flooding in Bangladesh using hydrographic, GPS, and Gravity Recovery and Climate Experiment (GRACE) data, J. Geophys. Res., 115, B08407, doi:10.1029/2009JB007018.

Steckler, Michael S., Bar Oryan, Carol A. Wilson, Céline Grall, Scott L. Nooner, Dhiman R. Mondal, S. Humayun Akhter, Scott DeWolf, Steve L. Goodbred, Synthesis of the distribution of subsidence of the lower Ganges-Brahmaputra Delta, Bangladesh, Earth-Science Reviews, Volume 224, 2022, https://doi.org/10.1016/j.earscirev.2021.103887.

Syvitski, J. P. M., et al. (2009), Sinking deltas due to human activities, Nat. Geosci., 2, 681–686, doi:10.1038/NGEO629.

Tempfli, Klaus & Huurneman, G.C. & Bakker, Wim & Janssen, L.L.F. & Feringa, W.F. & Gieske, Ambro & Grabmaier, K.A. & Hecker, Christoph & Horn, John & Kerle, Norman & Meer, F.D. & Parodi, Gabriel & Pohl, Christine & Reeves, C.V. & Ruitenbeek, F.J.A. & Schetselaar, Ernst & Weir, Michael & Westinga, Eduard & Woldai, Tsehaie. (2009). Principles of remote sensing : an introductory textbook.

(a) Tiampo, K., Huang, L., Simmons, C., Woods, C., Glasscoe, M..; A Machine Learning Approach to the detection of Flood Extent using Sentinel-1A/B Synthetic Aperture Radar. Remote Sens. 2021, 14, x. https://doi.org/10.3390/xxxxx. Publication Pending.

(b) Tiampo, K., Woods, C., et al. "A Machine Learning Approach to Flood Depth and Extent Detection Using Sentinel 1A/B Synthetic Aperture Radar," 2021 IEEE International Geoscience and Remote Sensing Symposium IGARSS, 2021, pp. 558-561, doi: 10.1109/IGARSS47720.2021.9553601.

Ticconi, F., Pulvirenti, L., Pierdicca, N.: Models for scattering from rough surfaces. In: Zhurbenko, V. (ed.) Electromagnetic Waves, Croatia. In Tech. ISBN: 978–953–307–304–0 (2011).

Tikhonov, A.N. and Arsenin, V.Y. (1977) Solutions of Ill-Posed Problems. Winston, New York.

Uddin, K.; Matin, M.A.; Meyer, F.J. Operational Flood Mapping Using Multi-Temporal Sentinel-1 SAR Images: A Case Study from Bangladesh. Remote Sens. 2019, 11, 1581.

Vitousek S, Wood N, Hayden MK, Jones JM. Dynamic flood modeling essential to assess the coastal impacts of climate change. Sci Rep. 2019 Mar 13;9(1):4309. doi: 10.1038/s41598-019-40742-z. PubMed PMID: 30867474; PubMed Central PMCID: PMC6416275.

Westerhoff, R. S., Kleuskens, M. P. H., Winsemius, H. C., Huizinga, H. J., Brakenridge, G. R., and Bishop, C.: Automated global water mapping based on wide-swath orbital synthetic-aperture radar, Hydrol. Earth Syst. Sci., 17, 651–663, 2013, https://doi.org/10.5194/hess-17-651-2013.

Yu Li, Sandro Martinis, Marc Wieland, Urban flood mapping with an active self-learning convolutional neural network based on TerraSAR-X intensity and interferometric coherence,

ISPRS Journal of Photogrammetry and Remote Sensing, Volume 152, 2019, Pages 178-191, ISSN 0924-2716, https://doi.org/10.1016/j.isprsjprs.2019.04.014

Yu, C., Li, Z., & Penna, N. T. (2018). Interferometric synthetic aperture radar atmospheric correction using a GPS-based iterative tropospheric decomposition model. Remote Sensing of Environment, 204, 109-121

Yu, C., Li, Z., Penna, N. T., & Crippa, P. (2018). Generic atmospheric correction model for Interferometric Synthetic Aperture Radar observations. Journal of Geophysical Research: Solid Earth, 123(10), 9202-9222

Yu, C., Penna, N. T., & Li, Z. (2017). Generation of real-time mode high-resolution water vapor fields from GPS observations. Journal of Geophysical Research: Atmospheres, 122(3), 2008-2025Zhang Haiying, NIU Zhenguo, LIU Chuang, SHI Ruixiang. Sundarbans Wetland in 2015 (Bangladesh）[J/DB/OL]. Digital Journal of Global Change Data Repository, 2015. https://doi.org/10.3974/geodb.2015.01.14.V1.

Zelentsov V. et al. (2018) River Flood Forecasting System: An Interdisciplinary Approach. In: Refice A., D'Addabbo A., Capolongo D. (eds) Flood Monitoring through Remote Sensing. Springer Remote Sensing/Photogrammetry. Springer, Cham

Zhang, H. Y., Niu, Z. G., Liu, C., et al. Sundarbans Wetland boundary data (Bangladesh) [J]. Journal of Global Change Data & Discovery, 2017, 1(3): 368. DOI: 10.3974/geodp.2017.03.18.

## Appendix

## Python code snippets

### 1. Code to remove linear planar trends from interferograms

```
import numpy as np
from numpy.linalg import inv

# remove linear trends that exist in image
def detrend_function(array_2_detrend):
    # (ATA)-1ATB
    tif_width = array_2_detrend.shape[1]
    tif_height = array_2_detrend.shape[0]
    x_vector = np.array([i for i in range(0, tif_width, 1)])
    y_vector = np.array([i for i in range(0, tif_height, 1)])

    xx, yy = np.meshgrid(x_vector, y_vector)
    xx_flat = xx.flatten()
    yy_flat = yy.flatten()
    ones_ = np.ones(len(xx_flat))
    b = array_2_detrend.flatten()

    a = np.column_stack((xx_flat, yy_flat, ones_))
    part_1 = inv(np.matmul(a.T, a))
    part_2 = np.matmul(part_1, a.T)
    plane_fit = np.matmul(part_2, b)
    z = xx * plane_fit[0] + yy * plane_fit[1] + plane_fit[2]
    tif_detrend_array = np.where(array_2_detrend == 0.,
                                 0,
                                 array_2_detrend - z).astype('float32')
    return tif_detrend_array
```

## Ascending Orbits Data Granules

### 1. Path 114 Frame 65

"https://datapool.asf.alaska.edu/SLC/SA/S1A_IW_SLC__1SDV_20210720T120406_20210720T120434_038861_0495EC_D2E8.zip",

"https://datapool.asf.alaska.edu/SLC/SA/S1A_IW_SLC__1SDV_20210708T120405_20210708T120433_038686_0490AD_5BD7.zip",

"https://datapool.asf.alaska.edu/SLC/SA/S1A_IW_SLC__1SDV_20210626T120405_20210626T120432_038511_048B6C_20D2.zip",

"https://datapool.asf.alaska.edu/SLC/SA/S1A_IW_SLC__1SDV_20210614T120404_20210614T120432_038336_04862F_30D7.zip",

"https://datapool.asf.alaska.edu/SLC/SA/S1A_IW_SLC__1SDV_20210602T120403_20210602T120431_038161_0480FD_3B06.zip",

"https://datapool.asf.alaska.edu/SLC/SA/S1A_IW_SLC__1SDV_20210521T120402_20210521T120430_037986_047BBD_7D97.zip",

"https://datapool.asf.alaska.edu/SLC/SA/S1A_IW_SLC__1SDV_20210509T120402_20210509T120430_037811_047676_D516.zip",

"https://datapool.asf.alaska.edu/SLC/SA/S1A_IW_SLC__1SDV_20210427T120401_20210427T120429_037636_0470A6_DB76.zip",

"https://datapool.asf.alaska.edu/SLC/SA/S1A_IW_SLC__1SDV_20210415T120401_20210415T120429_037461_046A8E_505C.zip",

"https://datapool.asf.alaska.edu/SLC/SA/S1A_IW_SLC__1SDV_20210403T120400_20210403T120428_037286_046480_3373.zip",

"https://datapool.asf.alaska.edu/SLC/SA/S1A_IW_SLC__1SDV_20210322T120400_20210322T120428_037111_045E7A_911A.zip",

"https://datapool.asf.alaska.edu/SLC/SA/S1A_IW_SLC__1SDV_20210310T120400_20210310T120428_036936_045868_68EB.zip",

"https://datapool.asf.alaska.edu/SLC/SA/S1A_IW_SLC__1SDV_20210226T120400_20210226T120428_036761_04524C_FF4B.zip",

"https://datapool.asf.alaska.edu/SLC/SA/S1A_IW_SLC__1SDV_20210214T120400_20210214T120428_036586_044C38_BB2C.zip",

"https://datapool.asf.alaska.edu/SLC/SA/S1A_IW_SLC__1SDV_20210202T120400_20210202T120428_036411_044618_7C35.zip",

"https://datapool.asf.alaska.edu/SLC/SA/S1A_IW_SLC__1SDV_20210121T120401_20210121T120428_036236_044009_DF34.zip",

"https://datapool.asf.alaska.edu/SLC/SA/S1A_IW_SLC__1SDV_20210109T120401_20210109T120429_036061_0439EE_484C.zip",

"https://datapool.asf.alaska.edu/SLC/SA/S1A_IW_SLC__1SDV_20201228T120402_20201228T120430_035886_0433DB_DB3A.zip",

"https://datapool.asf.alaska.edu/SLC/SA/S1A_IW_SLC__1SDV_20201216T120402_20201216T120430_035711_042DC6_05D7.zip",

"https://datapool.asf.alaska.edu/SLC/SA/S1A_IW_SLC__1SDV_20201204T120403_20201204T120431_035536_0427AA_923D.zip",

"https://datapool.asf.alaska.edu/SLC/SA/S1A_IW_SLC__1SDV_20201122T120403_20201122T120431_035361_0421AA_DEF3.zip",

"https://datapool.asf.alaska.edu/SLC/SA/S1A_IW_SLC__1SDV_20201110T120403_20201110T120431_035186_041BA0_34BD.zip",

"https://datapool.asf.alaska.edu/SLC/SA/S1A_IW_SLC__1SDV_20201029T120404_20201029T120432_035011_041587_D191.zip",

"https://datapool.asf.alaska.edu/SLC/SA/S1A_IW_SLC__1SDV_20201017T120404_20201017T120432_034836_040F8F_8A27.zip",

"https://datapool.asf.alaska.edu/SLC/SA/S1A_IW_SLC__1SDV_20201005T120404_20201005T120432_034661_04096B_4FE6.zip",

"https://datapool.asf.alaska.edu/SLC/SA/S1A_IW_SLC__1SDV_20200923T120403_20200923T120431_034486_040348_3DB6.zip",

"https://datapool.asf.alaska.edu/SLC/SA/S1A_IW_SLC__1SDV_20200911T120403_20200911T120431_034311_03FD13_E41C.zip",

"https://datapool.asf.alaska.edu/SLC/SA/S1A_IW_SLC__1SDV_20200830T120403_20200830T120430_034136_03F6F3_C331.zip",

"https://datapool.asf.alaska.edu/SLC/SA/S1A_IW_SLC__1SDV_20200818T120402_20200818T120430_033961_03F0C7_10A1.zip",

"https://datapool.asf.alaska.edu/SLC/SA/S1A_IW_SLC__1SDV_20200806T120401_20200806T120429_033786_03EAA2_B86C.zip",

"https://datapool.asf.alaska.edu/SLC/SA/S1A_IW_SLC__1SDV_20200725T120400_20200725T120428_033611_03E538_3839.zip",

"https://datapool.asf.alaska.edu/SLC/SA/S1A_IW_SLC__1SDV_20200713T120400_20200713T120427_033436_03DFD8_0A26.zip",

"https://datapool.asf.alaska.edu/SLC/SA/S1A_IW_SLC__1SDV_20200701T120359_20200701T120427_033261_03DA82_038D.zip",

"https://datapool.asf.alaska.edu/SLC/SA/S1A_IW_SLC__1SDV_20200619T120358_20200619T120426_033086_03D533_B6AF.zip",

"https://datapool.asf.alaska.edu/SLC/SA/S1A_IW_SLC__1SDV_20200607T120358_20200607T120425_032911_03CFEC_7C03.zip",

"https://datapool.asf.alaska.edu/SLC/SA/S1A_IW_SLC__1SDV_20200526T120357_20200526T120425_032736_03CAC0_843E.zip",

"https://datapool.asf.alaska.edu/SLC/SA/S1A_IW_SLC__1SDV_20200514T120356_20200514T120424_032561_03C571_D7B3.zip",

"https://datapool.asf.alaska.edu/SLC/SA/S1A_IW_SLC__1SDV_20200502T120355_20200502T120423_032386_03BFDE_58C5.zip",

"https://datapool.asf.alaska.edu/SLC/SA/S1A_IW_SLC__1SDV_20200420T120355_20200420T120423_032211_03B9B5_88D1.zip",

"https://datapool.asf.alaska.edu/SLC/SA/S1A_IW_SLC__1SDV_20200408T120354_20200408T120422_032036_03B390_8029.zip",

"https://datapool.asf.alaska.edu/SLC/SA/S1A_IW_SLC__1SDV_20200327T120354_20200327T120422_031861_03AD62_7B90.zip",

"https://datapool.asf.alaska.edu/SLC/SA/S1A_IW_SLC__1SDV_20200315T120354_20200315T120422_031686_03A739_9399.zip",

"https://datapool.asf.alaska.edu/SLC/SA/S1A_IW_SLC__1SDV_20200303T120354_20200303T120422_031511_03A128_92EC.zip",

"https://datapool.asf.alaska.edu/SLC/SA/S1A_IW_SLC__1SDV_20200220T120354_20200220T120422_031336_039B1C_24EA.zip",

"https://datapool.asf.alaska.edu/SLC/SA/S1A_IW_SLC__1SDV_20200208T120354_20200208T120422_031161_039519_E907.zip",

"https://datapool.asf.alaska.edu/SLC/SA/S1A_IW_SLC__1SDV_20200127T120354_20200127T120422_030986_038EFB_6401.zip",

"https://datapool.asf.alaska.edu/SLC/SA/S1A_IW_SLC__1SDV_20200115T120355_20200115T120423_030811_0388D1_4098.zip",

"https://datapool.asf.alaska.edu/SLC/SA/S1A_IW_SLC__1SDV_20200103T120355_20200103T120423_030636_0382B3_22F4.zip",

"https://datapool.asf.alaska.edu/SLC/SA/S1A_IW_SLC__1SDV_20191222T120356_20191222T120424_030461_037CAA_5A8C.zip",

"https://datapool.asf.alaska.edu/SLC/SA/S1A_IW_SLC__1SDV_20191210T120356_20191210T120424_030286_0376A1_D23A.zip",

"https://datapool.asf.alaska.edu/SLC/SA/S1A_IW_SLC__1SDV_20191128T120357_20191128T120425_030111_03709C_C7DD.zip",

"https://datapool.asf.alaska.edu/SLC/SA/S1A_IW_SLC__1SDV_20191116T120357_20191116T120425_029936_036A8A_4A0F.zip",

"https://datapool.asf.alaska.edu/SLC/SA/S1A_IW_SLC__1SDV_20191104T120357_20191104T120425_029761_036465_E4CA.zip",

"https://datapool.asf.alaska.edu/SLC/SA/S1A_IW_SLC__1SDV_20191023T120357_20191023T120425_029586_035E44_4009.zip",

"https://datapool.asf.alaska.edu/SLC/SA/S1A_IW_SLC__1SDV_20191011T120357_20191011T120425_029411_035844_8BDB.zip",

"https://datapool.asf.alaska.edu/SLC/SA/S1A_IW_SLC__1SDV_20190929T120357_20190929T120425_029236_035242_5A53.zip",

"https://datapool.asf.alaska.edu/SLC/SA/S1A_IW_SLC__1SDV_20190905T120356_20190905T120424_028886_03462C_DB48.zip",

"https://datapool.asf.alaska.edu/SLC/SA/S1A_IW_SLC__1SDV_20190824T120356_20190824T120424_028711_034010_9BCC.zip",

"https://datapool.asf.alaska.edu/SLC/SA/S1A_IW_SLC__1SDV_20190812T120355_20190812T120423_028536_033A08_B4EC.zip",

"https://datapool.asf.alaska.edu/SLC/SA/S1A_IW_SLC__1SDV_20190731T120354_20190731T120422_028361_03346D_18CD.zip",

"https://datapool.asf.alaska.edu/SLC/SA/S1A_IW_SLC__1SDV_20190719T120353_20190719T120421_028186_032F14_1845.zip",

"https://datapool.asf.alaska.edu/SLC/SA/S1A_IW_SLC__1SDV_20190707T120353_20190707T120420_028011_0329CD_7B90.zip",

"https://datapool.asf.alaska.edu/SLC/SA/S1A_IW_SLC__1SDV_20190625T120352_20190625T120420_027836_03247A_47A3.zip",

"https://datapool.asf.alaska.edu/SLC/SA/S1A_IW_SLC__1SDV_20190613T120351_20190613T120419_027661_031F43_4B51.zip",

"https://datapool.asf.alaska.edu/SLC/SA/S1A_IW_SLC__1SDV_20190601T120350_20190601T120418_027486_0319F2_F8A7.zip",

"https://datapool.asf.alaska.edu/SLC/SA/S1A_IW_SLC__1SDV_20190520T120350_20190520T120418_027311_031480_1D13.zip",

"https://datapool.asf.alaska.edu/SLC/SA/S1A_IW_SLC__1SDV_20190508T120349_20190508T120417_027136_030F08_F173.zip",

"https://datapool.asf.alaska.edu/SLC/SA/S1A_IW_SLC__1SDV_20190426T120349_20190426T120417_026961_0308C7_F21C.zip",

"https://datapool.asf.alaska.edu/SLC/SA/S1A_IW_SLC__1SDV_20190414T120348_20190414T120416_026786_030276_66FC.zip",

"https://datapool.asf.alaska.edu/SLC/SA/S1A_IW_SLC__1SDV_20190402T120348_20190402T120416_026611_02FC10_291C.zip",

"https://datapool.asf.alaska.edu/SLC/SA/S1A_IW_SLC__1SDV_20190321T120348_20190321T120416_026436_02F598_FAE9.zip",

"https://datapool.asf.alaska.edu/SLC/SA/S1A_IW_SLC__1SDV_20190309T120348_20190309T120415_026261_02EF29_7445.zip",

"https://datapool.asf.alaska.edu/SLC/SA/S1A_IW_SLC__1SDV_20190225T120348_20190225T120416_026086_02E8D9_4A40.zip",

"https://datapool.asf.alaska.edu/SLC/SA/S1A_IW_SLC__1SDV_20190213T120348_20190213T120416_025911_02E292_5396.zip",

"https://datapool.asf.alaska.edu/SLC/SA/S1A_IW_SLC__1SDV_20190201T120348_20190201T120416_025736_02DC62_328B.zip",

"https://datapool.asf.alaska.edu/SLC/SA/S1A_IW_SLC__1SDV_20190120T120348_20190120T120416_025561_02D602_E8B5.zip",

"https://datapool.asf.alaska.edu/SLC/SA/S1A_IW_SLC__1SDV_20190108T120349_20190108T120417_025386_02CFA8_7F36.zip",

"https://datapool.asf.alaska.edu/SLC/SA/S1A_IW_SLC__1SDV_20181227T120349_20181227T120417_025211_02C956_D24E.zip",

"https://datapool.asf.alaska.edu/SLC/SA/S1A_IW_SLC__1SDV_20181215T120350_20181215T120417_025036_02C2FF_4D0C.zip",

"https://datapool.asf.alaska.edu/SLC/SA/S1A_IW_SLC__1SDV_20181203T120350_20181203T120418_024861_02BCD8_90C1.zip",

"https://datapool.asf.alaska.edu/SLC/SA/S1A_IW_SLC__1SDV_20181121T120351_20181121T120418_024686_02B6BF_409F.zip",

"https://datapool.asf.alaska.edu/SLC/SA/S1A_IW_SLC__1SDV_20181109T120351_20181109T120419_024511_02B04D_2CBE.zip",

"https://datapool.asf.alaska.edu/SLC/SA/S1A_IW_SLC__1SDV_20181028T120351_20181028T120419_024336_02AA1D_589A.zip",

"https://datapool.asf.alaska.edu/SLC/SA/S1A_IW_SLC__1SDV_20181016T120351_20181016T120419_024161_02A47A_CC4C.zip",

"https://datapool.asf.alaska.edu/SLC/SA/S1A_IW_SLC__1SDV_20181004T120351_20181004T120419_023986_029EC8_FBF8.zip",

"https://datapool.asf.alaska.edu/SLC/SA/S1A_IW_SLC__1SDV_20180922T120351_20180922T120418_023811_02990F_EAB0.zip",

"https://datapool.asf.alaska.edu/SLC/SA/S1A_IW_SLC__1SDV_20180910T120350_20180910T120418_023636_02935F_E57E.zip",

"https://datapool.asf.alaska.edu/SLC/SA/S1A_IW_SLC__1SDV_20180829T120350_20180829T120418_023461_028DC3_4EA3.zip",

"https://datapool.asf.alaska.edu/SLC/SA/S1A_IW_SLC__1SDV_20180817T120349_20180817T120417_023286_028835_8388.zip",

"https://datapool.asf.alaska.edu/SLC/SA/S1A_IW_SLC__1SDV_20180805T120348_20180805T120416_023111_028289_9CEE.zip",

"https://datapool.asf.alaska.edu/SLC/SA/S1A_IW_SLC__1SDV_20180724T120348_20180724T120416_022936_027D11_84B7.zip",

"https://datapool.asf.alaska.edu/SLC/SA/S1A_IW_SLC__1SDV_20180712T120347_20180712T120415_022761_02778E_16A6.zip",

"https://datapool.asf.alaska.edu/SLC/SA/S1A_IW_SLC__1SDV_20180630T120346_20180630T120414_022586_02725D_994D.zip",

"https://datapool.asf.alaska.edu/SLC/SA/S1A_IW_SLC__1SDV_20180618T120346_20180618T120413_022411_026D46_B7E0.zip",

"https://datapool.asf.alaska.edu/SLC/SA/S1A_IW_SLC__1SDV_20180606T120345_20180606T120413_022236_0267DF_208D.zip",

"https://datapool.asf.alaska.edu/SLC/SA/S1A_IW_SLC__1SDV_20180525T120344_20180525T120412_022061_02625F_A62B.zip",

"https://datapool.asf.alaska.edu/SLC/SA/S1A_IW_SLC__1SDV_20180513T120343_20180513T120411_021886_025CD7_4649.zip",

"https://datapool.asf.alaska.edu/SLC/SA/S1A_IW_SLC__1SDV_20180501T120343_20180501T120411_021711_02573C_87A4.zip",

"https://datapool.asf.alaska.edu/SLC/SA/S1A_IW_SLC__1SDV_20180419T120342_20180419T120410_021536_0251BB_6926.zip",

"https://datapool.asf.alaska.edu/SLC/SA/S1A_IW_SLC__1SDV_20180407T120342_20180407T120410_021361_024C46_0759.zip",

"https://datapool.asf.alaska.edu/SLC/SA/S1A_IW_SLC__1SDV_20180326T120341_20180326T120409_021186_0246CB_4C3A.zip",

"https://datapool.asf.alaska.edu/SLC/SA/S1A_IW_SLC__1SDV_20180314T120341_20180314T120409_021011_02413B_7CCF.zip",

"https://datapool.asf.alaska.edu/SLC/SA/S1A_IW_SLC__1SDV_20180302T120341_20180302T120409_020836_023BAE_BB89.zip",

"https://datapool.asf.alaska.edu/SLC/SA/S1A_IW_SLC__1SDV_20180218T120341_20180218T120409_020661_023622_4549.zip",

"https://datapool.asf.alaska.edu/SLC/SA/S1A_IW_SLC__1SDV_20180206T120341_20180206T120409_020486_02308C_D981.zip",

"https://datapool.asf.alaska.edu/SLC/SA/S1A_IW_SLC__1SDV_20180125T120342_20180125T120409_020311_022AF6_12FC.zip",

"https://datapool.asf.alaska.edu/SLC/SA/S1A_IW_SLC__1SDV_20180113T120342_20180113T120410_020136_022569_57E2.zip",

"https://datapool.asf.alaska.edu/SLC/SA/S1A_IW_SLC__1SDV_20180101T120342_20180101T120410_019961_021FE1_5900.zip",

"https://datapool.asf.alaska.edu/SLC/SA/S1A_IW_SLC__1SDV_20171220T120343_20171220T120411_019786_021A70_FB0C.zip",

"https://datapool.asf.alaska.edu/SLC/SA/S1A_IW_SLC__1SDV_20171208T120343_20171208T120411_019611_0214FC_1FDD.zip",

"https://datapool.asf.alaska.edu/SLC/SA/S1A_IW_SLC__1SDV_20171126T120344_20171126T120412_019436_020F89_E627.zip",

"https://datapool.asf.alaska.edu/SLC/SA/S1A_IW_SLC__1SDV_20171114T120344_20171114T120412_019261_0209FF_410D.zip",

"https://datapool.asf.alaska.edu/SLC/SA/S1A_IW_SLC__1SDV_20171102T120344_20171102T120412_019086_02048A_05BA.zip",

"https://datapool.asf.alaska.edu/SLC/SA/S1A_IW_SLC__1SDV_20171021T120344_20171021T120412_018911_01FF3B_9AB3.zip",

"https://datapool.asf.alaska.edu/SLC/SA/S1A_IW_SLC__1SDV_20171009T120344_20171009T120412_018736_01F9D6_214D.zip",

"https://datapool.asf.alaska.edu/SLC/SA/S1A_IW_SLC__1SDV_20170927T120344_20170927T120412_018561_01F486_DA05.zip",

"https://datapool.asf.alaska.edu/SLC/SA/S1A_IW_SLC__1SDV_20170915T120344_20170915T120412_018386_01EF2B_1E9F.zip",

"https://datapool.asf.alaska.edu/SLC/SA/S1A_IW_SLC__1SDV_20170903T120343_20170903T120411_018211_01E9B7_CE1F.zip",

"https://datapool.asf.alaska.edu/SLC/SA/S1A_IW_SLC__1SDV_20170822T120343_20170822T120411_018036_01E472_2766.zip",

"https://datapool.asf.alaska.edu/SLC/SA/S1A_IW_SLC__1SDV_20170810T120342_20170810T120410_017861_01DF21_CAFE.zip",

"https://datapool.asf.alaska.edu/SLC/SA/S1A_IW_SLC__1SDV_20170729T120342_20170729T120410_017686_01D9CD_7EC4.zip",

"https://datapool.asf.alaska.edu/SLC/SA/S1A_IW_SLC__1SDV_20170717T120341_20170717T120409_017511_01D472_0CFE.zip",

"https://datapool.asf.alaska.edu/SLC/SA/S1A_IW_SLC__1SDV_20170705T120340_20170705T120408_017336_01CF21_11B4.zip",

"https://datapool.asf.alaska.edu/SLC/SA/S1A_IW_SLC__1SDV_20170623T120340_20170623T120407_017161_01C9D6_9D36.zip",

"https://datapool.asf.alaska.edu/SLC/SA/S1A_IW_SLC__1SDV_20170611T120339_20170611T120407_016986_01C47D_13AC.zip",

"https://datapool.asf.alaska.edu/SLC/SA/S1A_IW_SLC__1SDV_20170530T120338_20170530T120406_016811_01BF0F_7A98.zip",

"https://datapool.asf.alaska.edu/SLC/SA/S1A_IW_SLC__1SDV_20170518T120337_20170518T120405_016636_01B9AB_605B.zip",

"https://datapool.asf.alaska.edu/SLC/SA/S1A_IW_SLC__1SDV_20170506T120337_20170506T120405_016461_01B453_54F2.zip",

"https://datapool.asf.alaska.edu/SLC/SA/S1A_IW_SLC__1SDV_20170424T120336_20170424T120404_016286_01AF0F_95D3.zip",

"https://datapool.asf.alaska.edu/SLC/SA/S1A_IW_SLC__1SDV_20170412T120336_20170412T120403_016111_01A9AE_25D1.zip",

"https://datapool.asf.alaska.edu/SLC/SA/S1A_IW_SLC__1SDV_20170331T120335_20170331T120403_015936_01A461_0390.zip",

"https://datapool.asf.alaska.edu/SLC/SA/S1A_IW_SLC__1SDV_20170319T120335_20170319T120403_015761_019F2B_175D.zip"

2. **Path 114 Frame 71**

"https://datapool.asf.alaska.edu/SLC/SA/S1A_IW_SLC__1SDV_20210614T120430_20210614T120457_038336_04862F_4E08.zip",

"https://datapool.asf.alaska.edu/SLC/SA/S1A_IW_SLC__1SDV_20210602T120429_20210602T120456_038161_0480FD_0E3A.zip",

"https://datapool.asf.alaska.edu/SLC/SA/S1A_IW_SLC__1SDV_20210521T120428_20210521T120455_037986_047BBD_CC40.zip",

"https://datapool.asf.alaska.edu/SLC/SA/S1A_IW_SLC__1SDV_20210509T120428_20210509T120454_037811_047676_1564.zip",

"https://datapool.asf.alaska.edu/SLC/SA/S1A_IW_SLC__1SDV_20210427T120427_20210427T120454_037636_0470A6_70B9.zip",

"https://datapool.asf.alaska.edu/SLC/SA/S1A_IW_SLC__1SDV_20210415T120426_20210415T120453_037461_046A8E_E010.zip",

"https://datapool.asf.alaska.edu/SLC/SA/S1A_IW_SLC__1SDV_20210403T120426_20210403T120453_037286_046480_F176.zip",

"https://datapool.asf.alaska.edu/SLC/SA/S1A_IW_SLC__1SDV_20210322T120426_20210322T120453_037111_045E7A_2026.zip",

"https://datapool.asf.alaska.edu/SLC/SA/S1A_IW_SLC__1SDV_20210310T120426_20210310T120452_036936_045868_5D4A.zip",

"https://datapool.asf.alaska.edu/SLC/SA/S1A_IW_SLC__1SDV_20210226T120425_20210226T120452_036761_04524C_98C3.zip",

"https://datapool.asf.alaska.edu/SLC/SA/S1A_IW_SLC__1SDV_20210214T120426_20210214T120453_036586_044C38_7BF8.zip",

"https://datapool.asf.alaska.edu/SLC/SA/S1A_IW_SLC__1SDV_20210202T120426_20210202T120453_036411_044618_EFC6.zip",

"https://datapool.asf.alaska.edu/SLC/SA/S1A_IW_SLC__1SDV_20210121T120426_20210121T120453_036236_044009_8BE0.zip",

"https://datapool.asf.alaska.edu/SLC/SA/S1A_IW_SLC__1SDV_20210109T120427_20210109T120454_036061_0439EE_2B29.zip",

"https://datapool.asf.alaska.edu/SLC/SA/S1A_IW_SLC__1SDV_20201228T120428_20201228T120454_035886_0433DB_2ADF.zip",

"https://datapool.asf.alaska.edu/SLC/SA/S1A_IW_SLC__1SDV_20201216T120428_20201216T120455_035711_042DC6_72FC.zip",

"https://datapool.asf.alaska.edu/SLC/SA/S1A_IW_SLC__1SDV_20201204T120429_20201204T120455_035536_0427AA_6868.zip",

"https://datapool.asf.alaska.edu/SLC/SA/S1A_IW_SLC__1SDV_20201122T120429_20201122T120456_035361_0421AA_4489.zip",

"https://datapool.asf.alaska.edu/SLC/SA/S1A_IW_SLC__1SDV_20201110T120429_20201110T120456_035186_041BA0_77FE.zip",

"https://datapool.asf.alaska.edu/SLC/SA/S1A_IW_SLC__1SDV_20201029T120430_20201029T120456_035011_041587_B9C5.zip",

"https://datapool.asf.alaska.edu/SLC/SA/S1A_IW_SLC__1SDV_20201017T120430_20201017T120456_034836_040F8F_0728.zip",

"https://datapool.asf.alaska.edu/SLC/SA/S1A_IW_SLC__1SDV_20201005T120429_20201005T120456_034661_04096B_FD92.zip",

"https://datapool.asf.alaska.edu/SLC/SA/S1A_IW_SLC__1SDV_20200923T120429_20200923T120456_034486_040348_1A47.zip",

"https://datapool.asf.alaska.edu/SLC/SA/S1A_IW_SLC__1SDV_20200911T120429_20200911T120456_034311_03FD13_BAA1.zip",

"https://datapool.asf.alaska.edu/SLC/SA/S1A_IW_SLC__1SDV_20200830T120428_20200830T120455_034136_03F6F3_432D.zip",

"https://datapool.asf.alaska.edu/SLC/SA/S1A_IW_SLC__1SDV_20200818T120427_20200818T120454_033961_03F0C7_F7DB.zip",

"https://datapool.asf.alaska.edu/SLC/SA/S1A_IW_SLC__1SDV_20200806T120427_20200806T120454_033786_03EAA2_1327.zip",

"https://datapool.asf.alaska.edu/SLC/SA/S1A_IW_SLC__1SDV_20200725T120426_20200725T120453_033611_03E538_44FF.zip",

"https://datapool.asf.alaska.edu/SLC/SA/S1A_IW_SLC__1SDV_20200713T120425_20200713T120452_033436_03DFD8_ED6F.zip",

"https://datapool.asf.alaska.edu/SLC/SA/S1A_IW_SLC__1SDV_20200701T120425_20200701T120451_033261_03DA82_27F2.zip",

"https://datapool.asf.alaska.edu/SLC/SA/S1A_IW_SLC__1SDV_20200619T120424_20200619T120451_033086_03D533_E307.zip",

"https://datapool.asf.alaska.edu/SLC/SA/S1A_IW_SLC__1SDV_20200607T120423_20200607T120450_032911_03CFEC_9E4B.zip",

"https://datapool.asf.alaska.edu/SLC/SA/S1A_IW_SLC__1SDV_20200526T120423_20200526T120450_032736_03CAC0_E139.zip",

"https://datapool.asf.alaska.edu/SLC/SA/S1A_IW_SLC__1SDV_20200514T120422_20200514T120449_032561_03C571_639C.zip",

"https://datapool.asf.alaska.edu/SLC/SA/S1A_IW_SLC__1SDV_20200502T120421_20200502T120448_032386_03BFDE_3CDB.zip",

"https://datapool.asf.alaska.edu/SLC/SA/S1A_IW_SLC__1SDV_20200420T120421_20200420T120448_032211_03B9B5_649A.zip",

"https://datapool.asf.alaska.edu/SLC/SA/S1A_IW_SLC__1SDV_20200408T120420_20200408T120447_032036_03B390_827C.zip",

"https://datapool.asf.alaska.edu/SLC/SA/S1A_IW_SLC__1SDV_20200327T120420_20200327T120447_031861_03AD62_462F.zip",

"https://datapool.asf.alaska.edu/SLC/SA/S1A_IW_SLC__1SDV_20200315T120420_20200315T120447_031686_03A739_05FA.zip",

"https://datapool.asf.alaska.edu/SLC/SA/S1A_IW_SLC__1SDV_20200303T120420_20200303T120447_031511_03A128_BCF8.zip",

"https://datapool.asf.alaska.edu/SLC/SA/S1A_IW_SLC__1SDV_20200220T120420_20200220T120447_031336_039B1C_34E5.zip",

"https://datapool.asf.alaska.edu/SLC/SA/S1A_IW_SLC__1SDV_20200208T120420_20200208T120447_031161_039519_9EFC.zip",

"https://datapool.asf.alaska.edu/SLC/SA/S1A_IW_SLC__1SDV_20200127T120420_20200127T120447_030986_038EFB_2B55.zip",

"https://datapool.asf.alaska.edu/SLC/SA/S1A_IW_SLC__1SDV_20200115T120421_20200115T120447_030811_0388D1_81A6.zip",

"https://datapool.asf.alaska.edu/SLC/SA/S1A_IW_SLC__1SDV_20200103T120421_20200103T120448_030636_0382B3_0088.zip",

"https://datapool.asf.alaska.edu/SLC/SA/S1A_IW_SLC__1SDV_20191222T120422_20191222T120449_030461_037CAA_AC06.zip",

"https://datapool.asf.alaska.edu/SLC/SA/S1A_IW_SLC__1SDV_20191210T120422_20191210T120449_030286_0376A1_FF67.zip",

"https://datapool.asf.alaska.edu/SLC/SA/S1A_IW_SLC__1SDV_20191128T120423_20191128T120449_030111_03709C_118E.zip",

"https://datapool.asf.alaska.edu/SLC/SA/S1A_IW_SLC__1SDV_20191116T120423_20191116T120450_029936_036A8A_7DAC.zip",

"https://datapool.asf.alaska.edu/SLC/SA/S1A_IW_SLC__1SDV_20191104T120423_20191104T120450_029761_036465_C31D.zip",

"https://datapool.asf.alaska.edu/SLC/SA/S1A_IW_SLC__1SDV_20191023T120423_20191023T120450_029586_035E44_C549.zip",

"https://datapool.asf.alaska.edu/SLC/SA/S1A_IW_SLC__1SDV_20191011T120423_20191011T120450_029411_035844_9D7A.zip",

"https://datapool.asf.alaska.edu/SLC/SA/S1A_IW_SLC__1SDV_20190929T120423_20190929T120450_029236_035242_2DC8.zip",

"https://datapool.asf.alaska.edu/SLC/SA/S1A_IW_SLC__1SDV_20190905T120422_20190905T120449_028886_03462C_B5FD.zip",

"https://datapool.asf.alaska.edu/SLC/SA/S1A_IW_SLC__1SDV_20190824T120421_20190824T120448_028711_034010_1952.zip",

"https://datapool.asf.alaska.edu/SLC/SA/S1A_IW_SLC__1SDV_20190812T120421_20190812T120448_028536_033A08_9BBE.zip",

"https://datapool.asf.alaska.edu/SLC/SA/S1A_IW_SLC__1SDV_20190731T120420_20190731T120447_028361_03346D_3D1E.zip",

"https://datapool.asf.alaska.edu/SLC/SA/S1A_IW_SLC__1SDV_20190719T120419_20190719T120446_028186_032F14_6D40.zip",

"https://datapool.asf.alaska.edu/SLC/SA/S1A_IW_SLC__1SDV_20190707T120418_20190707T120445_028011_0329CD_13EC.zip",

"https://datapool.asf.alaska.edu/SLC/SA/S1A_IW_SLC__1SDV_20190625T120418_20190625T120445_027836_03247A_3E0C.zip",

"https://datapool.asf.alaska.edu/SLC/SA/S1A_IW_SLC__1SDV_20190613T120417_20190613T120444_027661_031F43_E989.zip",

"https://datapool.asf.alaska.edu/SLC/SA/S1A_IW_SLC__1SDV_20190601T120416_20190601T120443_027486_0319F2_B66E.zip",

"https://datapool.asf.alaska.edu/SLC/SA/S1A_IW_SLC__1SDV_20190520T120416_20190520T120443_027311_031480_2A1C.zip",

"https://datapool.asf.alaska.edu/SLC/SA/S1A_IW_SLC__1SDV_20190508T120415_20190508T120442_027136_030F08_4CA8.zip",

"https://datapool.asf.alaska.edu/SLC/SA/S1A_IW_SLC__1SDV_20190426T120415_20190426T120442_026961_0308C7_5030.zip",

"https://datapool.asf.alaska.edu/SLC/SA/S1A_IW_SLC__1SDV_20190414T120414_20190414T120441_026786_030276_E623.zip",

"https://datapool.asf.alaska.edu/SLC/SA/S1A_IW_SLC__1SDV_20190402T120414_20190402T120441_026611_02FC10_0EA6.zip",

"https://datapool.asf.alaska.edu/SLC/SA/S1A_IW_SLC__1SDV_20190321T120413_20190321T120440_026436_02F598_B734.zip",

"https://datapool.asf.alaska.edu/SLC/SA/S1A_IW_SLC__1SDV_20190309T120413_20190309T120440_026261_02EF29_A576.zip",

"https://datapool.asf.alaska.edu/SLC/SA/S1A_IW_SLC__1SDV_20190225T120413_20190225T120440_026086_02E8D9_02A3.zip",

"https://datapool.asf.alaska.edu/SLC/SA/S1A_IW_SLC__1SDV_20190213T120413_20190213T120440_025911_02E292_BD08.zip",

"https://datapool.asf.alaska.edu/SLC/SA/S1A_IW_SLC__1SDV_20190201T120414_20190201T120441_025736_02DC62_021C.zip",

"https://datapool.asf.alaska.edu/SLC/SA/S1A_IW_SLC__1SDV_20190120T120414_20190120T120441_025561_02D602_9704.zip",

"https://datapool.asf.alaska.edu/SLC/SA/S1A_IW_SLC__1SDV_20190108T120414_20190108T120441_025386_02CFA8_7D0D.zip",

"https://datapool.asf.alaska.edu/SLC/SA/S1A_IW_SLC__1SDV_20181227T120415_20181227T120442_025211_02C956_696A.zip",

"https://datapool.asf.alaska.edu/SLC/SA/S1A_IW_SLC__1SDV_20181215T120415_20181215T120442_025036_02C2FF_93CD.zip",

"https://datapool.asf.alaska.edu/SLC/SA/S1A_IW_SLC__1SDV_20181203T120416_20181203T120443_024861_02BCD8_ECEB.zip",

"https://datapool.asf.alaska.edu/SLC/SA/S1A_IW_SLC__1SDV_20181121T120416_20181121T120443_024686_02B6BF_B0A2.zip",

"https://datapool.asf.alaska.edu/SLC/SA/S1A_IW_SLC__1SDV_20181109T120417_20181109T120443_024511_02B04D_6567.zip",

"https://datapool.asf.alaska.edu/SLC/SA/S1A_IW_SLC__1SDV_20181028T120417_20181028T120444_024336_02AA1D_92F0.zip",

"https://datapool.asf.alaska.edu/SLC/SA/S1A_IW_SLC__1SDV_20181016T120417_20181016T120444_024161_02A47A_A5E7.zip",

"https://datapool.asf.alaska.edu/SLC/SA/S1A_IW_SLC__1SDV_20181004T120416_20181004T120443_023986_029EC8_3E96.zip",

"https://datapool.asf.alaska.edu/SLC/SA/S1A_IW_SLC__1SDV_20180922T120416_20180922T120443_023811_02990F_7A61.zip",

"https://datapool.asf.alaska.edu/SLC/SA/S1A_IW_SLC__1SDV_20180910T120416_20180910T120443_023636_02935F_DB01.zip",

"https://datapool.asf.alaska.edu/SLC/SA/S1A_IW_SLC__1SDV_20180829T120416_20180829T120443_023461_028DC3_C5A2.zip",

"https://datapool.asf.alaska.edu/SLC/SA/S1A_IW_SLC__1SDV_20180817T120415_20180817T120442_023286_028835_6AB4.zip",

"https://datapool.asf.alaska.edu/SLC/SA/S1A_IW_SLC__1SDV_20180805T120414_20180805T120441_023111_028289_C248.zip",

"https://datapool.asf.alaska.edu/SLC/SA/S1A_IW_SLC__1SDV_20180724T120413_20180724T120440_022936_027D11_FAF0.zip",

"https://datapool.asf.alaska.edu/SLC/SA/S1A_IW_SLC__1SDV_20180712T120413_20180712T120440_022761_02778E_1AD6.zip",

"https://datapool.asf.alaska.edu/SLC/SA/S1A_IW_SLC__1SDV_20180630T120412_20180630T120439_022586_02725D_DBBE.zip",

"https://datapool.asf.alaska.edu/SLC/SA/S1A_IW_SLC__1SDV_20180618T120411_20180618T120438_022411_026D46_66BB.zip",

"https://datapool.asf.alaska.edu/SLC/SA/S1A_IW_SLC__1SDV_20180606T120410_20180606T120437_022236_0267DF_6356.zip",

"https://datapool.asf.alaska.edu/SLC/SA/S1A_IW_SLC__1SDV_20180525T120410_20180525T120437_022061_02625F_1C03.zip",

"https://datapool.asf.alaska.edu/SLC/SA/S1A_IW_SLC__1SDV_20180513T120409_20180513T120436_021886_025CD7_4F3C.zip",

"https://datapool.asf.alaska.edu/SLC/SA/S1A_IW_SLC__1SDV_20180501T120408_20180501T120435_021711_02573C_3055.zip",

"https://datapool.asf.alaska.edu/SLC/SA/S1A_IW_SLC__1SDV_20180419T120408_20180419T120435_021536_0251BB_F4DE.zip",

"https://datapool.asf.alaska.edu/SLC/SA/S1A_IW_SLC__1SDV_20180407T120407_20180407T120434_021361_024C46_60AE.zip",

"https://datapool.asf.alaska.edu/SLC/SA/S1A_IW_SLC__1SDV_20180326T120407_20180326T120434_021186_0246CB_B6C6.zip",

"https://datapool.asf.alaska.edu/SLC/SA/S1A_IW_SLC__1SDV_20180314T120407_20180314T120434_021011_02413B_F032.zip",

"https://datapool.asf.alaska.edu/SLC/SA/S1A_IW_SLC__1SDV_20180302T120407_20180302T120434_020836_023BAE_47A7.zip",

"https://datapool.asf.alaska.edu/SLC/SA/S1A_IW_SLC__1SDV_20180218T120407_20180218T120434_020661_023622_A0BB.zip",

"https://datapool.asf.alaska.edu/SLC/SA/S1A_IW_SLC__1SDV_20180206T120407_20180206T120434_020486_02308C_3DCD.zip",

"https://datapool.asf.alaska.edu/SLC/SA/S1A_IW_SLC__1SDV_20180125T120407_20180125T120434_020311_022AF6_E636.zip",

"https://datapool.asf.alaska.edu/SLC/SA/S1A_IW_SLC__1SDV_20180113T120408_20180113T120435_020136_022569_A56A.zip",

"https://datapool.asf.alaska.edu/SLC/SA/S1A_IW_SLC__1SDV_20180101T120408_20180101T120435_019961_021FE1_7335.zip",

"https://datapool.asf.alaska.edu/SLC/SA/S1A_IW_SLC__1SDV_20171220T120409_20171220T120436_019786_021A70_4DC4.zip",

"https://datapool.asf.alaska.edu/SLC/SA/S1A_IW_SLC__1SDV_20171208T120409_20171208T120436_019611_0214FC_4E43.zip",

"https://datapool.asf.alaska.edu/SLC/SA/S1A_IW_SLC__1SDV_20171126T120410_20171126T120437_019436_020F89_F124.zip",

"https://datapool.asf.alaska.edu/SLC/SA/S1A_IW_SLC__1SDV_20171114T120410_20171114T120437_019261_0209FF_A58A.zip",

"https://datapool.asf.alaska.edu/SLC/SA/S1A_IW_SLC__1SDV_20171102T120410_20171102T120437_019086_02048A_137C.zip",

"https://datapool.asf.alaska.edu/SLC/SA/S1A_IW_SLC__1SDV_20171021T120410_20171021T120437_018911_01FF3B_958E.zip",

"https://datapool.asf.alaska.edu/SLC/SA/S1A_IW_SLC__1SDV_20171009T120410_20171009T120437_018736_01F9D6_21DA.zip",

"https://datapool.asf.alaska.edu/SLC/SA/S1A_IW_SLC__1SDV_20170927T120410_20170927T120437_018561_01F486_5E01.zip",

"https://datapool.asf.alaska.edu/SLC/SA/S1A_IW_SLC__1SDV_20170915T120410_20170915T120436_018386_01EF2B_7F53.zip",

"https://datapool.asf.alaska.edu/SLC/SA/S1A_IW_SLC__1SDV_20170903T120409_20170903T120436_018211_01E9B7_897D.zip",

"https://datapool.asf.alaska.edu/SLC/SA/S1A_IW_SLC__1SDV_20170822T120409_20170822T120436_018036_01E472_E062.zip",

"https://datapool.asf.alaska.edu/SLC/SA/S1A_IW_SLC__1SDV_20170810T120408_20170810T120435_017861_01DF21_3CEE.zip",

"https://datapool.asf.alaska.edu/SLC/SA/S1A_IW_SLC__1SDV_20170729T120407_20170729T120434_017686_01D9CD_3B78.zip",

"https://datapool.asf.alaska.edu/SLC/SA/S1A_IW_SLC__1SDV_20170717T120407_20170717T120434_017511_01D472_0B09.zip",

"https://datapool.asf.alaska.edu/SLC/SA/S1A_IW_SLC__1SDV_20170705T120406_20170705T120433_017336_01CF21_3926.zip",

"https://datapool.asf.alaska.edu/SLC/SA/S1A_IW_SLC__1SDV_20170623T120405_20170623T120432_017161_01C9D6_89CC.zip",

"https://datapool.asf.alaska.edu/SLC/SA/S1A_IW_SLC__1SDV_20170611T120405_20170611T120432_016986_01C47D_B7DE.zip",

"https://datapool.asf.alaska.edu/SLC/SA/S1A_IW_SLC__1SDV_20170530T120404_20170530T120431_016811_01BF0F_9B44.zip",

"https://datapool.asf.alaska.edu/SLC/SA/S1A_IW_SLC__1SDV_20170518T120403_20170518T120430_016636_01B9AB_57BF.zip",

"https://datapool.asf.alaska.edu/SLC/SA/S1A_IW_SLC__1SDV_20170506T120403_20170506T120430_016461_01B453_D99A.zip",

"https://datapool.asf.alaska.edu/SLC/SA/S1A_IW_SLC__1SDV_20170424T120402_20170424T120429_016286_01AF0F_9832.zip",

"https://datapool.asf.alaska.edu/SLC/SA/S1A_IW_SLC__1SDV_20170412T120401_20170412T120428_016111_01A9AE_E705.zip",

"https://datapool.asf.alaska.edu/SLC/SA/S1A_IW_SLC__1SDV_20170331T120401_20170331T120428_015936_01A461_982E.zip",

"https://datapool.asf.alaska.edu/SLC/SA/S1A_IW_SLC__1SDV_20170319T120401_20170319T120427_015761_019F2B_09B2.zip"

3. **Path 114 Frame 76**

"https://datapool.asf.alaska.edu/SLC/SA/S1A_IW_SLC__1SDV_20210720T120457_20210720T120524_038861_0495EC_E97D.zip",

"https://datapool.asf.alaska.edu/SLC/SA/S1A_IW_SLC__1SDV_20210708T120456_20210708T120523_038686_0490AD_88E8.zip",

"https://datapool.asf.alaska.edu/SLC/SA/S1A_IW_SLC__1SDV_20210626T120455_20210626T120522_038511_048B6C_F312.zip",

"https://datapool.asf.alaska.edu/SLC/SA/S1A_IW_SLC__1SDV_20210614T120455_20210614T120521_038336_04862F_2127.zip",

"https://datapool.asf.alaska.edu/SLC/SA/S1A_IW_SLC__1SDV_20210602T120454_20210602T120521_038161_0480FD_51D3.zip",

"https://datapool.asf.alaska.edu/SLC/SA/S1A_IW_SLC__1SDV_20210521T120453_20210521T120520_037986_047BBD_E73E.zip",

"https://datapool.asf.alaska.edu/SLC/SA/S1A_IW_SLC__1SDV_20210509T120452_20210509T120519_037811_047676_FF3C.zip",

"https://datapool.asf.alaska.edu/SLC/SA/S1A_IW_SLC__1SDV_20210427T120452_20210427T120519_037636_0470A6_D275.zip",

"https://datapool.asf.alaska.edu/SLC/SA/S1A_IW_SLC__1SDV_20210415T120451_20210415T120518_037461_046A8E_693D.zip",

"https://datapool.asf.alaska.edu/SLC/SA/S1A_IW_SLC__1SDV_20210403T120451_20210403T120518_037286_046480_6AF9.zip",

"https://datapool.asf.alaska.edu/SLC/SA/S1A_IW_SLC__1SDV_20210322T120450_20210322T120517_037111_045E7A_D4E0.zip",

"https://datapool.asf.alaska.edu/SLC/SA/S1A_IW_SLC__1SDV_20210310T120450_20210310T120517_036936_045868_09D9.zip",

"https://datapool.asf.alaska.edu/SLC/SA/S1A_IW_SLC__1SDV_20210226T120450_20210226T120517_036761_04524C_DE0E.zip",

"https://datapool.asf.alaska.edu/SLC/SA/S1A_IW_SLC__1SDV_20210214T120450_20210214T120517_036586_044C38_14D0.zip",

"https://datapool.asf.alaska.edu/SLC/SA/S1A_IW_SLC__1SDV_20210202T120451_20210202T120518_036411_044618_1DE9.zip",

"https://datapool.asf.alaska.edu/SLC/SA/S1A_IW_SLC__1SDV_20210121T120451_20210121T120518_036236_044009_A700.zip",

"https://datapool.asf.alaska.edu/SLC/SA/S1A_IW_SLC__1SDV_20210109T120452_20210109T120519_036061_0439EE_A76B.zip",

"https://datapool.asf.alaska.edu/SLC/SA/S1A_IW_SLC__1SDV_20201228T120452_20201228T120519_035886_0433DB_BD8E.zip",

"https://datapool.asf.alaska.edu/SLC/SA/S1A_IW_SLC__1SDV_20201216T120453_20201216T120520_035711_042DC6_C0BA.zip",

"https://datapool.asf.alaska.edu/SLC/SA/S1A_IW_SLC__1SDV_20201204T120453_20201204T120520_035536_0427AA_21CF.zip",

"https://datapool.asf.alaska.edu/SLC/SA/S1A_IW_SLC__1SDV_20201122T120454_20201122T120521_035361_0421AA_13A3.zip",

"https://datapool.asf.alaska.edu/SLC/SA/S1A_IW_SLC__1SDV_20201110T120454_20201110T120521_035186_041BA0_9FCB.zip",

"https://datapool.asf.alaska.edu/SLC/SA/S1A_IW_SLC__1SDV_20201029T120454_20201029T120521_035011_041587_F9B1.zip",

"https://datapool.asf.alaska.edu/SLC/SA/S1A_IW_SLC__1SDV_20201017T120454_20201017T120521_034836_040F8F_9C13.zip",

"https://datapool.asf.alaska.edu/SLC/SA/S1A_IW_SLC__1SDV_20201005T120454_20201005T120521_034661_04096B_1DFF.zip",

"https://datapool.asf.alaska.edu/SLC/SA/S1A_IW_SLC__1SDV_20200923T120454_20200923T120521_034486_040348_14E6.zip",

"https://datapool.asf.alaska.edu/SLC/SA/S1A_IW_SLC__1SDV_20200911T120454_20200911T120521_034311_03FD13_2311.zip",

"https://datapool.asf.alaska.edu/SLC/SA/S1A_IW_SLC__1SDV_20200830T120453_20200830T120520_034136_03F6F3_A829.zip",

"https://datapool.asf.alaska.edu/SLC/SA/S1A_IW_SLC__1SDV_20200818T120452_20200818T120519_033961_03F0C7_7C61.zip",

"https://datapool.asf.alaska.edu/SLC/SA/S1A_IW_SLC__1SDV_20200806T120452_20200806T120519_033786_03EAA2_6CA7.zip",

"https://datapool.asf.alaska.edu/SLC/SA/S1A_IW_SLC__1SDV_20200725T120451_20200725T120518_033611_03E538_5D61.zip",

"https://datapool.asf.alaska.edu/SLC/SA/S1A_IW_SLC__1SDV_20200713T120450_20200713T120517_033436_03DFD8_A0DF.zip",

"https://datapool.asf.alaska.edu/SLC/SA/S1A_IW_SLC__1SDV_20200701T120449_20200701T120516_033261_03DA82_7F00.zip",

"https://datapool.asf.alaska.edu/SLC/SA/S1A_IW_SLC__1SDV_20200619T120449_20200619T120516_033086_03D533_4734.zip",

"https://datapool.asf.alaska.edu/SLC/SA/S1A_IW_SLC__1SDV_20200607T120448_20200607T120515_032911_03CFEC_E335.zip",

"https://datapool.asf.alaska.edu/SLC/SA/S1A_IW_SLC__1SDV_20200526T120447_20200526T120514_032736_03CAC0_598C.zip",

"https://datapool.asf.alaska.edu/SLC/SA/S1A_IW_SLC__1SDV_20200514T120447_20200514T120514_032561_03C571_4B14.zip",

"https://datapool.asf.alaska.edu/SLC/SA/S1A_IW_SLC__1SDV_20200502T120446_20200502T120513_032386_03BFDE_F6F9.zip",

"https://datapool.asf.alaska.edu/SLC/SA/S1A_IW_SLC__1SDV_20200420T120445_20200420T120512_032211_03B9B5_0FF9.zip",

"https://datapool.asf.alaska.edu/SLC/SA/S1A_IW_SLC__1SDV_20200408T120445_20200408T120512_032036_03B390_60FA.zip",

"https://datapool.asf.alaska.edu/SLC/SA/S1A_IW_SLC__1SDV_20200327T120445_20200327T120512_031861_03AD62_34C4.zip",

"https://datapool.asf.alaska.edu/SLC/SA/S1A_IW_SLC__1SDV_20200315T120445_20200315T120512_031686_03A739_0748.zip",

"https://datapool.asf.alaska.edu/SLC/SA/S1A_IW_SLC__1SDV_20200303T120444_20200303T120511_031511_03A128_2AC2.zip",

"https://datapool.asf.alaska.edu/SLC/SA/S1A_IW_SLC__1SDV_20200220T120444_20200220T120511_031336_039B1C_6E22.zip",

"https://datapool.asf.alaska.edu/SLC/SA/S1A_IW_SLC__1SDV_20200208T120445_20200208T120512_031161_039519_9B9D.zip",

"https://datapool.asf.alaska.edu/SLC/SA/S1A_IW_SLC__1SDV_20200127T120445_20200127T120512_030986_038EFB_BE2E.zip",

"https://datapool.asf.alaska.edu/SLC/SA/S1A_IW_SLC__1SDV_20200115T120445_20200115T120512_030811_0388D1_7940.zip",

"https://datapool.asf.alaska.edu/SLC/SA/S1A_IW_SLC__1SDV_20200103T120446_20200103T120513_030636_0382B3_9AC3.zip",

"https://datapool.asf.alaska.edu/SLC/SA/S1A_IW_SLC__1SDV_20191222T120446_20191222T120513_030461_037CAA_607C.zip",

"https://datapool.asf.alaska.edu/SLC/SA/S1A_IW_SLC__1SDV_20191210T120447_20191210T120514_030286_0376A1_65BB.zip",

"https://datapool.asf.alaska.edu/SLC/SA/S1A_IW_SLC__1SDV_20191128T120447_20191128T120514_030111_03709C_9022.zip",

"https://datapool.asf.alaska.edu/SLC/SA/S1A_IW_SLC__1SDV_20191116T120448_20191116T120515_029936_036A8A_D94A.zip",

"https://datapool.asf.alaska.edu/SLC/SA/S1A_IW_SLC__1SDV_20191104T120448_20191104T120515_029761_036465_AE39.zip",

"https://datapool.asf.alaska.edu/SLC/SA/S1A_IW_SLC__1SDV_20191023T120448_20191023T120515_029586_035E44_E5F3.zip",

"https://datapool.asf.alaska.edu/SLC/SA/S1A_IW_SLC__1SDV_20191011T120448_20191011T120515_029411_035844_1666.zip",

"https://datapool.asf.alaska.edu/SLC/SA/S1A_IW_SLC__1SDV_20190929T120448_20190929T120515_029236_035242_7063.zip",

"https://datapool.asf.alaska.edu/SLC/SA/S1A_IW_SLC__1SDV_20190905T120447_20190905T120514_028886_03462C_1E3D.zip",

"https://datapool.asf.alaska.edu/SLC/SA/S1A_IW_SLC__1SDV_20190824T120446_20190824T120513_028711_034010_359D.zip",

"https://datapool.asf.alaska.edu/SLC/SA/S1A_IW_SLC__1SDV_20190812T120446_20190812T120513_028536_033A08_7601.zip",

"https://datapool.asf.alaska.edu/SLC/SA/S1A_IW_SLC__1SDV_20190731T120445_20190731T120512_028361_03346D_DCD6.zip",

"https://datapool.asf.alaska.edu/SLC/SA/S1A_IW_SLC__1SDV_20190719T120444_20190719T120511_028186_032F14_D4BF.zip",

"https://datapool.asf.alaska.edu/SLC/SA/S1A_IW_SLC__1SDV_20190707T120443_20190707T120510_028011_0329CD_7527.zip",

"https://datapool.asf.alaska.edu/SLC/SA/S1A_IW_SLC__1SDV_20190625T120442_20190625T120509_027836_03247A_B194.zip",

"https://datapool.asf.alaska.edu/SLC/SA/S1A_IW_SLC__1SDV_20190613T120442_20190613T120508_027661_031F43_B767.zip",

"https://datapool.asf.alaska.edu/SLC/SA/S1A_IW_SLC__1SDV_20190601T120441_20190601T120508_027486_0319F2_9C32.zip",

"https://datapool.asf.alaska.edu/SLC/SA/S1A_IW_SLC__1SDV_20190520T120441_20190520T120508_027311_031480_55D1.zip",

"https://datapool.asf.alaska.edu/SLC/SA/S1A_IW_SLC__1SDV_20190508T120440_20190508T120507_027136_030F08_FD08.zip",

"https://datapool.asf.alaska.edu/SLC/SA/S1A_IW_SLC__1SDV_20190426T120440_20190426T120507_026961_0308C7_EB95.zip",

"https://datapool.asf.alaska.edu/SLC/SA/S1A_IW_SLC__1SDV_20190414T120439_20190414T120506_026786_030276_90A0.zip",

"https://datapool.asf.alaska.edu/SLC/SA/S1A_IW_SLC__1SDV_20190402T120439_20190402T120506_026611_02FC10_7BAA.zip",

"https://datapool.asf.alaska.edu/SLC/SA/S1A_IW_SLC__1SDV_20190321T120438_20190321T120505_026436_02F598_8345.zip",

"https://datapool.asf.alaska.edu/SLC/SA/S1A_IW_SLC__1SDV_20190309T120438_20190309T120505_026261_02EF29_2F40.zip",

"https://datapool.asf.alaska.edu/SLC/SA/S1A_IW_SLC__1SDV_20190225T120438_20190225T120505_026086_02E8D9_1AEC.zip",

"https://datapool.asf.alaska.edu/SLC/SA/S1A_IW_SLC__1SDV_20190213T120438_20190213T120505_025911_02E292_5BBA.zip",

"https://datapool.asf.alaska.edu/SLC/SA/S1A_IW_SLC__1SDV_20190201T120439_20190201T120506_025736_02DC62_C856.zip",

"https://datapool.asf.alaska.edu/SLC/SA/S1A_IW_SLC__1SDV_20190120T120439_20190120T120506_025561_02D602_B1D7.zip",

"https://datapool.asf.alaska.edu/SLC/SA/S1A_IW_SLC__1SDV_20190108T120439_20190108T120506_025386_02CFA8_5314.zip",

"https://datapool.asf.alaska.edu/SLC/SA/S1A_IW_SLC__1SDV_20181227T120440_20181227T120507_025211_02C956_CC52.zip",

"https://datapool.asf.alaska.edu/SLC/SA/S1A_IW_SLC__1SDV_20181215T120440_20181215T120507_025036_02C2FF_8379.zip",

"https://datapool.asf.alaska.edu/SLC/SA/S1A_IW_SLC__1SDV_20181203T120441_20181203T120508_024861_02BCD8_CD60.zip",

"https://datapool.asf.alaska.edu/SLC/SA/S1A_IW_SLC__1SDV_20181121T120441_20181121T120508_024686_02B6BF_4B9D.zip",

"https://datapool.asf.alaska.edu/SLC/SA/S1A_IW_SLC__1SDV_20181109T120441_20181109T120508_024511_02B04D_D04E.zip",

"https://datapool.asf.alaska.edu/SLC/SA/S1A_IW_SLC__1SDV_20181028T120442_20181028T120509_024336_02AA1D_4C1B.zip",

"https://datapool.asf.alaska.edu/SLC/SA/S1A_IW_SLC__1SDV_20181016T120442_20181016T120509_024161_02A47A_6416.zip",

"https://datapool.asf.alaska.edu/SLC/SA/S1A_IW_SLC__1SDV_20181004T120441_20181004T120508_023986_029EC8_9A4D.zip",

"https://datapool.asf.alaska.edu/SLC/SA/S1A_IW_SLC__1SDV_20180922T120441_20180922T120508_023811_02990F_3B27.zip",

"https://datapool.asf.alaska.edu/SLC/SA/S1A_IW_SLC__1SDV_20180910T120441_20180910T120508_023636_02935F_AEC0.zip",

"https://datapool.asf.alaska.edu/SLC/SA/S1A_IW_SLC__1SDV_20180829T120440_20180829T120507_023461_028DC3_3125.zip",

"https://datapool.asf.alaska.edu/SLC/SA/S1A_IW_SLC__1SDV_20180817T120440_20180817T120507_023286_028835_EA35.zip",

"https://datapool.asf.alaska.edu/SLC/SA/S1A_IW_SLC__1SDV_20180805T120439_20180805T120506_023111_028289_1C8D.zip",

"https://datapool.asf.alaska.edu/SLC/SA/S1A_IW_SLC__1SDV_20180724T120438_20180724T120505_022936_027D11_9799.zip",

"https://datapool.asf.alaska.edu/SLC/SA/S1A_IW_SLC__1SDV_20180712T120437_20180712T120504_022761_02778E_6DF2.zip",

"https://datapool.asf.alaska.edu/SLC/SA/S1A_IW_SLC__1SDV_20180630T120437_20180630T120504_022586_02725D_71ED.zip",

"https://datapool.asf.alaska.edu/SLC/SA/S1A_IW_SLC__1SDV_20180618T120436_20180618T120503_022411_026D46_FC3D.zip",

"https://datapool.asf.alaska.edu/SLC/SA/S1A_IW_SLC__1SDV_20180606T120435_20180606T120502_022236_0267DF_357F.zip",

"https://datapool.asf.alaska.edu/SLC/SA/S1A_IW_SLC__1SDV_20180525T120435_20180525T120502_022061_02625F_283F.zip",

"https://datapool.asf.alaska.edu/SLC/SA/S1A_IW_SLC__1SDV_20180513T120434_20180513T120501_021886_025CD7_92AE.zip",

"https://datapool.asf.alaska.edu/SLC/SA/S1A_IW_SLC__1SDV_20180501T120433_20180501T120500_021711_02573C_1EBC.zip",

"https://datapool.asf.alaska.edu/SLC/SA/S1A_IW_SLC__1SDV_20180419T120433_20180419T120500_021536_0251BB_BE93.zip",

"https://datapool.asf.alaska.edu/SLC/SA/S1A_IW_SLC__1SDV_20180407T120432_20180407T120459_021361_024C46_F8D4.zip",

"https://datapool.asf.alaska.edu/SLC/SA/S1A_IW_SLC__1SDV_20180326T120432_20180326T120459_021186_0246CB_928F.zip",

"https://datapool.asf.alaska.edu/SLC/SA/S1A_IW_SLC__1SDV_20180314T120432_20180314T120459_021011_02413B_D514.zip",

"https://datapool.asf.alaska.edu/SLC/SA/S1A_IW_SLC__1SDV_20180302T120432_20180302T120459_020836_023BAE_612D.zip",

"https://datapool.asf.alaska.edu/SLC/SA/S1A_IW_SLC__1SDV_20180218T120432_20180218T120459_020661_023622_FF4D.zip",

"https://datapool.asf.alaska.edu/SLC/SA/S1A_IW_SLC__1SDV_20180206T120432_20180206T120459_020486_02308C_32F8.zip",

"https://datapool.asf.alaska.edu/SLC/SA/S1A_IW_SLC__1SDV_20180125T120432_20180125T120459_020311_022AF6_130A.zip",

"https://datapool.asf.alaska.edu/SLC/SA/S1A_IW_SLC__1SDV_20180113T120433_20180113T120500_020136_022569_C9CA.zip",

"https://datapool.asf.alaska.edu/SLC/SA/S1A_IW_SLC__1SDV_20180101T120433_20180101T120500_019961_021FE1_880B.zip",

"https://datapool.asf.alaska.edu/SLC/SA/S1A_IW_SLC__1SDV_20171220T120433_20171220T120500_019786_021A70_E70C.zip",

"https://datapool.asf.alaska.edu/SLC/SA/S1A_IW_SLC__1SDV_20171208T120434_20171208T120501_019611_0214FC_B37A.zip",

"https://datapool.asf.alaska.edu/SLC/SA/S1A_IW_SLC__1SDV_20171126T120434_20171126T120501_019436_020F89_C572.zip",

"https://datapool.asf.alaska.edu/SLC/SA/S1A_IW_SLC__1SDV_20171114T120435_20171114T120502_019261_0209FF_8ED0.zip",

"https://datapool.asf.alaska.edu/SLC/SA/S1A_IW_SLC__1SDV_20171102T120435_20171102T120502_019086_02048A_0473.zip",

"https://datapool.asf.alaska.edu/SLC/SA/S1A_IW_SLC__1SDV_20171021T120435_20171021T120502_018911_01FF3B_4E44.zip",

"https://datapool.asf.alaska.edu/SLC/SA/S1A_IW_SLC__1SDV_20171009T120435_20171009T120502_018736_01F9D6_0B97.zip",

"https://datapool.asf.alaska.edu/SLC/SA/S1A_IW_SLC__1SDV_20170927T120435_20170927T120502_018561_01F486_E646.zip",

"https://datapool.asf.alaska.edu/SLC/SA/S1A_IW_SLC__1SDV_20170915T120434_20170915T120501_018386_01EF2B_4286.zip",

"https://datapool.asf.alaska.edu/SLC/SA/S1A_IW_SLC__1SDV_20170903T120434_20170903T120501_018211_01E9B7_E8B7.zip",

"https://datapool.asf.alaska.edu/SLC/SA/S1A_IW_SLC__1SDV_20170822T120433_20170822T120500_018036_01E472_038D.zip",

"https://datapool.asf.alaska.edu/SLC/SA/S1A_IW_SLC__1SDV_20170810T120433_20170810T120500_017861_01DF21_A1F5.zip",

"https://datapool.asf.alaska.edu/SLC/SA/S1A_IW_SLC__1SDV_20170729T120432_20170729T120459_017686_01D9CD_C581.zip",

"https://datapool.asf.alaska.edu/SLC/SA/S1A_IW_SLC__1SDV_20170717T120431_20170717T120458_017511_01D472_46F9.zip",

"https://datapool.asf.alaska.edu/SLC/SA/S1A_IW_SLC__1SDV_20170705T120431_20170705T120458_017336_01CF21_A0EF.zip",

"https://datapool.asf.alaska.edu/SLC/SA/S1A_IW_SLC__1SDV_20170623T120430_20170623T120457_017161_01C9D6_DB61.zip",

"https://datapool.asf.alaska.edu/SLC/SA/S1A_IW_SLC__1SDV_20170611T120429_20170611T120456_016986_01C47D_E0CE.zip",

"https://datapool.asf.alaska.edu/SLC/SA/S1A_IW_SLC__1SDV_20170530T120429_20170530T120456_016811_01BF0F_41F8.zip",

"https://datapool.asf.alaska.edu/SLC/SA/S1A_IW_SLC__1SDV_20170518T120428_20170518T120455_016636_01B9AB_5AEB.zip",

"https://datapool.asf.alaska.edu/SLC/SA/S1A_IW_SLC__1SDV_20170506T120427_20170506T120454_016461_01B453_5B38.zip",

"https://datapool.asf.alaska.edu/SLC/SA/S1A_IW_SLC__1SDV_20170424T120427_20170424T120454_016286_01AF0F_EA9B.zip",

"https://datapool.asf.alaska.edu/SLC/SA/S1A_IW_SLC__1SDV_20170412T120426_20170412T120444_016111_01A9AE_0063.zip",

"https://datapool.asf.alaska.edu/SLC/SA/S1A_IW_SLC__1SDV_20170331T120426_20170331T120453_015936_01A461_52B6.zip",

"https://datapool.asf.alaska.edu/SLC/SA/S1A_IW_SLC__1SDV_20170319T120425_20170319T120452_015761_019F2B_20CA.zip"

4. **Path 12 Frame 64**

"https://datapool.asf.alaska.edu/SLC/SA/S1A_IW_SLC__1SDV_20210607T121211_20210607T121238_038234_048318_F70E.zip",

"https://datapool.asf.alaska.edu/SLC/SA/S1A_IW_SLC__1SDV_20210526T121210_20210526T121238_038059_047DE5_CBF0.zip",

"https://datapool.asf.alaska.edu/SLC/SA/S1A_IW_SLC__1SDV_20210514T121209_20210514T121237_037884_047898_B996.zip",

"https://datapool.asf.alaska.edu/SLC/SA/S1A_IW_SLC__1SDV_20210502T121208_20210502T121236_037709_047321_E16A.zip",

"https://datapool.asf.alaska.edu/SLC/SA/S1A_IW_SLC__1SDV_20210420T121208_20210420T121236_037534_046D0C_9E83.zip",

"https://datapool.asf.alaska.edu/SLC/SA/S1A_IW_SLC__1SDV_20210408T121208_20210408T121236_037359_0466FA_6B36.zip",

"https://datapool.asf.alaska.edu/SLC/SA/S1A_IW_SLC__1SDV_20210327T121207_20210327T121235_037184_0460F2_D139.zip",

"https://datapool.asf.alaska.edu/SLC/SA/S1A_IW_SLC__1SDV_20210315T121207_20210315T121235_037009_045AE4_BB58.zip",

"https://datapool.asf.alaska.edu/SLC/SA/S1A_IW_SLC__1SDV_20210303T121207_20210303T121235_036834_0454C9_3790.zip",

"https://datapool.asf.alaska.edu/SLC/SA/S1A_IW_SLC__1SDV_20210219T121207_20210219T121235_036659_044EBC_FFE8.zip",

"https://datapool.asf.alaska.edu/SLC/SA/S1A_IW_SLC__1SDV_20210207T121207_20210207T121235_036484_04489D_F39E.zip",

"https://datapool.asf.alaska.edu/SLC/SA/S1A_IW_SLC__1SDV_20210126T121208_20210126T121236_036309_04428F_4719.zip",

"https://datapool.asf.alaska.edu/SLC/SA/S1A_IW_SLC__1SDV_20210114T121208_20210114T121236_036134_043C7E_D45D.zip",

"https://datapool.asf.alaska.edu/SLC/SA/S1A_IW_SLC__1SDV_20210102T121209_20210102T121237_035959_043653_6D3D.zip",

"https://datapool.asf.alaska.edu/SLC/SA/S1A_IW_SLC__1SDV_20201221T121209_20201221T121237_035784_04303F_6757.zip",

"https://datapool.asf.alaska.edu/SLC/SA/S1A_IW_SLC__1SDV_20201209T121210_20201209T121238_035609_042A3E_2F19.zip",

"https://datapool.asf.alaska.edu/SLC/SA/S1A_IW_SLC__1SDV_20201127T121210_20201127T121238_035434_042430_0B35.zip",

"https://datapool.asf.alaska.edu/SLC/SA/S1A_IW_SLC__1SDV_20201115T121211_20201115T121239_035259_041E24_CF73.zip",

"https://datapool.asf.alaska.edu/SLC/SA/S1A_IW_SLC__1SDV_20201103T121211_20201103T121239_035084_041809_DE25.zip",

"https://datapool.asf.alaska.edu/SLC/SA/S1A_IW_SLC__1SDV_20201022T121211_20201022T121239_034909_0411FF_C2CB.zip",

"https://datapool.asf.alaska.edu/SLC/SA/S1A_IW_SLC__1SDV_20201010T121211_20201010T121239_034734_040BED_8DEA.zip",

"https://datapool.asf.alaska.edu/SLC/SA/S1A_IW_SLC__1SDV_20200928T121211_20200928T121239_034559_0405CE_B94C.zip",

"https://datapool.asf.alaska.edu/SLC/SA/S1A_IW_SLC__1SDV_20200916T121210_20200916T121238_034384_03FF9D_647E.zip",

"https://datapool.asf.alaska.edu/SLC/SA/S1A_IW_SLC__1SDV_20200904T121210_20200904T121238_034209_03F975_139C.zip",

"https://datapool.asf.alaska.edu/SLC/SA/S1A_IW_SLC__1SDV_20200823T121209_20200823T121237_034034_03F34F_8ABD.zip",

"https://datapool.asf.alaska.edu/SLC/SA/S1A_IW_SLC__1SDV_20200811T121209_20200811T121237_033859_03ED25_4BC2.zip",

"https://datapool.asf.alaska.edu/SLC/SA/S1A_IW_SLC__1SDV_20200730T121208_20200730T121236_033684_03E765_15AA.zip",

"https://datapool.asf.alaska.edu/SLC/SA/S1A_IW_SLC__1SDV_20200718T121207_20200718T121235_033509_03E207_6E62.zip",

"https://datapool.asf.alaska.edu/SLC/SA/S1A_IW_SLC__1SDV_20200706T121206_20200706T121234_033334_03DCAD_A931.zip",

"https://datapool.asf.alaska.edu/SLC/SA/S1A_IW_SLC__1SDV_20200624T121206_20200624T121234_033159_03D761_8878.zip",

"https://datapool.asf.alaska.edu/SLC/SA/S1A_IW_SLC__1SDV_20200612T121205_20200612T121233_032984_03D20C_01BB.zip",

"https://datapool.asf.alaska.edu/SLC/SA/S1A_IW_SLC__1SDV_20200531T121204_20200531T121232_032809_03CCE0_6ABD.zip",

"https://datapool.asf.alaska.edu/SLC/SA/S1A_IW_SLC__1SDV_20200519T121204_20200519T121232_032634_03C797_2B6F.zip",

"https://datapool.asf.alaska.edu/SLC/SA/S1A_IW_SLC__1SDV_20200507T121203_20200507T121231_032459_03C246_A3B8.zip",

"https://datapool.asf.alaska.edu/SLC/SA/S1A_IW_SLC__1SDV_20200425T121202_20200425T121230_032284_03BC35_51A8.zip",

"https://datapool.asf.alaska.edu/SLC/SA/S1A_IW_SLC__1SDV_20200413T121202_20200413T121230_032109_03B610_CC8D.zip",

"https://datapool.asf.alaska.edu/SLC/SA/S1A_IW_SLC__1SDV_20200401T121201_20200401T121229_031934_03AFE6_157F.zip",

"https://datapool.asf.alaska.edu/SLC/SA/S1A_IW_SLC__1SDV_20200320T121201_20200320T121229_031759_03A9BC_6F4A.zip",

"https://datapool.asf.alaska.edu/SLC/SA/S1A_IW_SLC__1SDV_20200308T121201_20200308T121229_031584_03A39B_35EB.zip",

"https://datapool.asf.alaska.edu/SLC/SA/S1A_IW_SLC__1SDV_20200225T121201_20200225T121229_031409_039D91_C65C.zip",

"https://datapool.asf.alaska.edu/SLC/SA/S1A_IW_SLC__1SDV_20200213T121201_20200213T121229_031234_039785_F6F5.zip",

"https://datapool.asf.alaska.edu/SLC/SA/S1A_IW_SLC__1SDV_20200201T121202_20200201T121229_031059_039174_08A3.zip",

"https://datapool.asf.alaska.edu/SLC/SA/S1A_IW_SLC__1SDV_20200120T121202_20200120T121230_030884_038B59_CC18.zip",

"https://datapool.asf.alaska.edu/SLC/SA/S1A_IW_SLC__1SDV_20200108T121202_20200108T121230_030709_038533_EF9C.zip",

"https://datapool.asf.alaska.edu/SLC/SA/S1A_IW_SLC__1SDV_20191227T121203_20191227T121231_030534_037F23_E5EE.zip",

"https://datapool.asf.alaska.edu/SLC/SA/S1A_IW_SLC__1SDV_20191215T121203_20191215T121231_030359_03791A_865B.zip",

"https://datapool.asf.alaska.edu/SLC/SA/S1A_IW_SLC__1SDV_20191203T121204_20191203T121232_030184_03730F_3E86.zip",

"https://datapool.asf.alaska.edu/SLC/SA/S1A_IW_SLC__1SDV_20191121T121204_20191121T121232_030009_036CFD_BA99.zip",

"https://datapool.asf.alaska.edu/SLC/SA/S1A_IW_SLC__1SDV_20191109T121204_20191109T121232_029834_0366F3_5B63.zip",

"https://datapool.asf.alaska.edu/SLC/SA/S1A_IW_SLC__1SDV_20191028T121204_20191028T121232_029659_0360C3_ADEE.zip",

"https://datapool.asf.alaska.edu/SLC/SA/S1A_IW_SLC__1SDV_20191016T121204_20191016T121232_029484_035ABB_1B8D.zip",

"https://datapool.asf.alaska.edu/SLC/SA/S1A_IW_SLC__1SDV_20191004T121204_20191004T121232_029309_0354B0_6427.zip",

"https://datapool.asf.alaska.edu/SLC/SA/S1A_IW_SLC__1SDV_20190922T121204_20190922T121232_029134_034EAB_4B11.zip",

"https://datapool.asf.alaska.edu/SLC/SA/S1A_IW_SLC__1SDV_20190910T121204_20190910T121231_028959_0348B6_88F0.zip",

"https://datapool.asf.alaska.edu/SLC/SA/S1A_IW_SLC__1SDV_20190829T121203_20190829T121231_028784_03429E_34FB.zip",

"https://datapool.asf.alaska.edu/SLC/SA/S1A_IW_SLC__1SDV_20190817T121203_20190817T121230_028609_033C79_61DD.zip",

"https://datapool.asf.alaska.edu/SLC/SA/S1A_IW_SLC__1SDV_20190805T121202_20190805T121230_028434_033690_10ED.zip",

"https://datapool.asf.alaska.edu/SLC/SA/S1A_IW_SLC__1SDV_20190724T121201_20190724T121229_028259_033136_A990.zip",

"https://datapool.asf.alaska.edu/SLC/SA/S1A_IW_SLC__1SDV_20190712T121200_20190712T121228_028084_032BED_9BA9.zip",

"https://datapool.asf.alaska.edu/SLC/SA/S1A_IW_SLC__1SDV_20190630T121159_20190630T121227_027909_03269F_64A4.zip",

"https://datapool.asf.alaska.edu/SLC/SA/S1A_IW_SLC__1SDV_20190618T121159_20190618T121227_027734_032165_4781.zip",

"https://datapool.asf.alaska.edu/SLC/SA/S1A_IW_SLC__1SDV_20190606T121158_20190606T121226_027559_031C1F_E152.zip",

"https://datapool.asf.alaska.edu/SLC/SA/S1A_IW_SLC__1SDV_20190513T121157_20190513T121225_027209_031140_8F98.zip",

"https://datapool.asf.alaska.edu/SLC/SA/S1A_IW_SLC__1SDV_20190501T121156_20190501T121224_027034_030B64_22D0.zip",

"https://datapool.asf.alaska.edu/SLC/SA/S1A_IW_SLC__1SDV_20190419T121156_20190419T121224_026859_030507_93A0.zip",

"https://datapool.asf.alaska.edu/SLC/SA/S1A_IW_SLC__1SDV_20190407T121155_20190407T121223_026684_02FEAD_2E3C.zip",

"https://datapool.asf.alaska.edu/SLC/SA/S1A_IW_SLC__1SDV_20190326T121155_20190326T121223_026509_02F838_42E1.zip",

"https://datapool.asf.alaska.edu/SLC/SA/S1A_IW_SLC__1SDV_20190314T121155_20190314T121223_026334_02F1CB_FC0E.zip",

"https://datapool.asf.alaska.edu/SLC/SA/S1A_IW_SLC__1SDV_20190302T121155_20190302T121223_026159_02EB68_A84C.zip",

"https://datapool.asf.alaska.edu/SLC/SA/S1A_IW_SLC__1SDV_20190218T121155_20190218T121223_025984_02E51F_C8AA.zip",

"https://datapool.asf.alaska.edu/SLC/SA/S1A_IW_SLC__1SDV_20190206T121155_20190206T121223_025809_02DEE0_D770.zip",

"https://datapool.asf.alaska.edu/SLC/SA/S1A_IW_SLC__1SDV_20190125T121155_20190125T121223_025634_02D899_5FF4.zip",

"https://datapool.asf.alaska.edu/SLC/SA/S1A_IW_SLC__1SDV_20190113T121156_20190113T121224_025459_02D234_464B.zip",

"https://datapool.asf.alaska.edu/SLC/SA/S1A_IW_SLC__1SDV_20190101T121156_20190101T121224_025284_02CBEB_A6FC.zip",

"https://datapool.asf.alaska.edu/SLC/SA/S1A_IW_SLC__1SDV_20181220T121157_20181220T121225_025109_02C597_FBC3.zip",

"https://datapool.asf.alaska.edu/SLC/SA/S1A_IW_SLC__1SDV_20181208T121157_20181208T121225_024934_02BF41_AFEC.zip",

"https://datapool.asf.alaska.edu/SLC/SA/S1A_IW_SLC__1SDV_20181126T121157_20181126T121225_024759_02B969_F73A.zip",

"https://datapool.asf.alaska.edu/SLC/SA/S1A_IW_SLC__1SDV_20181114T121158_20181114T121226_024584_02B2FA_7AF9.zip",

"https://datapool.asf.alaska.edu/SLC/SA/S1A_IW_SLC__1SDV_20181102T121158_20181102T121226_024409_02AC8E_8492.zip",

"https://datapool.asf.alaska.edu/SLC/SA/S1A_IW_SLC__1SDV_20181021T121158_20181021T121226_024234_02A6C9_9EC7.zip",

"https://datapool.asf.alaska.edu/SLC/SA/S1A_IW_SLC__1SDV_20181009T121158_20181009T121226_024059_02A118_B45E.zip",

"https://datapool.asf.alaska.edu/SLC/SA/S1A_IW_SLC__1SDV_20180927T121158_20180927T121226_023884_029B53_FC44.zip",

"https://datapool.asf.alaska.edu/SLC/SA/S1A_IW_SLC__1SDV_20180915T121158_20180915T121226_023709_0295A8_301B.zip",

"https://datapool.asf.alaska.edu/SLC/SA/S1A_IW_SLC__1SDV_20180903T121157_20180903T121225_023534_02900C_BDBC.zip",

"https://datapool.asf.alaska.edu/SLC/SA/S1A_IW_SLC__1SDV_20180822T121156_20180822T121224_023359_028A7D_0E87.zip",

"https://datapool.asf.alaska.edu/SLC/SA/S1A_IW_SLC__1SDV_20180810T121156_20180810T121224_023184_0284D5_6229.zip",

"https://datapool.asf.alaska.edu/SLC/SA/S1A_IW_SLC__1SDV_20180729T121155_20180729T121223_023009_027F5A_6649.zip",

"https://datapool.asf.alaska.edu/SLC/SA/S1A_IW_SLC__1SDV_20180717T121154_20180717T121222_022834_0279D2_C1D7.zip",

"https://datapool.asf.alaska.edu/SLC/SA/S1A_IW_SLC__1SDV_20180705T121154_20180705T121221_022659_027482_F6BF.zip",

"https://datapool.asf.alaska.edu/SLC/SA/S1A_IW_SLC__1SDV_20180623T121153_20180623T121221_022484_026F65_23D7.zip",

"https://datapool.asf.alaska.edu/SLC/SA/S1A_IW_SLC__1SDV_20180611T121152_20180611T121220_022309_026A26_B6F8.zip",

"https://datapool.asf.alaska.edu/SLC/SA/S1A_IW_SLC__1SDV_20180530T121151_20180530T121219_022134_0264B1_8945.zip",

"https://datapool.asf.alaska.edu/SLC/SA/S1A_IW_SLC__1SDV_20180518T121151_20180518T121219_021959_025F10_85EE.zip",

"https://datapool.asf.alaska.edu/SLC/SA/S1A_IW_SLC__1SDV_20180506T121150_20180506T121218_021784_02597F_BEA4.zip",

"https://datapool.asf.alaska.edu/SLC/SA/S1A_IW_SLC__1SDV_20180424T121150_20180424T121218_021609_0253F3_CE7C.zip",

"https://datapool.asf.alaska.edu/SLC/SA/S1A_IW_SLC__1SDV_20180412T121149_20180412T121217_021434_024E7E_4C21.zip",

"https://datapool.asf.alaska.edu/SLC/SA/S1A_IW_SLC__1SDV_20180331T121149_20180331T121217_021259_02490D_ED62.zip",

"https://datapool.asf.alaska.edu/SLC/SA/S1A_IW_SLC__1SDV_20180319T121148_20180319T121216_021084_02437D_5553.zip",

"https://datapool.asf.alaska.edu/SLC/SA/S1A_IW_SLC__1SDV_20180307T121148_20180307T121216_020909_023DF8_271C.zip",

"https://datapool.asf.alaska.edu/SLC/SA/S1A_IW_SLC__1SDV_20180223T121148_20180223T121216_020734_02386E_012C.zip",

"https://datapool.asf.alaska.edu/SLC/SA/S1A_IW_SLC__1SDV_20180211T121149_20180211T121216_020559_0232D9_7C91.zip",

"https://datapool.asf.alaska.edu/SLC/SA/S1A_IW_SLC__1SDV_20180130T121149_20180130T121217_020384_022D42_1E6B.zip",

"https://datapool.asf.alaska.edu/SLC/SA/S1A_IW_SLC__1SDV_20180118T121149_20180118T121217_020209_0227B2_C76F.zip",

"https://datapool.asf.alaska.edu/SLC/SA/S1A_IW_SLC__1SDV_20180106T121149_20180106T121217_020034_022226_C09F.zip",

"https://datapool.asf.alaska.edu/SLC/SA/S1A_IW_SLC__1SDV_20171225T121150_20171225T121218_019859_021C9A_F3A9.zip",

"https://datapool.asf.alaska.edu/SLC/SA/S1A_IW_SLC__1SDV_20171213T121150_20171213T121218_019684_021735_CB94.zip",

"https://datapool.asf.alaska.edu/SLC/SA/S1A_IW_SLC__1SDV_20171201T121151_20171201T121219_019509_0211BA_242A.zip",

"https://datapool.asf.alaska.edu/SLC/SA/S1A_IW_SLC__1SDV_20171119T121151_20171119T121219_019334_020C41_1CE1.zip",

"https://datapool.asf.alaska.edu/SLC/SA/S1A_IW_SLC__1SDV_20171107T121151_20171107T121219_019159_0206C5_7E59.zip",

"https://datapool.asf.alaska.edu/SLC/SA/S1A_IW_SLC__1SDV_20171026T121152_20171026T121220_018984_020158_F311.zip",

"https://datapool.asf.alaska.edu/SLC/SA/S1A_IW_SLC__1SDV_20171014T121152_20171014T121219_018809_01FC09_B26F.zip",

"https://datapool.asf.alaska.edu/SLC/SA/S1A_IW_SLC__1SDV_20171002T121151_20171002T121219_018634_01F6B9_FFB5.zip",

"https://datapool.asf.alaska.edu/SLC/SA/S1A_IW_SLC__1SDV_20170920T121151_20170920T121219_018459_01F155_CC2D.zip",

"https://datapool.asf.alaska.edu/SLC/SA/S1A_IW_SLC__1SDV_20170908T121151_20170908T121219_018284_01EBF3_F57A.zip",

"https://datapool.asf.alaska.edu/SLC/SA/S1A_IW_SLC__1SDV_20170827T121150_20170827T121218_018109_01E69C_2460.zip",

"https://datapool.asf.alaska.edu/SLC/SA/S1A_IW_SLC__1SDV_20170815T121150_20170815T121218_017934_01E151_B683.zip",

"https://datapool.asf.alaska.edu/SLC/SA/S1A_IW_SLC__1SDV_20170803T121149_20170803T121217_017759_01DBFC_19CA.zip",

"https://datapool.asf.alaska.edu/SLC/SA/S1A_IW_SLC__1SDV_20170722T121148_20170722T121216_017584_01D6A4_1ABB.zip",

"https://datapool.asf.alaska.edu/SLC/SA/S1A_IW_SLC__1SDV_20170710T121148_20170710T121216_017409_01D151_0620.zip",

"https://datapool.asf.alaska.edu/SLC/SA/S1A_IW_SLC__1SDV_20170628T121147_20170628T121215_017234_01CC09_67C1.zip",

"https://datapool.asf.alaska.edu/SLC/SA/S1A_IW_SLC__1SDV_20170604T121146_20170604T121214_016884_01C156_D68F.zip",

"https://datapool.asf.alaska.edu/SLC/SA/S1A_IW_SLC__1SDV_20170523T121145_20170523T121213_016709_01BBEA_D581.zip",

"https://datapool.asf.alaska.edu/SLC/SA/S1A_IW_SLC__1SDV_20170511T121144_20170511T121212_016534_01B681_07E1.zip",

"https://datapool.asf.alaska.edu/SLC/SA/S1A_IW_SLC__1SDV_20170429T121144_20170429T121211_016359_01B13B_DD61.zip",

"https://datapool.asf.alaska.edu/SLC/SA/S1A_IW_SLC__1SDV_20170417T121143_20170417T121211_016184_01ABEA_042B.zip",

"https://datapool.asf.alaska.edu/SLC/SA/S1A_IW_SLC__1SDV_20170405T121142_20170405T121210_016009_01A68C_E84E.zip",

"https://datapool.asf.alaska.edu/SLC/SA/S1A_IW_SLC__1SDV_20170324T121142_20170324T121210_015834_01A15C_2452.zip",

"https://datapool.asf.alaska.edu/SLC/SA/S1A_IW_SLC__1SDV_20170312T121142_20170312T121210_015659_019C2A_6435.zip"

5. **Path 12 Frame 69**

"https://datapool.asf.alaska.edu/SLC/SA/S1A_IW_SLC__1SDV_20210607T121236_20210607T121303_038234_048318_7C1A.zip",

"https://datapool.asf.alaska.edu/SLC/SA/S1A_IW_SLC__1SDV_20210526T121236_20210526T121303_038059_047DE5_2B03.zip",

"https://datapool.asf.alaska.edu/SLC/SA/S1A_IW_SLC__1SDV_20210514T121235_20210514T121302_037884_047898_F41B.zip",

"https://datapool.asf.alaska.edu/SLC/SA/S1A_IW_SLC__1SDV_20210502T121234_20210502T121301_037709_047321_DF5A.zip",

"https://datapool.asf.alaska.edu/SLC/SA/S1A_IW_SLC__1SDV_20210420T121234_20210420T121301_037534_046D0C_9383.zip",

"https://datapool.asf.alaska.edu/SLC/SA/S1A_IW_SLC__1SDV_20210408T121233_20210408T121300_037359_0466FA_8C05.zip",

"https://datapool.asf.alaska.edu/SLC/SA/S1A_IW_SLC__1SDV_20210327T121233_20210327T121300_037184_0460F2_ACF9.zip",

"https://datapool.asf.alaska.edu/SLC/SA/S1A_IW_SLC__1SDV_20210315T121233_20210315T121300_037009_045AE4_D0C3.zip",

"https://datapool.asf.alaska.edu/SLC/SA/S1A_IW_SLC__1SDV_20210303T121233_20210303T121300_036834_0454C9_8F43.zip",

"https://datapool.asf.alaska.edu/SLC/SA/S1A_IW_SLC__1SDV_20210219T121233_20210219T121300_036659_044EBC_B9AD.zip",

"https://datapool.asf.alaska.edu/SLC/SA/S1A_IW_SLC__1SDV_20210207T121233_20210207T121300_036484_04489D_CBF6.zip",

"https://datapool.asf.alaska.edu/SLC/SA/S1A_IW_SLC__1SDV_20210126T121233_20210126T121300_036309_04428F_6CB2.zip",

"https://datapool.asf.alaska.edu/SLC/SA/S1A_IW_SLC__1SDV_20210114T121234_20210114T121301_036134_043C7E_65E6.zip",

"https://datapool.asf.alaska.edu/SLC/SA/S1A_IW_SLC__1SDV_20210102T121234_20210102T121301_035959_043653_7694.zip",

"https://datapool.asf.alaska.edu/SLC/SA/S1A_IW_SLC__1SDV_20201221T121235_20201221T121302_035784_04303F_50C9.zip",

"https://datapool.asf.alaska.edu/SLC/SA/S1A_IW_SLC__1SDV_20201209T121236_20201209T121303_035609_042A3E_76CF.zip",

"https://datapool.asf.alaska.edu/SLC/SA/S1A_IW_SLC__1SDV_20201127T121236_20201127T121303_035434_042430_6709.zip",

"https://datapool.asf.alaska.edu/SLC/SA/S1A_IW_SLC__1SDV_20201115T121236_20201115T121303_035259_041E24_F57D.zip",

"https://datapool.asf.alaska.edu/SLC/SA/S1A_IW_SLC__1SDV_20201103T121237_20201103T121304_035084_041809_D95D.zip",

"https://datapool.asf.alaska.edu/SLC/SA/S1A_IW_SLC__1SDV_20201022T121237_20201022T121304_034909_0411FF_BB62.zip",

"https://datapool.asf.alaska.edu/SLC/SA/S1A_IW_SLC__1SDV_20201010T121237_20201010T121304_034734_040BED_BC5D.zip",

"https://datapool.asf.alaska.edu/SLC/SA/S1A_IW_SLC__1SDV_20200928T121236_20200928T121303_034559_0405CE_0D81.zip",

"https://datapool.asf.alaska.edu/SLC/SA/S1A_IW_SLC__1SDV_20200916T121236_20200916T121303_034384_03FF9D_949B.zip",

"https://datapool.asf.alaska.edu/SLC/SA/S1A_IW_SLC__1SDV_20200904T121236_20200904T121303_034209_03F975_B3E6.zip",

"https://datapool.asf.alaska.edu/SLC/SA/S1A_IW_SLC__1SDV_20200823T121235_20200823T121302_034034_03F34F_77C9.zip",

"https://datapool.asf.alaska.edu/SLC/SA/S1A_IW_SLC__1SDV_20200811T121234_20200811T121301_033859_03ED25_EF2B.zip",

"https://datapool.asf.alaska.edu/SLC/SA/S1A_IW_SLC__1SDV_20200730T121234_20200730T121301_033684_03E765_C20B.zip",

"https://datapool.asf.alaska.edu/SLC/SA/S1A_IW_SLC__1SDV_20200718T121233_20200718T121300_033509_03E207_FD5B.zip",

"https://datapool.asf.alaska.edu/SLC/SA/S1A_IW_SLC__1SDV_20200706T121232_20200706T121259_033334_03DCAD_B0BB.zip",

"https://datapool.asf.alaska.edu/SLC/SA/S1A_IW_SLC__1SDV_20200624T121232_20200624T121259_033159_03D761_4C4D.zip",

"https://datapool.asf.alaska.edu/SLC/SA/S1A_IW_SLC__1SDV_20200612T121231_20200612T121258_032984_03D20C_37A2.zip",

"https://datapool.asf.alaska.edu/SLC/SA/S1A_IW_SLC__1SDV_20200531T121230_20200531T121257_032809_03CCE0_1881.zip",

"https://datapool.asf.alaska.edu/SLC/SA/S1A_IW_SLC__1SDV_20200519T121229_20200519T121256_032634_03C797_D207.zip",

"https://datapool.asf.alaska.edu/SLC/SA/S1A_IW_SLC__1SDV_20200507T121229_20200507T121256_032459_03C246_6BBD.zip",

"https://datapool.asf.alaska.edu/SLC/SA/S1A_IW_SLC__1SDV_20200425T121228_20200425T121255_032284_03BC35_5187.zip",

"https://datapool.asf.alaska.edu/SLC/SA/S1A_IW_SLC__1SDV_20200413T121228_20200413T121255_032109_03B610_18ED.zip",

"https://datapool.asf.alaska.edu/SLC/SA/S1A_IW_SLC__1SDV_20200401T121227_20200401T121254_031934_03AFE6_81C8.zip",

"https://datapool.asf.alaska.edu/SLC/SA/S1A_IW_SLC__1SDV_20200320T121227_20200320T121254_031759_03A9BC_54F8.zip",

"https://datapool.asf.alaska.edu/SLC/SA/S1A_IW_SLC__1SDV_20200308T121227_20200308T121254_031584_03A39B_95A9.zip",

"https://datapool.asf.alaska.edu/SLC/SA/S1A_IW_SLC__1SDV_20200225T121227_20200225T121254_031409_039D91_A4C7.zip",

"https://datapool.asf.alaska.edu/SLC/SA/S1A_IW_SLC__1SDV_20200213T121227_20200213T121254_031234_039785_0206.zip",

"https://datapool.asf.alaska.edu/SLC/SA/S1A_IW_SLC__1SDV_20200201T121227_20200201T121254_031059_039174_4E01.zip",

"https://datapool.asf.alaska.edu/SLC/SA/S1A_IW_SLC__1SDV_20200120T121228_20200120T121255_030884_038B59_C103.zip",

"https://datapool.asf.alaska.edu/SLC/SA/S1A_IW_SLC__1SDV_20200108T121228_20200108T121255_030709_038533_ED96.zip",

"https://datapool.asf.alaska.edu/SLC/SA/S1A_IW_SLC__1SDV_20191227T121229_20191227T121256_030534_037F23_E3CD.zip",

"https://datapool.asf.alaska.edu/SLC/SA/S1A_IW_SLC__1SDV_20191215T121229_20191215T121256_030359_03791A_31E0.zip",

"https://datapool.asf.alaska.edu/SLC/SA/S1A_IW_SLC__1SDV_20191203T121229_20191203T121256_030184_03730F_796E.zip",

"https://datapool.asf.alaska.edu/SLC/SA/S1A_IW_SLC__1SDV_20191121T121230_20191121T121257_030009_036CFD_CD2A.zip",

"https://datapool.asf.alaska.edu/SLC/SA/S1A_IW_SLC__1SDV_20191109T121230_20191109T121257_029834_0366F3_D352.zip",

"https://datapool.asf.alaska.edu/SLC/SA/S1A_IW_SLC__1SDV_20191028T121230_20191028T121257_029659_0360C3_75BB.zip",

"https://datapool.asf.alaska.edu/SLC/SA/S1A_IW_SLC__1SDV_20191016T121230_20191016T121257_029484_035ABB_8AF7.zip",

"https://datapool.asf.alaska.edu/SLC/SA/S1A_IW_SLC__1SDV_20191004T121230_20191004T121257_029309_0354B0_3BF0.zip",

"https://datapool.asf.alaska.edu/SLC/SA/S1A_IW_SLC__1SDV_20190922T121230_20190922T121257_029134_034EAB_7873.zip",

"https://datapool.asf.alaska.edu/SLC/SA/S1A_IW_SLC__1SDV_20190910T121229_20190910T121256_028959_0348B6_EC06.zip",

"https://datapool.asf.alaska.edu/SLC/SA/S1A_IW_SLC__1SDV_20190829T121229_20190829T121256_028784_03429E_E3A7.zip",

"https://datapool.asf.alaska.edu/SLC/SA/S1A_IW_SLC__1SDV_20190817T121228_20190817T121255_028609_033C79_629B.zip",

"https://datapool.asf.alaska.edu/SLC/SA/S1A_IW_SLC__1SDV_20190805T121228_20190805T121254_028434_033690_415A.zip",

"https://datapool.asf.alaska.edu/SLC/SA/S1A_IW_SLC__1SDV_20190724T121227_20190724T121254_028259_033136_2EFE.zip",

"https://datapool.asf.alaska.edu/SLC/SA/S1A_IW_SLC__1SDV_20190712T121226_20190712T121253_028084_032BED_91DA.zip",

"https://datapool.asf.alaska.edu/SLC/SA/S1A_IW_SLC__1SDV_20190630T121225_20190630T121252_027909_03269F_7503.zip",

"https://datapool.asf.alaska.edu/SLC/SA/S1A_IW_SLC__1SDV_20190618T121224_20190618T121251_027734_032165_A947.zip",

"https://datapool.asf.alaska.edu/SLC/SA/S1A_IW_SLC__1SDV_20190606T121224_20190606T121251_027559_031C1F_C7AB.zip",

"https://datapool.asf.alaska.edu/SLC/SA/S1A_IW_SLC__1SDV_20190513T121223_20190513T121249_027209_031140_DFAD.zip",

"https://datapool.asf.alaska.edu/SLC/SA/S1A_IW_SLC__1SDV_20190501T121222_20190501T121249_027034_030B64_9F80.zip",

"https://datapool.asf.alaska.edu/SLC/SA/S1A_IW_SLC__1SDV_20190419T121222_20190419T121248_026859_030507_7457.zip",

"https://datapool.asf.alaska.edu/SLC/SA/S1A_IW_SLC__1SDV_20190407T121221_20190407T121248_026684_02FEAD_31D1.zip",

"https://datapool.asf.alaska.edu/SLC/SA/S1A_IW_SLC__1SDV_20190326T121221_20190326T121248_026509_02F838_26C9.zip",

"https://datapool.asf.alaska.edu/SLC/SA/S1A_IW_SLC__1SDV_20190314T121221_20190314T121248_026334_02F1CB_A040.zip",

"https://datapool.asf.alaska.edu/SLC/SA/S1A_IW_SLC__1SDV_20190302T121221_20190302T121248_026159_02EB68_F0AE.zip",

"https://datapool.asf.alaska.edu/SLC/SA/S1A_IW_SLC__1SDV_20190218T121221_20190218T121248_025984_02E51F_CD73.zip",

"https://datapool.asf.alaska.edu/SLC/SA/S1A_IW_SLC__1SDV_20190206T121221_20190206T121247_025809_02DEE0_63AD.zip",

"https://datapool.asf.alaska.edu/SLC/SA/S1A_IW_SLC__1SDV_20190125T121221_20190125T121248_025634_02D899_CFD2.zip",

"https://datapool.asf.alaska.edu/SLC/SA/S1A_IW_SLC__1SDV_20190113T121222_20190113T121249_025459_02D234_8C26.zip",

"https://datapool.asf.alaska.edu/SLC/SA/S1A_IW_SLC__1SDV_20190101T121222_20190101T121249_025284_02CBEB_FED6.zip",

"https://datapool.asf.alaska.edu/SLC/SA/S1A_IW_SLC__1SDV_20181220T121222_20181220T121249_025109_02C597_257E.zip",

"https://datapool.asf.alaska.edu/SLC/SA/S1A_IW_SLC__1SDV_20181208T121223_20181208T121250_024934_02BF41_0B42.zip",

"https://datapool.asf.alaska.edu/SLC/SA/S1A_IW_SLC__1SDV_20181126T121223_20181126T121250_024759_02B969_51E8.zip",

"https://datapool.asf.alaska.edu/SLC/SA/S1A_IW_SLC__1SDV_20181114T121224_20181114T121251_024584_02B2FA_413F.zip",

"https://datapool.asf.alaska.edu/SLC/SA/S1A_IW_SLC__1SDV_20181102T121224_20181102T121251_024409_02AC8E_469F.zip",

"https://datapool.asf.alaska.edu/SLC/SA/S1A_IW_SLC__1SDV_20181021T121224_20181021T121251_024234_02A6C9_AFF7.zip",

"https://datapool.asf.alaska.edu/SLC/SA/S1A_IW_SLC__1SDV_20181009T121224_20181009T121251_024059_02A118_59D6.zip",

"https://datapool.asf.alaska.edu/SLC/SA/S1A_IW_SLC__1SDV_20180927T121224_20180927T121251_023884_029B53_1AD8.zip",

"https://datapool.asf.alaska.edu/SLC/SA/S1A_IW_SLC__1SDV_20180915T121223_20180915T121250_023709_0295A8_49B0.zip",

"https://datapool.asf.alaska.edu/SLC/SA/S1A_IW_SLC__1SDV_20180903T121223_20180903T121250_023534_02900C_6F6A.zip",

"https://datapool.asf.alaska.edu/SLC/SA/S1A_IW_SLC__1SDV_20180822T121222_20180822T121249_023359_028A7D_460E.zip",

"https://datapool.asf.alaska.edu/SLC/SA/S1A_IW_SLC__1SDV_20180810T121222_20180810T121249_023184_0284D5_FB2B.zip",

"https://datapool.asf.alaska.edu/SLC/SA/S1A_IW_SLC__1SDV_20180729T121221_20180729T121248_023009_027F5A_9EC0.zip",

"https://datapool.asf.alaska.edu/SLC/SA/S1A_IW_SLC__1SDV_20180717T121220_20180717T121247_022834_0279D2_4F05.zip",

"https://datapool.asf.alaska.edu/SLC/SA/S1A_IW_SLC__1SDV_20180705T121219_20180705T121246_022659_027482_1401.zip",

"https://datapool.asf.alaska.edu/SLC/SA/S1A_IW_SLC__1SDV_20180623T121219_20180623T121246_022484_026F65_CBCA.zip",

"https://datapool.asf.alaska.edu/SLC/SA/S1A_IW_SLC__1SDV_20180611T121218_20180611T121245_022309_026A26_A41D.zip",

"https://datapool.asf.alaska.edu/SLC/SA/S1A_IW_SLC__1SDV_20180530T121217_20180530T121244_022134_0264B1_61B0.zip",

"https://datapool.asf.alaska.edu/SLC/SA/S1A_IW_SLC__1SDV_20180518T121217_20180518T121244_021959_025F10_06D6.zip",

"https://datapool.asf.alaska.edu/SLC/SA/S1A_IW_SLC__1SDV_20180506T121216_20180506T121243_021784_02597F_8D35.zip",

"https://datapool.asf.alaska.edu/SLC/SA/S1A_IW_SLC__1SDV_20180424T121215_20180424T121242_021609_0253F3_5FF7.zip",

"https://datapool.asf.alaska.edu/SLC/SA/S1A_IW_SLC__1SDV_20180412T121215_20180412T121242_021434_024E7E_A47E.zip",

"https://datapool.asf.alaska.edu/SLC/SA/S1A_IW_SLC__1SDV_20180331T121215_20180331T121241_021259_02490D_3055.zip",

"https://datapool.asf.alaska.edu/SLC/SA/S1A_IW_SLC__1SDV_20180319T121214_20180319T121241_021084_02437D_E5E4.zip",

"https://datapool.asf.alaska.edu/SLC/SA/S1A_IW_SLC__1SDV_20180307T121214_20180307T121241_020909_023DF8_ADC9.zip",

"https://datapool.asf.alaska.edu/SLC/SA/S1A_IW_SLC__1SDV_20180223T121214_20180223T121241_020734_02386E_B22B.zip",

"https://datapool.asf.alaska.edu/SLC/SA/S1A_IW_SLC__1SDV_20180211T121214_20180211T121241_020559_0232D9_9BAB.zip",

"https://datapool.asf.alaska.edu/SLC/SA/S1A_IW_SLC__1SDV_20180130T121214_20180130T121241_020384_022D42_1959.zip",

"https://datapool.asf.alaska.edu/SLC/SA/S1A_IW_SLC__1SDV_20180118T121215_20180118T121242_020209_0227B2_D7A7.zip",

"https://datapool.asf.alaska.edu/SLC/SA/S1A_IW_SLC__1SDV_20180106T121215_20180106T121242_020034_022226_A3B7.zip",

"https://datapool.asf.alaska.edu/SLC/SA/S1A_IW_SLC__1SDV_20171225T121216_20171225T121243_019859_021C9A_9C81.zip",

"https://datapool.asf.alaska.edu/SLC/SA/S1A_IW_SLC__1SDV_20171213T121216_20171213T121243_019684_021735_8787.zip",

"https://datapool.asf.alaska.edu/SLC/SA/S1A_IW_SLC__1SDV_20171201T121217_20171201T121244_019509_0211BA_24E9.zip",

"https://datapool.asf.alaska.edu/SLC/SA/S1A_IW_SLC__1SDV_20171119T121217_20171119T121244_019334_020C41_D545.zip",

"https://datapool.asf.alaska.edu/SLC/SA/S1A_IW_SLC__1SDV_20171107T121217_20171107T121244_019159_0206C5_CB2D.zip",

"https://datapool.asf.alaska.edu/SLC/SA/S1A_IW_SLC__1SDV_20171026T121217_20171026T121244_018984_020158_116A.zip",

"https://datapool.asf.alaska.edu/SLC/SA/S1A_IW_SLC__1SDV_20171014T121217_20171014T121244_018809_01FC09_A95D.zip",

"https://datapool.asf.alaska.edu/SLC/SA/S1A_IW_SLC__1SDV_20171002T121217_20171002T121244_018634_01F6B9_F075.zip",

"https://datapool.asf.alaska.edu/SLC/SA/S1A_IW_SLC__1SDV_20170920T121217_20170920T121244_018459_01F155_D0B8.zip",

"https://datapool.asf.alaska.edu/SLC/SA/S1A_IW_SLC__1SDV_20170908T121216_20170908T121243_018284_01EBF3_E267.zip",

"https://datapool.asf.alaska.edu/SLC/SA/S1A_IW_SLC__1SDV_20170827T121216_20170827T121243_018109_01E69C_86A5.zip",

"https://datapool.asf.alaska.edu/SLC/SA/S1A_IW_SLC__1SDV_20170815T121215_20170815T121242_017934_01E151_84A1.zip",

"https://datapool.asf.alaska.edu/SLC/SA/S1A_IW_SLC__1SDV_20170803T121215_20170803T121242_017759_01DBFC_B1EA.zip",

"https://datapool.asf.alaska.edu/SLC/SA/S1A_IW_SLC__1SDV_20170722T121214_20170722T121241_017584_01D6A4_5799.zip",

"https://datapool.asf.alaska.edu/SLC/SA/S1A_IW_SLC__1SDV_20170710T121213_20170710T121240_017409_01D151_765E.zip",

"https://datapool.asf.alaska.edu/SLC/SA/S1A_IW_SLC__1SDV_20170628T121213_20170628T121240_017234_01CC09_5021.zip",

"https://datapool.asf.alaska.edu/SLC/SA/S1A_IW_SLC__1SDV_20170604T121211_20170604T121238_016884_01C156_AFD4.zip",

"https://datapool.asf.alaska.edu/SLC/SA/S1A_IW_SLC__1SDV_20170523T121211_20170523T121237_016709_01BBEA_4DF9.zip",

"https://datapool.asf.alaska.edu/SLC/SA/S1A_IW_SLC__1SDV_20170511T121210_20170511T121237_016534_01B681_0928.zip",

"https://datapool.asf.alaska.edu/SLC/SA/S1A_IW_SLC__1SDV_20170429T121209_20170429T121236_016359_01B13B_4D85.zip",

"https://datapool.asf.alaska.edu/SLC/SA/S1A_IW_SLC__1SDV_20170417T121209_20170417T121236_016184_01ABEA_7AC2.zip",

"https://datapool.asf.alaska.edu/SLC/SA/S1A_IW_SLC__1SDV_20170405T121208_20170405T121235_016009_01A68C_354D.zip",

"https://datapool.asf.alaska.edu/SLC/SA/S1A_IW_SLC__1SDV_20170324T121208_20170324T121235_015834_01A15C_04A5.zip",

"https://datapool.asf.alaska.edu/SLC/SA/S1A_IW_SLC__1SDV_20170312T121208_20170312T121235_015659_019C2A_4D27.zip"

**Descending Orbits Data Granules**

6. **Path 150 Frame 510**

"https://datapool.asf.alaska.edu/SLC/SA/S1A_IW_SLC__1SDV_20210722T235555_20210722T235623_038897_0496F9_9175.zip",

"https://datapool.asf.alaska.edu/SLC/SA/S1A_IW_SLC__1SDV_20210710T235555_20210710T235622_038722_0491BA_FFB1.zip",

"https://datapool.asf.alaska.edu/SLC/SA/S1A_IW_SLC__1SDV_20210628T235554_20210628T235621_038547_048C7B_D6E5.zip",

"https://datapool.asf.alaska.edu/SLC/SA/S1A_IW_SLC__1SDV_20210616T235553_20210616T235620_038372_048735_1E3D.zip",

"https://datapool.asf.alaska.edu/SLC/SA/S1A_IW_SLC__1SDV_20210604T235553_20210604T235620_038197_048206_E957.zip",

"https://datapool.asf.alaska.edu/SLC/SA/S1A_IW_SLC__1SDV_20210523T235552_20210523T235619_038022_047CCC_9FFA.zip",

"https://datapool.asf.alaska.edu/SLC/SA/S1A_IW_SLC__1SDV_20210511T235551_20210511T235618_037847_047785_9D2F.zip",

"https://datapool.asf.alaska.edu/SLC/SA/S1A_IW_SLC__1SDV_20210429T235550_20210429T235617_037672_0471D5_084B.zip",

"https://datapool.asf.alaska.edu/SLC/SA/S1A_IW_SLC__1SDV_20210417T235550_20210417T235617_037497_046BBE_A17A.zip",

"https://datapool.asf.alaska.edu/SLC/SA/S1A_IW_SLC__1SDV_20210405T235550_20210405T235617_037322_0465B8_551B.zip",

"https://datapool.asf.alaska.edu/SLC/SA/S1A_IW_SLC__1SDV_20210324T235549_20210324T235616_037147_045FA8_3865.zip",

"https://datapool.asf.alaska.edu/SLC/SA/S1A_IW_SLC__1SDV_20210312T235549_20210312T235616_036972_04599A_C9A5.zip",

"https://datapool.asf.alaska.edu/SLC/SA/S1A_IW_SLC__1SDV_20210228T235549_20210228T235616_036797_04537D_DF44.zip",

"https://datapool.asf.alaska.edu/SLC/SA/S1A_IW_SLC__1SDV_20210216T235549_20210216T235616_036622_044D6A_1BAB.zip",

"https://datapool.asf.alaska.edu/SLC/SA/S1A_IW_SLC__1SDV_20210204T235550_20210204T235617_036447_04474A_9264.zip",

"https://datapool.asf.alaska.edu/SLC/SA/S1A_IW_SLC__1SDV_20210123T235550_20210123T235617_036272_044140_90C7.zip",

"https://datapool.asf.alaska.edu/SLC/SA/S1A_IW_SLC__1SDV_20210111T235550_20210111T235617_036097_043B2D_F6CB.zip",

"https://datapool.asf.alaska.edu/SLC/SA/S1A_IW_SLC__1SDV_20201230T235551_20201230T235618_035922_04350E_95BA.zip",

"https://datapool.asf.alaska.edu/SLC/SA/S1A_IW_SLC__1SDV_20201218T235552_20201218T235619_035747_042EEA_B128.zip",

"https://datapool.asf.alaska.edu/SLC/SA/S1A_IW_SLC__1SDV_20201206T235552_20201206T235619_035572_0428E9_E7B9.zip",

"https://datapool.asf.alaska.edu/SLC/SA/S1A_IW_SLC__1SDV_20201124T235552_20201124T235619_035397_0422E1_841B.zip",

"https://datapool.asf.alaska.edu/SLC/SA/S1A_IW_SLC__1SDV_20201112T235553_20201112T235620_035222_041CD7_94E6.zip",

"https://datapool.asf.alaska.edu/SLC/SA/S1A_IW_SLC__1SDV_20201031T235553_20201031T235620_035047_0416B7_ACEF.zip",

"https://datapool.asf.alaska.edu/SLC/SA/S1A_IW_SLC__1SDV_20201019T235553_20201019T235620_034872_0410C4_E040.zip",

"https://datapool.asf.alaska.edu/SLC/SA/S1A_IW_SLC__1SDV_20201007T235553_20201007T235620_034697_040A9F_347F.zip",

"https://datapool.asf.alaska.edu/SLC/SA/S1A_IW_SLC__1SDV_20200925T235553_20200925T235620_034522_04047C_2CED.zip",

"https://datapool.asf.alaska.edu/SLC/SA/S1A_IW_SLC__1SDV_20200913T235552_20200913T235619_034347_03FE52_C134.zip",

"https://datapool.asf.alaska.edu/SLC/SA/S1A_IW_SLC__1SDV_20200901T235552_20200901T235619_034172_03F831_F207.zip",

"https://datapool.asf.alaska.edu/SLC/SA/S1A_IW_SLC__1SDV_20200820T235551_20200820T235618_033997_03F204_6965.zip",

"https://datapool.asf.alaska.edu/SLC/SA/S1A_IW_SLC__1SDV_20200808T235551_20200808T235618_033822_03EBE2_B133.zip",

"https://datapool.asf.alaska.edu/SLC/SA/S1A_IW_SLC__1SDV_20200727T235550_20200727T235617_033647_03E64C_55A9.zip",

"https://datapool.asf.alaska.edu/SLC/SA/S1A_IW_SLC__1SDV_20200715T235549_20200715T235616_033472_03E0EC_6507.zip",

"https://datapool.asf.alaska.edu/SLC/SA/S1A_IW_SLC__1SDV_20200703T235548_20200703T235615_033297_03DB97_3C1C.zip",

"https://datapool.asf.alaska.edu/SLC/SA/S1A_IW_SLC__1SDV_20200621T235548_20200621T235615_033122_03D646_FDAC.zip",

"https://datapool.asf.alaska.edu/SLC/SA/S1A_IW_SLC__1SDV_20200609T235547_20200609T235614_032947_03D0F8_98E0.zip",

"https://datapool.asf.alaska.edu/SLC/SA/S1A_IW_SLC__1SDV_20200528T235546_20200528T235613_032772_03CBCF_5A6E.zip",

"https://datapool.asf.alaska.edu/SLC/SA/S1A_IW_SLC__1SDV_20200516T235546_20200516T235613_032597_03C685_90BF.zip",

"https://datapool.asf.alaska.edu/SLC/SA/S1A_IW_SLC__1SDV_20200504T235545_20200504T235612_032422_03C11C_D334.zip",

"https://datapool.asf.alaska.edu/SLC/SA/S1A_IW_SLC__1SDV_20200422T235544_20200422T235611_032247_03BAF0_87CA.zip",

"https://datapool.asf.alaska.edu/SLC/SA/S1A_IW_SLC__1SDV_20200410T235544_20200410T235611_032072_03B4CE_5EEC.zip",

"https://datapool.asf.alaska.edu/SLC/SA/S1A_IW_SLC__1SDV_20200329T235544_20200329T235611_031897_03AE9C_DDBE.zip",

"https://datapool.asf.alaska.edu/SLC/SA/S1A_IW_SLC__1SDV_20200317T235543_20200317T235610_031722_03A876_2025.zip",

"https://datapool.asf.alaska.edu/SLC/SA/S1A_IW_SLC__1SDV_20200305T235543_20200305T235610_031547_03A262_3A93.zip",

"https://datapool.asf.alaska.edu/SLC/SA/S1A_IW_SLC__1SDV_20200222T235543_20200222T235610_031372_039C57_2AC9.zip",

"https://datapool.asf.alaska.edu/SLC/SA/S1A_IW_SLC__1SDV_20200210T235543_20200210T235610_031197_039651_1CDB.zip",

"https://datapool.asf.alaska.edu/SLC/SA/S1A_IW_SLC__1SDV_20200129T235544_20200129T235611_031022_039038_CF69.zip",

"https://datapool.asf.alaska.edu/SLC/SA/S1A_IW_SLC__1SDV_20200117T235544_20200117T235611_030847_038A14_FC78.zip",

"https://datapool.asf.alaska.edu/SLC/SA/S1A_IW_SLC__1SDV_20200105T235545_20200105T235612_030672_0383F2_F963.zip",

"https://datapool.asf.alaska.edu/SLC/SA/S1A_IW_SLC__1SDV_20191224T235545_20191224T235612_030497_037DE8_5319.zip",

"https://datapool.asf.alaska.edu/SLC/SA/S1A_IW_SLC__1SDV_20191212T235546_20191212T235613_030322_0377DC_1871.zip",

"https://datapool.asf.alaska.edu/SLC/SA/S1A_IW_SLC__1SDV_20191130T235546_20191130T235613_030147_0371D0_AEE1.zip",

"https://datapool.asf.alaska.edu/SLC/SA/S1A_IW_SLC__1SDV_20191118T235546_20191118T235614_029972_036BC0_6597.zip",

"https://datapool.asf.alaska.edu/SLC/SA/S1A_IW_SLC__1SDV_20191106T235547_20191106T235614_029797_0365AF_0A7F.zip",

"https://datapool.asf.alaska.edu/SLC/SA/S1A_IW_SLC__1SDV_20191025T235547_20191025T235614_029622_035F7E_CD3E.zip",

"https://datapool.asf.alaska.edu/SLC/SA/S1A_IW_SLC__1SDV_20191013T235547_20191013T235614_029447_03597F_0EC5.zip",

"https://datapool.asf.alaska.edu/SLC/SA/S1A_IW_SLC__1SDV_20191001T235547_20191001T235614_029272_035378_C182.zip",

"https://datapool.asf.alaska.edu/SLC/SA/S1A_IW_SLC__1SDV_20190919T235546_20190919T235613_029097_034D72_7BDC.zip",

"https://datapool.asf.alaska.edu/SLC/SA/S1A_IW_SLC__1SDV_20190907T235546_20190907T235613_028922_034767_56DE.zip",

"https://datapool.asf.alaska.edu/SLC/SA/S1A_IW_SLC__1SDV_20190826T235545_20190826T235612_028747_03414E_D125.zip",

"https://datapool.asf.alaska.edu/SLC/SA/S1A_IW_SLC__1SDV_20190802T235544_20190802T235611_028397_03357D_F66A.zip",

"https://datapool.asf.alaska.edu/SLC/SA/S1A_IW_SLC__1SDV_20190721T235543_20190721T235610_028222_033027_A32E.zip",

"https://datapool.asf.alaska.edu/SLC/SA/S1A_IW_SLC__1SDV_20190709T235542_20190709T235609_028047_032AE1_0264.zip",

"https://datapool.asf.alaska.edu/SLC/SA/S1A_IW_SLC__1SDV_20190627T235541_20190627T235608_027872_03258C_1FCA.zip",

"https://datapool.asf.alaska.edu/SLC/SA/S1A_IW_SLC__1SDV_20190615T235540_20190615T235608_027697_032055_A465.zip",

"https://datapool.asf.alaska.edu/SLC/SA/S1A_IW_SLC__1SDV_20190603T235540_20190603T235607_027522_031B0C_D45C.zip",

"https://datapool.asf.alaska.edu/SLC/SA/S1A_IW_SLC__1SDV_20190510T235539_20190510T235606_027172_031023_6717.zip",

"https://datapool.asf.alaska.edu/SLC/SA/S1A_IW_SLC__1SDV_20190428T235538_20190428T235605_026997_030A0E_9826.zip",

"https://datapool.asf.alaska.edu/SLC/SA/S1A_IW_SLC__1SDV_20190416T235538_20190416T235605_026822_0303BE_9B60.zip",

"https://datapool.asf.alaska.edu/SLC/SA/S1A_IW_SLC__1SDV_20190404T235537_20190404T235604_026647_02FD61_7474.zip",

"https://datapool.asf.alaska.edu/SLC/SA/S1A_IW_SLC__1SDV_20190323T235537_20190323T235604_026472_02F6E8_B0AB.zip",

"https://datapool.asf.alaska.edu/SLC/SA/S1A_IW_SLC__1SDV_20190311T235537_20190311T235604_026297_02F071_ACEF.zip",

"https://datapool.asf.alaska.edu/SLC/SA/S1A_IW_SLC__1SDV_20190227T235537_20190227T235604_026122_02EA16_754C.zip",

"https://datapool.asf.alaska.edu/SLC/SA/S1A_IW_SLC__1SDV_20190215T235537_20190215T235604_025947_02E3DD_8768.zip",

"https://datapool.asf.alaska.edu/SLC/SA/S1A_IW_SLC__1SDV_20190203T235537_20190203T235604_025772_02DDAA_E09E.zip",

"https://datapool.asf.alaska.edu/SLC/SA/S1A_IW_SLC__1SDV_20190122T235538_20190122T235605_025597_02D74F_AA50.zip",

"https://datapool.asf.alaska.edu/SLC/SA/S1A_IW_SLC__1SDV_20190110T235538_20190110T235605_025422_02D0E9_20D1.zip",

"https://datapool.asf.alaska.edu/SLC/SA/S1A_IW_SLC__1SDV_20181229T235539_20181229T235606_025247_02CAA0_D8B6.zip",

"https://datapool.asf.alaska.edu/SLC/SA/S1A_IW_SLC__1SDV_20181217T235539_20181217T235606_025072_02C446_6D03.zip",

"https://datapool.asf.alaska.edu/SLC/SA/S1A_IW_SLC__1SDV_20181123T235540_20181123T235607_024722_02B811_BB6F.zip",

"https://datapool.asf.alaska.edu/SLC/SA/S1A_IW_SLC__1SDV_20181111T235540_20181111T235607_024547_02B19F_2D4C.zip",

"https://datapool.asf.alaska.edu/SLC/SA/S1A_IW_SLC__1SDV_20181030T235540_20181030T235607_024372_02AB43_DBD0.zip",

"https://datapool.asf.alaska.edu/SLC/SA/S1A_IW_SLC__1SDV_20181018T235540_20181018T235608_024197_02A59F_6EBB.zip",

"https://datapool.asf.alaska.edu/SLC/SA/S1A_IW_SLC__1SDV_20181006T235540_20181006T235607_024022_029FEB_6F73.zip",

"https://datapool.asf.alaska.edu/SLC/SA/S1A_IW_SLC__1SDV_20180924T235540_20180924T235607_023847_029A32_847A.zip",

"https://datapool.asf.alaska.edu/SLC/SA/S1A_IW_SLC__1SDV_20180912T235540_20180912T235607_023672_02947F_3C60.zip",

"https://datapool.asf.alaska.edu/SLC/SA/S1A_IW_SLC__1SDV_20180831T235539_20180831T235606_023497_028EE7_ADFE.zip",

"https://datapool.asf.alaska.edu/SLC/SA/S1A_IW_SLC__1SDV_20180819T235538_20180819T235606_023322_028959_5659.zip",

"https://datapool.asf.alaska.edu/SLC/SA/S1A_IW_SLC__1SDV_20180807T235538_20180807T235605_023147_0283AC_5422.zip",

"https://datapool.asf.alaska.edu/SLC/SA/S1A_IW_SLC__1SDV_20180726T235537_20180726T235604_022972_027E33_0920.zip",

"https://datapool.asf.alaska.edu/SLC/SA/S1A_IW_SLC__1SDV_20180714T235536_20180714T235603_022797_0278AA_2EB6.zip",

"https://datapool.asf.alaska.edu/SLC/SA/S1A_IW_SLC__1SDV_20180608T235534_20180608T235601_022272_026907_0EEB.zip",

"https://datapool.asf.alaska.edu/SLC/SA/S1A_IW_SLC__1SDV_20180527T235534_20180527T235601_022097_02638A_8603.zip",

"https://datapool.asf.alaska.edu/SLC/SA/S1A_IW_SLC__1SDV_20180515T235533_20180515T235600_021922_025DFC_519E.zip",

"https://datapool.asf.alaska.edu/SLC/SA/S1A_IW_SLC__1SDV_20180503T235532_20180503T235559_021747_02585F_F993.zip",

"https://datapool.asf.alaska.edu/SLC/SA/S1A_IW_SLC__1SDV_20180421T235532_20180421T235559_021572_0252DF_F2FD.zip",

"https://datapool.asf.alaska.edu/SLC/SA/S1A_IW_SLC__1SDV_20180409T235531_20180409T235558_021397_024D6E_5EF3.zip",

"https://datapool.asf.alaska.edu/SLC/SA/S1A_IW_SLC__1SDV_20180328T235531_20180328T235558_021222_0247EE_1C16.zip",

"https://datapool.asf.alaska.edu/SLC/SA/S1A_IW_SLC__1SDV_20180316T235531_20180316T235558_021047_024260_3EA3.zip",

"https://datapool.asf.alaska.edu/SLC/SA/S1A_IW_SLC__1SDV_20180304T235530_20180304T235557_020872_023CD2_E827.zip",

"https://datapool.asf.alaska.edu/SLC/SA/S1A_IW_SLC__1SDV_20180220T235530_20180220T235557_020697_023749_B314.zip",

"https://datapool.asf.alaska.edu/SLC/SA/S1A_IW_SLC__1SDV_20180208T235531_20180208T235558_020522_0231B8_E9B9.zip",

"https://datapool.asf.alaska.edu/SLC/SA/S1A_IW_SLC__1SDV_20180127T235531_20180127T235558_020347_022C20_B1D4.zip",

"https://datapool.asf.alaska.edu/SLC/SA/S1A_IW_SLC__1SDV_20180115T235531_20180115T235558_020172_022695_10B6.zip",

"https://datapool.asf.alaska.edu/SLC/SA/S1A_IW_SLC__1SDV_20180103T235531_20180103T235559_019997_022104_00F5.zip",

"https://datapool.asf.alaska.edu/SLC/SA/S1A_IW_SLC__1SDV_20171222T235532_20171222T235559_019822_021B82_C9CF.zip",

"https://datapool.asf.alaska.edu/SLC/SA/S1A_IW_SLC__1SDV_20171210T235533_20171210T235600_019647_021620_6652.zip",

"https://datapool.asf.alaska.edu/SLC/SA/S1A_IW_SLC__1SDV_20171128T235533_20171128T235600_019472_0210AA_359C.zip",

"https://datapool.asf.alaska.edu/SLC/SA/S1A_IW_SLC__1SDV_20171116T235533_20171116T235600_019297_020B23_C089.zip",

"https://datapool.asf.alaska.edu/SLC/SA/S1A_IW_SLC__1SDV_20171104T235534_20171104T235601_019122_0205AC_5241.zip",

"https://datapool.asf.alaska.edu/SLC/SA/S1A_IW_SLC__1SDV_20171023T235534_20171023T235601_018947_020056_F588.zip",

"https://datapool.asf.alaska.edu/SLC/SA/S1A_IW_SLC__1SDV_20171011T235534_20171011T235601_018772_01FAF6_C9EB.zip",

"https://datapool.asf.alaska.edu/SLC/SA/S1A_IW_SLC__1SDV_20170929T235533_20170929T235601_018597_01F5A4_7C8B.zip",

"https://datapool.asf.alaska.edu/SLC/SA/S1A_IW_SLC__1SDV_20170917T235533_20170917T235600_018422_01F04D_6BB5.zip",

"https://datapool.asf.alaska.edu/SLC/SA/S1A_IW_SLC__1SDV_20170905T235533_20170905T235600_018247_01EAD9_6A53.zip",

"https://datapool.asf.alaska.edu/SLC/SA/S1A_IW_SLC__1SDV_20170824T235532_20170824T235559_018072_01E586_27C2.zip",

"https://datapool.asf.alaska.edu/SLC/SA/S1A_IW_SLC__1SDV_20170812T235532_20170812T235559_017897_01E03B_7BF4.zip",

"https://datapool.asf.alaska.edu/SLC/SA/S1A_IW_SLC__1SDV_20170731T235531_20170731T235558_017722_01DAEC_8ECD.zip",

"https://datapool.asf.alaska.edu/SLC/SA/S1A_IW_SLC__1SDV_20170601T235528_20170601T235555_016847_01C031_1AD0.zip",

"https://datapool.asf.alaska.edu/SLC/SA/S1A_IW_SLC__1SDV_20170520T235527_20170520T235554_016672_01BACE_7E91.zip",

"https://datapool.asf.alaska.edu/SLC/SA/S1A_IW_SLC__1SDV_20170508T235526_20170508T235553_016497_01B575_5C45.zip",

"https://datapool.asf.alaska.edu/SLC/SA/S1A_IW_SLC__1SDV_20170426T235525_20170426T235552_016322_01B021_2E81.zip",

"https://datapool.asf.alaska.edu/SLC/SA/S1A_IW_SLC__1SDV_20170414T235525_20170414T235552_016147_01AACB_547C.zip",

"https://datapool.asf.alaska.edu/SLC/SA/S1A_IW_SLC__1SDV_20170402T235525_20170402T235552_015972_01A572_00F3.zip",

"https://datapool.asf.alaska.edu/SLC/SA/S1A_IW_SLC__1SDV_20170321T235524_20170321T235551_015797_01A044_2D23.zip"

7. **Path 150 Frame 515**

"https://datapool.asf.alaska.edu/SLC/SA/S1A_IW_SLC__1SDV_20210722T235620_20210722T235647_038897_0496F9_C137.zip",

"https://datapool.asf.alaska.edu/SLC/SA/S1A_IW_SLC__1SDV_20210710T235620_20210710T235647_038722_0491BA_5C97.zip",

"https://datapool.asf.alaska.edu/SLC/SA/S1A_IW_SLC__1SDV_20210628T235619_20210628T235646_038547_048C7B_F070.zip",

"https://datapool.asf.alaska.edu/SLC/SA/S1A_IW_SLC__1SDV_20210616T235618_20210616T235645_038372_048735_58B7.zip",

"https://datapool.asf.alaska.edu/SLC/SA/S1A_IW_SLC__1SDV_20210604T235617_20210604T235644_038197_048206_ABE0.zip",

"https://datapool.asf.alaska.edu/SLC/SA/S1A_IW_SLC__1SDV_20210523T235617_20210523T235644_038022_047CCC_E547.zip",

"https://datapool.asf.alaska.edu/SLC/SA/S1A_IW_SLC__1SDV_20210511T235616_20210511T235643_037847_047785_981B.zip",

"https://datapool.asf.alaska.edu/SLC/SA/S1A_IW_SLC__1SDV_20210429T235615_20210429T235642_037672_0471D5_FB0B.zip",

"https://datapool.asf.alaska.edu/SLC/SA/S1A_IW_SLC__1SDV_20210417T235615_20210417T235642_037497_046BBE_1497.zip",

"https://datapool.asf.alaska.edu/SLC/SA/S1A_IW_SLC__1SDV_20210405T235614_20210405T235642_037322_0465B8_BA49.zip",

"https://datapool.asf.alaska.edu/SLC/SA/S1A_IW_SLC__1SDV_20210324T235614_20210324T235641_037147_045FA8_68B4.zip",

"https://datapool.asf.alaska.edu/SLC/SA/S1A_IW_SLC__1SDV_20210312T235614_20210312T235641_036972_04599A_FE73.zip",

"https://datapool.asf.alaska.edu/SLC/SA/S1A_IW_SLC__1SDV_20210228T235614_20210228T235641_036797_04537D_2DAF.zip",

"https://datapool.asf.alaska.edu/SLC/SA/S1A_IW_SLC__1SDV_20210216T235614_20210216T235641_036622_044D6A_6DD9.zip",

"https://datapool.asf.alaska.edu/SLC/SA/S1A_IW_SLC__1SDV_20210204T235614_20210204T235641_036447_04474A_6923.zip",

"https://datapool.asf.alaska.edu/SLC/SA/S1A_IW_SLC__1SDV_20210123T235615_20210123T235642_036272_044140_226B.zip",

"https://datapool.asf.alaska.edu/SLC/SA/S1A_IW_SLC__1SDV_20210111T235615_20210111T235642_036097_043B2D_35BB.zip",

"https://datapool.asf.alaska.edu/SLC/SA/S1A_IW_SLC__1SDV_20201230T235616_20201230T235643_035922_04350E_FDC0.zip",

"https://datapool.asf.alaska.edu/SLC/SA/S1A_IW_SLC__1SDV_20201218T235616_20201218T235643_035747_042EEA_79C3.zip",

"https://datapool.asf.alaska.edu/SLC/SA/S1A_IW_SLC__1SDV_20201206T235617_20201206T235644_035572_0428E9_2486.zip",

"https://datapool.asf.alaska.edu/SLC/SA/S1A_IW_SLC__1SDV_20201124T235617_20201124T235644_035397_0422E1_701F.zip",

"https://datapool.asf.alaska.edu/SLC/SA/S1A_IW_SLC__1SDV_20201112T235618_20201112T235645_035222_041CD7_FBA3.zip",

"https://datapool.asf.alaska.edu/SLC/SA/S1A_IW_SLC__1SDV_20201031T235618_20201031T235645_035047_0416B7_3211.zip",

"https://datapool.asf.alaska.edu/SLC/SA/S1A_IW_SLC__1SDV_20201019T235618_20201019T235645_034872_0410C4_73D5.zip",

"https://datapool.asf.alaska.edu/SLC/SA/S1A_IW_SLC__1SDV_20201007T235618_20201007T235645_034697_040A9F_9660.zip",

"https://datapool.asf.alaska.edu/SLC/SA/S1A_IW_SLC__1SDV_20200925T235618_20200925T235645_034522_04047C_CD3C.zip",

"https://datapool.asf.alaska.edu/SLC/SA/S1A_IW_SLC__1SDV_20200913T235617_20200913T235644_034347_03FE52_DC8A.zip",

"https://datapool.asf.alaska.edu/SLC/SA/S1A_IW_SLC__1SDV_20200901T235617_20200901T235644_034172_03F831_35C3.zip",

"https://datapool.asf.alaska.edu/SLC/SA/S1A_IW_SLC__1SDV_20200820T235616_20200820T235643_033997_03F204_7C3C.zip",

"https://datapool.asf.alaska.edu/SLC/SA/S1A_IW_SLC__1SDV_20200808T235615_20200808T235642_033822_03EBE2_699C.zip",

"https://datapool.asf.alaska.edu/SLC/SA/S1A_IW_SLC__1SDV_20200727T235615_20200727T235642_033647_03E64C_6C5D.zip",

"https://datapool.asf.alaska.edu/SLC/SA/S1A_IW_SLC__1SDV_20200715T235614_20200715T235641_033472_03E0EC_6FC6.zip",

"https://datapool.asf.alaska.edu/SLC/SA/S1A_IW_SLC__1SDV_20200703T235613_20200703T235640_033297_03DB97_EB9C.zip",

"https://datapool.asf.alaska.edu/SLC/SA/S1A_IW_SLC__1SDV_20200621T235613_20200621T235640_033122_03D646_C76B.zip",

"https://datapool.asf.alaska.edu/SLC/SA/S1A_IW_SLC__1SDV_20200609T235612_20200609T235639_032947_03D0F8_2725.zip",

"https://datapool.asf.alaska.edu/SLC/SA/S1A_IW_SLC__1SDV_20200528T235611_20200528T235638_032772_03CBCF_D966.zip",

"https://datapool.asf.alaska.edu/SLC/SA/S1A_IW_SLC__1SDV_20200516T235610_20200516T235638_032597_03C685_FDC0.zip",

"https://datapool.asf.alaska.edu/SLC/SA/S1A_IW_SLC__1SDV_20200504T235610_20200504T235637_032422_03C11C_13B0.zip",

"https://datapool.asf.alaska.edu/SLC/SA/S1A_IW_SLC__1SDV_20200422T235609_20200422T235636_032247_03BAF0_C953.zip",

"https://datapool.asf.alaska.edu/SLC/SA/S1A_IW_SLC__1SDV_20200410T235609_20200410T235636_032072_03B4CE_816B.zip",

"https://datapool.asf.alaska.edu/SLC/SA/S1A_IW_SLC__1SDV_20200329T235608_20200329T235635_031897_03AE9C_986A.zip",

"https://datapool.asf.alaska.edu/SLC/SA/S1A_IW_SLC__1SDV_20200317T235608_20200317T235635_031722_03A876_C772.zip",

"https://datapool.asf.alaska.edu/SLC/SA/S1A_IW_SLC__1SDV_20200305T235608_20200305T235635_031547_03A262_0FAA.zip",

"https://datapool.asf.alaska.edu/SLC/SA/S1A_IW_SLC__1SDV_20200222T235608_20200222T235635_031372_039C57_593B.zip",

"https://datapool.asf.alaska.edu/SLC/SA/S1A_IW_SLC__1SDV_20200210T235608_20200210T235635_031197_039651_29B4.zip",

"https://datapool.asf.alaska.edu/SLC/SA/S1A_IW_SLC__1SDV_20200129T235608_20200129T235636_031022_039038_A4E0.zip",

"https://datapool.asf.alaska.edu/SLC/SA/S1A_IW_SLC__1SDV_20200117T235609_20200117T235636_030847_038A14_6D30.zip",

"https://datapool.asf.alaska.edu/SLC/SA/S1A_IW_SLC__1SDV_20200105T235609_20200105T235636_030672_0383F2_8CD4.zip",

"https://datapool.asf.alaska.edu/SLC/SA/S1A_IW_SLC__1SDV_20191224T235610_20191224T235637_030497_037DE8_42E1.zip",

"https://datapool.asf.alaska.edu/SLC/SA/S1A_IW_SLC__1SDV_20191212T235610_20191212T235637_030322_0377DC_A727.zip",

"https://datapool.asf.alaska.edu/SLC/SA/S1A_IW_SLC__1SDV_20191130T235611_20191130T235638_030147_0371D0_0EE6.zip",

"https://datapool.asf.alaska.edu/SLC/SA/S1A_IW_SLC__1SDV_20191118T235611_20191118T235638_029972_036BC0_69B0.zip",

"https://datapool.asf.alaska.edu/SLC/SA/S1A_IW_SLC__1SDV_20191106T235611_20191106T235639_029797_0365AF_DDB9.zip",

"https://datapool.asf.alaska.edu/SLC/SA/S1A_IW_SLC__1SDV_20191025T235611_20191025T235638_029622_035F7E_4762.zip",

"https://datapool.asf.alaska.edu/SLC/SA/S1A_IW_SLC__1SDV_20191013T235611_20191013T235638_029447_03597F_D86F.zip",

"https://datapool.asf.alaska.edu/SLC/SA/S1A_IW_SLC__1SDV_20191001T235611_20191001T235639_029272_035378_8DF3.zip",

"https://datapool.asf.alaska.edu/SLC/SA/S1A_IW_SLC__1SDV_20190919T235611_20190919T235638_029097_034D72_7397.zip",

"https://datapool.asf.alaska.edu/SLC/SA/S1A_IW_SLC__1SDV_20190907T235610_20190907T235638_028922_034767_D1FF.zip",

"https://datapool.asf.alaska.edu/SLC/SA/S1A_IW_SLC__1SDV_20190826T235610_20190826T235637_028747_03414E_9533.zip",

"https://datapool.asf.alaska.edu/SLC/SA/S1A_IW_SLC__1SDV_20190802T235608_20190802T235636_028397_03357D_725B.zip",

"https://datapool.asf.alaska.edu/SLC/SA/S1A_IW_SLC__1SDV_20190721T235608_20190721T235635_028222_033027_8101.zip",

"https://datapool.asf.alaska.edu/SLC/SA/S1A_IW_SLC__1SDV_20190709T235607_20190709T235634_028047_032AE1_824D.zip",

"https://datapool.asf.alaska.edu/SLC/SA/S1A_IW_SLC__1SDV_20190627T235606_20190627T235633_027872_03258C_E519.zip",

"https://datapool.asf.alaska.edu/SLC/SA/S1A_IW_SLC__1SDV_20190615T235605_20190615T235632_027697_032055_B4A2.zip",

"https://datapool.asf.alaska.edu/SLC/SA/S1A_IW_SLC__1SDV_20190603T235605_20190603T235632_027522_031B0C_0E08.zip",

"https://datapool.asf.alaska.edu/SLC/SA/S1A_IW_SLC__1SDV_20190522T235604_20190522T235631_027347_03159F_656C.zip",

"https://datapool.asf.alaska.edu/SLC/SA/S1A_IW_SLC__1SDV_20190510T235603_20190510T235631_027172_031023_B369.zip",

"https://datapool.asf.alaska.edu/SLC/SA/S1A_IW_SLC__1SDV_20190428T235603_20190428T235630_026997_030A0E_71B0.zip",

"https://datapool.asf.alaska.edu/SLC/SA/S1A_IW_SLC__1SDV_20190416T235603_20190416T235630_026822_0303BE_FD64.zip",

"https://datapool.asf.alaska.edu/SLC/SA/S1A_IW_SLC__1SDV_20190404T235602_20190404T235629_026647_02FD61_0D75.zip",

"https://datapool.asf.alaska.edu/SLC/SA/S1A_IW_SLC__1SDV_20190323T235602_20190323T235629_026472_02F6E8_C7A2.zip",

"https://datapool.asf.alaska.edu/SLC/SA/S1A_IW_SLC__1SDV_20190311T235602_20190311T235629_026297_02F071_A7C3.zip",

"https://datapool.asf.alaska.edu/SLC/SA/S1A_IW_SLC__1SDV_20190227T235602_20190227T235629_026122_02EA16_344C.zip",

"https://datapool.asf.alaska.edu/SLC/SA/S1A_IW_SLC__1SDV_20190215T235602_20190215T235629_025947_02E3DD_2230.zip",

"https://datapool.asf.alaska.edu/SLC/SA/S1A_IW_SLC__1SDV_20190203T235602_20190203T235629_025772_02DDAA_BF65.zip",

"https://datapool.asf.alaska.edu/SLC/SA/S1A_IW_SLC__1SDV_20190122T235603_20190122T235630_025597_02D74F_CB2A.zip",

"https://datapool.asf.alaska.edu/SLC/SA/S1A_IW_SLC__1SDV_20190110T235603_20190110T235630_025422_02D0E9_6482.zip",

"https://datapool.asf.alaska.edu/SLC/SA/S1A_IW_SLC__1SDV_20181229T235603_20181229T235630_025247_02CAA0_5DE8.zip",

"https://datapool.asf.alaska.edu/SLC/SA/S1A_IW_SLC__1SDV_20181217T235604_20181217T235631_025072_02C446_FE20.zip",

"https://datapool.asf.alaska.edu/SLC/SA/S1A_IW_SLC__1SDV_20181123T235605_20181123T235632_024722_02B811_0A84.zip",

"https://datapool.asf.alaska.edu/SLC/SA/S1A_IW_SLC__1SDV_20181111T235605_20181111T235632_024547_02B19F_4583.zip",

"https://datapool.asf.alaska.edu/SLC/SA/S1A_IW_SLC__1SDV_20181030T235605_20181030T235632_024372_02AB43_2052.zip",

"https://datapool.asf.alaska.edu/SLC/SA/S1A_IW_SLC__1SDV_20181018T235605_20181018T235632_024197_02A59F_2825.zip",

"https://datapool.asf.alaska.edu/SLC/SA/S1A_IW_SLC__1SDV_20181006T235605_20181006T235632_024022_029FEB_02A9.zip",

"https://datapool.asf.alaska.edu/SLC/SA/S1A_IW_SLC__1SDV_20180924T235605_20180924T235632_023847_029A32_0C6B.zip",

"https://datapool.asf.alaska.edu/SLC/SA/S1A_IW_SLC__1SDV_20180912T235604_20180912T235631_023672_02947F_0912.zip",

"https://datapool.asf.alaska.edu/SLC/SA/S1A_IW_SLC__1SDV_20180831T235604_20180831T235631_023497_028EE7_24DD.zip",

"https://datapool.asf.alaska.edu/SLC/SA/S1A_IW_SLC__1SDV_20180819T235603_20180819T235630_023322_028959_796F.zip",

"https://datapool.asf.alaska.edu/SLC/SA/S1A_IW_SLC__1SDV_20180807T235603_20180807T235630_023147_0283AC_F0A5.zip",

"https://datapool.asf.alaska.edu/SLC/SA/S1A_IW_SLC__1SDV_20180726T235602_20180726T235629_022972_027E33_EC23.zip",

"https://datapool.asf.alaska.edu/SLC/SA/S1A_IW_SLC__1SDV_20180714T235601_20180714T235628_022797_0278AA_12E8.zip",

"https://datapool.asf.alaska.edu/SLC/SA/S1A_IW_SLC__1SDV_20180608T235559_20180608T235626_022272_026907_10A3.zip",

"https://datapool.asf.alaska.edu/SLC/SA/S1A_IW_SLC__1SDV_20180527T235558_20180527T235625_022097_02638A_95F7.zip",

"https://datapool.asf.alaska.edu/SLC/SA/S1A_IW_SLC__1SDV_20180515T235558_20180515T235625_021922_025DFC_9AD2.zip",

"https://datapool.asf.alaska.edu/SLC/SA/S1A_IW_SLC__1SDV_20180503T235557_20180503T235624_021747_02585F_B3B1.zip",

"https://datapool.asf.alaska.edu/SLC/SA/S1A_IW_SLC__1SDV_20180421T235556_20180421T235624_021572_0252DF_6606.zip",

"https://datapool.asf.alaska.edu/SLC/SA/S1A_IW_SLC__1SDV_20180409T235556_20180409T235623_021397_024D6E_EF65.zip",

"https://datapool.asf.alaska.edu/SLC/SA/S1A_IW_SLC__1SDV_20180328T235556_20180328T235623_021222_0247EE_905E.zip",

"https://datapool.asf.alaska.edu/SLC/SA/S1A_IW_SLC__1SDV_20180316T235555_20180316T235622_021047_024260_8DE5.zip",

"https://datapool.asf.alaska.edu/SLC/SA/S1A_IW_SLC__1SDV_20180304T235555_20180304T235622_020872_023CD2_4558.zip",

"https://datapool.asf.alaska.edu/SLC/SA/S1A_IW_SLC__1SDV_20180220T235555_20180220T235622_020697_023749_BCAD.zip",

"https://datapool.asf.alaska.edu/SLC/SA/S1A_IW_SLC__1SDV_20180208T235556_20180208T235623_020522_0231B8_3F2E.zip",

"https://datapool.asf.alaska.edu/SLC/SA/S1A_IW_SLC__1SDV_20180127T235556_20180127T235623_020347_022C20_FB07.zip",

"https://datapool.asf.alaska.edu/SLC/SA/S1A_IW_SLC__1SDV_20180115T235556_20180115T235623_020172_022695_AA91.zip",

"https://datapool.asf.alaska.edu/SLC/SA/S1A_IW_SLC__1SDV_20180103T235556_20180103T235623_019997_022104_DB50.zip",

"https://datapool.asf.alaska.edu/SLC/SA/S1A_IW_SLC__1SDV_20171222T235557_20171222T235624_019822_021B82_B5BC.zip",

"https://datapool.asf.alaska.edu/SLC/SA/S1A_IW_SLC__1SDV_20171210T235557_20171210T235625_019647_021620_6CF7.zip",

"https://datapool.asf.alaska.edu/SLC/SA/S1A_IW_SLC__1SDV_20171128T235558_20171128T235625_019472_0210AA_99B1.zip",

"https://datapool.asf.alaska.edu/SLC/SA/S1A_IW_SLC__1SDV_20171116T235558_20171116T235625_019297_020B23_DE86.zip",

"https://datapool.asf.alaska.edu/SLC/SA/S1A_IW_SLC__1SDV_20171104T235558_20171104T235626_019122_0205AC_472A.zip",

"https://datapool.asf.alaska.edu/SLC/SA/S1A_IW_SLC__1SDV_20171023T235559_20171023T235626_018947_020056_346F.zip",

"https://datapool.asf.alaska.edu/SLC/SA/S1A_IW_SLC__1SDV_20171011T235558_20171011T235626_018772_01FAF6_3ACA.zip",

"https://datapool.asf.alaska.edu/SLC/SA/S1A_IW_SLC__1SDV_20170929T235558_20170929T235625_018597_01F5A4_7C21.zip",

"https://datapool.asf.alaska.edu/SLC/SA/S1A_IW_SLC__1SDV_20170917T235558_20170917T235625_018422_01F04D_E95C.zip",

"https://datapool.asf.alaska.edu/SLC/SA/S1A_IW_SLC__1SDV_20170905T235557_20170905T235625_018247_01EAD9_E6E0.zip",

"https://datapool.asf.alaska.edu/SLC/SA/S1A_IW_SLC__1SDV_20170824T235557_20170824T235624_018072_01E586_6B60.zip",

"https://datapool.asf.alaska.edu/SLC/SA/S1A_IW_SLC__1SDV_20170812T235556_20170812T235624_017897_01E03B_C961.zip",

"https://datapool.asf.alaska.edu/SLC/SA/S1A_IW_SLC__1SDV_20170731T235556_20170731T235623_017722_01DAEC_BC55.zip",

"https://datapool.asf.alaska.edu/SLC/SA/S1A_IW_SLC__1SDV_20170601T235552_20170601T235619_016847_01C031_6EC0.zip",

"https://datapool.asf.alaska.edu/SLC/SA/S1A_IW_SLC__1SDV_20170520T235552_20170520T235619_016672_01BACE_6198.zip",

"https://datapool.asf.alaska.edu/SLC/SA/S1A_IW_SLC__1SDV_20170508T235551_20170508T235618_016497_01B575_76BA.zip",

"https://datapool.asf.alaska.edu/SLC/SA/S1A_IW_SLC__1SDV_20170426T235550_20170426T235617_016322_01B021_7E02.zip",

"https://datapool.asf.alaska.edu/SLC/SA/S1A_IW_SLC__1SDV_20170414T235550_20170414T235617_016147_01AACB_13E9.zip",

"https://datapool.asf.alaska.edu/SLC/SA/S1A_IW_SLC__1SDV_20170402T235549_20170402T235616_015972_01A572_992C.zip",

"https://datapool.asf.alaska.edu/SLC/SA/S1A_IW_SLC__1SDV_20170321T235549_20170321T235616_015797_01A044_AD43.zip"

**8. Path 150 Frame 520**

"https://datapool.asf.alaska.edu/SLC/SA/S1A_IW_SLC__1SDV_20210722T235645_20210722T235712_038897_0496F9_A6AE.zip",

"https://datapool.asf.alaska.edu/SLC/SA/S1A_IW_SLC__1SDV_20210710T235644_20210710T235711_038722_0491BA_08C4.zip",

"https://datapool.asf.alaska.edu/SLC/SA/S1A_IW_SLC__1SDV_20210628T235644_20210628T235711_038547_048C7B_95B2.zip",

"https://datapool.asf.alaska.edu/SLC/SA/S1A_IW_SLC__1SDV_20210616T235643_20210616T235710_038372_048735_5212.zip",

"https://datapool.asf.alaska.edu/SLC/SA/S1A_IW_SLC__1SDV_20210604T235642_20210604T235709_038197_048206_ED72.zip",

"https://datapool.asf.alaska.edu/SLC/SA/S1A_IW_SLC__1SDV_20210523T235641_20210523T235709_038022_047CCC_F54F.zip",

"https://datapool.asf.alaska.edu/SLC/SA/S1A_IW_SLC__1SDV_20210511T235641_20210511T235708_037847_047785_81BF.zip",

"https://datapool.asf.alaska.edu/SLC/SA/S1A_IW_SLC__1SDV_20210429T235640_20210429T235707_037672_0471D5_B19A.zip",

"https://datapool.asf.alaska.edu/SLC/SA/S1A_IW_SLC__1SDV_20210417T235640_20210417T235707_037497_046BBE_37C5.zip",

"https://datapool.asf.alaska.edu/SLC/SA/S1A_IW_SLC__1SDV_20210405T235639_20210405T235706_037322_0465B8_AFB8.zip",

"https://datapool.asf.alaska.edu/SLC/SA/S1A_IW_SLC__1SDV_20210324T235639_20210324T235706_037147_045FA8_580C.zip",

"https://datapool.asf.alaska.edu/SLC/SA/S1A_IW_SLC__1SDV_20210312T235639_20210312T235706_036972_04599A_6C44.zip",

"https://datapool.asf.alaska.edu/SLC/SA/S1A_IW_SLC__1SDV_20210228T235639_20210228T235706_036797_04537D_B28E.zip",

"https://datapool.asf.alaska.edu/SLC/SA/S1A_IW_SLC__1SDV_20210216T235639_20210216T235706_036622_044D6A_CF83.zip",

"https://datapool.asf.alaska.edu/SLC/SA/S1A_IW_SLC__1SDV_20210204T235639_20210204T235706_036447_04474A_7B28.zip",

"https://datapool.asf.alaska.edu/SLC/SA/S1A_IW_SLC__1SDV_20210123T235640_20210123T235707_036272_044140_EFA5.zip",

"https://datapool.asf.alaska.edu/SLC/SA/S1A_IW_SLC__1SDV_20210111T235640_20210111T235707_036097_043B2D_D1CF.zip",

"https://datapool.asf.alaska.edu/SLC/SA/S1A_IW_SLC__1SDV_20201230T235641_20201230T235708_035922_04350E_6C30.zip",

"https://datapool.asf.alaska.edu/SLC/SA/S1A_IW_SLC__1SDV_20201218T235641_20201218T235708_035747_042EEA_DBD5.zip",

"https://datapool.asf.alaska.edu/SLC/SA/S1A_IW_SLC__1SDV_20201206T235642_20201206T235709_035572_0428E9_FA87.zip",

"https://datapool.asf.alaska.edu/SLC/SA/S1A_IW_SLC__1SDV_20201124T235642_20201124T235709_035397_0422E1_0E3C.zip",

"https://datapool.asf.alaska.edu/SLC/SA/S1A_IW_SLC__1SDV_20201112T235642_20201112T235710_035222_041CD7_98FA.zip",

"https://datapool.asf.alaska.edu/SLC/SA/S1A_IW_SLC__1SDV_20201031T235643_20201031T235710_035047_0416B7_9162.zip",

"https://datapool.asf.alaska.edu/SLC/SA/S1A_IW_SLC__1SDV_20201019T235643_20201019T235710_034872_0410C4_EA92.zip",

"https://datapool.asf.alaska.edu/SLC/SA/S1A_IW_SLC__1SDV_20201007T235643_20201007T235710_034697_040A9F_8F32.zip",

"https://datapool.asf.alaska.edu/SLC/SA/S1A_IW_SLC__1SDV_20200925T235642_20200925T235710_034522_04047C_56F5.zip",

"https://datapool.asf.alaska.edu/SLC/SA/S1A_IW_SLC__1SDV_20200913T235642_20200913T235709_034347_03FE52_E2E6.zip",

"https://datapool.asf.alaska.edu/SLC/SA/S1A_IW_SLC__1SDV_20200901T235642_20200901T235709_034172_03F831_9332.zip",

"https://datapool.asf.alaska.edu/SLC/SA/S1A_IW_SLC__1SDV_20200820T235641_20200820T235708_033997_03F204_4F59.zip",

"https://datapool.asf.alaska.edu/SLC/SA/S1A_IW_SLC__1SDV_20200808T235640_20200808T235707_033822_03EBE2_A10E.zip",

"https://datapool.asf.alaska.edu/SLC/SA/S1A_IW_SLC__1SDV_20200727T235640_20200727T235707_033647_03E64C_80A7.zip",

"https://datapool.asf.alaska.edu/SLC/SA/S1A_IW_SLC__1SDV_20200715T235639_20200715T235706_033472_03E0EC_C817.zip",

"https://datapool.asf.alaska.edu/SLC/SA/S1A_IW_SLC__1SDV_20200703T235638_20200703T235705_033297_03DB97_1F1F.zip",

"https://datapool.asf.alaska.edu/SLC/SA/S1A_IW_SLC__1SDV_20200621T235637_20200621T235704_033122_03D646_ADC8.zip",

"https://datapool.asf.alaska.edu/SLC/SA/S1A_IW_SLC__1SDV_20200609T235637_20200609T235704_032947_03D0F8_98A8.zip",

"https://datapool.asf.alaska.edu/SLC/SA/S1A_IW_SLC__1SDV_20200528T235636_20200528T235703_032772_03CBCF_8EA5.zip",

"https://datapool.asf.alaska.edu/SLC/SA/S1A_IW_SLC__1SDV_20200516T235635_20200516T235702_032597_03C685_01E5.zip",

"https://datapool.asf.alaska.edu/SLC/SA/S1A_IW_SLC__1SDV_20200504T235634_20200504T235702_032422_03C11C_7088.zip",

"https://datapool.asf.alaska.edu/SLC/SA/S1A_IW_SLC__1SDV_20200422T235634_20200422T235701_032247_03BAF0_361D.zip",

"https://datapool.asf.alaska.edu/SLC/SA/S1A_IW_SLC__1SDV_20200410T235633_20200410T235701_032072_03B4CE_0A65.zip",

"https://datapool.asf.alaska.edu/SLC/SA/S1A_IW_SLC__1SDV_20200329T235633_20200329T235700_031897_03AE9C_A636.zip",

"https://datapool.asf.alaska.edu/SLC/SA/S1A_IW_SLC__1SDV_20200317T235633_20200317T235700_031722_03A876_EE30.zip",

"https://datapool.asf.alaska.edu/SLC/SA/S1A_IW_SLC__1SDV_20200305T235633_20200305T235700_031547_03A262_CDE7.zip",

"https://datapool.asf.alaska.edu/SLC/SA/S1A_IW_SLC__1SDV_20200222T235633_20200222T235700_031372_039C57_F9D2.zip",

"https://datapool.asf.alaska.edu/SLC/SA/S1A_IW_SLC__1SDV_20200210T235633_20200210T235700_031197_039651_1D6E.zip",

"https://datapool.asf.alaska.edu/SLC/SA/S1A_IW_SLC__1SDV_20200129T235633_20200129T235700_031022_039038_EDF6.zip",

"https://datapool.asf.alaska.edu/SLC/SA/S1A_IW_SLC__1SDV_20200117T235634_20200117T235701_030847_038A14_8FAB.zip",

"https://datapool.asf.alaska.edu/SLC/SA/S1A_IW_SLC__1SDV_20200105T235634_20200105T235701_030672_0383F2_E6AE.zip",

"https://datapool.asf.alaska.edu/SLC/SA/S1A_IW_SLC__1SDV_20191224T235635_20191224T235702_030497_037DE8_73A7.zip",

"https://datapool.asf.alaska.edu/SLC/SA/S1A_IW_SLC__1SDV_20191212T235635_20191212T235702_030322_0377DC_5179.zip",

"https://datapool.asf.alaska.edu/SLC/SA/S1A_IW_SLC__1SDV_20191130T235636_20191130T235703_030147_0371D0_163E.zip",

"https://datapool.asf.alaska.edu/SLC/SA/S1A_IW_SLC__1SDV_20191118T235636_20191118T235703_029972_036BC0_F2F4.zip",

"https://datapool.asf.alaska.edu/SLC/SA/S1A_IW_SLC__1SDV_20191106T235636_20191106T235703_029797_0365AF_D8F4.zip",

"https://datapool.asf.alaska.edu/SLC/SA/S1A_IW_SLC__1SDV_20191025T235636_20191025T235703_029622_035F7E_1CDE.zip",

"https://datapool.asf.alaska.edu/SLC/SA/S1A_IW_SLC__1SDV_20191013T235636_20191013T235703_029447_03597F_6C0D.zip",

"https://datapool.asf.alaska.edu/SLC/SA/S1A_IW_SLC__1SDV_20191001T235636_20191001T235703_029272_035378_C51E.zip",

"https://datapool.asf.alaska.edu/SLC/SA/S1A_IW_SLC__1SDV_20190919T235636_20190919T235703_029097_034D72_6DA4.zip",

"https://datapool.asf.alaska.edu/SLC/SA/S1A_IW_SLC__1SDV_20190907T235635_20190907T235702_028922_034767_DF4B.zip",

"https://datapool.asf.alaska.edu/SLC/SA/S1A_IW_SLC__1SDV_20190826T235635_20190826T235702_028747_03414E_721B.zip",

"https://datapool.asf.alaska.edu/SLC/SA/S1A_IW_SLC__1SDV_20190802T235633_20190802T235700_028397_03357D_9A78.zip",

"https://datapool.asf.alaska.edu/SLC/SA/S1A_IW_SLC__1SDV_20190721T235633_20190721T235700_028222_033027_CCC0.zip",

"https://datapool.asf.alaska.edu/SLC/SA/S1A_IW_SLC__1SDV_20190709T235632_20190709T235659_028047_032AE1_3BCF.zip",

"https://datapool.asf.alaska.edu/SLC/SA/S1A_IW_SLC__1SDV_20190627T235631_20190627T235658_027872_03258C_73D5.zip",

"https://datapool.asf.alaska.edu/SLC/SA/S1A_IW_SLC__1SDV_20190615T235630_20190615T235657_027697_032055_87F2.zip",

"https://datapool.asf.alaska.edu/SLC/SA/S1A_IW_SLC__1SDV_20190603T235630_20190603T235657_027522_031B0C_89DB.zip",

"https://datapool.asf.alaska.edu/SLC/SA/S1A_IW_SLC__1SDV_20190522T235629_20190522T235656_027347_03159F_D87C.zip",

"https://datapool.asf.alaska.edu/SLC/SA/S1A_IW_SLC__1SDV_20190510T235628_20190510T235655_027172_031023_9BD2.zip",

"https://datapool.asf.alaska.edu/SLC/SA/S1A_IW_SLC__1SDV_20190428T235628_20190428T235655_026997_030A0E_C2EE.zip",

"https://datapool.asf.alaska.edu/SLC/SA/S1A_IW_SLC__1SDV_20190416T235627_20190416T235654_026822_0303BE_F656.zip",

"https://datapool.asf.alaska.edu/SLC/SA/S1A_IW_SLC__1SDV_20190404T235627_20190404T235654_026647_02FD61_A3DC.zip",

"https://datapool.asf.alaska.edu/SLC/SA/S1A_IW_SLC__1SDV_20190323T235627_20190323T235654_026472_02F6E8_3D22.zip",

"https://datapool.asf.alaska.edu/SLC/SA/S1A_IW_SLC__1SDV_20190311T235627_20190311T235654_026297_02F071_860A.zip",

"https://datapool.asf.alaska.edu/SLC/SA/S1A_IW_SLC__1SDV_20190227T235627_20190227T235654_026122_02EA16_F442.zip",

"https://datapool.asf.alaska.edu/SLC/SA/S1A_IW_SLC__1SDV_20190215T235627_20190215T235654_025947_02E3DD_E07A.zip",

"https://datapool.asf.alaska.edu/SLC/SA/S1A_IW_SLC__1SDV_20190203T235627_20190203T235654_025772_02DDAA_46D6.zip",

"https://datapool.asf.alaska.edu/SLC/SA/S1A_IW_SLC__1SDV_20190122T235627_20190122T235654_025597_02D74F_7721.zip",

"https://datapool.asf.alaska.edu/SLC/SA/S1A_IW_SLC__1SDV_20190110T235628_20190110T235655_025422_02D0E9_84BC.zip",

"https://datapool.asf.alaska.edu/SLC/SA/S1A_IW_SLC__1SDV_20181229T235628_20181229T235655_025247_02CAA0_DADC.zip",

"https://datapool.asf.alaska.edu/SLC/SA/S1A_IW_SLC__1SDV_20181217T235628_20181217T235656_025072_02C446_62AD.zip",

"https://datapool.asf.alaska.edu/SLC/SA/S1A_IW_SLC__1SDV_20181123T235629_20181123T235656_024722_02B811_2A35.zip",

"https://datapool.asf.alaska.edu/SLC/SA/S1A_IW_SLC__1SDV_20181111T235630_20181111T235657_024547_02B19F_55F6.zip",

"https://datapool.asf.alaska.edu/SLC/SA/S1A_IW_SLC__1SDV_20181030T235630_20181030T235657_024372_02AB43_71AB.zip",

"https://datapool.asf.alaska.edu/SLC/SA/S1A_IW_SLC__1SDV_20181018T235630_20181018T235657_024197_02A59F_C01C.zip",

"https://datapool.asf.alaska.edu/SLC/SA/S1A_IW_SLC__1SDV_20181006T235630_20181006T235657_024022_029FEB_EA5F.zip",

"https://datapool.asf.alaska.edu/SLC/SA/S1A_IW_SLC__1SDV_20180924T235630_20180924T235657_023847_029A32_175C.zip",

"https://datapool.asf.alaska.edu/SLC/SA/S1A_IW_SLC__1SDV_20180912T235629_20180912T235656_023672_02947F_92A6.zip",

"https://datapool.asf.alaska.edu/SLC/SA/S1A_IW_SLC__1SDV_20180831T235629_20180831T235656_023497_028EE7_ED33.zip",

"https://datapool.asf.alaska.edu/SLC/SA/S1A_IW_SLC__1SDV_20180819T235628_20180819T235655_023322_028959_C8F4.zip",

"https://datapool.asf.alaska.edu/SLC/SA/S1A_IW_SLC__1SDV_20180807T235627_20180807T235654_023147_0283AC_673D.zip",

"https://datapool.asf.alaska.edu/SLC/SA/S1A_IW_SLC__1SDV_20180726T235627_20180726T235654_022972_027E33_CE2C.zip",

"https://datapool.asf.alaska.edu/SLC/SA/S1A_IW_SLC__1SDV_20180714T235626_20180714T235653_022797_0278AA_7395.zip",

"https://datapool.asf.alaska.edu/SLC/SA/S1A_IW_SLC__1SDV_20180608T235624_20180608T235651_022272_026907_A227.zip",

"https://datapool.asf.alaska.edu/SLC/SA/S1A_IW_SLC__1SDV_20180527T235623_20180527T235650_022097_02638A_A9F1.zip",

"https://datapool.asf.alaska.edu/SLC/SA/S1A_IW_SLC__1SDV_20180515T235622_20180515T235650_021922_025DFC_11CB.zip",

"https://datapool.asf.alaska.edu/SLC/SA/S1A_IW_SLC__1SDV_20180503T235622_20180503T235649_021747_02585F_D4CD.zip",

"https://datapool.asf.alaska.edu/SLC/SA/S1A_IW_SLC__1SDV_20180421T235621_20180421T235648_021572_0252DF_EEE2.zip",

"https://datapool.asf.alaska.edu/SLC/SA/S1A_IW_SLC__1SDV_20180409T235621_20180409T235648_021397_024D6E_D289.zip",

"https://datapool.asf.alaska.edu/SLC/SA/S1A_IW_SLC__1SDV_20180328T235620_20180328T235648_021222_0247EE_D80B.zip",

"https://datapool.asf.alaska.edu/SLC/SA/S1A_IW_SLC__1SDV_20180316T235620_20180316T235647_021047_024260_6D5E.zip",

"https://datapool.asf.alaska.edu/SLC/SA/S1A_IW_SLC__1SDV_20180304T235620_20180304T235647_020872_023CD2_6183.zip",

"https://datapool.asf.alaska.edu/SLC/SA/S1A_IW_SLC__1SDV_20180220T235620_20180220T235647_020697_023749_1B41.zip",

"https://datapool.asf.alaska.edu/SLC/SA/S1A_IW_SLC__1SDV_20180208T235620_20180208T235647_020522_0231B8_6C49.zip",

"https://datapool.asf.alaska.edu/SLC/SA/S1A_IW_SLC__1SDV_20180127T235621_20180127T235648_020347_022C20_E5DF.zip",

"https://datapool.asf.alaska.edu/SLC/SA/S1A_IW_SLC__1SDV_20180115T235621_20180115T235648_020172_022695_5694.zip",

"https://datapool.asf.alaska.edu/SLC/SA/S1A_IW_SLC__1SDV_20180103T235621_20180103T235648_019997_022104_BB16.zip",

"https://datapool.asf.alaska.edu/SLC/SA/S1A_IW_SLC__1SDV_20171222T235622_20171222T235649_019822_021B82_5DEF.zip",

"https://datapool.asf.alaska.edu/SLC/SA/S1A_IW_SLC__1SDV_20171210T235622_20171210T235649_019647_021620_AE25.zip",

"https://datapool.asf.alaska.edu/SLC/SA/S1A_IW_SLC__1SDV_20171128T235623_20171128T235650_019472_0210AA_F1FE.zip",

"https://datapool.asf.alaska.edu/SLC/SA/S1A_IW_SLC__1SDV_20171116T235623_20171116T235650_019297_020B23_9046.zip",

"https://datapool.asf.alaska.edu/SLC/SA/S1A_IW_SLC__1SDV_20171104T235623_20171104T235650_019122_0205AC_A23E.zip",

"https://datapool.asf.alaska.edu/SLC/SA/S1A_IW_SLC__1SDV_20171023T235623_20171023T235650_018947_020056_B6BC.zip",

"https://datapool.asf.alaska.edu/SLC/SA/S1A_IW_SLC__1SDV_20171011T235623_20171011T235650_018772_01FAF6_2A3D.zip",

"https://datapool.asf.alaska.edu/SLC/SA/S1A_IW_SLC__1SDV_20170929T235623_20170929T235650_018597_01F5A4_1A72.zip",

"https://datapool.asf.alaska.edu/SLC/SA/S1A_IW_SLC__1SDV_20170917T235623_20170917T235650_018422_01F04D_72A5.zip",

"https://datapool.asf.alaska.edu/SLC/SA/S1A_IW_SLC__1SDV_20170905T235622_20170905T235649_018247_01EAD9_5547.zip",

"https://datapool.asf.alaska.edu/SLC/SA/S1A_IW_SLC__1SDV_20170824T235622_20170824T235649_018072_01E586_898C.zip",

"https://datapool.asf.alaska.edu/SLC/SA/S1A_IW_SLC__1SDV_20170812T235621_20170812T235648_017897_01E03B_A92B.zip",

"https://datapool.asf.alaska.edu/SLC/SA/S1A_IW_SLC__1SDV_20170731T235621_20170731T235648_017722_01DAEC_5D2F.zip",

"https://datapool.asf.alaska.edu/SLC/SA/S1A_IW_SLC__1SDV_20170601T235617_20170601T235644_016847_01C031_06A7.zip",

"https://datapool.asf.alaska.edu/SLC/SA/S1A_IW_SLC__1SDV_20170520T235616_20170520T235644_016672_01BACE_62CE.zip",

"https://datapool.asf.alaska.edu/SLC/SA/S1A_IW_SLC__1SDV_20170508T235616_20170508T235643_016497_01B575_F5F3.zip",

"https://datapool.asf.alaska.edu/SLC/SA/S1A_IW_SLC__1SDV_20170426T235615_20170426T235642_016322_01B021_C6B4.zip",

"https://datapool.asf.alaska.edu/SLC/SA/S1A_IW_SLC__1SDV_20170414T235615_20170414T235642_016147_01AACB_68E5.zip",

"https://datapool.asf.alaska.edu/SLC/SA/S1A_IW_SLC__1SDV_20170402T235614_20170402T235641_015972_01A572_381E.zip",

"https://datapool.asf.alaska.edu/SLC/SA/S1A_IW_SLC__1SDV_20170321T235614_20170321T235641_015797_01A044_5933.zip"

**9. Path 48 Frame 514**

"https://datapool.asf.alaska.edu/SLC/SA/S1A_IW_SLC__1SDV_20210610T000425_20210610T000452_038270_04841E_0951.zip",

"https://datapool.asf.alaska.edu/SLC/SA/S1A_IW_SLC__1SDV_20210529T000424_20210529T000451_038095_047EF4_274F.zip",

"https://datapool.asf.alaska.edu/SLC/SA/S1A_IW_SLC__1SDV_20210517T000423_20210517T000450_037920_0479A9_8D24.zip",

"https://datapool.asf.alaska.edu/SLC/SA/S1A_IW_SLC__1SDV_20210505T000423_20210505T000450_037745_047463_FB1E.zip",

"https://datapool.asf.alaska.edu/SLC/SA/S1A_IW_SLC__1SDV_20210423T000422_20210423T000449_037570_046E48_31EC.zip",

"https://datapool.asf.alaska.edu/SLC/SA/S1A_IW_SLC__1SDV_20210411T000422_20210411T000449_037395_046837_A7FC.zip",

"https://datapool.asf.alaska.edu/SLC/SA/S1A_IW_SLC__1SDV_20210330T000421_20210330T000448_037220_046230_E657.zip",

"https://datapool.asf.alaska.edu/SLC/SA/S1A_IW_SLC__1SDV_20210318T000421_20210318T000448_037045_045C26_7BBD.zip",

"https://datapool.asf.alaska.edu/SLC/SA/S1A_IW_SLC__1SDV_20210306T000421_20210306T000448_036870_045604_8EC5.zip",

"https://datapool.asf.alaska.edu/SLC/SA/S1A_IW_SLC__1SDV_20210222T000421_20210222T000448_036695_044FF8_9CE9.zip",

"https://datapool.asf.alaska.edu/SLC/SA/S1A_IW_SLC__1SDV_20210210T000421_20210210T000449_036520_0449D9_7D69.zip",

"https://datapool.asf.alaska.edu/SLC/SA/S1A_IW_SLC__1SDV_20210129T000422_20210129T000449_036345_0443C6_C946.zip",

"https://datapool.asf.alaska.edu/SLC/SA/S1A_IW_SLC__1SDV_20210117T000422_20210117T000449_036170_043DAD_E11B.zip",

"https://datapool.asf.alaska.edu/SLC/SA/S1A_IW_SLC__1SDV_20210105T000423_20210105T000450_035995_043787_964C.zip",

"https://datapool.asf.alaska.edu/SLC/SA/S1A_IW_SLC__1SDV_20201224T000423_20201224T000450_035820_043176_B171.zip",

"https://datapool.asf.alaska.edu/SLC/SA/S1A_IW_SLC__1SDV_20201212T000424_20201212T000451_035645_042B6E_452E.zip",

"https://datapool.asf.alaska.edu/SLC/SA/S1A_IW_SLC__1SDV_20201130T000424_20201130T000451_035470_04256D_EF94.zip",

"https://datapool.asf.alaska.edu/SLC/SA/S1A_IW_SLC__1SDV_20201118T000425_20201118T000452_035295_041F65_B47C.zip",

"https://datapool.asf.alaska.edu/SLC/SA/S1A_IW_SLC__1SDV_20201106T000425_20201106T000452_035120_041940_7C9C.zip",

"https://datapool.asf.alaska.edu/SLC/SA/S1A_IW_SLC__1SDV_20201025T000425_20201025T000452_034945_041343_1AD0.zip",

"https://datapool.asf.alaska.edu/SLC/SA/S1A_IW_SLC__1SDV_20201013T000425_20201013T000452_034770_040D2E_DC49.zip",

"https://datapool.asf.alaska.edu/SLC/SA/S1A_IW_SLC__1SDV_20201001T000425_20201001T000452_034595_040719_E3F9.zip",

"https://datapool.asf.alaska.edu/SLC/SA/S1A_IW_SLC__1SDV_20200919T000425_20200919T000452_034420_0400E8_CE78.zip",

"https://datapool.asf.alaska.edu/SLC/SA/S1A_IW_SLC__1SDV_20200907T000424_20200907T000451_034245_03FABD_E1BF.zip",

"https://datapool.asf.alaska.edu/SLC/SA/S1A_IW_SLC__1SDV_20200826T000424_20200826T000451_034070_03F49B_3AB6.zip",

"https://datapool.asf.alaska.edu/SLC/SA/S1A_IW_SLC__1SDV_20200814T000423_20200814T000450_033895_03EE63_B37F.zip",

"https://datapool.asf.alaska.edu/SLC/SA/S1A_IW_SLC__1SDV_20200802T000422_20200802T000449_033720_03E87F_F8FB.zip",

"https://datapool.asf.alaska.edu/SLC/SA/S1A_IW_SLC__1SDV_20200721T000422_20200721T000449_033545_03E31B_963F.zip",

"https://datapool.asf.alaska.edu/SLC/SA/S1A_IW_SLC__1SDV_20200709T000421_20200709T000448_033370_03DDC1_1FE4.zip",

"https://datapool.asf.alaska.edu/SLC/SA/S1A_IW_SLC__1SDV_20200627T000420_20200627T000447_033195_03D870_88BE.zip",

"https://datapool.asf.alaska.edu/SLC/SA/S1A_IW_SLC__1SDV_20200615T000419_20200615T000446_033020_03D320_BA79.zip",

"https://datapool.asf.alaska.edu/SLC/SA/S1A_IW_SLC__1SDV_20200603T000419_20200603T000446_032845_03CDEB_0D00.zip",

"https://datapool.asf.alaska.edu/SLC/SA/S1A_IW_SLC__1SDV_20200522T000418_20200522T000445_032670_03C8AC_759D.zip",

"https://datapool.asf.alaska.edu/SLC/SA/S1A_IW_SLC__1SDV_20200428T000417_20200428T000444_032320_03BD7E_9F52.zip",

"https://datapool.asf.alaska.edu/SLC/SA/S1A_IW_SLC__1SDV_20200416T000416_20200416T000443_032145_03B758_D7C9.zip",

"https://datapool.asf.alaska.edu/SLC/SA/S1A_IW_SLC__1SDV_20200404T000416_20200404T000443_031970_03B12F_CC18.zip",

"https://datapool.asf.alaska.edu/SLC/SA/S1A_IW_SLC__1SDV_20200323T000415_20200323T000443_031795_03AB07_F8B9.zip",

"https://datapool.asf.alaska.edu/SLC/SA/S1A_IW_SLC__1SDV_20200311T000415_20200311T000442_031620_03A4E1_963C.zip",

"https://datapool.asf.alaska.edu/SLC/SA/S1A_IW_SLC__1SDV_20200228T000415_20200228T000442_031445_039ECC_6C1B.zip",

"https://datapool.asf.alaska.edu/SLC/SA/S1A_IW_SLC__1SDV_20200216T000415_20200216T000442_031270_0398C8_C749.zip",

"https://datapool.asf.alaska.edu/SLC/SA/S1A_IW_SLC__1SDV_20200204T000416_20200204T000443_031095_0392BE_DD0E.zip",

"https://datapool.asf.alaska.edu/SLC/SA/S1A_IW_SLC__1SDV_20200123T000416_20200123T000443_030920_038C98_65B2.zip",

"https://datapool.asf.alaska.edu/SLC/SA/S1A_IW_SLC__1SDV_20200111T000416_20200111T000443_030745_038671_0525.zip",

"https://datapool.asf.alaska.edu/SLC/SA/S1A_IW_SLC__1SDV_20191230T000417_20191230T000444_030570_038063_9E82.zip",

"https://datapool.asf.alaska.edu/SLC/SA/S1A_IW_SLC__1SDV_20191218T000417_20191218T000444_030395_037A62_1C10.zip",

"https://datapool.asf.alaska.edu/SLC/SA/S1A_IW_SLC__1SDV_20191206T000418_20191206T000445_030220_037451_729D.zip",

"https://datapool.asf.alaska.edu/SLC/SA/S1A_IW_SLC__1SDV_20191124T000418_20191124T000445_030045_036E43_9D69.zip",

"https://datapool.asf.alaska.edu/SLC/SA/S1A_IW_SLC__1SDV_20191112T000419_20191112T000446_029870_036835_4ACD.zip",

"https://datapool.asf.alaska.edu/SLC/SA/S1A_IW_SLC__1SDV_20191031T000419_20191031T000446_029695_036215_681B.zip",

"https://datapool.asf.alaska.edu/SLC/SA/S1A_IW_SLC__1SDV_20191019T000419_20191019T000446_029520_035BFD_3CE2.zip",

"https://datapool.asf.alaska.edu/SLC/SA/S1A_IW_SLC__1SDV_20191007T000419_20191007T000446_029345_0355F7_EA97.zip",

"https://datapool.asf.alaska.edu/SLC/SA/S1A_IW_SLC__1SDV_20190925T000418_20190925T000445_029170_034FEC_D1EE.zip",

"https://datapool.asf.alaska.edu/SLC/SA/S1A_IW_SLC__1SDV_20190913T000418_20190913T000445_028995_0349F3_8B48.zip",

"https://datapool.asf.alaska.edu/SLC/SA/S1A_IW_SLC__1SDV_20190901T000417_20190901T000444_028820_0343E1_35CF.zip",

"https://datapool.asf.alaska.edu/SLC/SA/S1A_IW_SLC__1SDV_20190820T000417_20190820T000444_028645_033DC3_707D.zip",

"https://datapool.asf.alaska.edu/SLC/SA/S1A_IW_SLC__1SDV_20190808T000416_20190808T000443_028470_0337B5_C001.zip",

"https://datapool.asf.alaska.edu/SLC/SA/S1A_IW_SLC__1SDV_20190727T000415_20190727T000442_028295_033259_4B40.zip",

"https://datapool.asf.alaska.edu/SLC/SA/S1A_IW_SLC__1SDV_20190422T000410_20190422T000437_026895_030652_959B.zip",

"https://datapool.asf.alaska.edu/SLC/SA/S1A_IW_SLC__1SDV_20190410T000409_20190410T000437_026720_030006_02CE.zip",

"https://datapool.asf.alaska.edu/SLC/SA/S1A_IW_SLC__1SDV_20190329T000409_20190329T000436_026545_02F993_61F3.zip",

"https://datapool.asf.alaska.edu/SLC/SA/S1A_IW_SLC__1SDV_20190317T000409_20190317T000436_026370_02F32A_DF57.zip",

"https://datapool.asf.alaska.edu/SLC/SA/S1A_IW_SLC__1SDV_20190221T000409_20190221T000436_026020_02E673_CE3B.zip",

"https://datapool.asf.alaska.edu/SLC/SA/S1A_IW_SLC__1SDV_20190209T000409_20190209T000436_025845_02E03C_C556.zip",

"https://datapool.asf.alaska.edu/SLC/SA/S1A_IW_SLC__1SDV_20190128T000410_20190128T000437_025670_02D9F3_8E18.zip",

"https://datapool.asf.alaska.edu/SLC/SA/S1A_IW_SLC__1SDV_20190116T000410_20190116T000437_025495_02D389_55AA.zip",

"https://datapool.asf.alaska.edu/SLC/SA/S1A_IW_SLC__1SDV_20190104T000410_20190104T000437_025320_02CD37_62B9.zip",

"https://datapool.asf.alaska.edu/SLC/SA/S1A_IW_SLC__1SDV_20181223T000411_20181223T000438_025145_02C6E9_E677.zip",

"https://datapool.asf.alaska.edu/SLC/SA/S1A_IW_SLC__1SDV_20181211T000411_20181211T000438_024970_02C09B_1DFF.zip",

"https://datapool.asf.alaska.edu/SLC/SA/S1A_IW_SLC__1SDV_20181129T000411_20181129T000439_024795_02BAB1_19ED.zip",

"https://datapool.asf.alaska.edu/SLC/SA/S1A_IW_SLC__1SDV_20181117T000412_20181117T000439_024620_02B44A_616F.zip",

"https://datapool.asf.alaska.edu/SLC/SA/S1A_IW_SLC__1SDV_20181105T000412_20181105T000439_024445_02ADE3_5D93.zip",

"https://datapool.asf.alaska.edu/SLC/SA/S1A_IW_SLC__1SDV_20181024T000412_20181024T000439_024270_02A7F5_4BBB.zip",

"https://datapool.asf.alaska.edu/SLC/SA/S1A_IW_SLC__1SDV_20181012T000412_20181012T000439_024095_02A248_6770.zip",

"https://datapool.asf.alaska.edu/SLC/SA/S1A_IW_SLC__1SDV_20180930T000412_20180930T000439_023920_029C86_7DD7.zip",

"https://datapool.asf.alaska.edu/SLC/SA/S1A_IW_SLC__1SDV_20180918T000412_20180918T000439_023745_0296D7_30F7.zip",

"https://datapool.asf.alaska.edu/SLC/SA/S1A_IW_SLC__1SDV_20180906T000412_20180906T000439_023570_02913F_CA8D.zip",

"https://datapool.asf.alaska.edu/SLC/SA/S1A_IW_SLC__1SDV_20180825T000411_20180825T000438_023395_028BA9_B985.zip",

"https://datapool.asf.alaska.edu/SLC/SA/S1A_IW_SLC__1SDV_20180801T000409_20180801T000436_023045_028071_37AD.zip",

"https://datapool.asf.alaska.edu/SLC/SA/S1A_IW_SLC__1SDV_20180720T000409_20180720T000436_022870_027AE8_11CA.zip",

"https://datapool.asf.alaska.edu/SLC/SA/S1A_IW_SLC__1SDV_20180708T000408_20180708T000435_022695_02758B_7837.zip",

"https://datapool.asf.alaska.edu/SLC/SA/S1A_IW_SLC__1SDV_20180626T000407_20180626T000434_022520_027072_E667.zip",

"https://datapool.asf.alaska.edu/SLC/SA/S1A_IW_SLC__1SDV_20180614T000407_20180614T000434_022345_026B4E_F722.zip",

"https://datapool.asf.alaska.edu/SLC/SA/S1A_IW_SLC__1SDV_20180521T000405_20180521T000432_021995_026046_8C4B.zip",

"https://datapool.asf.alaska.edu/SLC/SA/S1A_IW_SLC__1SDV_20180509T000404_20180509T000432_021820_025AB2_CAC4.zip",

"https://datapool.asf.alaska.edu/SLC/SA/S1A_IW_SLC__1SDV_20180427T000404_20180427T000431_021645_025523_01BE.zip",

"https://datapool.asf.alaska.edu/SLC/SA/S1A_IW_SLC__1SDV_20180322T000403_20180322T000430_021120_0244B7_2447.zip",

"https://datapool.asf.alaska.edu/SLC/SA/S1A_IW_SLC__1SDV_20180310T000402_20180310T000430_020945_023F25_A3A4.zip",

"https://datapool.asf.alaska.edu/SLC/SA/S1A_IW_SLC__1SDV_20180226T000402_20180226T000430_020770_0239A2_9132.zip",

"https://datapool.asf.alaska.edu/SLC/SA/S1A_IW_SLC__1SDV_20180214T000403_20180214T000430_020595_02340C_F3FA.zip",

"https://datapool.asf.alaska.edu/SLC/SA/S1A_IW_SLC__1SDV_20180202T000403_20180202T000430_020420_022E70_8EAC.zip",

"https://datapool.asf.alaska.edu/SLC/SA/S1A_IW_SLC__1SDV_20180121T000403_20180121T000430_020245_0228DC_D318.zip",

"https://datapool.asf.alaska.edu/SLC/SA/S1A_IW_SLC__1SDV_20180109T000404_20180109T000431_020070_02234E_7436.zip",

"https://datapool.asf.alaska.edu/SLC/SA/S1A_IW_SLC__1SDV_20171228T000404_20171228T000431_019895_021DCF_B4C3.zip",

"https://datapool.asf.alaska.edu/SLC/SA/S1A_IW_SLC__1SDV_20171204T000405_20171204T000432_019545_0212ED_285D.zip",

"https://datapool.asf.alaska.edu/SLC/SA/S1A_IW_SLC__1SDV_20171110T000405_20171110T000433_019195_0207F0_10A6.zip",

"https://datapool.asf.alaska.edu/SLC/SA/S1A_IW_SLC__1SDV_20171029T000406_20171029T000433_019020_020289_729C.zip",

"https://datapool.asf.alaska.edu/SLC/SA/S1A_IW_SLC__1SDV_20171017T000406_20171017T000433_018845_01FD3E_7AB0.zip",

"https://datapool.asf.alaska.edu/SLC/SA/S1A_IW_SLC__1SDV_20171005T000406_20171005T000433_018670_01F7DF_A3E5.zip",

"https://datapool.asf.alaska.edu/SLC/SA/S1A_IW_SLC__1SDV_20170923T000405_20170923T000432_018495_01F286_B17C.zip",

"https://datapool.asf.alaska.edu/SLC/SA/S1A_IW_SLC__1SDV_20170911T000405_20170911T000432_018320_01ED29_4D6A.zip",

"https://datapool.asf.alaska.edu/SLC/SA/S1A_IW_SLC__1SDV_20170818T000404_20170818T000431_017970_01E26E_8EE4.zip",

"https://datapool.asf.alaska.edu/SLC/SA/S1A_IW_SLC__1SDV_20170806T000403_20170806T000430_017795_01DD21_1652.zip",

"https://datapool.asf.alaska.edu/SLC/SA/S1A_IW_SLC__1SDV_20170725T000403_20170725T000430_017620_01D7C9_6499.zip",

"https://datapool.asf.alaska.edu/SLC/SA/S1A_IW_SLC__1SDV_20170701T000401_20170701T000428_017270_01CD28_52A7.zip",

"https://datapool.asf.alaska.edu/SLC/SA/S1A_IW_SLC__1SDV_20170619T000401_20170619T000428_017095_01C7E1_0127.zip",

"https://datapool.asf.alaska.edu/SLC/SA/S1A_IW_SLC__1SDV_20170607T000400_20170607T000427_016920_01C27F_A8D2.zip",

"https://datapool.asf.alaska.edu/SLC/SA/S1A_IW_SLC__1SDV_20170526T000359_20170526T000426_016745_01BD09_4B78.zip",

"https://datapool.asf.alaska.edu/SLC/SA/S1A_IW_SLC__1SDV_20170514T000359_20170514T000426_016570_01B7A9_AC53.zip",

"https://datapool.asf.alaska.edu/SLC/SA/S1A_IW_SLC__1SDV_20170502T000358_20170502T000425_016395_01B25B_7748.zip",

"https://datapool.asf.alaska.edu/SLC/SA/S1A_IW_SLC__1SDV_20170420T000357_20170420T000424_016220_01AD0F_C4FF.zip",

"https://datapool.asf.alaska.edu/SLC/SA/S1A_IW_SLC__1SDV_20170408T000357_20170408T000424_016045_01A7AC_6003.zip",

"https://datapool.asf.alaska.edu/SLC/SA/S1A_IW_SLC__1SDV_20170327T000356_20170327T000423_015870_01A273_5257.zip"

**10. Path 48 Frame 519**

"https://datapool.asf.alaska.edu/SLC/SA/S1A_IW_SLC__1SDV_20210610T000450_20210610T000517_038270_04841E_68D1.zip",

"https://datapool.asf.alaska.edu/SLC/SA/S1A_IW_SLC__1SDV_20210529T000449_20210529T000516_038095_047EF4_DCF9.zip",

"https://datapool.asf.alaska.edu/SLC/SA/S1A_IW_SLC__1SDV_20210517T000448_20210517T000515_037920_0479A9_7782.zip",

"https://datapool.asf.alaska.edu/SLC/SA/S1A_IW_SLC__1SDV_20210505T000448_20210505T000515_037745_047463_7682.zip",

"https://datapool.asf.alaska.edu/SLC/SA/S1A_IW_SLC__1SDV_20210423T000447_20210423T000514_037570_046E48_8317.zip",

"https://datapool.asf.alaska.edu/SLC/SA/S1A_IW_SLC__1SDV_20210411T000447_20210411T000514_037395_046837_3A30.zip",

"https://datapool.asf.alaska.edu/SLC/SA/S1A_IW_SLC__1SDV_20210330T000446_20210330T000513_037220_046230_0558.zip",

"https://datapool.asf.alaska.edu/SLC/SA/S1A_IW_SLC__1SDV_20210318T000446_20210318T000513_037045_045C26_5557.zip",

"https://datapool.asf.alaska.edu/SLC/SA/S1A_IW_SLC__1SDV_20210306T000446_20210306T000513_036870_045604_1F6A.zip",

"https://datapool.asf.alaska.edu/SLC/SA/S1A_IW_SLC__1SDV_20210222T000446_20210222T000513_036695_044FF8_5311.zip",

"https://datapool.asf.alaska.edu/SLC/SA/S1A_IW_SLC__1SDV_20210210T000446_20210210T000513_036520_0449D9_AEA5.zip",

"https://datapool.asf.alaska.edu/SLC/SA/S1A_IW_SLC__1SDV_20210129T000447_20210129T000514_036345_0443C6_D3D8.zip",

"https://datapool.asf.alaska.edu/SLC/SA/S1A_IW_SLC__1SDV_20210117T000447_20210117T000514_036170_043DAD_B0E5.zip",

"https://datapool.asf.alaska.edu/SLC/SA/S1A_IW_SLC__1SDV_20210105T000447_20210105T000515_035995_043787_3E0A.zip",

"https://datapool.asf.alaska.edu/SLC/SA/S1A_IW_SLC__1SDV_20201224T000448_20201224T000515_035820_043176_63B9.zip",

"https://datapool.asf.alaska.edu/SLC/SA/S1A_IW_SLC__1SDV_20201212T000449_20201212T000516_035645_042B6E_D2D4.zip",

"https://datapool.asf.alaska.edu/SLC/SA/S1A_IW_SLC__1SDV_20201130T000449_20201130T000516_035470_04256D_63EA.zip",

"https://datapool.asf.alaska.edu/SLC/SA/S1A_IW_SLC__1SDV_20201118T000450_20201118T000517_035295_041F65_A079.zip",

"https://datapool.asf.alaska.edu/SLC/SA/S1A_IW_SLC__1SDV_20201106T000450_20201106T000517_035120_041940_AF18.zip",

"https://datapool.asf.alaska.edu/SLC/SA/S1A_IW_SLC__1SDV_20201025T000450_20201025T000517_034945_041343_D3E9.zip",

"https://datapool.asf.alaska.edu/SLC/SA/S1A_IW_SLC__1SDV_20201013T000450_20201013T000517_034770_040D2E_0AD5.zip",

"https://datapool.asf.alaska.edu/SLC/SA/S1A_IW_SLC__1SDV_20201001T000450_20201001T000517_034595_040719_BC98.zip",

"https://datapool.asf.alaska.edu/SLC/SA/S1A_IW_SLC__1SDV_20200919T000449_20200919T000516_034420_0400E8_1465.zip",

"https://datapool.asf.alaska.edu/SLC/SA/S1A_IW_SLC__1SDV_20200907T000449_20200907T000516_034245_03FABD_0EE4.zip",

"https://datapool.asf.alaska.edu/SLC/SA/S1A_IW_SLC__1SDV_20200826T000449_20200826T000516_034070_03F49B_2EE6.zip",

"https://datapool.asf.alaska.edu/SLC/SA/S1A_IW_SLC__1SDV_20200814T000448_20200814T000515_033895_03EE63_E728.zip",

"https://datapool.asf.alaska.edu/SLC/SA/S1A_IW_SLC__1SDV_20200802T000447_20200802T000514_033720_03E87F_F491.zip",

"https://datapool.asf.alaska.edu/SLC/SA/S1A_IW_SLC__1SDV_20200721T000446_20200721T000513_033545_03E31B_16CD.zip",

"https://datapool.asf.alaska.edu/SLC/SA/S1A_IW_SLC__1SDV_20200709T000446_20200709T000513_033370_03DDC1_479E.zip",

"https://datapool.asf.alaska.edu/SLC/SA/S1A_IW_SLC__1SDV_20200627T000445_20200627T000512_033195_03D870_ACB4.zip",

"https://datapool.asf.alaska.edu/SLC/SA/S1A_IW_SLC__1SDV_20200615T000444_20200615T000511_033020_03D320_668F.zip",

"https://datapool.asf.alaska.edu/SLC/SA/S1A_IW_SLC__1SDV_20200603T000443_20200603T000510_032845_03CDEB_3AD2.zip",

"https://datapool.asf.alaska.edu/SLC/SA/S1A_IW_SLC__1SDV_20200522T000443_20200522T000510_032670_03C8AC_89D1.zip",

"https://datapool.asf.alaska.edu/SLC/SA/S1A_IW_SLC__1SDV_20200428T000441_20200428T000509_032320_03BD7E_E28E.zip",

"https://datapool.asf.alaska.edu/SLC/SA/S1A_IW_SLC__1SDV_20200416T000441_20200416T000508_032145_03B758_9D0C.zip",

"https://datapool.asf.alaska.edu/SLC/SA/S1A_IW_SLC__1SDV_20200404T000441_20200404T000508_031970_03B12F_FF40.zip",

"https://datapool.asf.alaska.edu/SLC/SA/S1A_IW_SLC__1SDV_20200323T000440_20200323T000507_031795_03AB07_9201.zip",

"https://datapool.asf.alaska.edu/SLC/SA/S1A_IW_SLC__1SDV_20200311T000440_20200311T000507_031620_03A4E1_1381.zip",

"https://datapool.asf.alaska.edu/SLC/SA/S1A_IW_SLC__1SDV_20200228T000440_20200228T000507_031445_039ECC_9B22.zip",

"https://datapool.asf.alaska.edu/SLC/SA/S1A_IW_SLC__1SDV_20200216T000440_20200216T000507_031270_0398C8_F97F.zip",

"https://datapool.asf.alaska.edu/SLC/SA/S1A_IW_SLC__1SDV_20200204T000440_20200204T000508_031095_0392BE_C3AA.zip",

"https://datapool.asf.alaska.edu/SLC/SA/S1A_IW_SLC__1SDV_20200123T000441_20200123T000508_030920_038C98_9650.zip",

"https://datapool.asf.alaska.edu/SLC/SA/S1A_IW_SLC__1SDV_20200111T000441_20200111T000508_030745_038671_34D0.zip",

"https://datapool.asf.alaska.edu/SLC/SA/S1A_IW_SLC__1SDV_20191230T000442_20191230T000509_030570_038063_688D.zip",

"https://datapool.asf.alaska.edu/SLC/SA/S1A_IW_SLC__1SDV_20191218T000442_20191218T000509_030395_037A62_AB19.zip",

"https://datapool.asf.alaska.edu/SLC/SA/S1A_IW_SLC__1SDV_20191206T000443_20191206T000510_030220_037451_4A67.zip",

"https://datapool.asf.alaska.edu/SLC/SA/S1A_IW_SLC__1SDV_20191124T000443_20191124T000510_030045_036E43_114B.zip",

"https://datapool.asf.alaska.edu/SLC/SA/S1A_IW_SLC__1SDV_20191112T000443_20191112T000511_029870_036835_A77A.zip",

"https://datapool.asf.alaska.edu/SLC/SA/S1A_IW_SLC__1SDV_20191031T000443_20191031T000511_029695_036215_050B.zip",

"https://datapool.asf.alaska.edu/SLC/SA/S1A_IW_SLC__1SDV_20191019T000443_20191019T000510_029520_035BFD_3F0F.zip",

"https://datapool.asf.alaska.edu/SLC/SA/S1A_IW_SLC__1SDV_20191007T000443_20191007T000511_029345_0355F7_2A20.zip",

"https://datapool.asf.alaska.edu/SLC/SA/S1A_IW_SLC__1SDV_20190925T000443_20190925T000510_029170_034FEC_A99B.zip",

"https://datapool.asf.alaska.edu/SLC/SA/S1A_IW_SLC__1SDV_20190913T000443_20190913T000510_028995_0349F3_3C41.zip",

"https://datapool.asf.alaska.edu/SLC/SA/S1A_IW_SLC__1SDV_20190901T000442_20190901T000509_028820_0343E1_9860.zip",

"https://datapool.asf.alaska.edu/SLC/SA/S1A_IW_SLC__1SDV_20190820T000442_20190820T000509_028645_033DC3_00AD.zip",

"https://datapool.asf.alaska.edu/SLC/SA/S1A_IW_SLC__1SDV_20190808T000441_20190808T000508_028470_0337B5_808F.zip",

"https://datapool.asf.alaska.edu/SLC/SA/S1A_IW_SLC__1SDV_20190727T000440_20190727T000507_028295_033259_EEF1.zip",

"https://datapool.asf.alaska.edu/SLC/SA/S1A_IW_SLC__1SDV_20190422T000435_20190422T000502_026895_030652_4D3E.zip",

"https://datapool.asf.alaska.edu/SLC/SA/S1A_IW_SLC__1SDV_20190410T000434_20190410T000501_026720_030006_AF4E.zip",

"https://datapool.asf.alaska.edu/SLC/SA/S1A_IW_SLC__1SDV_20190329T000434_20190329T000501_026545_02F993_4601.zip",

"https://datapool.asf.alaska.edu/SLC/SA/S1A_IW_SLC__1SDV_20190317T000434_20190317T000501_026370_02F32A_64E6.zip",

"https://datapool.asf.alaska.edu/SLC/SA/S1A_IW_SLC__1SDV_20190221T000434_20190221T000501_026020_02E673_5856.zip",

"https://datapool.asf.alaska.edu/SLC/SA/S1A_IW_SLC__1SDV_20190209T000434_20190209T000501_025845_02E03C_52BA.zip",

"https://datapool.asf.alaska.edu/SLC/SA/S1A_IW_SLC__1SDV_20190128T000434_20190128T000502_025670_02D9F3_C461.zip",

"https://datapool.asf.alaska.edu/SLC/SA/S1A_IW_SLC__1SDV_20190116T000435_20190116T000502_025495_02D389_955C.zip",

"https://datapool.asf.alaska.edu/SLC/SA/S1A_IW_SLC__1SDV_20190104T000435_20190104T000502_025320_02CD37_A5D8.zip",

"https://datapool.asf.alaska.edu/SLC/SA/S1A_IW_SLC__1SDV_20181223T000436_20181223T000503_025145_02C6E9_F260.zip",

"https://datapool.asf.alaska.edu/SLC/SA/S1A_IW_SLC__1SDV_20181211T000436_20181211T000503_024970_02C09B_F783.zip",

"https://datapool.asf.alaska.edu/SLC/SA/S1A_IW_SLC__1SDV_20181129T000436_20181129T000503_024795_02BAB1_111C.zip",

"https://datapool.asf.alaska.edu/SLC/SA/S1A_IW_SLC__1SDV_20181117T000437_20181117T000504_024620_02B44A_88DA.zip",

"https://datapool.asf.alaska.edu/SLC/SA/S1A_IW_SLC__1SDV_20181105T000437_20181105T000504_024445_02ADE3_B6C3.zip",

"https://datapool.asf.alaska.edu/SLC/SA/S1A_IW_SLC__1SDV_20181024T000437_20181024T000504_024270_02A7F5_F942.zip",

"https://datapool.asf.alaska.edu/SLC/SA/S1A_IW_SLC__1SDV_20181012T000437_20181012T000504_024095_02A248_A6BB.zip",

"https://datapool.asf.alaska.edu/SLC/SA/S1A_IW_SLC__1SDV_20180930T000437_20180930T000504_023920_029C86_AF2A.zip",

"https://datapool.asf.alaska.edu/SLC/SA/S1A_IW_SLC__1SDV_20180918T000437_20180918T000504_023745_0296D7_475C.zip",

"https://datapool.asf.alaska.edu/SLC/SA/S1A_IW_SLC__1SDV_20180906T000436_20180906T000503_023570_02913F_C6C4.zip",

"https://datapool.asf.alaska.edu/SLC/SA/S1A_IW_SLC__1SDV_20180825T000436_20180825T000503_023395_028BA9_2319.zip",

"https://datapool.asf.alaska.edu/SLC/SA/S1A_IW_SLC__1SDV_20180801T000434_20180801T000501_023045_028071_AF2E.zip",

"https://datapool.asf.alaska.edu/SLC/SA/S1A_IW_SLC__1SDV_20180720T000434_20180720T000501_022870_027AE8_31E1.zip",

"https://datapool.asf.alaska.edu/SLC/SA/S1A_IW_SLC__1SDV_20180708T000433_20180708T000500_022695_02758B_9825.zip",

"https://datapool.asf.alaska.edu/SLC/SA/S1A_IW_SLC__1SDV_20180626T000432_20180626T000459_022520_027072_0A14.zip",

"https://datapool.asf.alaska.edu/SLC/SA/S1A_IW_SLC__1SDV_20180614T000432_20180614T000459_022345_026B4E_2BFF.zip",

"https://datapool.asf.alaska.edu/SLC/SA/S1A_IW_SLC__1SDV_20180521T000430_20180521T000457_021995_026046_6624.zip",

"https://datapool.asf.alaska.edu/SLC/SA/S1A_IW_SLC__1SDV_20180509T000429_20180509T000456_021820_025AB2_6078.zip",

"https://datapool.asf.alaska.edu/SLC/SA/S1A_IW_SLC__1SDV_20180427T000429_20180427T000456_021645_025523_272B.zip",

"https://datapool.asf.alaska.edu/SLC/SA/S1A_IW_SLC__1SDV_20180322T000427_20180322T000454_021120_0244B7_3841.zip",

"https://datapool.asf.alaska.edu/SLC/SA/S1A_IW_SLC__1SDV_20180310T000427_20180310T000454_020945_023F25_BE0C.zip",

"https://datapool.asf.alaska.edu/SLC/SA/S1A_IW_SLC__1SDV_20180226T000427_20180226T000454_020770_0239A2_65CC.zip",

"https://datapool.asf.alaska.edu/SLC/SA/S1A_IW_SLC__1SDV_20180214T000427_20180214T000454_020595_02340C_D7F8.zip",

"https://datapool.asf.alaska.edu/SLC/SA/S1A_IW_SLC__1SDV_20180202T000428_20180202T000455_020420_022E70_BF08.zip",

"https://datapool.asf.alaska.edu/SLC/SA/S1A_IW_SLC__1SDV_20180121T000428_20180121T000455_020245_0228DC_13E1.zip",

"https://datapool.asf.alaska.edu/SLC/SA/S1A_IW_SLC__1SDV_20180109T000428_20180109T000455_020070_02234E_7259.zip",

"https://datapool.asf.alaska.edu/SLC/SA/S1A_IW_SLC__1SDV_20171228T000429_20171228T000456_019895_021DCF_16FC.zip",

"https://datapool.asf.alaska.edu/SLC/SA/S1A_IW_SLC__1SDV_20171204T000430_20171204T000457_019545_0212ED_F69E.zip",

"https://datapool.asf.alaska.edu/SLC/SA/S1A_IW_SLC__1SDV_20171110T000430_20171110T000457_019195_0207F0_1B23.zip",

"https://datapool.asf.alaska.edu/SLC/SA/S1A_IW_SLC__1SDV_20171029T000431_20171029T000458_019020_020289_7A75.zip",

"https://datapool.asf.alaska.edu/SLC/SA/S1A_IW_SLC__1SDV_20171017T000431_20171017T000458_018845_01FD3E_B77E.zip",

"https://datapool.asf.alaska.edu/SLC/SA/S1A_IW_SLC__1SDV_20171005T000430_20171005T000457_018670_01F7DF_2E8C.zip",

"https://datapool.asf.alaska.edu/SLC/SA/S1A_IW_SLC__1SDV_20170923T000430_20170923T000457_018495_01F286_19F1.zip",

"https://datapool.asf.alaska.edu/SLC/SA/S1A_IW_SLC__1SDV_20170911T000430_20170911T000457_018320_01ED29_247F.zip",

"https://datapool.asf.alaska.edu/SLC/SA/S1A_IW_SLC__1SDV_20170818T000429_20170818T000456_017970_01E26E_5559.zip",

"https://datapool.asf.alaska.edu/SLC/SA/S1A_IW_SLC__1SDV_20170806T000428_20170806T000455_017795_01DD21_CF7A.zip",

"https://datapool.asf.alaska.edu/SLC/SA/S1A_IW_SLC__1SDV_20170725T000427_20170725T000455_017620_01D7C9_1CAE.zip",

"https://datapool.asf.alaska.edu/SLC/SA/S1A_IW_SLC__1SDV_20170701T000426_20170701T000453_017270_01CD28_69FC.zip",

"https://datapool.asf.alaska.edu/SLC/SA/S1A_IW_SLC__1SDV_20170619T000425_20170619T000453_017095_01C7E1_2CF8.zip",

"https://datapool.asf.alaska.edu/SLC/SA/S1A_IW_SLC__1SDV_20170607T000425_20170607T000452_016920_01C27F_9383.zip",

"https://datapool.asf.alaska.edu/SLC/SA/S1A_IW_SLC__1SDV_20170526T000424_20170526T000451_016745_01BD09_952D.zip",

"https://datapool.asf.alaska.edu/SLC/SA/S1A_IW_SLC__1SDV_20170514T000423_20170514T000450_016570_01B7A9_9899.zip",

"https://datapool.asf.alaska.edu/SLC/SA/S1A_IW_SLC__1SDV_20170502T000423_20170502T000450_016395_01B25B_3918.zip",

"https://datapool.asf.alaska.edu/SLC/SA/S1A_IW_SLC__1SDV_20170420T000422_20170420T000449_016220_01AD0F_CCE8.zip",

"https://datapool.asf.alaska.edu/SLC/SA/S1A_IW_SLC__1SDV_20170408T000422_20170408T000449_016045_01A7AC_ED8E.zip",

"https://datapool.asf.alaska.edu/SLC/SA/S1A_IW_SLC__1SDV_20170327T000421_20170327T000448_015870_01A273_2A81.zip"